Proceedings of the

16th International Conference on Location Based Services

Anahid Basiri, Georg Gartner and Haosheng Huang (Editors)

Online
November 24–25, 2021

ICA Commission on Location Based Services

Editors

Anahid Basiri, Ana.Basiri@glasgow.ac.uk

School of Geographical & Earth Sciences, University of Glasgow, UK

Georg Gartner, Georg.Gartner@tuwien.ac.at

Research Group Cartography, TU Wien, Austria

Haosheng Huang, Haosheng.Huang@ugent.be

Department of Geography, Ghent University, Belgium

This document contains the proceedings of the 16th International Conference on Location Based Services (LBS 2021), held online on November 24–25, 2021.

The conference is organized by the ICA Commission on Location Based Services, and the School of Geographical & Earth Sciences at the University of Glasgow.

The editors would like to thank all the scientific committee members of LBS 2021 for help ensuring an excellent conference program, as well as Wangshu Wang for compiling the whole proceedings.

DOI: 10.34726/1741

Preface

We are now living in a mobile information era, which is fundamentally changing science and society. Location Based Services (LBS), which deliver information depending on the location and context of the (mobile) device and user, play a key role in this mobile information era. In recent years, lots of progress has been achieved in the research field of LBS, due to the increasingly maturity of the underpinning communication technologies and mobile devices. LBS have become more and more popular in not only citywide outdoor environments, but also shopping malls, museums, and many other indoor environments. They have been applied for emergency services, tourism services, intelligent transport services, social networking, gaming, assistive services, etc.

Since its initiation by Georg Gartner from TU Wien in 2002, the LBS conference series has become one of the most important scientific events decided to LBS. The conferences have been held in Vienna (2002, 2004, 2005), Hong Kong (2007), Salzburg (2008), Nottingham (2009), Guangzhou (2010), Vienna (2011), Munich (2012), Shanghai (2013), Vienna (2014), Augsburg (2015), Vienna (2016), Zurich (2018), Vienna (2019). Starting from 2015, the LBS conferences have become the annual event of the Commission on Location Based Services of the International Cartographic Association (ICA). In November 2021, the 16th LBS conference (LBS 2021) will be hosted by the University of Glasgow.

The conference proceedings contain a selection of short papers submitted to LBS 2021. The book provides a general picture of recent research activities related to the domain of LBS. Such activities emerged in the last years, especially concerning issues of outdoor/indoor positioning, wayfinding and navigation systems, location tracking, mobility and activity analytics, social media, usability and privacy, and innovative LBS systems

We would like to thank all the authors for their excellent work. We hope you enjoy reading these papers, and look forward to your participation in the future LBS conferences.

Anahid Basiri, Georg Gartner and Haosheng Huang

November 2021 in Glasgow, UK, Vienna, Austria and Ghent, Belgium

Scientific Committee

Conference Chairs:

Anahid Basiri, University of Glasgow, UK

Haosheng Huang, Ghent University, BE / ICA Commission on Location Based Services

Program Committee:

Georg Gartner, TU Wien, AT (Chair)

Anto Aasa, University of Tartu, EE

Tinghua Ai, Wuhan University, CN

Gennady Andrienko, Fraunhofer, DE

Masatoshi Arikawa, The University of Tokyo, JP

Thierry Badard, Laval University, CA

Dirk Burghardt, TU Dresden, DE

William Cartwright, RMIT University, AU

Christophe Claramunt, Naval Academy Research Institute, FR

Sagi Dalyot, Technion, IL

Mahmoud Reza Delavar, University of Tehran, IR

Urska Demsar, University of St Andrews, UK

Sara Irina Fabrikant, University of Zurich, CH

Zhixiang Fang, Wuhan University, CN

Ioannis Giannopoulos, Vienna University of Technology, AT

Nico Van de Weghe, Ghent University, BE

Monica Wachowicz, RMIT University, AU

Wangshu Wang, TU Wien, AT

Robert Weibel, University of Zurich, CH

Stephan Winter, The University of Melbourne, AU

Frank Witlox, Ghent University, BE

Table of Contents

Section I: Wayfinding and Navigation Systems

Section II: Positioning

Section III: Location tracking and systems

Section IV: Mobility and Activity Analytics

Section V: User Studies, Visualization, and Analysis

Towards a hierarchical indoor data model from a route perspective

Zhiyong Zhou*, Robert Weibel*, Kai-Florian Richter**, Haosheng Huang***

* Department of Geography, University of Zurich, Zurich, Switzerland
** Department of Computing Science, Umeå University, Sweden
*** Department of Geography, Ghent University, Ghent, Belgium

Abstract. In mobile navigation systems, an appropriate level of detail of the route instructions provided is important for navigation users to understand, memorise, and follow routes. However, few existing indoor navigation systems are capable of providing route instructions with multiple levels of detail. To close this gap, it is critical to model indoor environments with multiple granularities for route instructions to be generated on varying levels of detail. We propose a hierarchical model for route instructions in multi-storey buildings by allowing for representing actions (i.e., turning left or right, and going straight) in conceptualising route instructions. As a proof of concept, a case study is being conducted to present the feasibility of the proposed hierarchical model.

Keywords. Hierarchy, Indoor data model, Route instruction

1. Introduction

When a person, who is termed a route-giver in the route communication contexts, plans and instructs route information, to another person who requests and receives route information (i.e., the route-receiver), the route-giver tends to adapt the level of detail of the given route information to the assumed familiarity of the route receiver (Ziegler et al., 2011; Zhou et al., 2021), and the route complexity (Richter, 2007; Tenbrink, 2012). There are primarily two approaches to generating route instructions with varying levels of detail (LOD): destination descriptions (Tomko and Winter, 2009) and route directions (Klippel, 2003). The former approach makes use of various spatial features to describe the location of destinations, whereas the latter approach aggregates fully detailed turn-by-turn instructions from an

Published in "Proceedings of the 16th International Conference on Location Based Services (LBS 2021)", edited by Anahid Basiri, Georg Gartner and Haosheng Huang, LBS 2021, 24-25 November 2021, Glasgow, UK/online.

https://doi.org/10.34726/1742 | © Authors 2021. CC BY 4.0 License.

origin to a destination using various chunking principles. In mobile navigation systems, a hierarchical data model that accounts for the salience or granularity of spatial features is required for the generation of multiple LODs of route instructions (Klippel et al., 2009).

As indoor spaces are significantly distinct from outdoor environments (Worboys, 2011; Winter et al., 2019), there have been a number of studies conducted to model indoor spaces (Afyouni et al., 2012). Some of them (Richter et al., 2011; Stoffel et al., 2008; Liu et al., 2019) attempted to develop hierarchical indoor data models to enable efficient route planning and place descriptions in buildings. However, these models are unable to support route directions at multiple LODs because the underlying basic graph primarily represents individual cellular indoor spaces (e.g., rooms, corridors) as nodes, without embedding the precise geometric information.

In summary, there is a need for a hierarchical indoor data model that supports both destination descriptions and route directions in route instructions with multiple LODs. Accordingly, we propose a route-based hierarchical indoor data model that enables route instructions in multi-storey buildings at multiple LODs. This work-in-progress paper is mainly concerned with conceptualising the hierarchy of indoor spaces in route instructions. A case study is used to demonstrate the usability of the proposed model.

2. Conceptual Model of Indoor Hierarchy

As illustrated in Figure 1, the conceptualised hierarchy for indoor route instructions is composed of seven levels: building, floor, axial, segment, junction, side, and basic. The building level represents individual buildings that contain multiple floors. The floor level captures the movement in the vertical direction of a building. The axial level models the longest straight line in corridor areas. The segment level further details segment components that constitute each axial element of that level. The junction level distinguishes decision points from other positions that are from the same cluster in the segment level. The side level characterises whether portal nodes in a cluster at the junction level are situated on the same or opposite side relative to a corridor section. And the basic level is composed of these specific positions (e.g., doors, POIs) in a building.

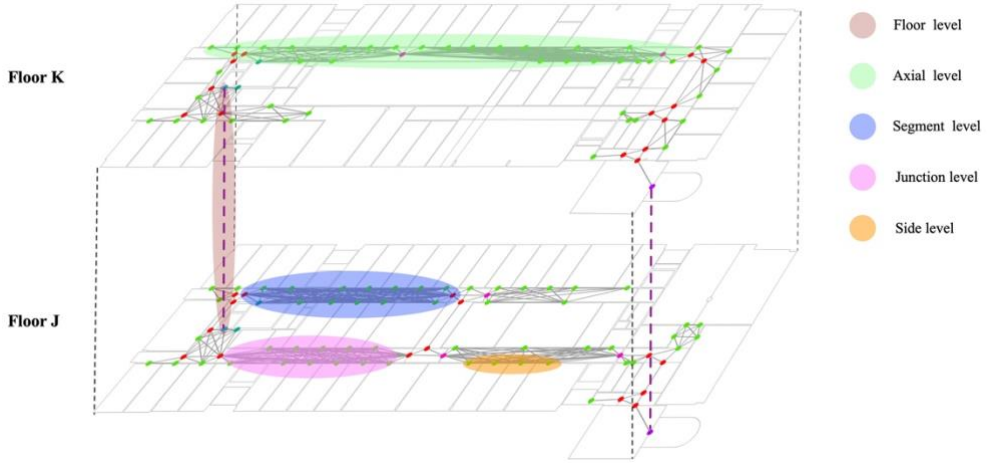

Figure 1. Illustration of the conceptualized hierarchy for indoor spaces from a route perspective.

3. Case Study

We selected the Y25 building at the University of Zurich as the case study for indoor route instructions based on the proposed hierarchical model. Currently, we are developing and testing an algorithm that allows mapping the conceptualised hierarchy to the given building to generate different LODs

4. Conclusion

This work-in-progress paper proposes a hierarchical indoor data model from a route perspective in order to enable the generation of multiple LODs of route instructions. Unlike conventional hierarchical indoor data models, which exclusively focus on the global architectural structure (e.g., floors, wings) of buildings, our model incorporates the local structures used for conceptualising both route directions and place descriptions. In the future, we intend to develop an approach to automatically construct the proposed hierarchy based on the commonly used floor plans. Then, we will conduct case studies to demonstrate the capability of the proposed model to facilitate destination descriptions and route directions in multi-storey buildings.

References

Afyouni, I., Ray, C., and Claramunt, C. (2012). Spatial models for context-aware indoor navigation systems: A survey. Journal of Spatial Information Science, 2012(4):85–123.

Klippel, A. (2003). Wayfinding choremes: Conceptualizing wayfinding and route direction elements. University of Bremen.

Klippel, A., Hansen, S., Richter, K.-F., and Winter, S. (2009). Urban granularities—a data structure for cognitively ergonomic route directions. GeoInformatica, 13(2):223–247.

Liu, L., Zlatanova, S., Li, B., van Oosterom, P., Liu, H., and Barton, J. (2019). Indoor routing on logical network using space semantics. ISPRS International Journal of Geo-Information, 8(3):126.

Richter, K.-F. (2007). From turn-by-turn directions to overview information on the way to take. In Location based services and telecartography, pages 205–216. Springer.

Richter, K.-F., Winter, S., and Santosa, S. (2011). Hierarchical representations of indoor spaces. Environment and Planning B: Planning and Design, 38(6):1052–1070.

Stoffel, E.-P., Schoder, K., and Ohlbach, H. J. (2008). Applying hierarchical graphs to pedestrian indoor navigation. In Proceedings of the 16th ACM SIGSPATIAL international conference on Advances in geographic information systems, page 54. ACM.

Tenbrink, T. (2012). Relevance in spatial navigation and communication. In International Conference on Spatial Cognition, pages 358–377. Springer.

Tomko, M. and Winter, S. (2009). Pragmatic construction of destination descriptions for urban environments. Spatial Cognition and Computation, 9(1):1–29.

Winter, S., Tomko, M., Vasardani, M., Richter, K.-F., Khoshelham, K., and Kalantari, M. (2019). Infrastructure-independent indoor localization and navigation. ACM Computing Surveys (CSUR), 52(3):61.

Worboys, M. (2011). Modeling indoor space. In Proceedings of the 3rd ACM SIGSPATIAL International Workshop on Indoor Spatial Awareness, pages 1–6. ACM.

Zhou, Z., Weibel, R., Fu, C., Winter, S., and Huang, H. (2021). Indoor landmarkselection for route communication: the influence of route-givers' social roles andreceivers' familiarity with the environment. Spatial Cognition & Computation, 21(4):257–289.

Ziegler, J., Hussein, T., M¨unter, D., Hofmann, J., and Linder, T. (2011). Generating route instructions with varying levels of detail. Proceedings of the 3rd International Conference on Automotive User Interfaces and Interactive Vehicular Applications, pages 31–38.

Representation and modelling of the complexity of street intersections for navigation guidance

Fangli Guan*,**, Zhixiang Fang*, Haosheng Huang**

* The State Key Laboratory of Information Engineering in Surveying, Mapping and Remote Sensing, Wuhan University, Wuhan, China.
** Department of Geography, Ghent University, Ghent, Belgium.

Abstract. There is growing recognition that the complexity of road intersections within navigation environments is a critical factor of wayfinding. A complex intersection can increase the difficulty of spatial cognition and environment perception for pedestrians, leading to wrong decision-making and deviated navigation. Existing methods quantify the complexity of a decision point by simply outputting a single value, thus fail to match the perceived content under different passage strategies. Besides, most methods merely include the structural or visual features, and rarely contain a comprehensive integration of multi-dimensional characteristics. This study proposes a passage strategy-based computational method to assess the complexity of road intersections with their perceptual contents of street scenes. Specifically, we analyze several types of real-world perceived features when crossing intersections. Then, develop a combination of conceptual features regarding the visual, structural and semantic aspects based on different route strategies (i.e., whether pedestrians focus on a particular branch as an entrance or an exit), to depict the perceived complexity features of the road intersections. This study provides further implication that the innovative method can be integrated into route planning and communication, and navigation guidance services in complex scenarios.

Keywords. Decision-making; Intersection's complexity; Passage strategy; Navigation guidance

LBS 2021
16th Conference on Location Based Services
24-25 November 2021 Online

Published in "Proceedings of the 16th International Conference on Location Based Services (LBS 2021)", edited by Anahid Basiri, Georg Gartner and Haosheng Huang, LBS 2021, 24-25 November 2021, Glasgow, UK/online.

https://doi.org/10.34726/1743 | © Authors 2021. CC BY 4.0 License.

1. Introduction

Road intersections are critical areas during wayfinding. They are the locations where decision-making and route-following errors occur. The complexity of navigation environments directly affects the guidance performance (O'Neill 1991) and raises the operation difficulty, involving the perception and understanding of environments, spatial cognition and mental representation (Richter 2009). Especially, in the context of road intersections, where the wayfinder needs to make turning decisions.

Current researches on road intersections' complexity ignore specific passage strategies. It outputs merely a single value, which leads to a mismatch between a single complexity result and the perceived scenes' content under **different passage strategies** (i.e., entrance branch and exit branch). The existing methods mainly construct complexity computation models for roads and intersections by extracting environmental features on structural or visual aspects. The former commonly detected the structural features of road networks (e.g., the length of road segments, the number of turnings, road intersections and their branches) (Sladewski et al. 2017, Zhou et al. 2019). The latter extracted basic image features (e.g., color, shape) to measure the visual complexity and cognitive elements (e.g., sky, building) to reflect wayfinder's psychological stress (Golledge 1999, Sanocki et al. 2015). Note that the above mentioned two fields address computational modelling of complexity somewhat separately, either in visual or structural aspects. Methods on combining both or more aspects are still under explored.

As a result, this study first considers the passage strategies when passing intersections (i.e., which branch the pedestrian concerns to be the entrance and which branch to be the exit) as a prerequisite, and proposes a model for evaluating the complexity of a wayfinding decision at road intersections. We argue that the calculation model, depending on the passage strategy and outputs multiple results, perform better than the model that only outputs a single value in describing the complexity of a wayfinding decision at a road intersection. From which an n-branches intersection will correspond to A_n^2 complexity values, respectively. This model incorporates the specific passage strategy as constraints and describes the intersection's visual, structural, and semantic characteristics. Eight features are extracted from easy-access geodata (i.e., street-view panoramas, road network, and POI data), to represent the intersection, and finally are integrated for decision-making complexity computation.

2. Research motivation

2.1. Overview

This study aims to represent the complexity of road intersections from navigation perspectives and develop a passage strategy-based computational method to quantify a single intersection more realistic and refined with multiple values of decision-making complexity. *Figure 1* demonstrates the framework of this 'working in progress' study.

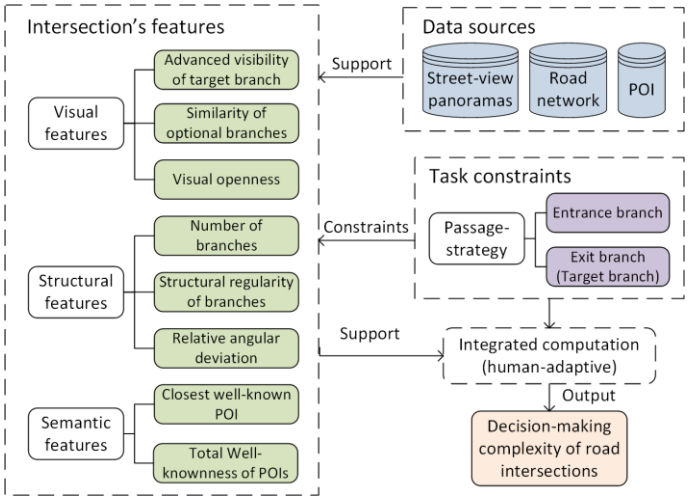

Figure 1. Framework of computational model.

2.2. Passage strategy-based features

Different passing routes provide diverse perceptual information to pedestrians, including perceived visual and semantic information, spatial attributes, and its mental representation of the road network. We believe that the computation of intersections' complexity needs to follow the specific traversal strategies. Therefore, we propose the following features to characterize the intersection visually, structurally, and semantically based on the passage strategy.

The **visual features** visually describe the global and local impressions of the real-world street scenes. Cognitive science research shows that human beings acquire external information mainly through vision, which is the main driver behind human perception (Brakus et al. 2009) and consequent experience). Previous studies extracted basic image features (e.g., color, shape, and size) and cognitive features (e.g., field of vision with sky and building areas) to measure the image/visual complexity of the scenes and wayfinder's psychology stress during the navigation process. Therefore, we

investigate the visual attributes with the specific entrance and exit branch, and design the following visual features.

- ***Advanced visibility of target branch*** (to measure the visibility characteristics of the target branch as it approaches the intersection (Klippel and Winter, 2005)).
- ***Similarity of optional branches*** (to measure the visual similarity of the target branch versus its neighboring branches).
- ***Visual openness of the forward direction*** (to measure the openness of the field of vision on human perspectives at street level).

The **structural features** of the road network physically and spatially measure the fundamental properties of navigation environments. As Richter (2009) mentioned, intersections with regular branches are easier to understand and make correct decisions than irregular intersections. Intersections that offer multiple turns in the same conceptual direction are more complex, and intersections with oblique turns are more complex than those with prototypical turns. We focus on the specific routes and intersections' branches, and design the following structural features to answer the question of 'how many branches of this road intersection?', then come to 'how many branches in the same direction?', and further 'how the relative angular deviation of adjacent branches'.

- ***Number of branches***.
- ***Structural regularity of branches*** (to measure the structural regularity of the remaining branches).
- ***Relative angular deviation of adjacent branches*** (to quantify the spatial angular proximity of a target branch to its neighboring branches).

The **semantic features** represent the social-cultural attributes of environments. Generally, POIs work as adequate spatial references with their significant meanings and functions in real-world scenes and digital maps. Further, well-known POIs have prominent historical and cultural characteristics that always facilitate people's understanding of street scenes. Consequently, this study adopts the well-known POIs and their reviews data, and designs the following semantic features to capture all potential visible spatial reference objects on each route segment, and measures the semantically impacts on the complexity of decision-making at road intersections.

- ***Closest well-known POI*** (to quantify the semantically impact by the closest well-known POI locally).
- ***Total well-knownness of POIs*** (to quantify the global popularity properties of the target branch).

2.3. Modelling of the complexity of road intersections

This section incorporates the features mentioned above and designs an adaptive weighted-based computation method to integrate the above features. It can be summarized as $F(f_{vis}, f_{str}, f_{sem}) = F(f_{vis}) \oplus F(f_{str}) \oplus F(f_{sem})$, where f_{vis}, f_{str}, f_{sem} are resulting visual complexity, structural complexity, and semantic complexity separately, which can account for more or less complexity of the wayfinding decision.

3. Conclusion and future work

This paper develops an innovation framework for computing the decision-making complexity of road intersections based on the passage strategy. We further propose eight features based on visual, structural, and semantic aspects to characterize the road intersection of the real-world environments in terms of human perspectives. This study provides further insight into the multi-outcome results of decision-making complexity for specific road intersection. The results will provide solid support the user-friendly route planning services without complicated intersections and aid scene complexity evaluation to enhance signals for route communication and guidance.

References

Brakus JJ, Schmitt BH, Zarantonello L (2009) Brand experience: what is it? How is it measured? Does it affect loyalty? J. Market. 73 (3), 52–68.

Golledge RG (1999) COGNITIVE MAPPING AND OTHER SPATIAL PROCESSES. The Johns Hopkins University Press, Washington, D.C.

Klippel A, Winter S (2005) Structural Salience of Landmarks for Route Directions, in: Spatial Information Theory, Lecture Notes in Computer Science. Springer Berlin Heidelberg, Berlin, Heidelberg, pp. 347–362.

O'Neill MJ (1991) Evaluation of a conceptual model of architectural legibility. Environment and Behavior, 23(3), 259-284.

Richter KF (2009) Adaptable Path Planning in Regionalized Environments, in: Spatial Information Theory, Lecture Notes in Computer Science. Springer Berlin Heidelberg, Berlin, Heidelberg, pp. 453–470.

Sanocki T, Islam M, Doyon JK, et al (2015) Rapid scene perception with tragic consequences: observers miss perceiving vulnerable road users, especially in crowded traffic scenes. Atten. Percept. Psychophys. 77, 1252–1262.

Sladewski RS, Keler A, Divanis A (2017) Computing the least complex path for vehicle drivers based on classified intersections 4.

Zhou Sh, Wang R, Ding J, et al (2019) An approach for computing routes without complicated decision points in landmark-based pedestrian navigation. International Journal of Geographical Information Science. 33, 1829–1846.

Adaptive Mobile Indoor Route Guidance, The Next Big Step

Laure De Cock*, Nico Van de Weghe*, Kristien Ooms*, Philippe De Maeyer*

* Ghent University, department of Geography

Abstract. Not all those who wander are lost… but when you are lost, there is a high chance that you are inside a building as we spend 90% of our time indoors. As opposed to outdoors, mobile indoor route guidance is not yet common practice, while the indoor environment can be far more complex than the outdoor one. As indoor navigation can be very challenging, we need supportive navigation systems that can ease the process. To this end, adaptive mobile indoor route guidance systems are being developed, which adapt the type of route instruction to the building configuration. This way, the right amount of information is provided at the right time and place. This work studies this type of smart route communication, and more specifically, its influence on the user. An online survey, a field experiment and a VR experiment were conducted to find out how building configuration can be quantified by the space syntax theory, which route instruction types should be used at which decision points and how this affects the performance, cognitive map, cognitive load and perception of the users. Prototypes were developed and eye tracking and position tracking were used to build the bridge between indoor route guidance technologies in smart buildings on the one hand, and the users of those smart buildings on the other hand. The results of this research can be translated into practical guidelines or implications for the design of adaptive mobile indoor route guidance systems, because this work has shown this is the way to go.

Keywords. Adaptive mobile route guidance, route instructions, space syntax, eye tracking

1. Introduction

Outdoors, we have a lot of options for navigation. We can use several apps on our smartphones, calculate the route for a vehicle or another transport

Published in "Proceedings of the 16th International Conference on Location Based Services (LBS 2021)", edited by Anahid Basiri, Georg Gartner and Haosheng Huang, LBS 2021, 24-25 November 2021, Glasgow, UK/online.

https://doi.org/10.34726/1744 | © Authors 2021. CC BY 4.0 License.

mode, choose the time and date for which the route has to be calculated, avoid highways, estimate traffic and get notifications of speed controls. We can even change the voice in our app so that Batman can tell us we have reached our destination. Have we though? When we for example have arrived at the hospital entrance, have we really reached our destination? We still have to find the reception desk, we have to get to the waiting room and maybe grab a coffee on the way, but once we enter the building we're on our own. No apps that can say how long it will take, no funny voices to make us feel more comfortable.

In a world where many new construction projects have a digital twin, where not only people but also devices are connected through the internet of things, where sensors and cameras are generating big data and where everything has to be smart, indoor navigation is the next big step. However, this work does not focus on the technological implementation of indoor navigation. Instead, it focuses on the cognitive aspects of navigation in smart buildings, and more specifically on easing the decision making process during route guidance. As every decision point is different, the user's need for route information is also different at every point. Therefore, decision making can be eased by adapting the route instruction type to the needs of the users, and thus, to the decision point. Navigation systems that implement this idea provide the right amount of information at the right time and place. The usability of these systems is studied in the dissertation of De Cock (2021).

2. Three user studies

The first step in the design of an adaptive navigation system is to determine which route instruction types should be used on which decision points. In this research, this decision is based on the subjective preferences of the users, which was collected during an online survey. The case study building of this work is the iGent, the office lab of Ghent University, and for the online survey ten route videos were recorded in this smart building, and ten route instruction types were designed for these route videos (e.g., maps, symbols, photos, 3D-simulations). Participants had to indicate how complex they found a decision point and how they scored a route instruction type on every decision point of the recorded routes. The results indicated, first of all, which decision point categories were found to be most complex, and how this could be related to the building configuration, quantified by space syntax. Second of all, they indicated which route instruction type gained preference on which decision point category.

In a second step, the results of the online survey were used to develop a mobile indoor navigation prototype. The prototype was web-based, connected to the UWB sensors in iGent and automatically showed a new route

instruction on the smartphone of the users. This route instruction could either be adapted to the decision point (i.e. symbols at starts and ends, 3D-simulations at complex turns and photos at all other points) or not adapted (i.e. photos on all points). The usability of the adaptive and non-adaptive system was tested with objective measures (e.g. eye tracking) in a field experiment where participants had to walk three routes with either one of the systems. The results of this field experiment showed that the usability of the adaptive system was higher, both in terms of cognitive load and performance.

In a third step, a virtual model of a building floor was designed and a virtual copy was made of the adaptive prototype from the field experiment. The same parameters as in the previous step were used to test the usability of the prototype, but this time the experiment was conducted in virtual reality. Because the virtual model was much bigger than the physical building, an analysis on the building configuration could be included. This way, the results of both the online survey and field experiment could be cross-validated in virtual reality. The lower cognitive load of the adaptive instructions that was found in the field experiment was confirmed in the virtual reality experiment.

3. Recommendations

First, we would like to address the implications of using turn-by-turn instructions. The comparison of turn-by-turn instructions with other ways of conveying route information is out of scope here, so it is impossible to give a full account of the usability of turn-by-turn instructions in general, based on the results of this work. However, we believe that certain results are caused by the general format of turn-by-turn route instructions, rather than the route instruction types specifically. This is the case for the general lower satisfaction of men in the online survey. This can for example imply that men are less likely to try a navigation aid when they know it uses turn-by-turn instructions, or that they will rather choose a navigation aid without turn-by-turn instructions. When they do decide to try it, it will not affect their orientation in a way that it becomes lesser than the orientation of women. This might be important to consider for example when the largest share of the target audience are men. A second difference between the prejudice of a system and actually using it, is the preference for a route instruction type. In the online survey, photo instructions were most liked by users, but when they had to use a navigation aid with photos in the field and VR experiment, this was no longer the case. As such, users might have a higher tendency to start using navigation aids when they know it uses photorealistic route instructions. In brief, the above mentioned results of the online survey might especially be of use to estimate the acceptability of a naviga-

tion aid before users can actually try it, as these results were not found in the other experiments. A result of the online survey that was repeated is the higher cognitive load on convex turns. This might be the result with the largest impact on the design of route guidance systems, as this goes straight against the navigation strategies without aid. This difference might be caused by the directed isovist during route guidance, and this seems to be confirmed both in the online survey and field experiment as only the local isovist measures correlate significantly. This means that designers of indoor navigation aids have to pay extra attention to the convex spaces as these are the hotspots of indoor turns. The convex space can be identified in a building by its local isovist characteristics, and more specifically by the compactness and occlusivity. Users will be in need of more support at these points, as they might be more confused and insecure by the rise in cognitive load. Luckily for future designers, we also found a way to reduce the cognitive load at these points: use 3D-simulations. The dwells will be smaller, which results in less screentime and more working memory devoted to the task. Moreover, it will not affect the user's walking speed, which is the case for photo instructions. At the same time, this might also be an advantage of the photo instructions. For example, when a building has very few or no convex turns, photo instructions might facilitate a faster walking speed, while this is not the case for 3D-simulations. Turns are not the only decision points where photo instructions induce a variable walking speed: at starting points, participants were clearly faster with the photo instructions, only this time compared to symbol instructions. At ending points, the role of photo instructions is again dubious, so the use of the route instruction type at end points will strongly depend on the layout of the building and the goal of the application: if there are a lot of possible end points at central places in a building, you have a chance of reducing cognitive load there with symbol instructions; if the main goal of the navigation aid is to get users as fast as possible to their destination, then this chance is also higher with symbol instructions. We could also make a case for the use of photo instructions at end points, as the first dwell was lower with this type, but the photo instruction does not provide extra help at the most complex points. All things considered, this nicely describes the role of photo instructions: overall this type has some advantages, but not on the most complex decision points. This also nicely affirms the preference ratings of the route instruction types. Regardless of the chosen route instruction type, the global building characteristics determine the cognitive load on ending points, which is in contrast to turns, where the local isovist characteristics are decisive. As such, designers should pay extra attention to the integration of end points in the building. This is also reflected in the orientation error that was most clearly influenced by the MVD. Furthermore, two final, general implications for the design of indoor navigation aids can be discussed. First, adding text to an instruction has been proven to have a high usability. On the one hand in the

online survey, where users rated types with text consistently higher than the same type without text, and on the other hand in the VR experiment, as the timestamp analysis showed that users consistently read the text first. The final implication of adapting the route instruction type to the decision point for the design of indoor navigation aids speaks for itself: significantly less navigation errors will be made.

References

De Cock L (2021) Adaptive mobile indoor route guidance : the next big step. Ghent University. Faculty of Sciences, Ghent, Belgium.

Indoor Wayfinding in Real-world Environments and Virtual Reality: A Comparison

Tong Qin *, Weihua Dong **, Haosheng Huang*

* CartoGIS, Ghent University, Ghent, Belgium
(tong.qin@ugent.be, haosheng.huang@ugent.be)
** Faculty of Geographical Science, Beijing Normal University, Beijing, China
(dongweihua@bnu.edu.cn)

Abstract. Wayfinding has been widely studied in fields of location-based service and geospatial cognition. It is currently unclear how wayfinding behaviour and spatial knowledge acquisition in immersive virtual reality (iVR) differ from those in real-world environments (REs). To investigate this question, we conducted the wayfinding experiment in RE with twenty-five participants and in iVR with forty participants. Participants' eye movements, verbal reports and questionnaires were recorded. The results revealed that participants processed visual information more efficiently in RE but searched visual information more efficiently in iVR. For spatial learning, participants' distance estimation was more accurate in iVR. This empirical study proves the ecological validity of iVR and encourages further studies to use VR techniques in wayfinding research.

Keywords. Indoor wayfinding, Spatial learning, Immersive virtual realty

LBS 2021
16th Conference on Location Based Services
24-25 November 2021 Online

Published in "Proceedings of the 16th International Conference on Location Based Services (LBS 2021)", edited by Anahid Basiri, Georg Gartner and Haosheng Huang, LBS 2021, 24-25 November 2021, Glasgow, UK/online.

https://doi.org/10.34726/1745 | © Authors 2021. CC BY 4.0 License.

1. Introduction

Elucidating wayfinding behaviours can improve our understanding of spatial knowledge acquisition in an unfamiliar environment, and better provide location-based service. The rapid development of Virtual environment (VE) technologies, with a range of setups from desktop to fully immersive, provides new experimental approaches for investigating wayfinding behaviours and spatial knowledge acquisition (Darken et al., 1998; Ehinger et al., 2014). Immersive Virtual Reality (iVR) offers more naturalistic sensory information, which might reduce the gap between laboratory and the real-world environment (RE) (Ruddle et al., 2011). No matter how realistic a virtual environment, however, differences between REs and VEs are inevitable. The ecological validity (Schmuckler, 2001) of the iVR in the indoor wayfinding field is still poorly understood, it remains unclear whether people who navigate in iVR and RE settings exhibit the same wayfinding behaviours and acquire equivalent spatial knowledge.

Therefore, we here hypothesize that pedestrians exhibit the different wayfinding behaviours and obtain varying levels of spatial knowledge between iVR and RE experiments. To test this hypothesis, we conducted indoor wayfinding experiments in two different setups. We measured their behavioural (verbal report protocol and questionnaire) and physiological (eye movement) metrics and tested them difference by statistics, to verify the ecological validity of the iVR from multiple perspectives.

2. Methodology

We recruited 65 participants (25 in the group RE and 40 in the group iVR) to conduct eye-tracking wayfinding experiments. The experiment tasks are the same in both two environments: participants were first required to complete the first set of tasks including one free viewing and three wayfinding tasks. Subsequently, participants finished the spatial knowledge measurements. After data pre-processing, we did statistical tests to validate our hypothesis.

3. Results and Discussion

Results include their wayfinding performance, visual attention, and spatial knowledge acquisition (Figure 1). Behavioural results show that indoor wayfinding efficiency and effectiveness might be closer between two environments with increasing experimental time in the iVR. Eye movement reflects that it is more difficult to process visual information in the iVR. Conversely, they perform better in visual searching with a wider range.

However, the distribution of fixation locates in landmarks is similar in both environments. The flexibility of participants and the landmark salience in different experimental settings (Dong et al., 2020; Lessels and Ruddle, 2005) might cause these findings. For their spatial learning results, we don't detect the distinguish in their direction estimation and sketch map between two environments. To our surprise, participants in the iVR estimate distance more accurately than in the RE. Our study provides evidence for the ecological validity of the iVR in wayfinding research. Confirming these interesting results will require further research into the detailed mechanisms of spatial coding at the level of brain activation and response.

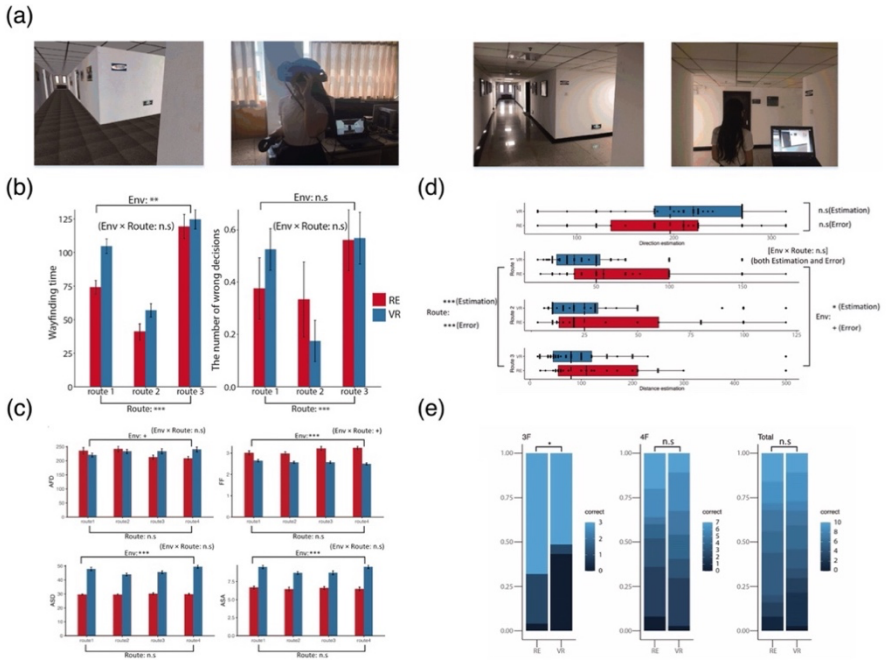

Figure 1. Overall results include wayfinding performance, visual attention, and spatial knowledge. (a) Experimental setups, two left pictures are in the iVR and right pictures are in the RE; (b) Wayfinding performance; (c) Visual attention; (d) Direction and distance estimation; (e) Sketch mapping distribution.

Notice: This extended abstract is based on the following paper:

Dong, W., Qin, T., Yang, T., Liao, H., Liu, B., Meng, L., & Liu, Y. (2021). Wayfinding Behavior and Spatial Knowledge Acquisition: Are They the Same in Virtual Reality and in Real-World Environments? *Annals of the American Association of Geographers, 1-21.*

References

Darken, R. P., T. Allard, and L. B. Achille (1998) Spatial orientation and wayfinding in large-scale. Virtual spaces: An introduction. Presence: Teleoperators and Virtual Environments 7 (2):101–7.

Dong, W., T. Qin, H. Liao, Y. Liu, and J. Liu (2020) Comparing the roles of landmark visual. salience and semantic salience in visual guidance during indoor wayfinding. Cartography and Geographic Information Science 47 (3):229–43.

Ehinger, B. V., P. Fischer, A. L. Gert, L. Kaufhold, F. Weber, G. Pipa, and P. Konig (2014) Kinesthetic and vestibular information modulate alpha activity during spatial navigation: A mobile EEG study. Frontiers in Human Neuroscience 8:71. Di Dio C, Macaluso E, Rizzolatti G (2007) The Golden Beauty: Brain Response to Classical and Renaissance Sculptures. PLoS ONE 2(11): e1201. doi: 10.1371/journal.pone.0001201

Lessels, S., and R. A. Ruddle (2005) Movement around real and virtual cluttered. environments. Presence: Teleoperators and Virtual Environments 14 (5):580–96.

Ruddle, R. A., E. Volkova, and H. H. Bulthoff (2011) Walking improves your cognitive map in. environments that are large-scale and large in extent. ACM Transactions on Computer–Human Interaction 18 (2):1–20.

Schmuckler, M. A (2001) What is ecological validity? A dimensional analysis. Infancy: The. Official Journal of the International Society on Infant Studies 2 (4):419–36.

Indoor navigation path visualization method considering the spatial characteristics

Jingyi Zhou [1,2,3], Jie Shen[1,2,3,*], Jiafeng Shi [1,2,3], Litao Zhu[1,2,3]

[1] Key Laboratory of Virtual Geographic Environment (Nanjing Normal University), Ministry of Education, Nanjing 210023, China;
[2] Jiangsu Center for Collaborative Innovation in Geographical Information Resource Development and Application, Nanjing 210023, China;
[3] School of Geography, Nanjing Normal University, Nanjing 210023, China.
211301034@njnu.edu.cn (J.Z.); 171302089@njnu.edu.cn (J.S.); 181301028@njnu.edu.cn (L.Z.)
[*] Corresponding author: shenjie@njnu.edu.cn (J.S.)

Abstract. Facing the complicated indoor space structure, people's demands for indoor location services such as navigation and emergency evacuation are also increasing. Indoor navigation map is an important tool for people to navigate and find way in large public buildings. Navigation path visualization is a key map element that guides users to complete navigation behavior, and its visualization method has attracted more and more attention. The difference between indoor and outdoor path characteristics makes it difficult for outdoor path visualization methods to be fully applicable indoors. It is urgent to propose a navigation path visualization method that meets the characteristics of indoor space in order to better assist users in completing navigation tasks. This paper summarizes the indoor space characteristics, indoor navigation path characteristics and visualization principles, in the future, it is planned to use different methods of overview and user perspective to visualize the indoor navigation path.

Keywords. Spatial characteristics, Path visualization, Indoor navigation map, Indoor location services

1. Introduction

With the gradual improvement of urban infrastructure and building coverage, various super large buildings emerge in endlessly, such as shopping malls, hospitals, airports, high-rise office buildings, exhibition halls, etc.

LBS 2021
16th Conference on Location Based Services
24-25 November 2021 Online

Published in "Proceedings of the 16th International Conference on Location Based Services (LBS 2021)", edited by Anahid Basiri, Georg Gartner and Haosheng Huang, LBS 2021, 24-25 November 2021, Glasgow, UK/online.

https://doi.org/10.34726/1746 | © Authors 2021. CC BY 4.0 License.

Research have shown that humans spend approximately 80% of their time in indoor activities (Klepeis et al. 2001). At present, indoor location services mainly focus on technical research such as positioning and path planning. As the calculation basis and information carrier of indoor location services, indoor navigation maps have received little attention for their own modeling and visualization. In particular, the navigation path is a key map element for the indoor navigation map to guide the user to complete the navigation behavior, and its visualization method is often ignored.

The indoor space structure and function are obviously different from the outdoor. Unlike the outdoor road network which is mainly two-dimensional, the multi-storey connection inside the building makes the indoor road present a three-dimensional spatial structure. Therefore, navigation in indoor environment involves more vertical movement, that is, inter-layer movement (Karimi 2015). At the same time, humans often exhibit a networked topology, that is, "sequential behavior" in the process of navigation and pathfinding (Kuipers 1979). Since the indoor environment does not have an obvious road network structure, most of them are open traffic areas. In this case, how to clearly visualize the indoor navigation path is worthy of in-depth discussion.

2. Analysis of indoor space characteristics

In the field of indoor cartography, Afyouni et al. (2010) defined the building environment where people frequent daily activities such as shopping malls and residential houses as indoor space. Yang et al. (2011) proposed that indoor space is a concept that is relative to the large-scale space in the natural environment. It refers to the inside and below of the building on the ground, which provides enclosed space for human activities, such as various large-scale buildings on the ground and underground parking, etc.

Compared with the outdoor open natural environment, the indoor space is a man-made and relatively closed environment, which mainly contains artificially constructed entities, the indoor space has the following characteristics:

(1) Indoor space presents a multi-layer three-dimensional structure. Due to the horizontal division and vertical connection between floors, the structures of each floor have similarity, consistency and overlap.

(2) Indoor space is restrictive. Some spaces have certain social, time and functional privacy restrictions.

(3) Poor visibility of indoor space. In the horizontal and vertical direction, the indoor space is divided by many walls, rooms, and the floors are

connected by elevators, escalators, and stairs, the user's line of sight is limited.

(4) Indoor space elements are special, densely distributed and highly variable. Affected by various emergencies, behaviors or activities, the layout of the indoor space is frequently changed.

3. Characteristics and visualization principles of indoor navigation path

In map visualization, generally select some elements for mapping based on the characteristics of the cartographic object, the specific purpose of the map, or the specific user object (Ryder 2015). The difference of indoor and outdoor space characteristics makes the path characteristics also show obvious differences.

- Dimensional characteristic

The multi-storey nature of the building makes the indoor space present a three-dimensional structure, and the indoor path, as a passage element connecting each floor, also presents a three-dimensional form.

Visualization principles: For cross-floor indoor paths, 2.5D and 3D are combined to visualize the transition positions and connection relationships between floors.

- Directional characteristic

The indoor path direction is diversified. It not only has the horizontal connection of the front, back, left and right directions, but also the vertical connection of the upper and lower sides.

Visualization principles: For indoor navigation paths, escape routes, etc., appropriate visual variables and visual forms should be designed for such clearly-indicated paths, and correct direction instructions should be given.

- Openness characteristic

In addition to the open passage for the public, some indoor scenes have special passages, such as staff passages, VIP passages, etc.

Visualization principles: For impassable paths, colors that are quite different from the base map should be used to visualize in order to achieve the function of reminding and warning.

- Semantic characteristic

As far as indoor space is concerned, there is no conventional or prescribed semantic description for indoor paths.

Visualization principles: Landmarks are important element for people to communicate route information (Denis 1997, Raubal & Winter 2002). Using landmarks as the semantic information of indoor paths can provide users with accurate location descriptions.

4. Conclusion

This paper studies the indoor navigation path visualization method that takes into account the space characteristics, analyzes the indoor space characteristics, the navigation path characteristics and visualization principles. In the future, it is planned to use different methods of overview and user perspective to visualize the indoor navigation path based on the hierarchical visualization of indoor navigation map elements.

Acknowledgment

This research was funded by National Key R&D Program of China (2021YFE0112300), National Natural Science Foundation of China (NSFC) (No. 41871371).

References

Afyouni I, Ray C, Claramunt C (2010) A fine-grained context-dependent model for indoor spaces. In Proceedings of the 2nd acm sigspatial international workshop on indoor spatial awareness (pp. 33-38).

Denis M (1997). The description of routes: A cognitive approach to the production of spatial discourse. Current psychology of cognition, 16, 409-458.

Karimi H A (2015) Indoor wayfinding and navigation. CRC Press.

Klepeis N E, Nelson W C, Ott W R, Robinson J P, Tsang A M, Switzer P, Behar J V, Hern S C, Engelmann W H (2001) The National Human Activity Pattern Survey (NHAPS): a resource for assessing exposure to environmental pollutants. Journal of Exposure Science & Environmental Epidemiology, 11(3), 231-252.

Kuipers B (1979). On representing commonsense knowledge. In Associative networks (pp. 393-408). Academic Press.

Raubal M, Winter S. (2002). Enriching wayfinding instructions with local landmarks. In International conference on geographic information science (pp. 243-259). Springer, Berlin, Heidelberg.

Ryder K J (2015). Designing and Publishing Indoor Maps for Patients and Visitors in an Academic Teaching Hospital (Doctoral dissertation, Royal College of Surgeons in Ireland).

Yang L, Worboys M (2011). A navigation ontology for outdoor-indoor space: (work-in-progress). In Proceedings of the 3rd ACM SIGSPATIAL international workshop on indoor spatial awareness (pp. 31-34).

Ontology-driven context-aware recommendation method for indoor navigation in large hospitals

Litao Zhu[1,2,3], Jie Shen[1,2,3,*], Georg Gartner[4]

[1] Key Laboratory of Virtual Geographic Environment (Nanjing Normal University), Ministry of Education, Nanjing 210023, China;
[2] Jiangsu Center for Collaborative Innovation in Geographical Information Resource Development and Application, Nanjing 210023, China;
[3] School of Geography Science, Nanjing Normal University, Nanjing 210023, China; 181301028@njnu.edu.cn (L.Z);
[4] Research Group Cartography, Technischen Universität Wien, 1040 Vienna, Austria; georg.gartner@tuwien.ac.at (G.G)
[*] Corresponding author: shenjie@njnu.edu.cn (J.S)

Abstract. Navigating in complex and dynamic indoor spaces of large hospitals is challenging. Since improving efficiency is a common goal for hospitals, there is an urgent need for an accurate and personalized service recommendation method in hospital navigation. To address this challenge, we propose a context-aware recommendation method for personalized hospital navigation. Firstly, an ontology-based contextual framework is designed for hospital navigation using Protégé Web Ontology Language (OWL)-2. Then rule-based contextual reasoning and information recommendation using Semantic Web Rule Language (SWRL) are proposed to overcome the limitations of ontology reasoning. Finally, some case queries are conducted using RDF Query Language (SPARQL) to evaluate the usability of the contextual ontology and rules.

Keywords. Context-aware, Ontology, Recommendation, Hospital navigation, SWRL rule, OWL

Hospitals contain rich contextual semantic information, including critical medical knowledge and facilities, complex spatial layouts, hospital-related processes, and intensive information exchange (Moon & Kim, 2013). The complex and dynamic environment of the hospital consists of staff, patients,

Published in "Proceedings of the 16th International Conference on Location Based Services (LBS 2021)", edited by Anahid Basiri, Georg Gartner and Haosheng Huang, LBS 2021, 24-25 November 2021, Glasgow, UK/online.

https://doi.org/10.34726/1747 | © Authors 2021. CC BY 4.0 License.

and devices that are constantly moving according to the changing healthcare tasks (Coyle, Neely, Nixon, & Quigley, 2006). Patients typically complete many tasks under time constraints and discomfort in large hospitals. Therefore, improving efficiency is a common need and goal for hospitals (Lakehal, Alti, Laborie, & Philippe, 2018). Much medical information and complex processes make location-based services recommendations challenging (Anagnostopoulos, Deriaz, Gaspoz, Konstantas, & Guessous, 2017). Compared to other indoor navigation (e.g., mall navigation, airport navigation), hospital navigation is unique which involves contextual information such as complex environments, user characteristics, medical processes, and medical knowledge. Specifically, different patients or groups (e.g., youth, elderly, newcomers, foreign visitors, immobility, people with various diseases) are heterogeneous. Therefore, they have different navigation needs and preferences (Ženka, Macháček, Michna, & Kořízek, 2021). Consequently, it is necessary to develop a context-based hospital navigation recommendation system to support user-centered services for personalized visits, rather than limited to traditional navigation from point A to point B.

Context-awareness plays a crucial role in the personalization and intelligence of navigation systems (Gartner, Huang, Millonig, Schmidt, & Ortag, 2011). Context-aware systems aim to improve computer-human interactions by using contextual information about the system, the user, and the environment (Lüddecke, Bergmann, & Schaefer, 2014). Previous studies develop various indoor applications based on context-awareness, such as indoor navigation (Afyouni, Ray, & Christophe, 2012; Huang & Gartner, 2009), location-related queries (Afyouni, Ilarri, Ray, & Claramunt, 2013), and recommended services (RSs) (Orciuoli & Parente, 2017). RSs have been an important research area of interest (del Carmen Rodríguez-Hernández & Ilarri, 2021). Intelligent RSs can generate personalized recommendations using contextual information describing the user's situation (e.g., individual, location, time, and tasks) (Adomavicius & Tuzhilin, 2011). Context-based recommendations can improve navigation efficiency and meet changing user needs (Villegas, Sánchez, Díaz-Cely, & Tamura, 2018).

Ontologies have attracted increasing interest as an essential means of modeling and reasoning about contextual information, especially in enhancing indoor semantic information to support indoor navigation, such as C-NGINE (Michou, Bikakis, Patkos, Antoniou, & Plexousakis, 2008), OntoNav (Anagnostopoulos, Tsetsos, & Kikiras, 2005), and CANE (Yao, Rolia, Basu, Singhal, & Kumar, 2012). Ontology-driven indoor navigation aims to provide semantic descriptions of certain events occurring in the indoor environment and support decision-making corresponding to recognized cases (Sriharee, 2015). However, there is limited research on intelligent hospital navigation services ontology for a personalized recommendation.

To address the above issues, this study proposes an ontology-driven context aware recommendation method to provide users personalized navigational information involving medical processes and knowledge. Firstly, a contextual ontology model is developed using Protégé Web Ontology Language (OWL)-2, consisting of user, time, location, indoor space, medical, process, and service. Then, a rule-based recommendation system is constructed using Semantic Web Rule Language (SWRL). Finally, the RDF Query Language (SPARQL) query service is utilized to evaluate the effectiveness of the recommendation method.

Acknowledgment

This research was funded by National Key R&D Program of China (2021YFE0112300), National Natural Science Foundation of China (NSFC) (No. 41871371), the Postgraduate Research and Practice Innovation Program of Jiangsu Province (No. KYCX21_1350), the State Scholarship Fund from the China Scholarship Council (CSC) (No. 201906860035).

References

Adomavicius G, Tuzhilin A (2011) Context-aware recommender systems. In Recommender systems handbook (pp. 217-253). Springer, Boston, MA. doi: 10.1007/978-0-387-85820-3_7

Afyouni I, Ilarri S, Ray C, Claramunt C (2013) Context-aware modelling of continuous location-dependent queries in indoor environments. Journal of Ambient Intelligence and Smart Environments, 5(1), 65-88. doi: 10.3233/AIS-120186

Afyouni I, Ray C, Christophe C (2012) Spatial models for context-aware indoor navigation systems: A survey. Journal of Spatial Information Science, 1(4), 85--123. doi: 10.5311/JOSIS.2012.4.73

Anagnostopoulos C, Tsetsos V, Kikiras P (2005) OntoNav: A semantic indoor navigation system. Paper presented at the 1st Workshop on Semantics in Mobile Environments (SME05), Ayia.

Anagnostopoulos G G, Deriaz M, Gaspoz J M, Konstantas D, Guessous I (2017) Navigational needs and requirements of hospital staff: Geneva University Hospitals case study. In 2017 International Conference on Indoor Positioning and Indoor Navigation (IPIN) (pp. 1-8). IEEE. doi: 10.1109/IPIN.2017.8115958

Coyle L, Neely S, Nixon P, Quigley A (2006, November) Sensor aggregation and integration in healthcare location based services. In 2006 Pervasive Health Conference and Workshops (pp. 1-4). IEEE. doi: 10.1109/PCTHEALTH.2006.361698

del Carmen Rodríguez-Hernández M, Ilarri S (2021) AI-based mobile context-aware recommender systems from an information management perspective: Progress and directions. Knowledge-Based Systems, 215, 106740. doi: 10.1016/j.knosys.2021.106740

Gartner, G., Huang, H., Millonig, A., Schmidt, M., & Ortag, F (2011) Human-centred mobile pedestrian navigation systems. Mitteilungen der Österreichischen Geographischen Gesellschaft, 153, 237-250.

Huang H, Gartner G (2009) A survey of mobile indoor navigation systems. In Cartography in Central and Eastern Europe (pp. 305-319). Springer, Berlin, Heidelberg. doi: 10.1007/978-3-642-03294-3_20

Lakehal A, Alti A, Laborie S, Philippe R (2018) Ontology-based context-aware recommendation approach for dynamic situations enrichment. In 2018 13th International Workshop on Semantic and Social Media Adaptation and Personalization (SMAP) (pp. 81-86). IEEE. doi: 10.1109/SMAP.2018.8501880

Lüddecke D, Bergmann N, Schaefer I (2014) Ontology-based modeling of context-aware systems. In International Conference on Model Driven Engineering Languages and Systems (pp. 484-500). Springer, Cham. doi: 10.1007/978-3-319-11653-2_30

Michou M, Bikakis A, Patkos T, Antoniou G, Plexousakis D (2008) A semantics-based user model for the support of personalized, context-aware navigational services. In 2008 First International Workshop on Ontologies in Interactive Systems (pp. 41-50). IEEE. doi: 10.1109/ONTORACT.2008.8

Moon J, Kim D (2013) Context-aware business process management for personalized healthcare services. In 2013 IEEE International Conference on Services Computing (pp. 757-758). IEEE. doi: 10.1109/SCC.2013.88

Orciuoli F, Parente M (2016) An ontology-driven context-aware recommender system for indoor shopping based on cellular automata. Journal of Ambient Intelligence and Humanized Computing, 8(6), 937–955. doi:10.1007/s12652-016-0411-2

Sriharee G (2015) A Symbolic-based Indoor Navigation System with Direction-based Navigation Instruction. Procedia Computer Science, 647-653. doi: 10.1016/j.procs.2015.05.065

Villegas N M, Sánchez C, Díaz-Cely J, Tamura G (2018) Characterizing context-aware recommender systems: A systematic literature review. Knowledge-Based Systems, 140, 173-200. doi: 10.1016/j.knosys.2017.11.003

Yao W, Rolia J, Basu S, Singhal S, Kumar A (2012) A Context-Aware framework for patient Navigation and Engagement (CANE). In 8th International Conference on Collaborative Computing: Networking, Applications and Worksharing (CollaborateCom) (pp. 316-325). IEEE. doi: 10.4108/icst.collaboratecom.2012.250454

Ženka J, Macháček J, Michna P, Kořízek P (2021) Navigational Needs and Preferences of Hospital Patients and Visitors: What Prospects for Smart Technologies?. International Journal of Environmental Research and Public Health, 18(3), 974. doi:10.3390/ijerph18030974

Bluetooth Distance Estimation for COVID-19 Contact Tracing

Guenther Retscher, Pajtim Zariqi, Ana Oliva Pinilla Pachon, José Pablo Ceballos Cantu, Sasanka Madawalagama

Department of Geodesy and Geoinformation, Engineering Geodesy,
TU Wien – Vienna University of Technology, Vienna, Austria

Abstract. Because of the covid-19 pandemic, Bluetooth is widely adopted for contact tracing Apps to keep and prove social distancing. If two persons are close at a short distance as defined for a period of usually at least 15 minutes, then the contact should be automatically detected using Bluetooth Low Energy (BLE) measurements on the mobile devices of the two persons. For that purpose, usually the signal strength of the Bluetooth signals, referred to as Received Signal Strength Indicator (RSSI), is measured and converted into a distance using path loss models. Logarithmic models are thereby commonly employed. In this study, the feasibility of the use of BLE for this type of application is investigated. A test field in an indoor environment has been defined and measurements taken with different smartphones serving either as signal broadcaster, the so-called advertisers, or as scanners recording the BLE signals from the advertisers. From the RSSI measurements, distances are estimated and aerial distributions in the form of interpolated radio maps (or heat maps) derived. Experiments were conducted in three scenarios where the smartphones were either placed unobstructed in free space on chairs, put into backpacks or handbags and into the trousers pockets of the users. The results indicate that a meaningful relationship between the RSSI values and models based on an approximation with a logarithmic path loss model can be derived in most cases especially at a very close range (> 1 m). This is very promising if we consider the contact tracing application. From the radio maps of the whole test area, it could be seen that the results of the distribution of RSSI in the main free space and backpack experiments were coherent to the distance from each selected advertiser. The results of the trousers pocket experiment, however, showed unexpected distributions due to the low granularity in the sampling points.

LBS 2021
16th Conference on Location Based Services
24-25 November 2021 Online

Published in "Proceedings of the 16th International Conference on Location Based Services (LBS 2021)", edited by Anahid Basiri, Georg Gartner and Haosheng Huang, LBS 2021, 24-25 November 2021, Glasgow, UK/online.

https://doi.org/10.34726/1748 | © Authors 2021. CC BY 4.0 License.

Keywords. Bluetooth Low Energy (BLE), Received Signal Strength Indicator (RSSI), Path Loss Model, Radio Map Interpolation

1. Introduction

Contact tracing for covid-19 is an important tool for reducing the number of infections (Apple and Google, 2020). Its goal is to reduce the number of infections by identifying the cases through contacts with infected people and provide early detection, guidance, and treatment (Bay et al., 2020; Leith et al., 2020; Nguyen et al., 2020). Using Bluetooth Low Energy (BLE) for estimating distance between users of mobile devices is a potential alternative which is evaluated in this study by measuring the Received Signal Strength Indicator (RSSI) in three different scenarios. We measured firstly in a free space, secondly in a scenario with the selected advertisers inside bags, and finally we measured the effect on RSSI caused by the human body by locating a cell phone in a trouser pocket. In this contribution the experiment design, statistics, distance estimations, leading to a derivation of radio maps (or heat maps) of RSSI distributions, are presented. A variety of smartphones serving either as so-called advertising mobile devices (short advertisers) broadcasting BLE signals or as scanning devices (i.e., the scanners) to scan for the RSSI of the advertisers were used in the tests. Distance estimation is supported by graphs that show each selected advertiser alongside the sampling points and the expected distance. Radio maps display the distribution of RSSI in each scenario per selected advertiser.

Thus, the main objectives of the study are:

- Understand better how Bluetooth signal interaction between different devices in order to asses better the effectiveness of using BLE technology as a contact tracing tool;
- Long-term Bluetooth observations in different scenarios, such as device is held in hand, in trousers pocket, backpack, handbag, etc.

2. Test Set-up and Design

The indoor experiments were designed to acquire data from different mobile devices at different scenarios: (1) unobstructed in free space (2) inside bags or backpacks and (3) inside trousers pockets. In order to get a good data range eight control points and 20 observation points are established in an open room as shown in Figure 1. After establishing the control points and observation points on the ground with chain surveying methods, identical plastic chairs were placed above each control point and

advertiser phones were placed on these chairs at the eight locations A to H. Figure 2 shows impressions from the set-up in the room.

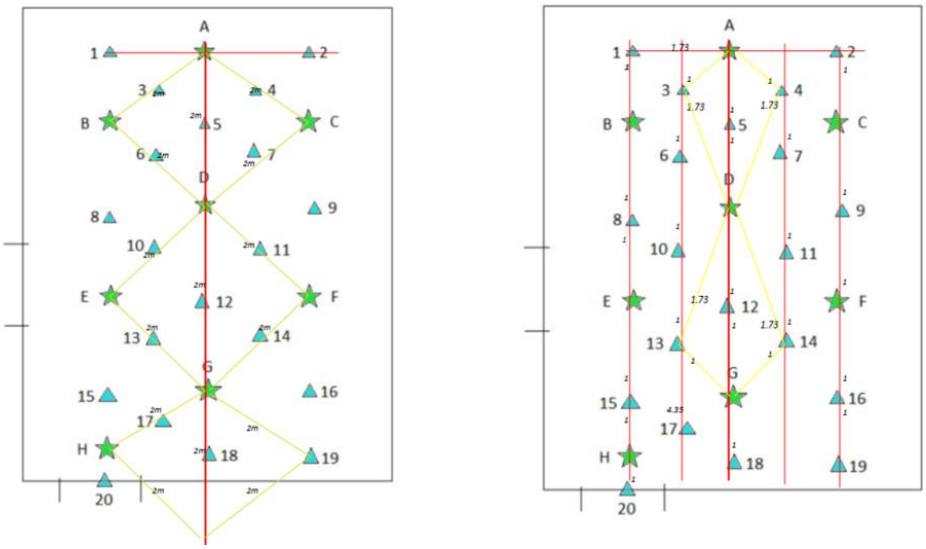

Figure 1. Layout of control points A to H and observation points 1 to 20.

Figure 2. Experimental set-up.

Eight different mobile devices were used in the test. Their specifications are summarized in Table 1. The Apple iPhone SE 2020 was used as the scanner

for all the experiments and the other phones were configured as advertisers. The open source nRF connect App developed by Nordic Semiconductor was used to collect the RSSI data (Nordic Semiconductor, 2020). nRF Connect for Mobile is a powerful generic tool that allows to scan and explore Bluetooth devices, communicate with them, and acquire data about the signal. RSSI data were recorded in CSV format and exported for post processing. Pre-processing of the observed RSSI data was done to remove outliers and calculate average RSSI for each observation points. This was done with a code written in Python using the Pandas package.

Location	Device	Bluetooth specification
A	iPad pro 2018	5.0, A2DP, LE, EDR
B	Samsung Galaxy S7	4.2, A2DP, LE, aptX
C	LG Nexus 5x	4.2, A2DP
D	Google Pixel 5	5.0, A2DP, LE, aptX HD
F	Sony Xperia Z3	4.0, A2DP, aptX
G	Samsung Galaxy S8	5.0, A2DP, LE, aptX
H	One Plus 7	5.0, A2DP, LE, aptX HD
moving scanner	iPhone SE 2020	4.2, A2DP, LE

Table 1. Specifications of the used mobile devices and their usual location on the control points A to H. A2DP stands for Advanced Audio Distribution Profile, LE for low energy, EDR for Enhanced Data Rate, aptX for audio processing technology and HD for high definition.

Bluetooth Low Energy (Bluetooth LE, colloquially BLE, formerly marketed as Bluetooth Smart) is a wireless personal area network technology designed and marketed by the Bluetooth Special Interest Group (Bluetooth SIG) aimed at novel applications in the healthcare, fitness, beacons, security, and home entertainment industries. The original specification was developed by Nokia in 2006 under the name Wibree, which was integrated into Bluetooth 4.0 in December 2009 as Bluetooth Low Energy. Bluetooth 2.0+EDR (Enhanced Data Rate) and Bluetooth 2.1+EDR are specifications for short-range wireless data exchange. Both Version 2.0 and 2.1 support EDR, a faster PSK (Phase Shift Key) modulation scheme capable of transmitting data 2 or 3 times faster than previous versions of Bluetooth. The audio processing technology aptX is a proven technology that compresses and then decompresses audio as it travels from a source device like a phone, to a receiving device like a wireless speaker, in a way that it

can be transmitted over Bluetooth without damaging the quality. This ensures that you get the very most from your audio.

3. Distance Estimation from BLE RSSI

Path loss models can be applied to convert the recorded RSSI to distances between the mobile devices. Usually a logarithmic path loss model for the relationship is employed. Such a model is a simple way to estimate distance with RSSI (Phunthawornwong, 2018). It can be expressed using the following equation:

$$d = 10^{\left(\frac{A-RSSI}{10\beta}\right)} \quad (1)$$

where d is the distance between the reference node and any nodes in [m], A is the RSSI at reference distance (1 m) and β is a propagation constant (in free space = 2).

A was determined as the average of all RSSI measurements taken at a 1 m distance and the propagation constant β was also set as 2 since the experiment was conducted at a free space between the phones.

After derivation of the estimated distance, a comparison with the true distance is performed and analysed how the model deviates from reality. The results were plotted for all phones and the resulting distance from equation (1) were compared with the true distance that the phones had from each other. The graphs in Figure 3 present these comparisons for the different mobile devices. Thereby the title letter corresponds to a specific phone and all sampling points are referenced on the scatter plot.

As part of the results, a logarithmic equation was estimated for each phone with an r^2 to indicate the correlation that each equation has to the ground truth data. The results are presented in Table 2. For the estimated equations the following applies: $x \rightarrow ||RSSI||$, $y(x) \rightarrow d(m)$.

As can be seen from Figure 3 some smartphones follow the logarithmic path loss model even at long distances. An example is the Samsung Galaxy S7 which has a very similar trend as the theoretical model and the data correlates somewhat fairly at -0.664. On the other side of the spectrum, there is the Sony Xperia Z3 phone whose RSSI values do not reflect at all the true distance of the phone and have a very low correlation coefficient at -0.055. Some phones clustered in the mid-regions such as the Samsung Galaxy S8 and the LG Nexus 5x which shows that some phones have

somewhat reliable RSSI at specific regions but deviate in other regions. Similar results for these smartphones were obtained by Retscher et al. (2021) in a similar test set-up. As for the estimated equations (see Table 2), it can be seen that the iPad pro 2018 and the Google Pixel 5 fit very well on the logarithmic model while the One Plus 7 and the Sony Xperia Z3 have a very poor fitting. Even though the One Plus 7 seems to show a somewhat similarity to the loss model. Lastly, something important is that all phones had a good RSSI estimation at a very close range (> 1 m) which is promising if we consider the contact tracing application. We can see that in all graphs with the exception of the Samsung Galaxy S8 (G) the model and the true distance match. This results have been achieved for smartphones unobstructed lying on the chairs in the testing room. In the following section, results are presented where smartphones are placed in backpacks, handbags and in trouser pockets.

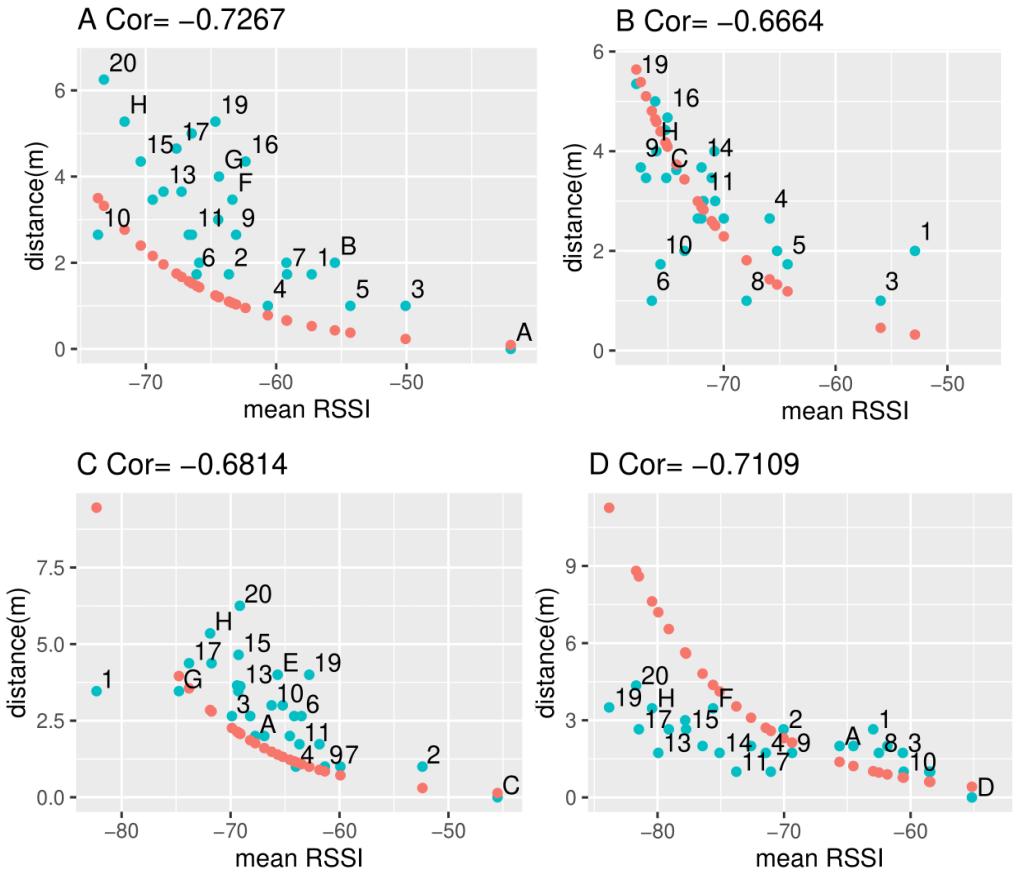

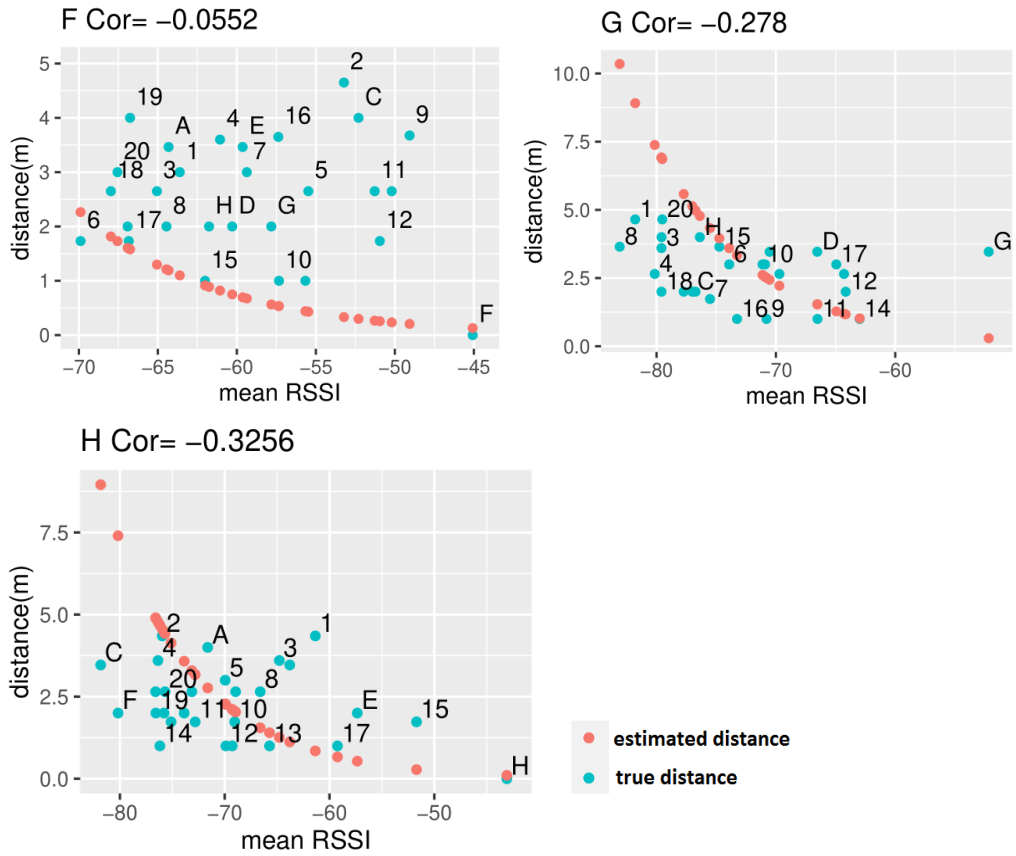

Figure 3. Distance comparison for each phone where the sampling points (blue) are plotted alongside the true distance (red) illustrating the deviation from the logarithmic path loss model.

Location	Smartphone	Equation	r^2
A	iPad pro 2018	-35.2 + 9.2 ln x	0.513
B	Samsung Galaxy S7	-23.6 + 6.26 ln x	0.397
C	LG Nexus 5x	-35.2 + 9.09 ln x	0.470
D	Google Pixel 5	-19.5 + 5.09 ln x	0.496
F	Sony Xperia Z3	-0.191 + 0.668 ln x	0.005
G	Samsung Galaxy S8	-7.87 + 2.5 ln x	0.048
H	One Plus 7	-19.5 + 5.09 ln x	0.121

Table 2. Logarithmic equation relationships and their respective correlation coefficients r^2.

4. Different Smartphone Placement Scenarios

Figure 4 shows comparisons of different scenarios where several phones were put into a backpack each or trousers pocket of the user. In these three plots the sampled points of each experiment are compared with each other to see how the change in condition affected the RSSI recorded. The difference in signals between the seven devices is obvious.

As can be seen clearly in the three plots in Figure 4, the placement of phones affects the RSSI significantly. For the observation points 5 and 12 the RSSI of the backpack is stronger than the one of the trousers pocket and for location 18 there is some similarity between the backpack and pocket scenarios but a similar trend can be inferred where the backpack scenario has stronger RSSI's.

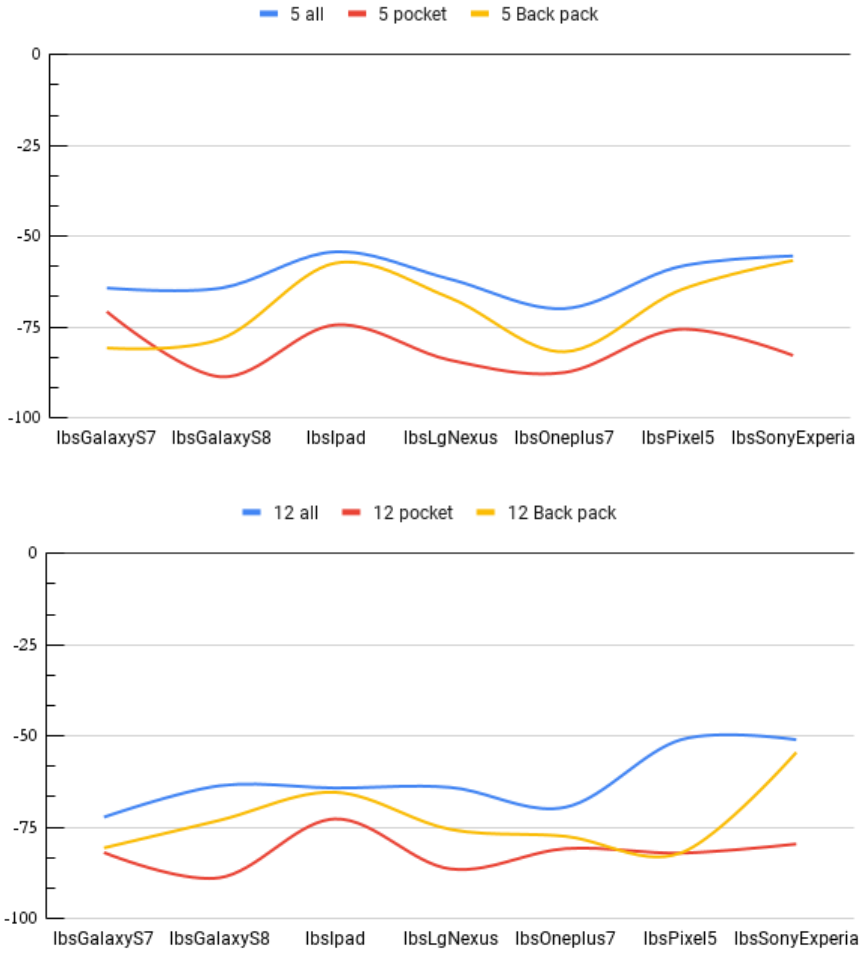

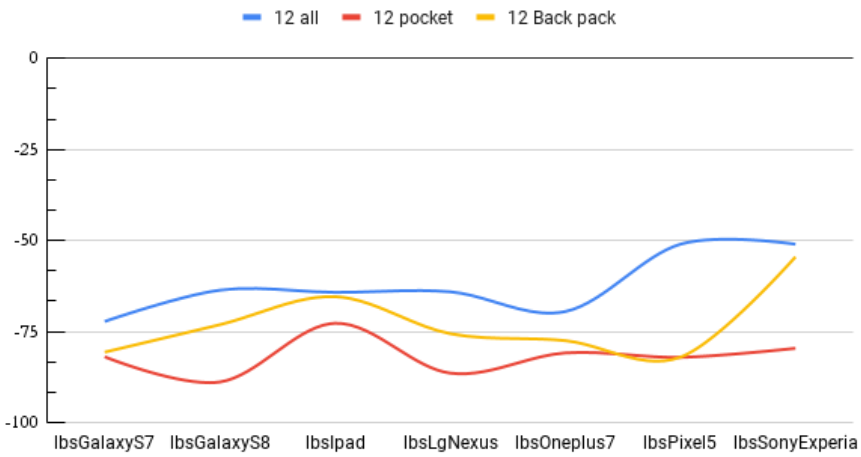

Figure 4. Different placement scenarios of smartphones on the observation points 5, 12 and 18 (see Figure 1 for their location in the test field).

5. Derivation of Radio Maps in the Test Field

Heat maps can be employed to show the distribution of the RSSI in the test field. In the case of RSSI distributions, these maps are usually referred to as radio maps. These maps were generated using the inverse distance weighted (IDW) interpolation method. This method determines the values of unknown points by assigning a weighted average of values from the known points depending on their distance from the unknown point (see Figure 5) (Qgis, n.d.). The known values closest to the unknown values have more influence, thus, a higher weight than the points farther away (Esri, n.d.).

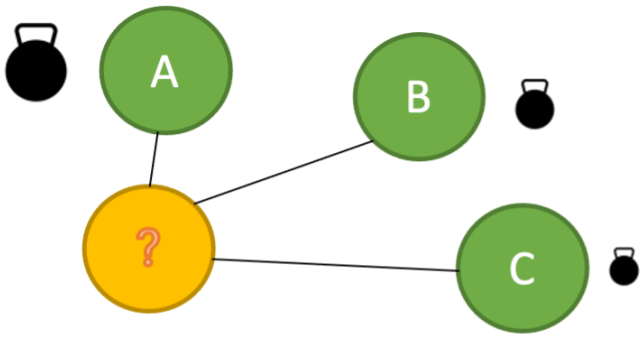

Figure 5. Illustration of the inverse distance weighted (IDW) interpolation method where the relative weights are assigned to each known point to determine the value of the unknown point.

Weights are proportional to the inversed distance raised to the power value p that in this case was 2 for all the maps. Figure 6 shows the variation in distance depending on the value of p. For p = 0, there are no changes in the distance so the values of the unknown points would be the mean of all the know values. The greater p is, the faster the weight assigned is decremented (see Figure 6) (Esri, n.d.). For this experiment, each known value represents the mean value of RSSI calculated for each advertiser position (A, B, C, D, F, G, and H).

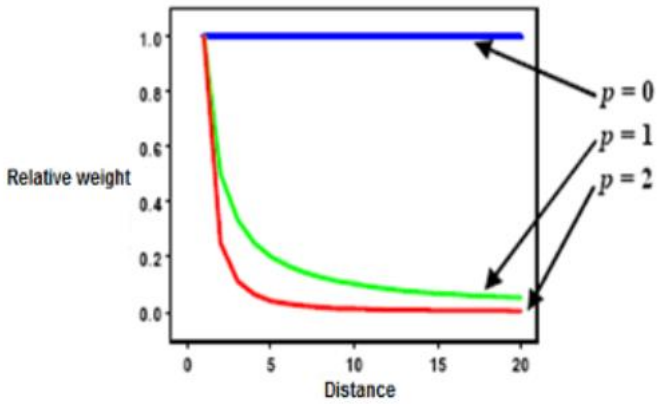

Figure 6. Decrease of weight with distance (https://pro.arcgis.com/en/pro-app/2.7/help/analysis/geostatistical-analyst/how-inverse-distance-weighted-interpolation-works.htm).

Figure 7 presents the radio maps for the main experiment where the smartphones were placed on the chairs. Figure 8 and 9 present examples of the radio maps for the scenarios where the smartphones were placed in backpacks or trousers pockets of the user sitting on the chairs, respectively. As can be seen from a cross-comparison between Figure 7 with Figures 8 and 9, the granularity of the RSSI values is higher than the represented for the experiments where the phones have been put in backpacks and trouser pockets. The RSSI for each selected advertiser in the main experiment (see green balloons with labels A, B, C, D, F, G, and H in Figure 7) is displayed by representing the mean RSSI from each point in the scenario (from 1 to 20 and from A to H). Figure 7 shows a clear distribution of the signal strength concerning the distance from the selected advertisers (see A, B, C, D, F, G, and H green balloons in Figure 7). However, there are some differences in the distribution of the RSSI. For instance, the RSSI for the selected advertiser C (Figure 7c) shows higher RSSI values in the whole scenario compared to the values of RSSI in Figures 7a and 7b. Since D is along the line in the middle of the test area between A to G (referred to as middle baseline; compare Figure 1), it is expected that the distribution of

RSSI to the right and left of it should be similar, however, the RSSI values on the left are higher than those on the right. For Figures 7e, 7f, and 7g, there is a clear distribution of the signal strength in respect to the distance from the selected advertiser.

Respect to the backpack and trouser pocket scenarios, the granularity is lower compared to the main experiment. For these two experiments (backpack and pocket), the measured points were only taken at stations 5, 12 and 18. Even though, most of the radio maps for these two experiments show a coherent distribution in respect to the distance from the selected advertiser, there are two unexpected results for the trousers pocket experiment. In both cases (see Figures 9a and 9c), the distribution is opposite to the expected. It could be cause to the low number of measured points for these two experiments.

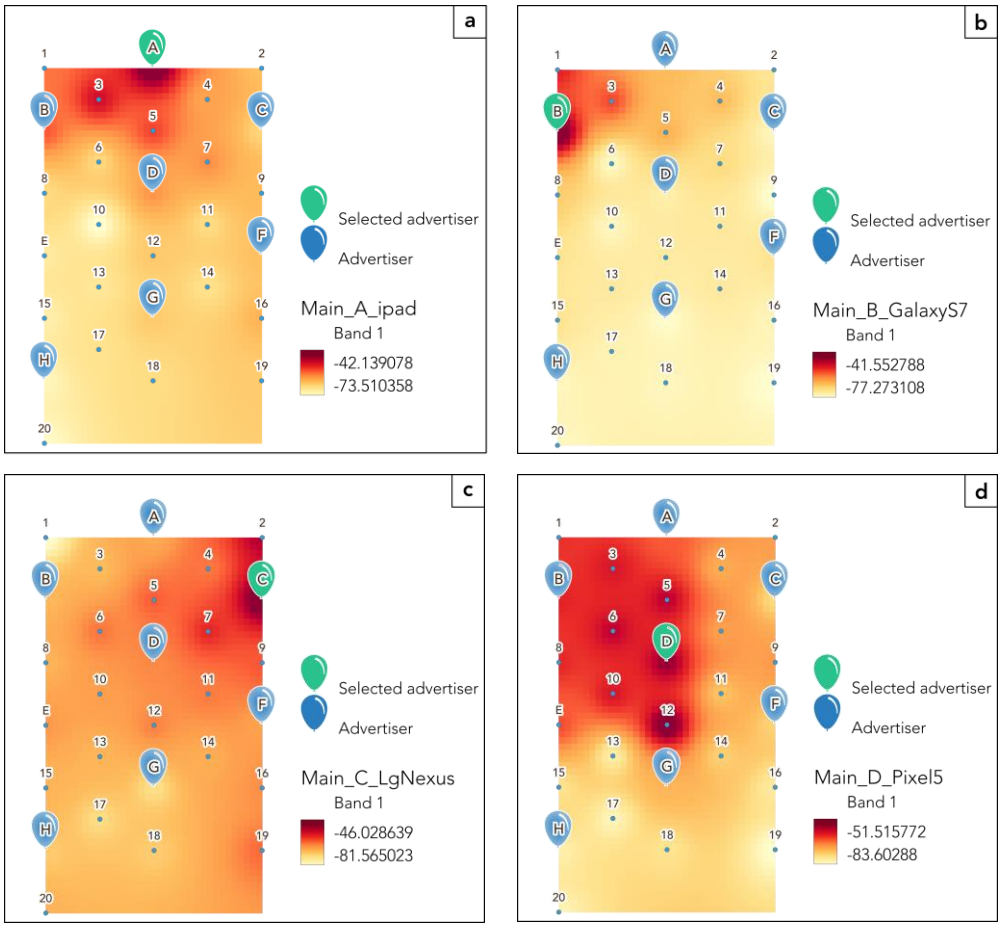

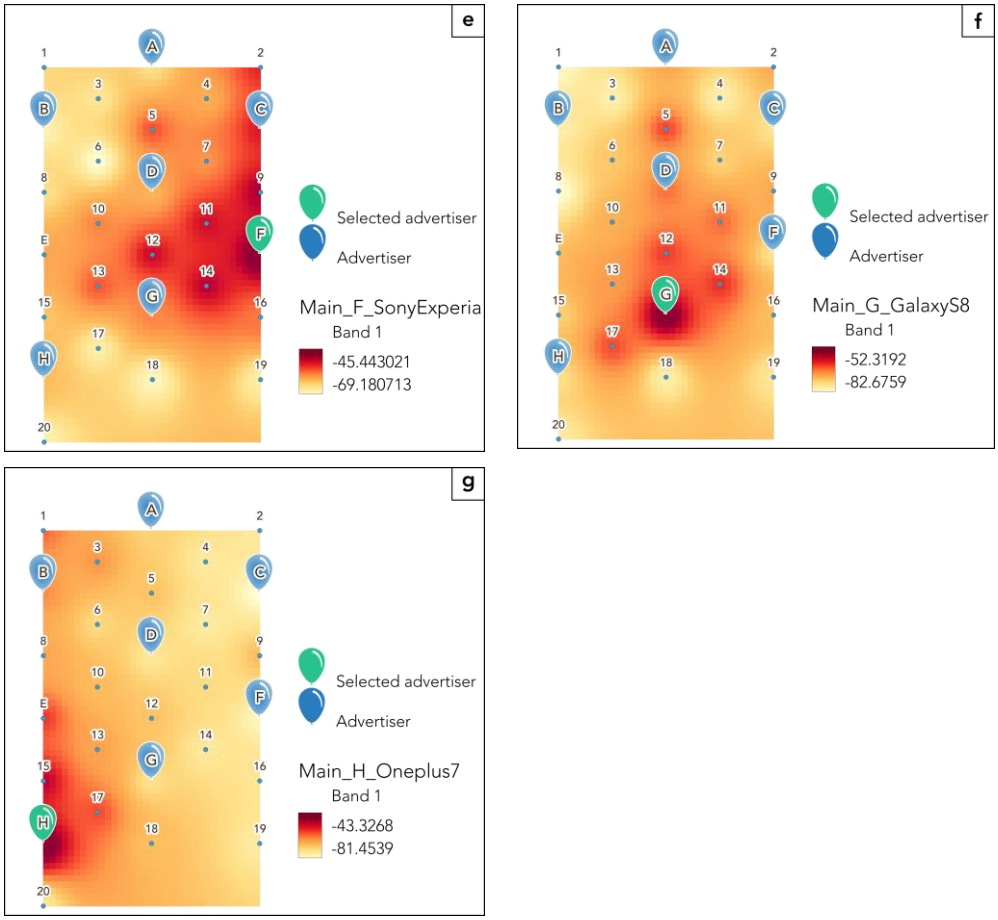

Figure 7. Radio maps of the RSSI distribution showing the results of the IDW interpolation method for the main experiments made for every point in the following positions: (a) point A, (b) point B, (c) point C, (d) point D, (e) point F, (f) point G, and (g) point H.

6. Conclusions

In this study, the usage of BLE RSSI measurements was investigated. From the experiments it can be concluded, that a relationship between the RSSI values and models based on an approximation with a logarithmic path loss model can be derived. In respect to the distance estimation from the measured RSSI values, some of the selected smartphones used in this study are following the predicted logarithmic model and some other phones deviate entirely. The trousers pocket scenario has the most impact on the obtained RSSI strength. If one looks at the radio maps derived from RSSI values in the whole test area, it can be seen that the results of the

distribution of RSSI in the main and backpack experiments were coherent to the distance from each selected advertiser. On the other hand, the results of the trousers pocket experiment showed unexpected distributions due to the low granularity in the sampling points.

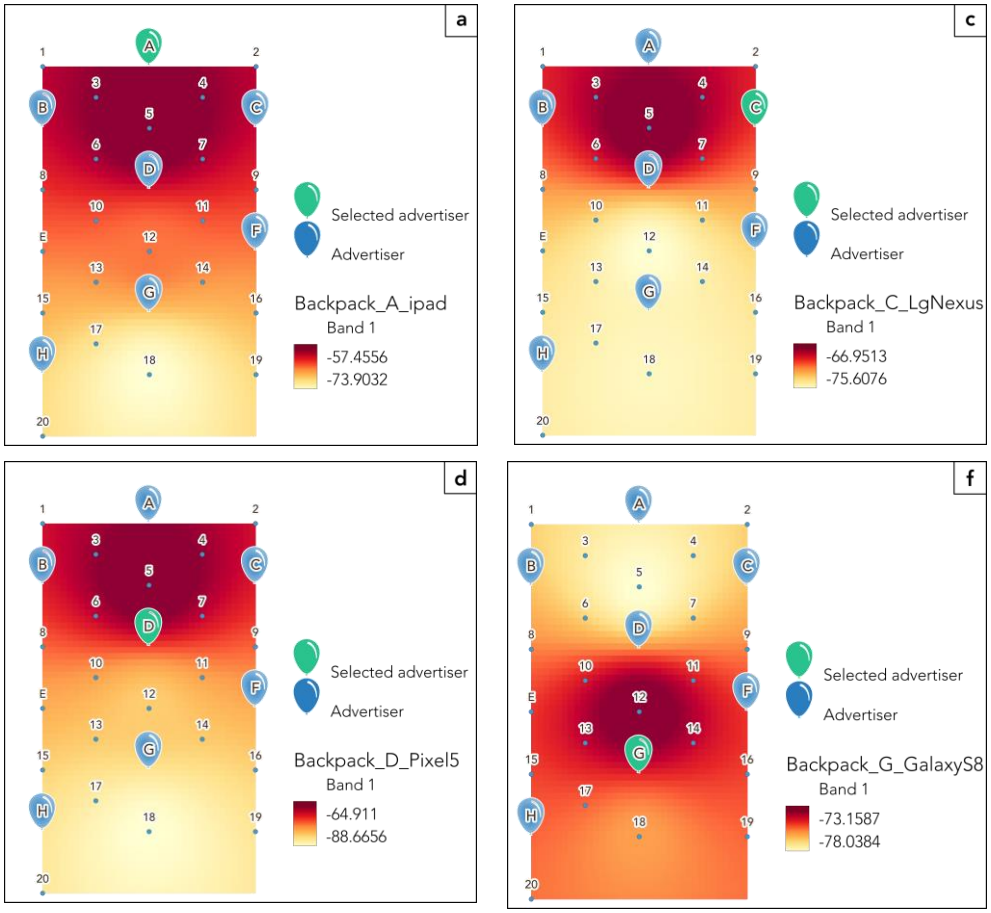

Figure 8. Selected radio maps of the RSSI distribution along the middle baseline ((a) point A; (d) point D and (f) point G) as well as point C (c) on the side for the experiments where the phones were in the backpacks.

References

Apple and Google (2020) Exposure Notification – Bluetooth Specification. Version 1.2, https://covid19.apple.com/contacttracing. Accessed 8 April 2020

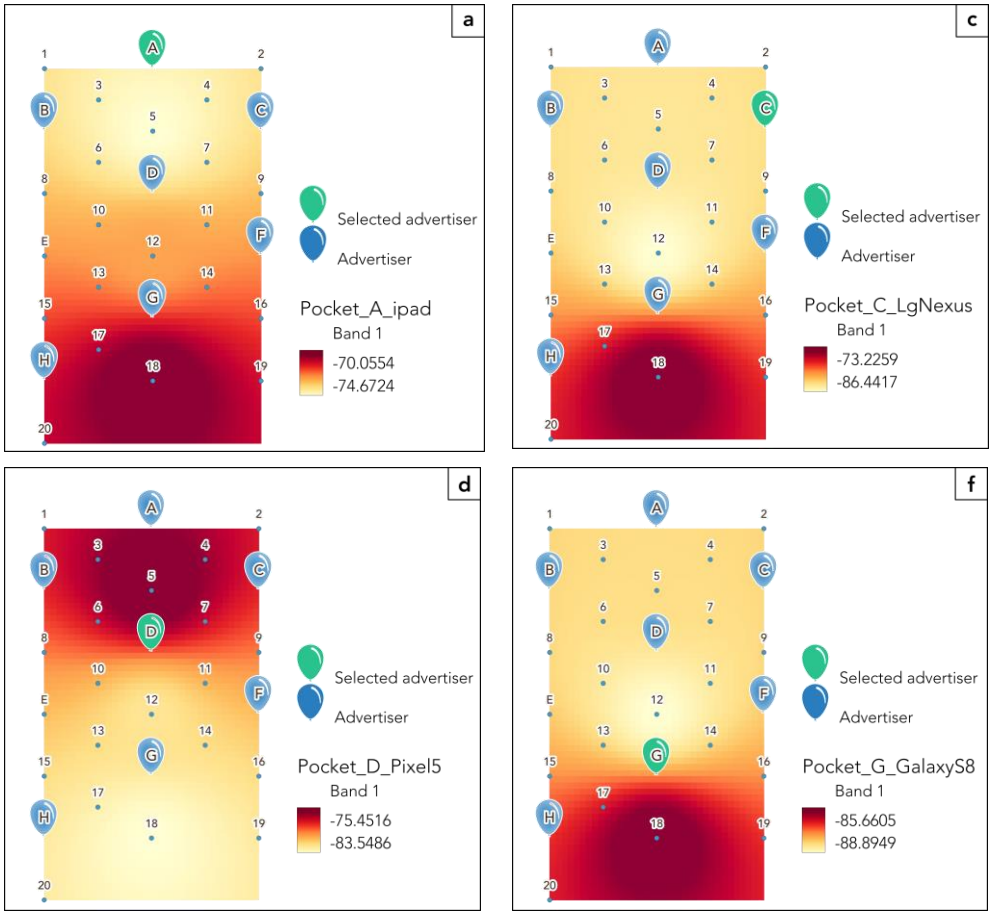

Figure 9. Selected radio maps of the RSSI distribution along the middle baseline ((a) point A; (d) point D and (f) point G) as well as point C (c) on the side for the experiments where the phones were in the trousers pocket.

Bay J, Kek, J, Tan A, Sheng Hau C, Yongquan L, Tan J, Anh Quy T (2020) BlueTrace: A Privacy-preserving Protocol for Community-driven Contact Tracing Across Borders. Government Technology Agency Singapore, Technical Report, 9 pgs

Esri (n.d.) How Inverse Distance Weighted Interpolation Works. https://pro.arcgis.com/en/pro-app/2.7/help/analysis/geostatistical-analyst/how-inverse-distance-weighted-interpolation-works.htm. Accessed 28 June 2021

Leith D J, Farrell S (2020) Coronavirus Contact Tracing: Evaluating The Potential Of Using Bluetooth Received Signal Strength For Proximity Detection. arXiv.org, eess, arXiv:2006.06822; 11 pgs

Nguyen K. A.; Luo Z.; Watkins C.; 2020. Epidemic Contact Tracing with Smartphone Sensors. Journal of Location Based Services, 14:2, 92-128, DOI: 10.1080/17489725.2020.1805521.

Nordic Semiconductor (2020) nRF Connect for Mobile. https://www.nordicsemi.com/Software-and-tools/Development-Tools/nRF-Connect-for-mobile. Accessed 8 April 2020

Phunthawornwong M, Pengwang E, Silapunt R (2018) Indoor Location Estimation of Wireless Devices Using the Log-Distance Path Loss Model. 2017 Proceedings of TENCON 2018 - 2018 IEEE Region 10 Conference

Qgis. (n.d.) Spatial Analysis (Interpolation). https://docs.qgis.org/2.18/en/docs/gentle_gis_introduction/spatial_analysis_interpolation.html. Accessed 28 June 2021

Retscher G, Zariqi P, Gartner G (2021) Analyses of Bluetooth Distance Measurements for Digital Contact Tracing. International Symposium on Geospatial Approaches to Combating Covid-19. Florence, Italy, 13-14 December, 2021 (accepted)

Positioning Performance Evaluation of a Dual Frequency Multi-GNSS Smartphone

Till Weigert, Guenther Retscher

Department of Geodesy and Geoinformation, Engineering Geodesy,
TU Wien – Vienna University of Technology, Vienna, Austria

Abstract. Smartphones with dual-frequency multi-constellation GNSS (Global Navigation Satellite Systems) receivers are now available on the market. This study examines their usage in simple surveying tasks, such as data acquisition for GIS, e.g. for a tree cadastre, lantern cadastre, traffic signs, etc., as well as line documentation, such as for underground power lines. For the experiments, the Pixel 5 from the manufacturer Google LLC is chosen. Code and phase observations are recorded in different scenarios. Evaluation in post-processing based on these observations in Single Positioning (SPP) and Precise Positioning (PPP) mode are carried out. In the analyses, the main focus is led on the achievable positioning accuracies and resulting deviations from reference points serving as ground truth. Apart from these parameters, other criteria, such as the measurement effort and costs, quality, accuracy and repeatability of the measurements are investigated. The results of the experiments indicate that the Pixel 5, although it enables the recording of satellite data on two frequency bands, can only be used to a limited extent in practical surveying tasks because it does not meet the accuracy requirements on the centimeter level. The main reason for this is the quite low quality of the observations. With long observation times, however, results with a positioning accuracy of less than half a meter are achievable with the smartphone. Thus, the Pixel 5 is capable to achieve the requirements in terms of positioning accuracy and reliability for applications such as data acquisition for Geographic Information Systems (GIS) and especially in Location-based Services (LBS).

Keywords. GNSS dual-frequency measurements, smartphone, positioning accuracies assessment, Single Point Positioning (SPP), Precise Point Positioning (PPP), static observations, stop-and-go and kinematic measurements.

LBS 2021
16th Conference on Location Based Services
24-25 November 2021 Online

Published in "Proceedings of the 16th International Conference on Location Based Services (LBS 2021)", edited by Anahid Basiri, Georg Gartner and Haosheng Huang, LBS 2021, 24-25 November 2021, Glasgow, UK/online.

https://doi.org/10.34726/1749 | © Authors 2021. CC BY 4.0 License.

1. Introduction

Due to recent developments in the last years in the smartphone market, some smartphone models are nowadays available providing multi-constellation GNSS with signals on two frequency bands (see e.g. Barbeau, 2018; Darugna, 2021). They are also capable to record the raw data of the GNSS signals, which facilitates high performance real-time and post-processing applications. Thus, using these new models more precise positioning with GNSS has become possible. In this study, it is analysed if simple tasks of applied surveying, GIS (Geographic Information System) data acquisition or in LBS can be performed with these smartphones. Their usage saves time and cost, since no additional hardware has to be purchased, such as PDAs or dedicated GIS receivers. One current smartphone is selected for the experiments. It is the Pixel 5 of the American manufacturer Google LLC, which has been available since October 2020.

For the experiments, measurements were carried out on the roof of the Electrical Engineering Institute (EI) building of the TU Wien (Vienna University of Technology) and in a park in front of the main building (i.e., Karlsplatz). In some of the tests the smartphone is placed on a coordinative known reference point, i.e., a measuring pillar on the building roof or at known points of the control network available on Karlsplatz. Furthermore, measurements at Karlsplatz were performed in stop-and-go and kinematic mode where a user with the smartphone held in his hand walked along a straight trajectory with usual walking speed. The main purpose of the experiments is the analysis of the achievable positioning accuracies. The stop-and-go and kinematic measurements are used to simulate real measurement tasks such as data acquisition for GIS, such as for a tree cadastre, lantern cadastre, traffic signs, etc., as well as line documentation, such as for underground power lines.

The paper is structured as follows: In section 2 the characteristics of the Google Pixel 5 smartphone and the basics of the chosen approach for the investigations are presented. Also the fundamentals of the positioning methods are reviewed. This is followed by comprehensive analyses of the observations carried out in the experiments in section 3. Here firstly the GNSS satellite availability and quality, then the results for static observations using the Single Point Positioning (SPP) and Precise Point Positioning (PPP) methods and the stop-and-go and kinematic measurements along the straight trajectory are presented in section 3.1 to 3.3, respectively. Section 4 summarizes the main findings and concludes the paper.

2. Basics and Approaches

2.1. Smartphone Basics

The Google Pixel 5 smartphone incorporates a Snapdragon 765G processor from Qualcomm which allows the recording of multi-GNSS signals on two frequencies (Qualcomm, 2019). Table 1 provides an overview of the supported satellite positioning systems and frequencies. As can be seen dual frequency operation is available for the US Navstar GPS, European Galileo and Japanese QZSS (Quasi-Zenith-Satellite-System) satellite based augmentation system. For data logging an App from Geo++ GmbH, Germany, was used. The App is based on the freely accessible source code of Google's GPS Measurement Tool. With this App, raw GNSS observations in RINEX (Receiver Independent Exchange Format) format from the smartphone can be recorded. Figure 1 shows a snapshot of the interface of the GNSS logger. The RINEX Logger can record signals of all GNSS listed in Table 1. Apart from QZSS, other augmentation systems such as the European Satellite Based Augmentation System (SBAS) called EGNOS (European Geostationary Overlay System) are not supported.

GPS	L1 / L5
Glonass	R1
Galileo	E1 / E5a
Beidou	B1
QZSS	L1 / L5

Table 1. : Supported GNSS and their useable frequency bands for the Google Pixel 5.

The measurements took place on the roof of the building of the TU Wien in the Gußhausstraße campus and on the nearby Karlsplatz. Eleven measuring pillars are located on the roof, the coordinates of which are known. On Karlsplatz there is a control point network.

In addition, a geodetic GNSS receiver from Spectra Geospatial, the SP80, is used as a reference station and placed in 12 meter distance from the smartphone on a second measuring pillar on the roof of the EI building. Figure 2 shows the set-up on the roof in the three pictures on the left. The SP80 receiver is capable to record GPS (L1, L2, L5) and GLONASS (R1, R2) data. In order to be able to use them, they are then converted to the RINEX format. The RINEX Converter 4.7.2 from Trimble is used for this conversion. Further data, such as the satellite ephemeris (RINEX navigation file) and clock corrections, are acquired from the CORS network

EPOSA (see EPOSA, 2021) and the IGS (International GNSS Service). Post-processing of the raw data is carried out with the freely available Real Time Kinematic Library (RTKLib) software package. Furthermore Matlab routines are used to eliminate outliers, to calculate statistical parameters and transformations between different reference systems, such as from the WGS84 (World Geodetic System 1984) of GPS and the ETRS89 (European Terrestrial Reference System 1984).

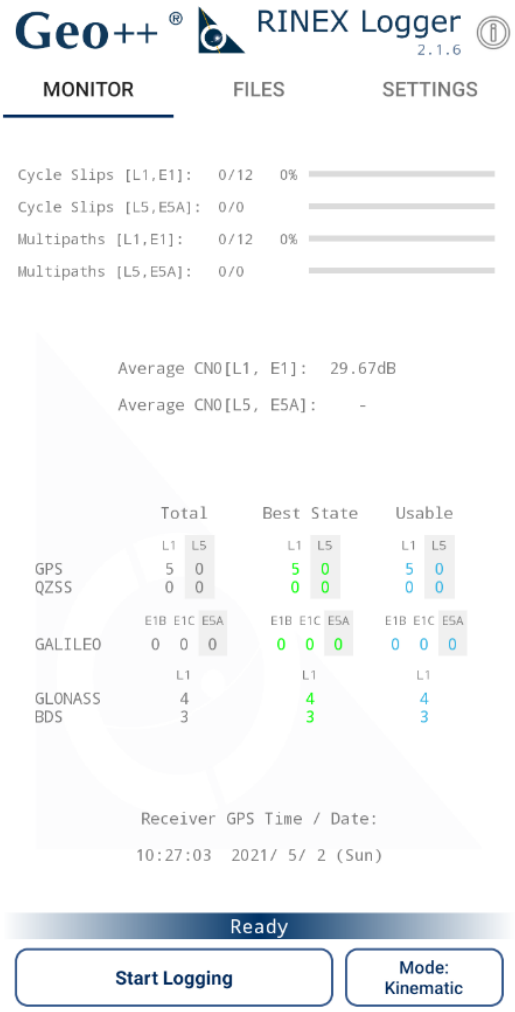

Figure 1. Interface of the Geo++ RINEX logger.

RTKLib includes positioning algorithms for all common GNSS systems. In addition to the evaluation of the data in post-processing, the software can be used for positioning in real-time. In the course of this work, however, only the post-processing applications are used. The software package contains several subroutines. In this work, we use the applications RTKPlot

and RTKPost. With RTKPlot, observations, navigation data and the solutions calculated with RTKPost can be visualized. In RTKPost the actual processing of the data takes place. The software includes different positioning methods. The methods Single Point Positioning (SPP), Precise Point Positioning (PPP)and the method static are used to calculate baselines.

Figure 2. Smartphone und reference receiver SP80 on two neighbouring measuring pillars on the roof of the EI building of TU Wien and mobile measuring set-up on Karlsplatz.

2.2. Single Point Positioning (SPP)

Positioning with the help of SPP is an absolute position determination method. The position is determined by code observation; for civil users with PRN (Pseudo-random Noise) code C/A (Coarse Acquisition). The satellites permanently transmit their position in the form of their orbit data and the current time. These signals are modulated on a specified carrier frequency with an individual PRN code for each satellite and transmitted via it. This allows them to be received and demodulated by a receiver on Earth (Reußner, 2016). Since the speed at which the signal travels there is a time difference between the actual time at the time when the signal is received and the time sent by the satellite. This difference is the signal travel time. Since the receiver clock is not synchronized with the satellite clock in practice and is usually not accurate enough, we speak of the pseudorange observation for the time being. From this the pseudorange or distance to the satellite can be calculated by multiplying it with the signal speed (approximately the speed of light). Three Cartesian coordinates (X, Y, Z) are required to define a position in three-dimensional space. Consequently, three observations or three satellite signals should suffice to identify these three unknowns. When positioning with GNSS, however, there is a fourth unknown: the receiver clock error. This is the difference between the receiver clock and the satellite clocks already mentioned. The measured signal travel times must be corrected for this error. In order to determine the clock error, a fourth observation is necessary. Thus, the signals of at least four satellites are needed to determine the four unknowns (3 position

coordinates and receiver clock error). Mathematically speaking, a system of equations with four equations and four unknowns is solved (Reußner, 2016). Geometrically, the position determination can be described as follows: The distance of the receiver to the satellites can be calculated from the signal travel times. The position of the satellites is known via the orbit data of the satellites. This allows spheres to be placed with the distance as a radius around three of the satellites. The point at which the surfaces of the three spheres intersect corresponds to the position of the receiver. The accuracy of single point positioning is in the range of several meters.

2.3. Atmospheric Error Sources

In addition to satellite and receiver-specific errors such as orbit, hardware or clock errors, the atmosphere has a major influence on the accuracy of the determined positions (Reußner, 2016). To reach the receiver, the signals must pass through the atmosphere. This affects the propagation speed of the signals and thus their travel time. The signals are slowed down and no longer propagate at the speed of light. This atmospheric refraction is dependent on time and place. If the precise signal speed is not known, the distances to the satellites can only be determined very inaccurately. Consequently, the identified position of the recipient differs from the actual position. The effects of atmospheric refraction can be divided into the neutral atmosphere (tropospheric parts) and ionospheric parts.

The neutral atmosphere ranges up to an altitude of 90 km which are the ranges from the troposphere to the stratosphere to the mesosphere. The influence of the neutral atmosphere on the travel time depends on the meteorological conditions along the signal pathway and can be divided into hydrostatic (dry) and wet (or humid) fractions. Hydrostatic fractions account for 90% and wet fractions 10% of the tropospheric travel time delay. The hydrostatic components can be easily modelled on the Earth's surface using meteorological measurements (pressure and temperature) or through the use of standard atmospheric models and can therefore be modelled quite easily. For the wet fraction, the moisture content is largely determined by the water vapour content of the atmosphere along the signal path. This is subject to temporal and spatial fluctuations and is difficult to model (Reußner, 2016).

The neutral atmosphere is followed by the ionosphere. It passes into interplanetary space at an altitude of about 2000 km. The ionosphere contains the thermo- and exosphere. It contains large amounts of ions and free electrons, which significantly influence the delay of electromagnetic waves. The strength of this influence depends on the density of the free electrons along the signal path. To characterise this usually the parameter Total Electron Content (TEC) is used. Density, in turn, is influenced by the intensity of solar radiation and the geographic latitude and is subject to

cyclical fluctuations. For example, the number of free electrons is ten times higher during the day than at night. The ionosphere is a dispersive medium for electromagnetic waves. This means that the propagation velocity depends on the frequency. This effect can be exploited to model the influence of ionospheric travel time delay. If the influence of the ionosphere is not eliminated, deviations in the order of several meters up to tens of meters for the measured pseudorange would occur. Although the satellites transmit several parameters modelling the state of the ionosphere, this non-negligible residual deviation remains. Dual-frequency observations can help in this respect as the ionosphere is dispersive. This means that the two frequencies travel with different propagation speed. Using the two frequencies recorded by the receiver linear combinations can be determined to reduce the effect of the ionospheric propagation travel time delays.

A further error influence is the multipath of the GNSS siganls. Through reflections on buildings, reflecting surfaces or other objects, a signal reaches the receiver in different ways. The direct signal is superimposed by the reflected signals which can cause interference. The received signals are time-delayed because the reflected portion has travelled a longer distance. Normally, the amplitudes of the reflected signals are lower than those of the direct signal. As the satellites move, the multipath effects also change over time (Reußner, 2016).

The dual-frequency observations with the newest smartphones can therefore help to reduce or model these error sources leading to higher positioning accuracies with higher reliability. The following section describes two positioning methods, i.e., PPP and DGNSS, and how they help reducing errors caused by the atmosphere and by multipath effects can be reduced, i.e. PPP and DGNSS.

2.4. Precise Point Positioning (PPP)

PPP is a method for reducing atmospheric error influences and for more accurate positioning. As with SPP, this is an absolute positioning method. In contrast to SPP, however, this is much more accurate, since the position determination is based on phase measurements of the carrier frequencies, e.g. from GPS L1 and L5 observations of the smartpohone. The code observations serve only to determine an approximate solution, which is necessary, since the phase measurement is ambiguous in contrast to the code measurement. The phase ambiguity is an unknown integer, which describes the number of whole wave cycles between the satellite and the receiver before phase synchronization is achieved in the receiver. If the carrier phase is detected, it is followed up until a signal interruption or phase jump, i.e., a so-called cycle slip, occurs. After each cycle slip the ambiguity must be solved anew. The solution requires a certain convergence period, during which there must be no signal interruption. It is

therefore of crucial importance that the observations are as uninterrupted as possible (Heßelbarth, 2011; Reußner, 2016).

With PPP, accuracy in the centimetre range can be achieved. The broadcast ephemeris are not sufficient for this purpose. More precise satellite orbit data and satellite clock corrections are needed. These are provided by the International GNSS Service (IGS) on different accuracy levels, i.e, rapid and ultra-rapid orbits for real-time applications and final orbits for post-processing (Reußner, 2016). Thus, in this work the final orbits from IGS are used for the calculation of the PPP solutions.

As described above, the ionosphere is responsible for most of the atmospheric error influences. In order to reduce this influence, the properties of the medium can be exploited, since the propagation velocity of electromagnetic waves in the ionosphere is frequency-dependent. As aforementioned, GNSS systems transmit their signals via more than one carrier frequency. Table 2 shows the carrier frequencies of the four systems studied in this paper. At least two carrier phases are observed during Precise Point Positioning. The difference in time between the two signals allows conclusions to be drawn about the electron content of the atmosphere and the measurements can be corrected (Reußner, 2016).

GPS		GLONASS		GALILEO		BEIDOU	
L1	*1575.42 MHz*	R1	*1598 - 1605 MHz*	E1	*1575.42 MHz*	B1	*1561.10 MHz*
L2	*1227.60 MHz*	R2	*1243 - 1249 MHz*	E5a	*1176.45 MHz*	B2	*1207.14 MHz*
L5	*1176.45 MHz*	R3	*1202.025 MHz*	E5b	*1207.14 MHz*	B3	*1268.52 MHz*
				E6	*1278.75 MHz*		

Table 2. Overview of the carrier frequencies of the used GNSS.

2.5. Differential GNSS (DGNSS)

Another method for increasing accuracy is DGNSS. As with PPP, the position determination is based on both phase and code observations. Unlike SPP and PPP, this is a relative method, since the position is determined in relation to a reference station with known coordinates. This procedure therefore requires at least two GNSS receivers. One is operated as a rover, the other as a base (reference) station. While the base receiver is stationary, the rover is a mobile GNSS receiver. The position of the rover is unknown and needs to be determined. As described in section 2.3, a travel time delay occurs along the signal path due to atmospheric conditions. If rover and base station are close to each other, the atmospheric influences can be assumed to be similar for both receivers. Measurements shall be carried out with both receivers, which shall cover the same measurement period. In addition to the already known coordinates of the base, one obtains a position determined by GNSS for the rover. From the difference between the measured position and the known coordinates of the base

station, conclusions can be drawn about the properties of the atmosphere and correction data can be determined. These correction data can be applied to the measured values of the rover. Thus, accuracy is increased. Since the atmospheric influences are local, this method becomes less precise as the two receptors are further apart. The line or vector between rover and base is called baseline or base vector, respectively (Heßelbarth, 2011; Reußner, 2016).

The correction of the measurement signals can be done either in post-processing or in real-time (so-called Real-Time Kinematic, RTK) during the measurement. In RTK, the correction data must be transmitted to the rover in real-time via a data link. This is usually done via the existing mobile network. In practice, it is often not necessary to set up an own reference station, since it is often possible to use an existing reference station network, so-called Continuously Operating Reference Station (CORS) networks. In Austria, such a network is operated by Energie Burgenland AG, ÖBB Infrastruktur AG and Wiener Netze GmbH. The station network, called EPOSA (Echtzeit Positionierung Austria), consists of 40 reference stations, which are distributed throughout Austria. The service provides both real-time data and RINEX data for post-processing. With the Austrian Positioning Service (APOS), the Federal Office of Surveying and Mapping (BEV) is providing another service with a similar function and its own reference stations. EPOSA is used in this work (EPOSA, 2021).

If there is no reference station at an acceptable distance near the measuring area, it is possible to calculate a Virtual Reference Station (VRS) by interpolation from the surrounding reference stations (EPOSA, 2021).

Results of DGNSS solutions for the conducted long-term observations with the Google Pixel 5 are not presented here in the following. They can be found in Retscher and Weigert (2021). Here the focus is led more on measurements with shorter observation periods of several minutes and down to seconds in gthe case of observations in the stop-and-go and kinematic mode.

2.6. Coordinate Systems and Transformations

To determine the satellite-ephemeris, a globally uniform reference system is needed. This is provided by the WGS84 in the case of GPS, which is based on the International Terrestrial Reference System (ITRS). If a position is determined using GNSS, coordinates are obtained in WGS84, since the determined position refers to the position of the satellites. In many cases, it is necessary to transform the coordinates into a regional system. The European Terrestrial Reference System 1989 (ETRS89) is used in large parts of Europe because it represents a uniform and stable system for the Eurasian Plate. The ETRS89 was aligned with the ITRS in 1989. Since then, due to the continental drift, the Eurasian Plate has moved about 2.5 cm to

the Northeast every year. The current positional deviation of the two systems is in the order of a few decimeters. The actual value is position dependent due to the additional rotation of the Eurasian plate. The ETRS89 is realized in Austria by the Austrian Positioning Service (APOS) (Höggerl et al, 2007; Killet, 2010).

3. Analyses of Static and Kinematic Observations

For the analyses, static long-term observations were carried out first (Retscher and Weigert, 2021). In these measurements, the smartphone was mounted on a measuring pillar with a holder in a tripod (see Figure 2 on the left). Moreover, measurements with static short observation periods of around 20 minutes were carried out. These measurement campaigns were followed by several tests along different trajectories which were observed either in stop-and-go or kinematic mode. In the following, the satellite availability and quality is briefly reviewed and then the main findings of the static long- and short-term observations and a detailed analysis of the kinematic observations are presented.

3.1. Satellite Availability and Quality of the Static Long-term Observations

The Google Pixel 5 was able to observe GNSS signals from a total of 56 satellites over the whole observation period of 150 minutes in the static long-term observations. Of these, however, only 21 satellites were recorded on both frequency bands L1 and L5. Thereby the number of satellites observed was highest for GPS, but only about half could be observed on two frequencies. This is expected as only half of all available GNSS satellites in space broadcast L5 signals at the time of the experiments. In contrast, the number of Galileo satellites was smaller, but almost all satellites were able to receive both frequencies. Figures 3 and 4 show the satellite constellation of the GPS and Galileo satellites for the GPS frequency bands L1 (left) and L5 (right) and the Galileo E1 (left) and E5a (right), respectively, in the form of skyplots. In these plots the satellite motion, signal strength and the number of signal interruptions can be seen clearly. The signal strength is described on the basis of a colour scale, signal interruptions caused by cycle slips are marked by a red bar. Eight GPS satellites could be observed on only one frequency (see Figure 3). Many of these satellites are located more in the West. It is obvious that some of the satellites, from which only the L1 band could be observed, have a higher signal strength. The high number of cycle slips in the Pixel 5 observations is clearly visible. From the skyplots of the Galileo satellites in the frequency Galileo bands E1 and E5a presented in Figure 4 can be seen that all satellites could be observed on two frequency bands. Similar as for the GPS observations, cycle slips occur more

frequently in the E5a band than in the E1 band. Overall, the signal quality of the Pixel 5 receiver is significantly lower compared to a professional geodetic GNSS receiver. The signals are considerably weaker and there are more frequent signal outages. In Retscher and Weigert (2021) the observations of the Pixel 5 with the nearby geodetic reference receiver SP80 placed on a second measuring pillar in a distance of only 12 m on the roof of the EI building (see Figure 2) are compared. With the SP80, signal outages occur only at a very low elevation. While the signal strength of the reference receiver is highest at the zenith, the Pixel 5 still shows signal interruptions. Only in the West were relatively continuous signals with an SNR (Signal to Noise Ratio) of more than 45 dBHz.

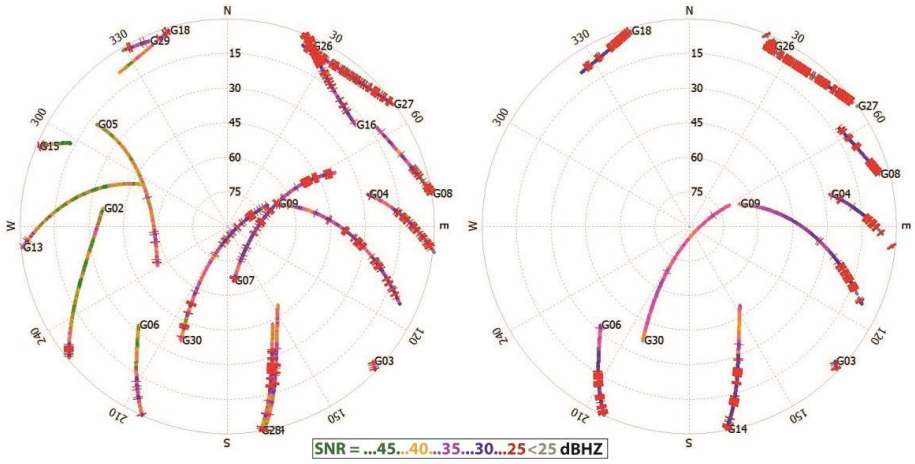

Figure 3. Skyplots showing the tracked GPS satellites of the Google Pixel 5 on L1 (left) and L5 (right) with coloured visualisation of the Signal to Noise Ration (SNR).

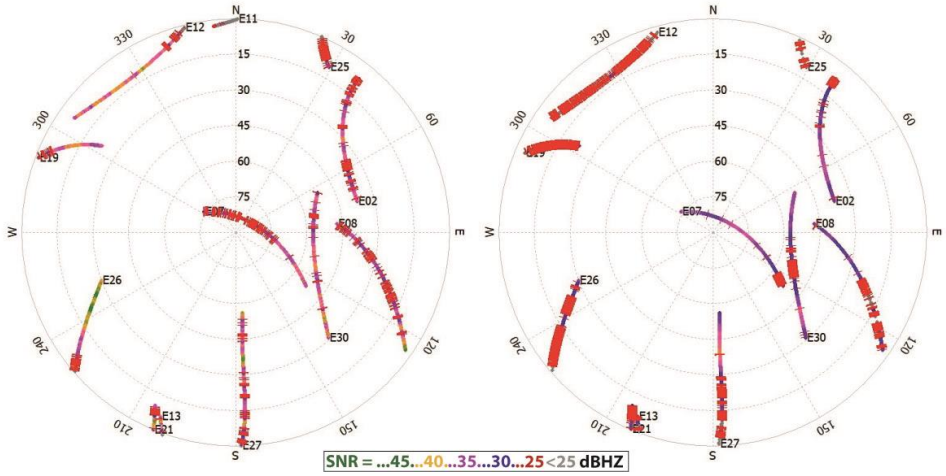

Figure 4. Skyplots showing the tracked Galileo satellites of the Google Pixel 5 on E1 (left) and E5a (right) with coloured visualisation of the Signal to Noise Ration (SNR).

3.2. Results of Short Static Observation Periods

Further measurements were carried out at Karlsplatz where a control point network including several reference points is available. These measurements represent typical real world measurement scenarios, such as GIS data acquisition, such as tree cadastre, lantern cadastre, etc. The Pixel 5 is mounted on a tripod and placed on known points (see Figure 2 on the right). Three surveys are carried out, each with 20 minutes of observation time. Different obstructions of the satellite signals are prevailing on the three chosen reference points N07, N08 and N09 of the control point network. While the points N09 and N08 are relatively in open space, N07 is located between several broad-leaved trees. Since the measurements have been carried out in winter, the trees do not bear any foliage. In the following, the calculated SPP and PPP solutions are presented and analysed.

3.2.1 SPP Solutions

For the three reference points N07, N08 and N09, SPP solutions for the individual systems and a multi-GNSS solution are calculated. In the multi-GNSS solution, the individual systems are combined with Matlab. This is done for the entire observation period of 20 minutes. Table 3 shows the solutions for position N07, Table 4 for N08 and Table 4 for N09.

SPP	20 Min	17.12.2020 11:10 - 11:30		N07							
	n	Std E	Std N	Std U	Std 2D	Std 3D	Dev E	Dev N	Dev U	Dev 2D	Dev 3D
GPS	539	17.235	32.911	48.135	37.151	60.804	4.450	18.117	-16.983	18.655	25.228
GLONASS	369	40.812	53.238	46.900	67.082	81.851	-0.957	16.274	-30.079	16.302	34.212
GALILEO	534	10.999	12.478	28.7971	16.634	33.256	-2.992	-3.392	-10.669	4.523	11.588
BEIDOU	480	12.002	8.954	31.268	14.974	34.668	5.832	-0.032	9.885	5.832	11.477
Multi GNSS	1922	16.862	21.407	38.651	27.250	47.292	1.337	4.161	-9.739	4.371	10.675

Table 3. Comparison of the SPP solutions over a 20-minute observation period for the reference point N07.

SPP	20 Min	17.12.2020 10:46 - 11:06		N08							
	n	Std E	Std N	Std U	Std 2D	Std 3D	Dev E	Dev N	Dev U	Dev 2D	Dev 3D
GPS	270	9.248	23.738	28.934	25.476	38.551	-0.217	0.288	-21.455	0.361	21.458
GLONASS	837	11.863	18.469	20.655	21.951	30.141	-9.349	4.618	-16.314	10.427	19.362
GALILEO	915	2.909	6.661	10.3231	7.268	12.625	-0.474	0.263	-11.376	0.542	11.389
BEIDOU	554	8.535	2.329	16.608	8.847	18.818	2.353	6.511	9.703	6.924	11.919
Multi GNSS	2576	7.427	9.129	17.754	11.768	21.300	-2.108	2.709	-9.441	3.433	10.045

Table 4. Comparison of the SPP solutions over a 20-minute observation period for the reference point N08.

SPP	20 Min	17.12.2020 10:20 - 10:40		N09							
	n	Std E	Std N	Std U	Std 2D	Std 3D	Dev E	Dev N	Dev U	Dev 2D	Dev 3D
GPS	393	10.129	11.289	12.889	15.167	19.904	-3.714	3.512	-12.201	5.112	13.229
GLONASS	640	16.821	17.708	39.453	24.424	46.401	-6.824	4.670	-14.565	8.268	16.748
GALILEO	276	12.318	38.452	31.6746	40.376	51.318	-7.085	-19.078	-45.453	20.351	49.801
BEIDOU	342	5.165	7.840	17.423	9.389	19.792	2.185	-8.563	-37.729	8.837	38.750
Multi GNSS	1651	11.915	14.093	26.506	18.455	32.297	-3.977	-0.830	-24.258	4.063	24.596

Table 5. Comparison of the SPP solutions over a 20-minute observation period for the reference point N09.

The number of calculated positions *n* varies greatly depending on the system used. The location also influences the measurement result. For reference point N07 the highest number of solutions (539) can be determined using GPS compared to the other points. For point N08, on the other hand, the lowest number (270) is determined with GPS. The number of solutions of the other systems also varies significantly depending on the point of view. Beidou delivers the most constant number of solutions. This varies only by 212 solutions between positions N07 and N09. Standard deviations are also subject to strong fluctuations and vary depending on the system and the point location. The smallest 2D standard deviation (i.e., Std 2D in the Tables) of around 7.3 m is achieved at position N07 with Galileo. The largest positional standard deviation of around 67.1 m is again at point N07 with Glonass. These GNSS and points also achieve the lowest (12.6 m) and largest (81.9 m) 3D standard deviations. In the following, the deviations from the known coordinates of the reference points are analysed. The results of Helmert's point position error (i.e., Dev 2D) differ by a few meters depending on the system and the point of view. The lowest deviation is achieved with GPS at point N08. It is only 0.36 m and is at the same time the solution for which the fewest individual solutions have been identified. The GPS solution for which the most solutions are available (N07, n=539) achieves an inaccurate result with a deviation of more than 18 m. This means most likely that more outliers in the data have influenced the result significantly. With more than 20 m, only the GLONASS solution for position N09 is less accurate. When the height component is included in the deviation, the best results are achieved with the multi-GNSS solutions. For points N08 and N07 these are just over 10 m, for point N09 a deviation of 24.6 m is achieved. Overall, the multi-GNSS solution achieves position deviations of about 4 m on all points.

3.2.2 PPP Solutions

In the following, PPP solutions are calculated for the three reference points. As in the case of long-term measurement, no solutions can be estimated for Galileo and Beidou because of their low signal quality. For GPS, two carrier frequencies can be included in the calculation. For Glonass, only the frequency R1 is available. Broadcast ephemeris are used. Figure 5 shows plots of the determined numbers of solutions for point N09 (left) and N07 (right). The distribution of the solutions for position N08 is similar to that for position N09 and is therefore not shown here. The GPS solutions are shown in green and the Glonass solutions in blue. If PPP solutions cannot be determined, the employed software package RTKPost automatically calculates SPP solutions. These are represented in red in the Figure. There is a distance of several meters between the GPS and GLONASS solutions at N09. At N07 this distance is even larger. Observations from point N07 have a lower quality and many SPP solutions are estimated only. Similar as for

the SPP solutions in section 3.2.1, Tables 6, 7 and 8 summarise the PPP results for each reference point. In addition to the number of identified solutions per system, the quality (Q) of the solutions is also given in percent. Q describes the proportion of PPP solutions. The remaining solutions are SPP solutions.

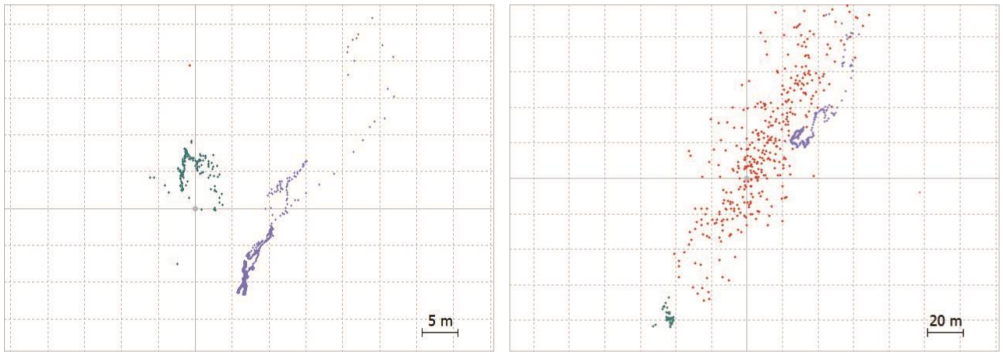

Figure 5. Comparison of PPP solutions for GPS (turquoise) and GLONASS (purple); on the left is point N09, on the right N07. Solutions for which only one SPP solution could be determined are shown in red. Note, the different scale of the grids.

PPP	20 Min		17.12.2020 11:10-11:30		N07							
	n	Q [%]	Std E	Std N	Std U	Std 2D	Std 3D	Dev E	Dev N	Dev U	Dev 2D	Dev 3D
GPS	380	17.6	21.585	40.022	65.366	45.472	79.627	9.174	25.459	-19.463	27.062	33.333
GLONASS	340	99.8	3.993	3.895	4.806	5.578	7.363	-20.501	0.810	-34.893	20.517	40.478
Multi GNSS	720	56.4	16.829	21.529	29.141	27.326	39.949	-8.518	8.700	-22.311	12.176	25.417

Table 6. Comparison of the PPP solutions for GPS and GLONASS over a 20-minute observation period at point N07.

PPP	20 Min		17.12.2020 10:46-11:06		N08							
	n	Q [%]	Std E	Std N	Std U	Std 2D	Std 3D	Dev E	Dev N	Dev U	Dev 2D	Dev 3D
GPS	189	84.4	1.596	4.636	9.613	4.903	10.791	-1.046	-11.199	-27.989	11.247	30.164
GLONASS	797	100.0	0.839	2.018	2.059	2.185	3.003	-8.731	2.052	-13.874	8.969	16.521
Multi GNSS	988	95.6	2.024	5.097	4.762	5.484	7.263	-8.017	-0.169	-15.723	8.018	17.650

Table 7. Comparison of the PPP solutions for GPS and GLONASS over a 20-minute observation period at point N08.

PPP	20 Min		17.12.2020 10:20-10:40		N09							
	n	Q [%]	Std E	Std N	Std U	Std 2D	Std 3D	Dev E	Dev N	Dev U	Dev 2D	Dev 3D
GPS	245	99.0	1.090	2.581	1.753	2.802	3.305	-1.097	-4.159	-12.044	4.301	12.789
GLONASS	556	100.0	2.289	2.414	2.770	3.326	4.328	-5.251	6.537	-17.473	8.385	19.380
Multi GNSS	799	99.9	2.582	4.404	3.065	5.105	5.955	-3.898	3.641	-15.642	5.334	16.527

Table 8. Comparison of the PPP solutions for GPS and GLONASS over a 20-minute observation period at point N09.

At the reference points N07 and N08 much more solutions are achieved with Glonass than with GPS. Especially at N07, where Q is only 17.6% for the GPS results. Overall, Glonass solutions are of a higher quality than GPS solutions. With Glonass, 100% PPP solutions can usually be calculated, even on point N07. Using GPS this result is not achievable. The quality of the solutions has a major influence on the standard deviations. The solution

with the lowest quality (GPS; N07; 17.6%) also has the largest standard deviation (in 2D 45.5 m; and in 3D 79.6 m). The smallest standard deviation is achieved with Glonass for point N08. This is about 2 m in 2D and about 3 m in 3D. The total deviations from ground truth are similar. The results with a low quality have a large deviation. This reaches for the reference points more than 27 m. The best result can be achieved with the GPS solution for position N09. The deviations are about 4 m in 2D and 12.9 m in 3D. The multi-GNSS solutions vary by several meters depending on the reference point. For the position, results for the standard deviations are obtained between 4 and 13 m, the total deviation from the known reference point coordinates is between 16 and 26 m.

Compared to long-term observations, the 20 minute observations are much more imprecise. Thus, if the requirements in terms of positioning accuracies are high, longer observation times are needed with PPP.

3.3. Measurements along a Straight Trajectory

For application scenarios such as line documentation, e.g. for underground power lines, or the approximate recording of trajectories, measurements are carried out along a straight line with a total length of 95.86 m on Karlsplatz. The measurement scenario is such that a user walks at a slow pace with the smartphone in his hand along a predefined line both ways in the outward and in the return direction between the two known reference points N07 and N09. Every five meters a short stop with a duration of several seconds is made. Thus, the measurements can be seen as pseudo-kinematic or in stop-and-go mode.

With RTKPost the GPS, Glonass, Galileo and Beidou solutions for the outward and return journey were calculated. The resulting 8 position files are transformed, merged and plotted with Matlab (Figure 6). A total of 3,497 positioning solutions are available. The resulting point cloud is widely scattered. The course and direction of the track can be roughly estimated in the form of a cluster. There are many faraway outliers and it is not possible to make precise statements about the path taken. Consequently, the results need to be further processed. For this purpose, an adjusted straight line is laid through the point cloud. This can then be compared with the calculated distance between the two known reference points. With Matlab, a neighbourhood analysis is performed to eliminate outliers and more distant points. For each point, the number of neighbours within a defined radius is determined. If the number falls below a predefined limit, the point is not included in the calculation. The radius and the limit are determined by experimentation. The adjusted line should be optimally adapted to the known straight path. The best result was achieved with a radius of 5 m and a minimum number of 30 neighbours (Figure 7). A total of 1,491 points are eliminated (blue) and 2006 points are included in the compensation (red).

The adjusted line is shown in red and the ground truth in green in Figure 7. The actual distance can be easily reproduced by the straight line. The estimated adjusted line, however, has a slightly lower slope. This results in an increasing distance between the two straight lines. The maximum distance obtained resulted in 0.97 m. A problem is the start and end point of the determined trajectory. The adjusted line is too long and extends more than 10 m beyond the distance between the known points serving as ground truth (Retscher and Weigert, 2021).

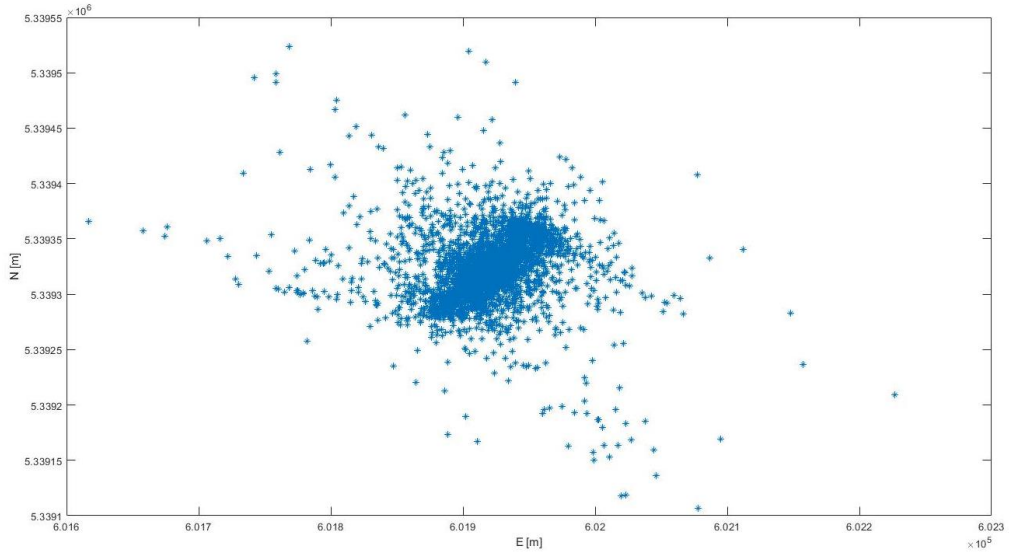

Figure 6. Point cloud with SPP solutions along the route to be investigated. The point cloud includes solutions for the round trip, as well as for all four GNSS.

In addition to the SPP solutions, the PPP solutions are estimated. As with previous measurements, PPP solutions can only be calculated for GPS and Glonass. A total of 1,142 individual solutions of the two systems are available for the round trip. This data is processed with Matlab similar as with the SPP solution. The unprocessed point cloud of the solutions gave similar results as the SPP solutions shown in Figure 8. There are fewer points in total than in the SPP solution. The point density along the reference line is lower and there are many outliers. Despite the variation of the radius and the boundary during the neighbourhood analysis, a good adaptation to the actual distance is not achieved. The deviations of the two lines are many meters apart. The main reason for the lower accuracies is here that only GPS and Glonass can be used instead of all four GNSS as in the SPP solutions.

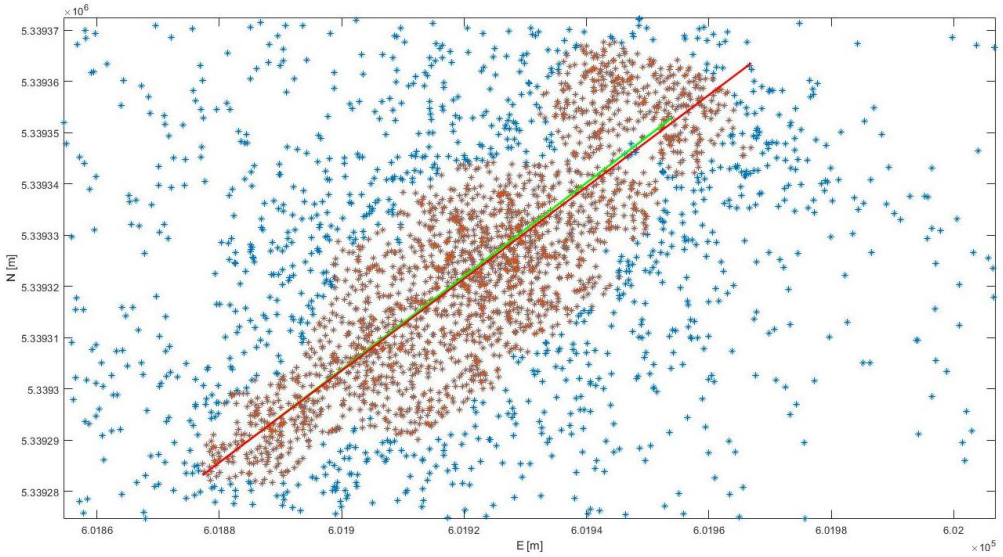

Figure 7. Adjusted line of the point cloud along the straight route. The distance calculated from the known coordinates is shown in green. The distance calculated with the help of the neighbourhood analysis from the points is shown in red. The red points have been included in the calculation of the adjusted line (Source: Retscher and Weigert (2021)).

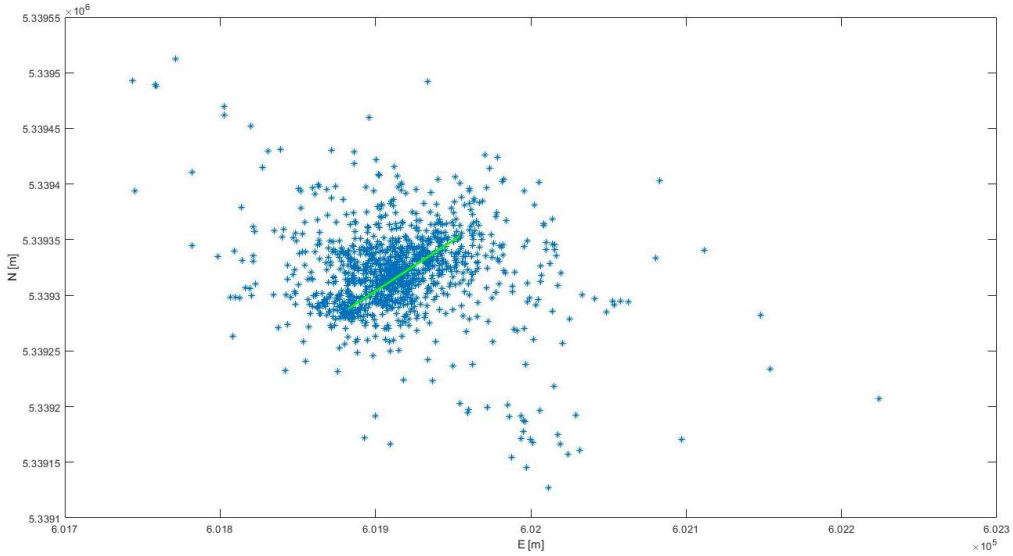

Figure 8. Point cloud with PPP solutions along the route to be investigated. The point cloud includes GPS and Glonass solutions for the round trip. In addition, the reference trajectory is shown as straight line.

4. Summary of the Main Results and Conclusions

Various experiments were carried out in this study, such as long-term measuremenst of 150 minutes, several practical measurements over an observation period of 20 minutes as well as stop-and-go and kinematic measurements. In this paper, short-term static observations and a straight trajectory measured in stop-and-go mode is analyzed. The measurement data were evaluated using the positioning methods SPP and PPP. The main findings and results are summarized in the following, with reference to the criteria investigated, i.e., measurement effort and costs, quality, accuracy and repeatability of the measurements.

4.1. Measurement Effort and Costs

The effort for the measurements is quite low. For equipment, only a mounting device for the mobile phone and a tripod are required for long-term observations on reference points depending on the measurement task. Especially if PPP is chosen as positioning method, longer observation times should be chosen, as the quality of the measurement data varies considerably over time. Here the smartphone must be placed reliably stationary. The analysis of the data is more complex. Only observation files can be created with the Geo++ RINEX Logger. The satellite ephemeris must be obtained elsewhere, such as from EPOSA for broadcast ephemeris and from IGS for precise final orbits. The position determination was performed with the freely available RTKLib software package. The calculated solution point clouds were then transformed with Matlab to UTM and further processed into a single positional solution

4.2. Signal Quality

Compared to geodetic GNSS receivers, the quality of the observations is significantly lower. The recorded satellite signals are weaker and there are frequent signal outages, which also occur for observations in the zenith. Obvious from the tests is that the satellites with strong L1 signals from GPS could not always be observed on the second frequency L5. Most of the Galileo satellites could be received on both frequencies, however, the signals of the bands L5 and E5a are weaker overall than the signals of the bands L1 and E1. The high number of signal outages and the often low signal strength indicated by the SNR make further evaluation difficult. PPP solutions can only be calculated for GPS and Glonass. However, this is often not possible for the entire observation period. At these points, RTKLib automatically switches to SPP mode. The fact that a dual-frequency receiver is installed in the Pixel 5 can therefore only be used to a limited extent in our experiments.

4.3. Achievable Positioning Accuracies

As expected, SPP solutions have significantly higher standard deviations than PPP. They resulted on the few meter level. For PPP, they are often less than one metre. The standard deviations of the Glonass solutions are significantly larger than the ones of GPS. If one considers the deviations from the ground truth from the coordinates of the reference points, the results could not be generalized as significant differences in achievable accuracies occurred for the individual methods. Clear differences of the results can only be seen for GPS in the long-term measurement. Both Galileo and Beidou provide SPP results with higher positioning accuracy for long-term measurements. However, these cannot be compared with the other solutions, as no PPP processing is possible for Galileo or Beidou. If the different GNSS are combined, SPP can achieve results with a deviation of less than half a meter in dependence of the chosen observation time period. The combined solution of all four systems is not always the best, however, as it is strongly influenced by the very inaccurate Glonass results. However, position deviations of less than 30 cm could be achieved with different GNSS combinations (see also Retscher and Weigert, 2021).

For the observations over 20 minutes the differences between the results are in the range of several meters for both methods SPP and PPP. The results vary significantly between the different GNSS combinations and the chosen reference points. Because of the high variation, it is difficult to say which system and method can be used to obtain the more accurate results. The SPP multi-GNSS solution, consisting of all four systems, can guarantee a positional deviation of less than 5 m for all three reference points on Karlsplatz. The PPP dual-GNSS solutions, consisting of GPS and GLONASS, provide a positional deviation of similar quality depending mainly on the length of the observation period.

SPP and PPP solutions were also calculated for the measurement along the chosen trajectory. From the point cloud of the SPP solutions, an adjusted straight line could be estimated, which represents the true trajectory well. The maximum deviation of the measured and true distance is less than one meter. However, the adjusted line resulted in a longer distance than the true distance of few meters which causes that the start and end point cannot be estimated precisely from the measurements.

4.4. Repeatability

In the paper of Retscher and Weigert (2021), the long-term observation for GPS were also divided into measuring intervals of 10 minutes each and position solutions were calculated using the methods SPP and PPP, using both broadcast ephemeris and final orbits from IGS for the PPP calculation. The standard deviations for these solutions remain largely constant in the intervals. However, the accuracy varies significantly regardless of the

method used. The measurement results therefore show poor repeatability for the short observation periods of 10 minutes. A major dependence on the prevailing satellite constellation in these 10-minute periods is seen. Further analyses are required for different length of observation periods.

4.5. Final Outcome Discussion

Observations on two frequency bands can only be made currently for GPS and Galileo with the Google Pixel 5. In this case, however, the observation data of the second frequency band L5 was of lower quality in the conducted experiments, so that unfortunately evaluation of both frequency bands is only possible to a limited extent. Due to the high number of signal outages, a position determination based on phase observations was not possible for all satellite systems. In most cases they could only be made for GPS. The results depend also on the chosen ephemeris data. If IGS final orbits are also used for PPP, the accuracy is significantly higher.

Whether the Google Pixel 5 or a similar smartphone is currently suitable for solving measurement tasks in surveying depends essentially on the requirements of the application. If accuracies of less than half a meter are sufficient smartphones can replace PDAs or receivers for GIS data acquisition. However, if short observation times are required, the deviations often amount to several meters. The in the literature reported cm-accuracies for the PPP with comparable smartphone models could not be confirmed from the experiments. These are mostly based on extensive calibrations for the smartphone GNSS antennae to determine the phase center variations, see e.g. in Darugna (2021) and Wanninger and Heßelbarth (2020), and are therefore not always for practical usage in GIS and LBS applications.

4.6. Outlook on Future Research Questions

For the future work, we will concentrate on the following research questions:

- Which results can be achieved for different observation time periods with PPP?
- How do the other GNSS and the SPP multi-GNSS solutions behave during the measurement?
- How do the L5 observations look like for different satellite constellations?
- How long is the convergence period of PPP solutions as a function of the observation time?
- Which positioning accuracies can be achieved in real-time?

- Which positioning accuracy is achieved in real-time positioning with the CORS RTK services?
- Do similar problems occur with comparable smartphones?
- Are the accuracies to be achieved comparable for different smartphones?
- Does the App used for data acquisition have an impact on the results?

References

Barbeau S (2018) Dual-frequency GNSS on Android devices. https://barbeau.medium.com/dual-frequency-gnss-on-android-devices-152b8826e1c Accessed 28 June 2021

Darugna F (2021) Improving Smartphone-Based GNSS Positioning Using State Space Augmentation Techniques. Veröffentlichungen der DGK, Ausschuss Geodäsie der Bayerischen Akademie der Wissenschaften, Reihe C, Dissertationen, Heft No. 864

EPOSA (2021): Echtzeit Positionierung Austria; https://www.eposa.at/ Accessed 24 February 2021

Heßelbarth A (2011) Statische und kinematische GNSS-Auswertung mittels Precise Point Positioning (PPP). Dissertation Fakultät für Forst-, Geo- und Hydrowissenschaften, Technische Universität Dresden (in German)

Höggerl N, Titz H, Zahn E (2007) APOS – Austrian Positioning Service. Österreichische Zeitschrift für Vermessung und Geoinformation (in German).

Killet F (2010) Sind die Bezugssysteme WGS84 und ETRS89 wirklich gleich? https://www.portalderwirtschaft.de/ Accessed 24 June 2021 (in German)

Qualcomm (2019) Snapdragon 765G 5G Mobile Platform https://www.qualcomm.com/products/snapdragon-765g-5g-mobile-platform Accessed 1 June 2021

Retscher G, Weigert T (2021) Analyses of a Dual Frequency Multi-GNSS Smartphone for Surveying Applications. Submitted to Electronics, MDPI.

Reußner N (2016) Die GLONASS-Mehrdeutigkeitslösung beim Precise Point Positioning (PPP). Dissertation Fakultät Umweltwissenschaften, Technische Universität Dresden (in German)

Wanninger L, Heßelbarth A (2020) GNSS Code and Carrier Phase Observations of a Huawei P30 Smartphone: Quality Assessment and Centimeter-Accurate Positioning. GPS Solutions (2020) 24:64, 10 S., https://doi.org/10.1007/s10291-020-00978-z

PPP-RTK : the advantageous result of a hybridization of GNSS accurate positioning techniques

Delphine Isambert**, Paul Chambon*, Alexandre Vervisch Picois**

* Exagone, Vitry sur Seine, France
** SAMOVAR, Telecom SudParis, Institut Polytechnique of Paris, Palaiseau, France

Abstract. Precise Global Navigation Satellite system (GNSS) positioning is one of the main keys to outdoor positioning. Different technologies exist, each with its own advantages and disadvantages in terms of performance or robustness. This is why the hybridization of two of these techniques is studied; PPP-RTK is the result of the combination of Precise Point Positioning (PPP) and Real Time Kinematic (RTK). This method allows to keep a global approach with a state space representation (SSR) and high performances close to RTK. Using an SSR approach could offer a considerable advantage in precise positioning with telecommunications.

Keywords. Positioning, PPP-RTK, PPP, RTK, SSR

1. Introduction

Precise Point Positioning (PPP) and Real Time Kinematic (RTK) are two different methods for accurate outdoor and Global Navigation Satellite system (GNSS) positioning. Each one has its own way to compute the position. RTK uses a differential positioning technique while PPP has an absolute positioning approach. RTK is the most used method in a lot of applications thanks to higher performances, and uses a network of base stations to collect data to determine the user position. The PPP does not use base stations but a technique of signal augmentation. However, PPP has one main drawback: a very long convergence time.

LBS 2021
16th Conference on Location Based Services
24-25 November 2021 Online

Published in “Proceedings of the 16th International Conference on Location Based Services (LBS 2021)”, edited by Anahid Basiri, Georg Gartner and Haosheng Huang, LBS 2021, 24-25 November 2021, Glasgow, UK/online.

https://doi.org/10.34726/1750 | © Authors 2021. CC BY 4.0 License.

First, we will study the two main techniques mentioned above by explaining their characteristics. Then, we will present a PPP-RTK precise positioning hybrid solution. Finally, we will show an example of the advantages of such a technique in telecommunications using Digital Audio Broadcasting (DAB) for example. We will finish by concluding and explaining a possible follow-up to this work.

2. Positining Techniques

2.1. Real Time Kinematic

The main idea of precise positioning method with RTK is the differentiation of phases and codes measurements between two receivers (de Salas & M. Torroja 2016). By this action, some terms will be removed from the GNSS observation equations: the atmospheric errors independent of the receivers and the clock terms have been removed and will not need to be estimated or calculated here. The solution of these equations, used to determine the user's position will therefore be simpler. The biggest unknown is the ambiguity related to the phase. Many techniques to solve the ambiguity exist in this case, like the LAMBDA method (Jokinen et al. 2012). One big advantage of RTK is about convergence: the performance of RTK positioning remains the best (convergence time <1min). However, this application is between two receivers, it is not global. One solution exists : the Network RTK (NRTK).

The main objective is to pool the data of several base stations. This creates an interconnected network. Each station is about 100 km apart in the network. The denser the network, the higher the performance. Indeed, the user will be on average 50km away from a base station. If this distance is respected, the performance of this positioning technique remains as good as that of RTK alone. The mobile receiver will apply the principle of the RTK with the nearest station of the network.

In practice, only one GNSS receiver is needed, the network data is sent to the receivers in corrections messages. There are different types of NRTK implementation: Virtual Reference Station (VRS), Master Auxiliary Concept (MAC) and FläschenKorrekturParameter (FKP) (Retscher 2002). The most commonly used and the one we will apply in our case is the VRS solution. Its principle is based on the creation of an imaginary reference station. The latter is modelled a few kilometres from the receiver. The RTK resolution will be made between this virtual station and the receiver. It is modelled thanks to the network of base

stations. The entire ambiguity to be determined can be calculated from the NRTK data.

2.2. Precise point Positioning

PPP is an augmentation technique. It is applied in the context of a global network. The main objective of this technique is to reduce the static side in data processing. Thus, PPP works for a dynamic approach. Its reliability and accuracy is based on the number of satellites, the geometry of the satellites, the availability of the signal and the quality of the measurements. Unlike RTK, this method does not use differentiation. This allows firstly to keep the positional measurement strength of the instrument and secondly to avoid the propagation and correlation of measurement errors. In addition, the PPP uses precise orbital data, precise satellite clock data, from the International GNSS Service (IGS) for example and two frequencies in the GNSS observation equations (Bisnath 2020). Indeed, the double frequency allows to apply the model without ionosphere. This model is the most widely used and allows ionosphere-free combinations of code pseudoranges and carrier phases.

The main factors limiting accuracy in PPP are orbit errors, clock errors and atmospheric variations. The latter is a consequence of multipath: there may be a lack of information on the refraction of the signal in the atmosphere (troposphere, ionosphere). All this will alter the accuracy of the pseudo distance measurements. To compensate for these inaccuracies, the observation equations can take into account several constellations (multi-constellations technique). It is necessary to be careful because errors of counting between the different constellations can appear. Despite these errors, the convergence in PPP will be faster and the accuracy will be improved.

However, the main drawback of this technique is the long convergence time due to the resolution of ambiguities (Jokinen et al. 2012). This is why the RTK explained above is often preferred.

3. A Hybrid Technique : PPP-RTK

3.1. An example of PPP-RTK model

PPP-RTK is an extension of the PPP model, it is a signal augmentation technique but it uses a network of base stations to correct some parameters. Thus, the objective in the GNSS observation equations is the same as in PPP: to make the equations as explicit as possible in

order to see the influence of the various parameters. It is an undifferentiated and uncombined model that is implemented (Teunissen & Khodabandeh 2014). There is an inconsistency in the resolution of theses equations: a rank defect. To overcome this, some parameters can be estimated like in the PPP. We can detail the different parameters in *Table 1.*

Parameters	PPP-RTK
Satellites Clock errors	Known precisely (IGS)
Receiver Clock errors	estimated
Bias receiver errors	Estimated
Bias satellite errors	Known precisely (IGS)
Ionospheric delay	Estimated
Tropospheric delay	Known (IGS)
Ambiguity	Estimated
Mapping function	Known (IGS)

Table 1. Parameters in PPP-RTK

Furthermore, in GNSS observation equations for PPP-RTK, a single station principle is applied because it improves the quality of the corrections. The advantages of the PPP-RTK implementation are a positioning system that operates in absolute mode, no mathematical correlation between observables, robustness against errors, and optimal reliability. This hybrid technique can have the same accuracy and performance of RTK.

3.2. An SSR approach

The main advantage of PPP-RTK is that it allows to have an accuracy close to RTK but with a State Space Reprensation (SSR). The SSR approach is opposed to the Observation State Representation (OSR) generally used in RTK and NRTK (Wabbena et al. 2005). The difference between these two approaches is that in OSR the corrections sent to the user are not the same for everyone and depend on the data from the stations closest to the user. On the other hand, in the SSR approach, the corrections are universal and are the same for everyone in the network. They are independent of the user position.

To show the advantage of SSR corrections over OSR-type corrections, we performed tests on the reception of corrections via Digital Audio Broadcasting (DAB). The corrections were put on DAB via a service called "teria" via channel 5B (176.640 MHz). We received this data via a DAB antenna and then transmitted it to a Septentrio GNSS card, connected to a receiver, which uses the corrections to determine its position.

Using the OSR corrections as a first step we noticed a latency of 19sec between the moment when the corrections are received and transmitted (*Figure 1*).

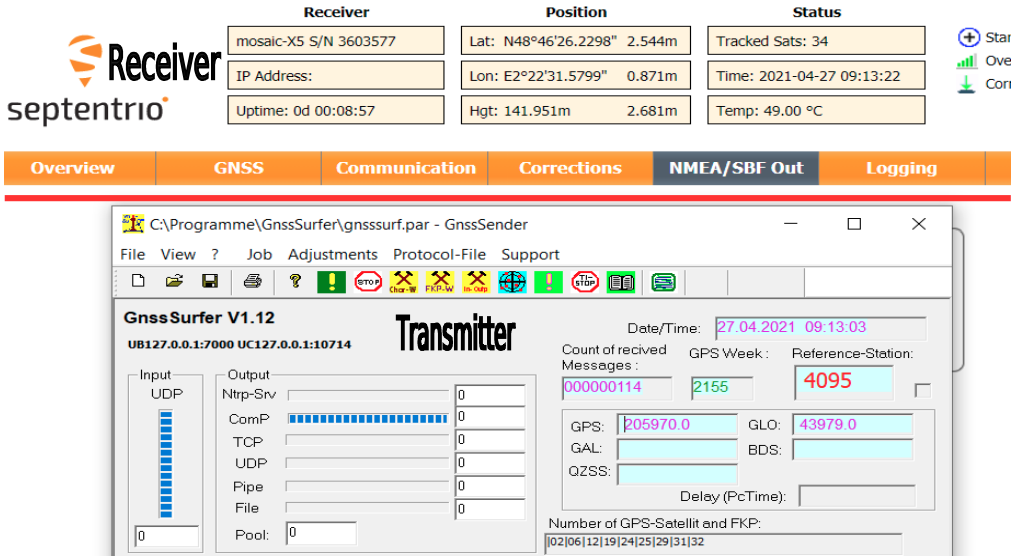

Figure 1. OSR Corrections latency between the received and sent corrections

This latency is a real problem because the receiver cannot take into account the OSR corrections and thus calculate its position. To compensate for this it is possible to use SSR corrections. These are taken into account even with latencies of up to 20sec. Thus, by using SSR corrections the receiver could take into account the corrections and determine its position. This example shows that SSR corrections, are a real asset compared to the latencies that can occur when receiving these corrections via DAB or 3GPP.

4. Conclusion

To conclude, this new approach hybridizing two GNSS accurate positioning techniques shows that having a global positioning method is possible with similar performances to RTK. Indeed, today in many applications, RTK is preferred because it has performances well above PPP. Moreover, RTK remains the standard because it has an OSR approach and devices are calibrated for this type of correction. Very few of them allow the use of corrections with SSR approach. However, in the future, it would be interesting to highlight this approach with an extended version of the PPP: PPP-RTK. Indeed, as shown earlier, having a State Space Representation is an advantage and brings a lot of good results for accurate postioning with telecommunications devices, a smartphone for example. The SSR corrections allow latencies and offer the same performancesof OSR corrections.

References

J. de Salas and M. Torroja (2016) Carrier phase positioning experiences in consumer GNSS devices, International Conference on Localization and GNSS (ICL-GNSS) pp. 1-6, doi: 10.1109/ICL-GNSS.2016.7533683.

G. Retscher (2002) Accuracy Performance of Virtual Reference Station (VRS) Networks Journal of Global Positioning Systems. 1. 40-47. 10.5081/jgps.1.1.40.

S. Bisnath (2020) PPP: Perhaps the natural processing mode for precise GNSS PNT, IEEE/ION Position, Location and Navigation Symposium (PLANS) pp. 419-425, doi: 10.1109/PLANS46316.2020.9110150.

A. Jokinen, S. Feng, W. Ochieng, C. Hide, T. Moore and C. Hill (2012) Fixed ambiguity Precise Point Positioning (PPP) with FDE RAIM, Proceedings of the 2012 IEEE/ION Position, Location and Navigation Symposium, pp. 643-658, doi: 10.1109/PLANS.2012.6236939.

G. Wabbena, M. Schmitz and A. Bagge (2005) PPP-RTK: Precise Point Positioning Using State-Space Representation in RTK Networks.

P. Teunissen and A. Khodabandeh (2014) Review and principles of PPP-RTK methods Journal of Geodesy 89: 217-240.

A New Method for Indoor Positioning Based on Integrating Wireless Local Area Network, Bluetooth Low Energy, and Inertial Sensors

Maryam Jafari Tafazzol, Mohammad Reza Malek

Ubiquitous and Mobile GIS Lab., Dept. of GIS, Faculty of Geodesy and Geomatics, K.N. Toosi University of Technology, Iran

Increasing the accuracy of indoor positioning is still a challenging issue. In this paper, we propose a novel integration structure for indoor positioning using a wireless local area network, Bluetooth low energy beacons, and inertial sensors to increase the positioning accuracy. The main steps of this method are initial and relative positioning. Wireless local area network fingerprinting and database filtering using Bluetooth low energy are applied to calculate the initial location. Relative location is computed using inertial sensors data and the pedestrian dead reckoning method. In order to increase the accuracy of pedestrian dead reckoning, two sources of information, wireless local area network, and Bluetooth low energy are used. This new correction method is performed using a double Kalman filter. Extensive experiments were conducted in a smartphone and under two indoor environments. Our correction structure using a double Kalman filter outperforms previous pedestrian dead reckoning structures in terms of accuracy. Moreover, experimental results show our correction structure achieves an average accuracy of 1.7 meters.

Keywords. Indoor positioning, Wireless Local Area Network (WLAN), Bluetooth low energy BLE), Pedestrian Dead Reckoning (PDR), Kalman filter, Data Fusion.

1. Introduction

Most people spend more than 70% of their time in indoor areas (Y. Li et al. 2017). Thus, location-based services are highly demanding in indoor areas,

Published in "Proceedings of the 16th International Conference on Location Based Services (LBS 2021)", edited by Anahid Basiri, Georg Gartner and Haosheng Huang, LBS 2021, 24-25 November 2021, Glasgow, UK/online.

https://doi.org/10.34726/1751 | © Authors 2021. CC BY 4.0 License.

especially in hospitals, airports, train stations, and shopping malls (Evennou and Marx 2006). These location-based services require indoor positioning and tracking systems (Mohammad R. Malek and Frank 2006; Carrera V. et al. 2018). Various indoor positioning methods using Wireless local area network (WLAN) (Vahidnia et al. 2013; Ma et al. 2015; Khalajmehrabadi, Gatsis, and Akopian 2017), Ultra-wideband (UWB) (Garcia et al. 2015), ZigBee (Niu et al. 2015), Bluetooth low energy beacons (BLE) (Röbesaat et al. 2017), Radio frequency identification (RFID) (H. Xu et al. 2017), and inertial sensors (Orujov et al. 2018; L. Xu et al. 2019), have been developed.

Any of these methods have limitations and disadvantages such as low accuracy, high cost to provide the required hardware or computational complexity. Moreover, there exists no technology that works perfectly in different buildings. Therefore, recent investigations have been conducted on improving indoor positioning (Röbesaat et al. 2017). Among all solutions, integrating different indoor positioning techniques is an optimal solution for increasing accuracy and reducing the limitations of every single method (Y. Li et al. 2017; Poulose, Kim, and Han 2019). In this paper, we propose a novel integration structure for indoor positioning using wireless local area network, Bluetooth low energy beacons, and inertial sensors to increase the positioning accuracy.

2. Related work

Several hybrid indoor positioning research using WLAN, BLE, and inertial sensors are discussed in this section. These researches combine information from two or all of these sources. Li et al. (2015) proposed two fusion structures using BLE data and PDR method. The first structure is determining location, using PDR and map matching, then correct it using the BLE data. The second structure is combining PDR and BLE using adapted noise extended Kalman filter. The results showed that both fusion structures have higher accuracy than single positioning algorithms. Li et al. (2017), proposed a hybrid indoor positioning algorithm using WLAN, PDR, and Magnetic matching.

Some researchers have focused on combining an absolute indoor positioning, such as WLAN or BLE, with a relative indoor positioning such as PDR (Orujov et al. 2018). Chen et al. (2015) proposed a hybrid indoor positioning method using the WLAN fingerprinting and PDR method.

A few number of research studied the hybrid indoor positioning structures using BLE, WLAN, and PDR. Zou et al. (2017) introduced a fusion structure using WLAN and BLE observations and inertial sensors data using a parti-

cle filter. They fused WLAN and inertial sensors data to reduce the drift of indoor positioning and in poor coverage of WLAN signals; they utilized BLE RSS to correct PDR. Chen et al. (2016) proposed a smartphone based indoor positioning method with BLE corrections using an extended Kalman filter. This article studied step detection, step length estimation, and walking direction estimation.

In our study, we used two different RF-based observations to reduce the PDR drift. Some of the presented research, such as Frank et al. (2009) and Zou et al. (2017), require processing on a server or special equipment. However, we introduced a method that can be run on smartphones without additional hardware. Some articles like Kanaris et al. (2017) only calculate the absolute location and do not consider real-time positioning. The purpose of this study is to solve the mentioned problems and limitations by combining WLAN and BLE RSS measurements and PDR method.

3. Preliminaries

The fingerprinting method is a positioning method, which uses the RSS measurements of RF signals. In the first phase, RSS measurements are collected, for example, from WLAN APs, and stored in a database called radio map. Then in the second phase, real-time collected RSS matches with radio map to estimate the location using definite or probabilistic methods (Vahidnia et al. 2013; Deng et al. 2015)

Vector of N measured RSS measurements at the unknown point from defined APs and vector of collected RSS measurements at the j-th RP from defined APs, respectively are $\boldsymbol{s}$ and $\boldsymbol{r}_i$. Equation 1 shows the Euclidean distance between the i-th reference point and the unknown point.

$$d_j = \sqrt{\sum_{i=1}^{n} (\boldsymbol{r}_{ij} - \boldsymbol{s}_i)^2} \qquad (1)$$

$\boldsymbol{s}_i$ and $\boldsymbol{r}_{ii}$ are the i-th element in $\boldsymbol{s}$ and $\boldsymbol{r}_i$, respectively. K nearest RPs are selected for positioning using Weighted K-Nearest Neighbour (WKNN). Then the weighted average of k nearest neighbours' positions estimates the unknown location.

PDR is a relative positioning method that uses previous position, step length, and direction to calculate the current position. Equation 2 shows the

PDR formula. In this equation, $\boldsymbol{x}_k$ is a two-dimensional coordinate vector of the previous position, l_K is step length, θ_k is step heading, and $\boldsymbol{x}_{k+1}$ is estimated coordinate vector (Malek 2020).

$$\boldsymbol{x}_{k+1} = \boldsymbol{x}_k + l_K \begin{bmatrix} \sin\theta_k \\ \cos\theta_k \end{bmatrix} \qquad (2)$$

Where, $\boldsymbol{x}_i$ is the position vector of j-th RP, $\hat{\boldsymbol{x}}$ is the estimated position vector, and d_i is calculated using equation 2.

4. Proposed method

Our proposed method is shown in **Error! Reference source not found.** which mainly consists of initial positioning, PDR, and PDR correction. Initial location is calculated using WLAN fingerprinting and BLE measurements. Radio map is filtered using the nearest BLE beacons RSS measurements. Finally, the initial location is estimated using the WKNN algorithm. PDR calculates Relative displacements of the user using gyroscope and accelerometer data. A Kalman filter with two measurement equations corrects PDR using WLAN and BLE observations. PDR, BLE observations, and WLAN measurements estimate the state equation of the Kalman filter, short-time measurement observation, and long-time measurement observation, respectively.

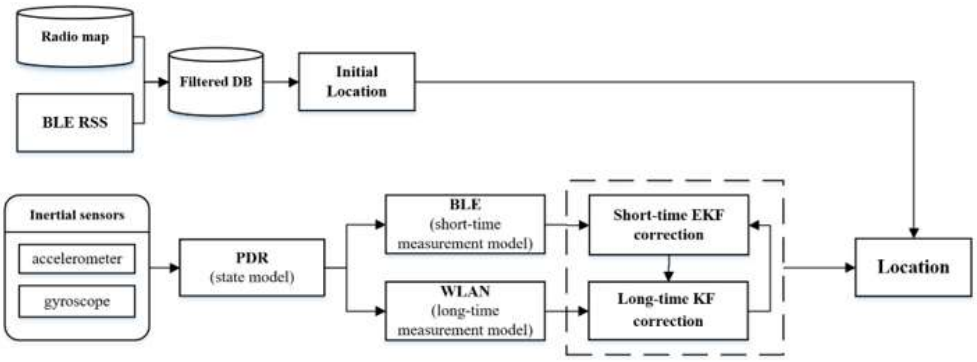

Figure 1. Overview of the proposed indoor localization approach.

4.1. Initial positioning

The Fingerprinting method is used to calculate the initial location of the user. To reduce blunders and decrease the search time in the database, BLE RSS measurements filter the WLAN fingerprinting database.

We used a one-dimensional Kalman filter for BLE RSS filtering and increasing positioning accuracy. Then a second order polynomial equation is used to model the distance between nearest beacon and user based on BLE RSS measurements. This polynomial equation is built after collecting data at different distances from each beacon and using least square estimation. Equation 3 shows a function for estimating the distance from a beacon.

$$r_i = 0.0073 rss_i{}^2 + 1.012 rss_i + 10.4 \qquad (3)$$

In equation 3, rss_i is the RSS from i-th beacon at an unknown location, and r_i is the estimated distance from i-th beacon. After comparing estimated distances from each beacon, the nearest beacon is detected, and based on the estimated distance to the nearest beacon, WLAN fingerprinting database is filtered. Thus, instead of searching in a large database, a smaller set of RPs is selected as the search area in the WKNN algorithm. The final initial location is calculated using the WKNN method.

4.2. PDR correction

PDR method is simple and common but suffers from drifting problems (Poulose et al. 2019). It has a cumulative error which increases over time. In order to reduce the cumulative error of PDR, we used a double correction method. WLAN and BLE measurements are used to correct PDR, and Kalman filter is used to fuse information. To use both observations, two different time intervals for using each measurement are defined. Because of the higher sampling rate of BLE measurements, we used them for short-time correction. WLAN measurements are used for long-time correction and when BLE RSS measurements are weak. We define each step as a short-time interval and every 12 steps as a long-term interval. Figure 2 shows the correcting process.

In our algorithm, after detecting a step, step length and heading are estimated using real-time accelerometer and gyroscope data. If the number of steps is not a multiple of 12, measurement mode is set to BLE. Then BLE RSS measurements are collected and distance to each beacon is estimated. If the RSS of the nearest beacon is more than -95 dBm, the measurement equation of the Kalman filter is defined using the estimated distance to it.

The state equation of Kalman filter is defined using the PDR method and Kalman filter is implemented.

PDR correction

```
1: Given: accelerometer and gyroscope real-time data, S←number of steps, measurement_mode
2: if a step is detected:
3: S++
4: calculate step length and heading
5:   if S is not a factor of 12:
6:       switch measurement_mode to BLE
7:       collect RSS measurements of beacons
8:         calculate distance from beacons
9:       find the nearest_beacon
10:          if RSS of nearest_beacon <= -95 dBm
11:             break
12:          end if
13:  end if
14:    if S is a factor of 12:
15:   collect WLAN RSS measurements of Defined APs
16:   switch measurement_mode to WLAN
17:   calculate the estimated_position using WKNN
18:    end if
19: calculate Kalman state equation using PDR
20:     if (measurement_mode is BLE)
21:          calculate measurement Eq from BLE
22:          run Kalman filter
23:     end if
24:     else if (measurement_mode is WLAN)
25:          calculate measurement Eq from WLAN
26:          run Kalman filter
27:      end if
28: end if
29: go to 1
```

Figure 2. PDR correction algorithm.

If the number of steps is a multiple of 12, measurement mode is switched to WLAN. Then WLAN RSS measurements from APs are collected and the user's location is estimated using fingerprinting and WKNN. Measurement equation of the Kalman filter is defined using the estimated location. Then, the Kalman filter with the PDR state model and WLAN measurement model is executed.

If the RSS of the nearest beacon is more than -95 dBm, the measurement equation of the Kalman filter is defined using the estimated distance to it. If the number of steps is a multiple of 12, measurement mode is switched to WLAN. Then WLAN RSS measurements from APs are collected and the user's location is estimated using fingerprinting and WKNN. Measurement equation of the Kalman filter is defined using the estimated location. Then, the Kalman filter with the PDR state model and WLAN measurement model is executed.

We developed short-time and long-time corrections. A Kalman filter is utilized to correct PDR cumulative error in each step using Bluetooth RSS measurements. In long time correction, WLAN measurements are used to build the Kalman observation model. A long-term correction interval was chosen every 12 steps.

5. Implementation and evaluation

We have developed an android app for real-time positioning and evaluation. The app can be run on any mobile device with a gyroscope, accelerometer, Wi-Fi, and Bluetooth receiver. All steps related to data collection and positioning were performed using the app. In this study, six beacons were used. All beacons were installed at the height of 1.5 meters above the grounds and on the walls. The transmission power for BLE beacons was set to 0 dBm.

The experiments have been carried out at the K.N. Toosi University of Technology. The third floor of the faculty of Geodesy and Geomatics that is in 70×14 m^2 was selected. The environment is a corridor along which there are stairways to the mezzanines, floors, and roof. The corridor is mainly used for walking in a linear path.

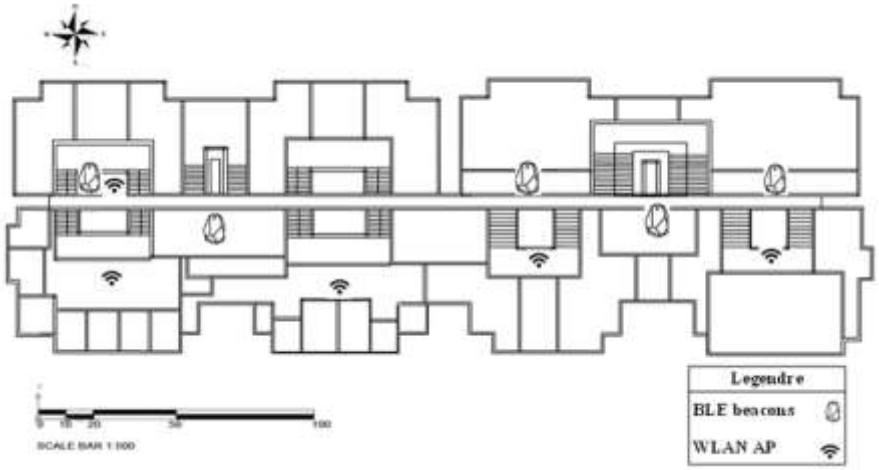

Figure 3. The plan of our case study

Figure 3 shows the experimental environment, location of beacons, and WLAN APs. RPs were selected in in 2×2 m^2 grids. RSS measurements were collected at four directions and 20 times in each direction. Then, the average of RSS readings was stored in the database. The RSS of an unavailable AP is set to -100 dBm. In the environment, 74 RPs using 5 APs were collected.

Initial positioning method using WLAN and BLE observations, PDR using inertial sensors, and PDR corrections using WLAN and BLE observations were performed to evaluate the proposed hybrid method. In this experiment, the user walked along the defined path and estimated locations was compared to the ground truth.

In order to evaluate the initial positioning method, 20 checkpoints were selected. Then, each checkpoints' locations were estimated using the defined method and was compared to the real locations. In Figure 4 real locations of checkpoints, estimated locations of checkpoints, and positioning error for each point are shown using circles, squares, and triangles, respectively. The average initial positioning error was estimated at 2.2 meters. The computational speed of searching in the filtered database increased by an average of 54% Compared to computational speed in the main database.

In Figure 4, the estimated locations using PDR, estimated locations using corrected PDR with BLE and estimated locations using corrected PDR with BLE and WLAN are shown by circles, squares, and triangles in the first environment, respectively. A straight line in Figure 5 shows the true path of walking. PDR cumulative error is corrected twice, and the final positioning

error after the two-step correction is less than PDR and short-time correction using BLE.

Figure 6 and Figure 7 illustrate the error of positioning methods at each step and cumulative distribution function (CDF) curves of position errors, respectively. The average PDR positioning error was estimated 4.03 m. After PDR correction using BLE through the Kalman filter, the average positioning error was decreased to 2.3 m. The average positioning error after the proposed two-step correction was reduced to 1.8 m, and the accuracy of positioning was increased compared to the other two methods.

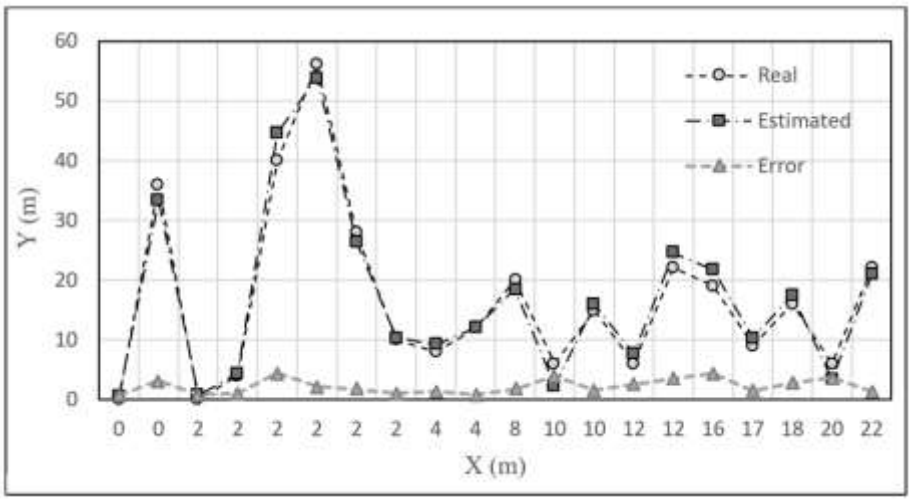

Figure 4. Initial positioning method evaluation (circles: true locations of checkpoints, squares: estimated locations, triangles: positioning error).

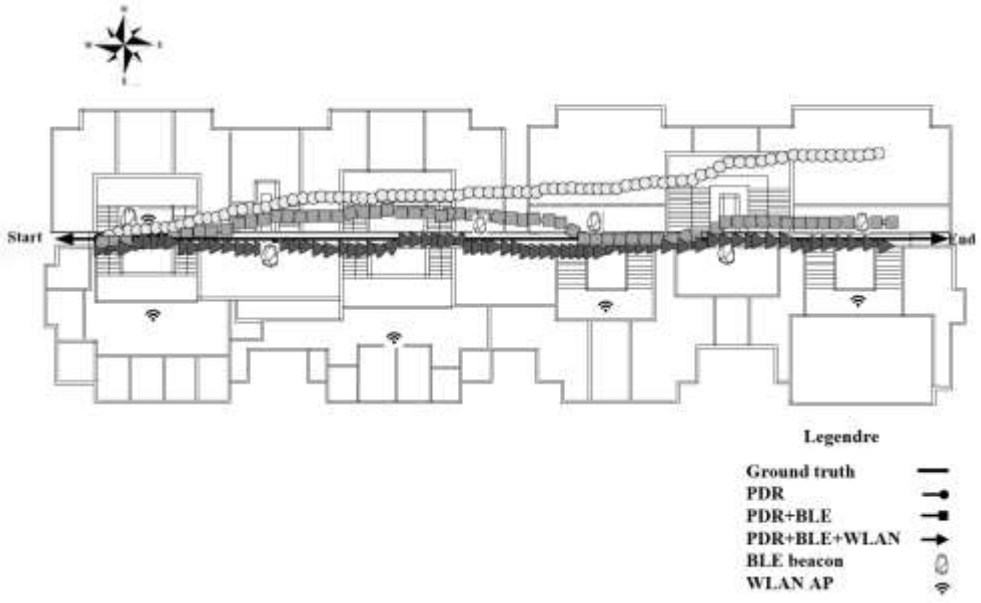

Figure 5. Ground truth and estimated locations using PDR, corrected PDR using BLE, corrected PDR using BLE and WLAN in the first environment.

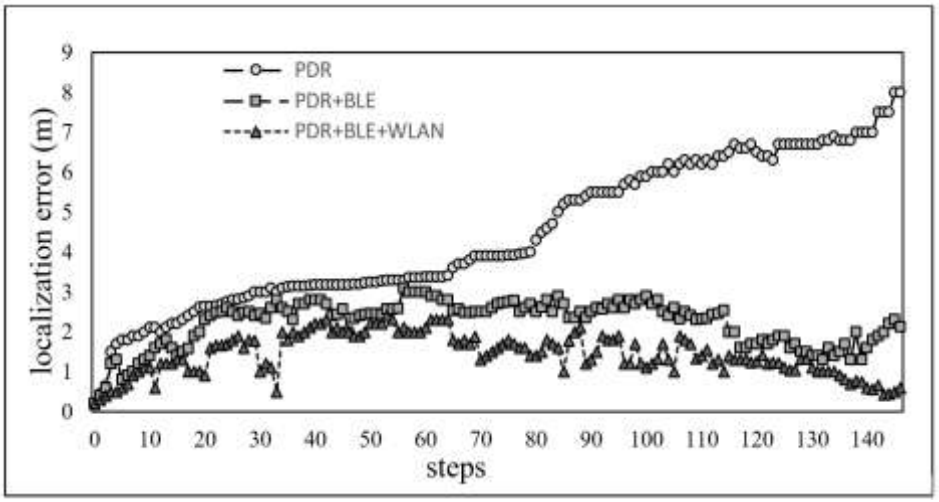

Figure 6. Positioning error of different methods per step.

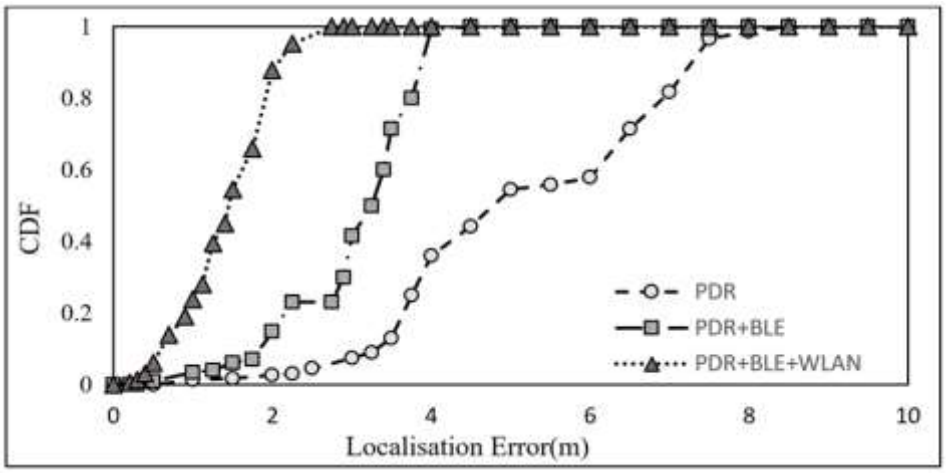

Figure 7. CDF of positioning errors for different methods.

6. Conclusion

In this paper, we proposed an integrated indoor positioning method with inertial sensors, WLAN, and BLE observations. To improve the PDR accuracy and reduce the cumulative error of PDR, we used a novel correction method using WLAN and BLE observations. Because of the high sampling rate of BLE RSS measurements, we used BLE observations for short-time correction, and WLAN observations with a lower sampling rate, for long-time correction. To reduce blunders, BLE RSS measurements were filtered and weak RSS measurements (lower than -95 dBm) were not sent to the correction phase. Moreover, initial positioning was achieved using a filtered fingerprinting database.

The final results of our experiment shows that the average positioning error of PDR correction using BLE and WLAN was lower than PDR and corrected PDR using BLE. The average positioning of the proposed correction method was estimated at 1.7 m, and the highest and lowest errors were about 0.6, and 2.7 respectively. Furthermore, our method could be used for real-time applications.

Future research will focus on improving the proposed method by using other methods like map matching, and we will also examine floor detection.

References

Carrera V., José Luis, Zhongliang Zhao, Torsten Braun, Zan Li, and Augusto Neto. 2018. “A Real-Time Robust Indoor Tracking System in Smartphones.” *Computer Communications* 117. Elsevier: 104–115. doi:10.1016/j.comcom.2017.09.004.

Chen, Guoliang, Xiaolin Meng, Yunjia Wang, Yanzhe Zhang, Peng Tian, and Huachao Yang. 2015. “Integrated WiFi/PDR/Smartphone Using an Unscented Kalman Filter Algorithm for 3D Indoor Localization.” *Sensors (Switzerland)* 15 (9). Multidisciplinary Digital Publishing Institute: 24595–24614. doi:10.3390/s150924595.

Chen, Zhenghua, Qingchang Zhu, and Yeng Chai Soh. 2016. “Smartphone Inertial Sensor-Based Indoor Localization and Tracking with IBeacon Corrections.” *IEEE Transactions on Industrial Informatics* 12 (4). IEEE: 1540–1549. doi:10.1109/TII.2016.2579265.

Deng, Zhi An, Ying Hu, Jianguo Yu, and Zhenyu Na. 2015. “Extended Kalman Filter for Real Time Indoor Localization by Fusing WiFi and Smartphone Inertial Sensors.” *Micromachines* 6 (4). Multidisciplinary Digital Publishing Institute: 523–543. doi:10.3390/mi6040523.

Evennou, Frédéric, and François Marx. 2006. “Advanced Integration of WiFi and Inertial Navigation Systems for Indoor Mobile Positioning.” *Eurasip Journal on Applied Signal Processing* 2006. Springer: 1–11. doi:10.1155/ASP/2006/86706.

Frank, Korbinian, Bernhard Kracht, Noel Catterall, and Patrick Robertson. 2009. “Development and Evaluation of a Combined WLAN & Inertial Indoor Pedestrian Positioning System.” In *22nd International Technical Meeting of the Satellite Division of the Institute of Navigation 2009, ION GNSS 2009*, 1:133–141.

Garcia, Enrique, Pablo Poudereux, Alvaro Hernandez, Jesus Urena, and David Gualda. 2015. “A Robust UWB Indoor Positioning System for Highly Complex Environments.” In *Proceedings of the IEEE International Conference on Industrial Technology*, 2015-June:3386–3391. IEEE. doi:10.1109/ICIT.2015.7125601.

Kanaris, Loizos, Akis Kokkinis, Antonio Liotta, and Stavros Stavrou. 2017. “Fusing Bluetooth Beacon Data with Wi-Fi Radiomaps for Improved Indoor Localization.” *Sensors (Switzerland)* 17 (4). Multidisciplinary Digital Publishing Institute: 812. doi:10.3390/s17040812.

Khalajmehrabadi, Ali, Nikolaos Gatsis, and David Akopian. 2017. “Modern WLAN Fingerprinting Indoor Positioning Methods and Deployment Challenges.” *IEEE Communications Surveys and Tutorials* 19 (3). IEEE: 1974–2002. doi:10.1109/COMST.2017.2671454.

Li, Xin, Jian Wang, and Chunyan Liu. 2015. “A Bluetooth/PDR Integration Algorithm for an Indoor Positioning System.” *Sensors* 15 (10). Multidisciplinary Digital Publishing Institute: 24862–24885.

Li, You, Yuan Zhuang, Peng Zhang, Haiyu Lan, Xiaoji Niu, and Naser El-Sheimy. 2017. “An Improved Inertial/Wifi/Magnetic Fusion Structure for Indoor Navigation.” *Information Fusion* 34. Elsevier: 101–119. doi:10.1016/j.inffus.2016.06.004.

Ma, Rui, Qiang Guo, Changzhen Hu, and Jingfeng Xue. 2015. “An Improved WiFi Indoor Positioning Algorithm by Weighted Fusion.” *Sensors (Switzerland)* 15 (9). Multidisciplinary Digital Publishing Institute: 21824–21843. doi:10.3390/s150921824.

Malek, Mohammad R., and Andrew U. Frank. 2006. “A Mobile Computing Approach for

Navigation Purposes." In *Lecture Notes in Computer Science (Including Subseries Lecture Notes in Artificial Intelligence and Lecture Notes in Bioinformatics)*, 4295 LNCS:123–134. Springer. doi:10.1007/11935148_12.

Malek, Mohammad R. 2020. *Context-Aware Geoinformation and Ubiquitous Computing (In Persian)*. Second. Tehran, Iran: K.N. Toosi university of Tech.

Niu, Jianwei, Bowei Wang, Lei Shu, Trung Q. Duong, and Yuanfang Chen. 2015. "ZIL: An Energy-Efficient Indoor Localization System Using ZigBee Radio to Detect WiFi Fingerprints." *IEEE Journal on Selected Areas in Communications* 33 (7). IEEE: 1431–1442. doi:10.1109/JSAC.2015.2430171.

Orujov, F., R. Maskeliūnas, R. Damaševičius, Wei Wei, and Ye Li. 2018. "Smartphone Based Intelligent Indoor Positioning Using Fuzzy Logic." *Future Generation Computer Systems* 89. Elsevier: 335–348. doi:10.1016/j.future.2018.06.030.

Poulose, Alwin, Jihun Kim, and Dong Seog Han. 2019. "A Sensor Fusion Framework for Indoor Localization Using Smartphone Sensors and Wi-Fi RSSI Measurements." *Applied Sciences (Switzerland)* 9 (20). Multidisciplinary Digital Publishing Institute: 4379. doi:10.3390/app9204379.

Röbesaat, Jenny, Peilin Zhang, Mohamed Abdelaal, and Oliver Theel. 2017. "An Improved BLE Indoor Localization with Kalman-Based Fusion: An Experimental Study." *Sensors (Switzerland)* 17 (5). Multidisciplinary Digital Publishing Institute: 951. doi:10.3390/s17050951.

Vahidnia, Mohammad H., Mohammad R. Malek, Nazila Mohammadi, and Ali A. Alesheikh. 2013. "A Hierarchical Signal-Space Partitioning Technique for Indoor Positioning with WLAN to Support Location-Awareness in Mobile Map Services." *Wireless Personal Communications* 69 (2). Springer: 689–719. doi:10.1007/s11277-012-0607-5.

Xu, He, Ye Ding, Peng Li, Ruchuan Wang, and Yizhu Li. 2017. "An RFID Indoor Positioning Algorithm Based on Bayesian Probability and K-Nearest Neighbor." *Sensors (Switzerland)* 17 (8). Multidisciplinary Digital Publishing Institute: 1806. doi:10.3390/s17081806.

Xu, Limin, Zhi Xiong, Jianye Liu, Zhengchun Wang, and Yiming Ding. 2019. "A Novel Pedestrian Dead Reckoning Algorithm for Multi-Mode Recognition Based on Smartphones." *Remote Sensing* 11 (3). Multidisciplinary Digital Publishing Institute: 294. doi:10.3390/rs11030294.

Zou, Han, Zhenghua Chen, Hao Jiang, Lihua Xie, and Costas Spanos. 2017. "Accurate Indoor Localization and Tracking Using Mobile Phone Inertial Sensors, WiFi and IBeacon." In *4th IEEE International Symposium on Inertial Sensors and Systems, INERTIAL 2017 - Proceedings*, 1–4. IEEE. doi:10.1109/ISISS.2017.7935650.

Dual-frequency GNSS/Wi-Fi Smartphone Navigation

Błaszczak-Bąk Wioleta*, Retscher Guenther **, Janicka Joanna*, Uradziński Marcin*, Bednarczyk Michał* and Gabela Jelena**

* University of Warmia and Mazury in Olsztyn, Faculty of Geoengineering, Olsztyn, Poland;
wioleta.blaszczak@uwm.edu.pl, janicka.joanna@uwm.edu.pl, uradzinski.marcin@uwm.edu.pl, bednarczyk.michal@uwm.edu.pl
** Vienna University of Technology, Faculty of Mathematics and Geoinformation, Vienna, Austria;
guenther.retscher@geo.tuwien.ac.at, jelena.gabela@geo.tuwien.ac.at

Abstract. More and more sensors and receivers are found nowadays in modern smartphones which can enable and improve positioning for Location-based Services and other navigation applications. They include multi-constellation GNSS (Global Navigation Satellite Systems) receivers and other sensors which can be employed for positioning. The state-of-the-art thereby is that dual frequency GNSS capable receivers in smartphones are now recently on the market. With these receivers not only the current 3D positions but also the raw data of the measurements can be utilized leading to higher positioning accuracies. New algorithms need to be developed to make use of the measured GNSS raw data to be able to achieve required positioning accuracies. Therefore, the goal of our research concept is to develop a methodology based on dual frequency GNSS/Wi-Fi smartphone (L1/L5 carrier phases and 2.4/5 GHz frequency bands) for supporting seamless out/indoor navigation. A methodology for processing the measurement results based on fusion of these techniques, its significance and the expected findings are presented in the paper.

Keywords. Dual-frequency smartphone, navigation, GNSS, Wi-Fi

LBS 2021
16th Conference on Location Based Services
24-25 November 2021 Online

Published in "Proceedings of the 16th International Conference on Location Based Services (LBS 2021)", edited by Anahid Basiri, Georg Gartner and Haosheng Huang, LBS 2021, 24-25 November 2021, Glasgow, UK/online.

https://doi.org/10.34726/1752 | © Authors 2021. CC BY 4.0 License.

1. Introduction

Until now, many measurement technologies based on different sensors have been used for indoor navigation. In outdoor navigation, the most important is positioning with GNSS. GNSS performance in out- to indoor transitional environments remains one of the most challenging problems due to inability to use satellites indoors. An indoor cooperative positioning (CP) system was deployed for this purpose. So far CP systems have demonstrated to be useful for positioning of mobile platforms navigating in challenging GNSS, as well as GNSS-denied environments (Wan et al. 2014; Rantakokko et al. 2011). The CP approach relies on information exchange in an inter-connected network of multiple nodes that could be static (called anchor or infrastructure nodes) or dynamic (such as Unmanned Aerial Vehicles (UAVs), pedestrians, vehicles, robots, etc.) in nature (Alam & Dempster 2013, Bargshady et al. 2010). Various CP systems-based on various sensors such as Ultra-Wide Band (UWB) (Chen et al. 2013), Wireless Fidelity (Wi-Fi) (Chen et al. 2009) were developed. Also Bluetooth, or other similar sensors (Savic & Zazo 2013) have been investigated in the literature. These positioning systems can be classified according to their type of sensor observations), type of processing architecture used and the presence or absence of static anchors. However, one of the major limitations of distributed algorithms is the presence of unknown correlation among the states of the nodes (Carrillo-Arce et al. 2013). Various distributed algorithms, such as Belief Propagation (BP) and the Covariance Intersection Filter (Hlinka et al. 2014) have been proposed for CP. Inclusion of static anchor (i.e., infrastructure) nodes has been shown to improve localization accuracy (Goel et al. 2018). On the other hand, anchor-free (or peer-to-peer (P2P) cooperative systems do not rely on the presence of a fixed infrastructure and can use ad hoc networks for positioning. In completely GNSS-denied environments, such as an indoor environment, a CP network can be best utilized by realization of the sufficient number of static anchor nodes, whose precise location is known in advance. Various authors have demonstrated the use of alternative positioning technologies for positioning in GNSS-denied environments (see e.g. Alam & Dempster 2013).

Compared to outdoor positioning, there is still no generally valid solution for indoor positioning. In buildings, a variety of technologies are available that are already installed on site and can be used for indoor positioning, such as infrared, Bluetooth, Wi-Fi, etc. (Bai et al. 2014, Chen et al. 2012). With smartphones, however, the selection of sensors and receivers and their quality differ depending on the device, which means that the position solution can also be influenced differently. In the literature there are different approaches for position determination, which can be divided into cell-based methods (Cell of-Origin CoO), Time of Arrival (ToA) or Round Trip Time (RTT) as well as Angle of Arrival (AoA) measurements, hyperbolic

trilateration (Time Difference of Arrival TDoA), scene analysis with measured signal strengths (Received Signal Strength RSS) and digital images as well as fingerprinting (Stojanović & Stojanović 2014). In vision-based positioning, scene analysis involves examination and matching a video/image or electromagnetic characteristics viewed or sensed from a target object (Robertsone & Cipolla 2012, Stojanović & Stojanović 2014). Another technique involves the matching of perspective images of the environment captured by a camera, carried by a person (e.g. camera in the smartphone) or mounted on a mobile robot platform, to prerecorded images or videos which have been collected to build-up 3D models stored in an image/video database. Furthermore, visual odometry with sequentially captured images can be performed while the user is walking along his trajectory (Kazemipur et al. 2013).

In this study, the selected method is trilateration fusing dual frequency Wi-Fi/GNSS smartphone observations.

2. Research Concept

2.1. Principles of Related and Novel Approach

With reference to the developed methods discussed in the introduction, Figure 1 presents our concept of a new approach that can be used in indoor navigation. The novel approach integrates dual frequency Wi-Fi in the 2.4 and 5 GHz frequency band and dual frequency GNSS (in the case of GPS the L1 and L5 signals) measurements.

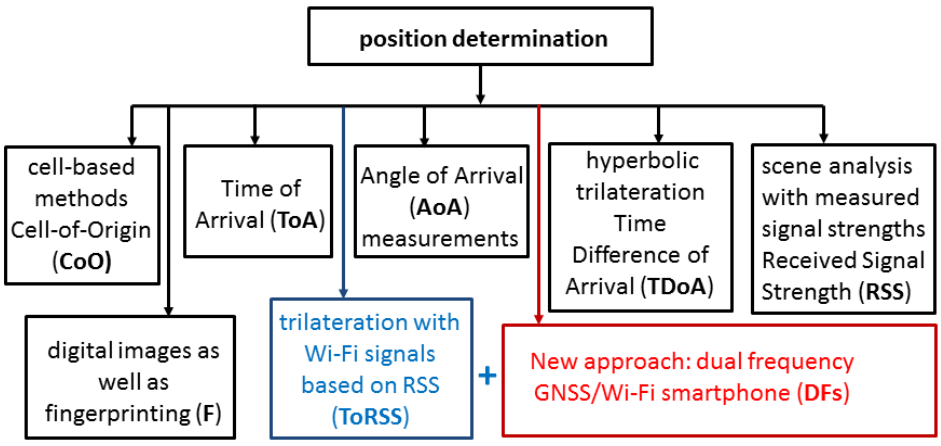

Figure 1. Related and new approach (source: own study)

2.2. Detailed Research Methodology

The main research aim is to investigate and prove the usefulness of emerging wireless sensing data for indoor positioning. Such a solution allows for real-time visualization of the location of people, materials, and equipment. The ability to calculate trajectories holds tremendous potential for indoor localization and visualization, especially if linked to Wi-Fi wireless sensing technologies. Making uses of such technology, we can provide two key pieces of spatial information: (1) the coordinates of objects needed for localization; and (2) the topology and geometry needed to navigate inside the building. Localization sensing technology can provide location and time information. Many various circumstances may appear where poor visibility makes detection of utilities difficult for a worker, causing problems to remain unnoticed and resources to remain inoperative. In such a situation, where this problem is located, additional time is lost while relaying the information to the facility manager for guidance on the necessary corrective measures that must be taken. Moreover, workers unfamiliar with a facility may have difficulties locating themselves, as well as locating a specific room within a facility. It is also very important that the facility can be navigated quickly in the event of an emergency, because a search and rescue crew has no time to waste in getting lost when human lives are the most important. Proposed research solution may provide working personnel, or emergency crews precise location information to navigate around and find their destinations.

Achieving the main goal of our tests requires the following research tasks:

1. Preparation of optimal Wi-Fi network calibration algorithms.
2. Verification of Wi-Fi network based on indoor positioning algorithms.
3. Development of intelligent positioning method using GNSS smartphone module in outdoor environments.
4. Refinement of the RTT method for reducing the number of RSSI data.
5. Implementation and refinement of integrated navigation software for testing positioning accuracy.

3. Significance and Expected Findings

As a result of the conducted research, we expect to obtain the following findings:

1. The most accurate position information being outdoors with various GNSS positioning techniques (mostly Real-time Kinematic RTK) using a dual frequency L1/L5 GNSS smartphone.
2. Indoor navigation software using RSSI data and RTT measurements obtained simultaneously from 2.4 and 5 GHz mobile Wi-Fi routers.

3. The emergence of a new calibration method based on least square fit algorithms for different distances to calculate parameters for obtaining the most accurate range information to all mobile routers serving as anchors.
4. A prototype indoor navigation software implemented on Android-based smartphones.
5. Evaluation of the accuracy of the proposed integrated navigation system.

4. Conclusion

The development of a method and algorithm for seamless and combined out-/indoor navigation integrating dual frequency GNSS and dual band Wi-Fi on smartphones will respond to the user's needs for indoor navigation providing the starting point for innovation and development.

References

Alam N, Dempster A G, (2013) Cooperative positioning for vehicular networks: Facts and future. IEEE Trans. Intell. Transp. Syst. doi.org/10.1109/TITS.2013.2266339

Bai Y B, Wu S, Retscher G, Kealy A, Holden L, Tomko M, Borriak A, Hu B, Wu H R, Zhang K (2014) A new method for improving Wi-Fi-based indoor positioning accuracy. J. Locat. Based Serv. doi.org/10.1080/17489725.2014.977362

Bargshady N, Alsindi N A, Pahlavan K, Ye Y, Akgul F O (2010) Bounds on performance of hybrid WiFi-UWB cooperative RF localization for robotic applications, in: IEEE International Symposium on Personal, Indoor and Mobile Radio Communications, PIMRC. doi.org/10.1109/PIMRCW.2010.5670379

Carrillo-Arce L C, Nerurkar E D, Gordillo J L, Roumeliotis S I (2013) Decentralized multi-robot cooperative localization using covariance intersection, in: IEEE International Conference on Intelligent Robots and Systems. doi.org/10.1109/IROS.2013.6696534

Chen X, Gao W, Wang J (2013) Robust all-source positioning of UAVs based on belief propagation. EURASIP J. Adv. Signal Process. doi.org/10.1186/1687-6180-2013-150

Chen R, Pei L, Liu J, Leppäkoski H (2012) WLAN and bluetooth positioning in smart phones, in: Ubiquitous Positioning and Mobile Location-Based Services in Smart Phones. doi.org/10.4018/978-1-4666-1827-5.ch003

Chen, Y.T., Yang, C.L., Chang, Y.K., Chu, C.P., 2009. A RSSI-based algorithm for indoor localization using ZigBee in wireless sensor network, in: Proceedings: DMS 2009 - 15th International Conference on Distributed Multimedia Systems.

Goel S, Kealy A, Lohani B (2018) Development and experimental evaluation of a low-cost cooperative UAV localization network prototype. J. Sens. Actuator Networks. doi.org/10.3390/jsan7040042

Hlinka O, Sluciak O, Hlawatsch F, Rupp M (2014) Distributed data fusion using iterative covariance intersection, in: ICASSP, IEEE International Conference on Acoustics, Speech and Signal Processing - Proceedings. doi.org/10.1109/ICASSP.2014.6853921

Kazemipur B, Syed Z, Georgy J, El-Sheimy N (2013) Vision-based real-time estimation of smartphone heading and misalignment, in: 26th International Technical Meeting of the Satellite Division of the Institute of Navigation, ION GNSS 2013.

Rantakokko J, Rydell J, Strömbäck P, Händel P, Callmer J, Törnqvist D, Gustafsson F, Jobs M, Grudén M (2011) Accurate and reliable soldier and first responder indoor positioning: Multisensor systems and cooperative localization. IEEE Wirel. Commun. doi.org/10.1109/MWC.2011.5751291

Robertsone D, Cipolla R (2012) An Image-Based System for Urban Navigation. doi.org/10.5244/c.18.84

Savic V, Zazo S (2013) Cooperative localization in mobile networks using nonparametric variants of belief propagation. Ad Hoc Networks. doi.org/10.1016/j.adhoc.2012.04.012

Stojanović D H, Stojanović N M (2014) Indoor Localization and Tracking: Methods, Technologies and Research Challenges. Facta Univ. Ser. Autom. Control Robot.

Wan J, Zhong L, Zhang F (2014) Cooperative localization of multi-UAVs via dynamic non-parametric belief propagation under GPS signal loss condition. Int. J. Distrib. Sens. Networks. doi.org/10.1155/2014/562380

Towards C-ITS-based communication between bicycles and automated vehicles

Simon Gröchenig, Karl Rehrl

Salzburg Research, Jakob Haringer Straße 5/3, 5020 Salzburg, Austria

Abstract. Cooperative Intelligent Transport Systems (C-ITS) technologies will play a significant role in the communication of automated vehicles. So far, vulnerable road users such as cyclists or pedestrians are often excluded from the communication and therefore are not able to actively create awareness for themselves. The Austrian research project Bike2CAV aims at improving bicyclists' safety via Cooperative Intelligent Transport Systems (C-ITS) technologies. The work introduces the implemented prototype of a C-ITS-enabled helmet consisting of a GNSS (Global Navigation Satellite System) device (XSens MTi 680G) to determine the current location and two additional IMUs (MetamotionR by Mbientlab) mounted on the left and right hand to recognize turn intentions indicated by hand signals. The overall goal is to evaluate the C-ITS-prototype in real-world situations, especially whether localization accuracies (0.1 m accuracy at 95% confidence) can be achieved. For the LBS 2021 conference, first results will be available.

Keywords. C-ITS, Vulnerable Road User, Road Safety

1. Introduction

According to the European Road Safety Council, 47% of all killed people on the road are vulnerable road users (pedestrians, cyclists, motorcyclists) and 83% of those deaths are caused by collisions with motorized vehicles (Adminaité-Fodor and Jos 2020). Since cycling is experiencing a boom in many countries (Nikolaeva et al. 2019), without dedicated measures, cycling safety will further be at risk. Beside safety-related improvements of the cycling infrastructure and regulatory measures (being considered by far most important) (Loidl and Zagel 2014), smart cycling accessories or wearables can contribute to enhanced safety, e.g. by making cyclists more visible for motorized vehicles (Oliveira et al. 2021). Furthermore, it is expected that progress in vehicle automation is able to lower risks, also for cyclists, but at

LBS 2021
16th Conference on Location Based Services
24-25 November 2021 Online

Published in "Proceedings of the 16th International Conference on Location Based Services (LBS 2021)", edited by Anahid Basiri, Georg Gartner and Haosheng Huang, LBS 2021, 24-25 November 2021, Glasgow, UK/online.

https://doi.org/10.34726/1753 | © Authors 2021. CC BY 4.0 License.

the same time new challenges arise (Botello et al. 2019; Sandt and Owens 2017). While automation can contribute to lower or avoid human errors, the reliable recognition of cyclists by automated vehicles' perception systems is still in its infancies (Ahmed et al. 2019).

The Austrian research project Bike2CAV[1] aims at improving bicyclists' safety via Cooperative Intelligent Transport Systems (C-ITS) technologies. C-ITS technologies such as ETSI ITS-G5 (Festag 2014) will play a significant role in the communication of automated vehicles (e.g. to share positions and intentions or to warn each other) and between vehicles and road operators via so-called roadside ITS stations (e.g. to get information on the state of the infrastructure). These technologies are worked out in Europe by the C-Roads Platform[2] and the Car2Car Communication Consortium[3] and standardized by ETSI[4]. So far, vulnerable road users such as cyclists or pedestrians are often excluded from the communication and therefore are not able to actively create awareness for themselves. In Bike2CAV, this should be changed by enabling bicycles to send Cooperative Awareness Messages (CAMs) (ETSI EN 302 637-2 2019) being received by other C-ITS-enabled vehicles, bicycles or roadside ITS stations. Besides raising awareness, automated vehicles and cyclists should be further warned by Decentralized Environmental Notification Messages (DENMs) (ETSI EN 302 637-3 2019) in case of collision risk situations. Such collision risks should be primarily detected based on CAMs but being also supported by environmental perception from the automated vehicle, the bicycle (via mounted radar or LiDAR sensors) as well as sensor-equipped intersections for local perception. Perceived moving objects are communicated via Cooperative Perception Messages (CPM) (ETSI TR 103 562 2019) which should contribute to a more reliable perception. Beside reliable perception and C-ITS-based communication, the main challenge arises from highly accurate localization of moving objects such as automated vehicles and cyclists (0.1 m accuracy; 0.95 % confidence) (Reid et al. 2019). In order to achieve high localization accuracies and to enable bicycles with C-ITS technology, the approach going to be evaluated in Bike2CAV is twofold: On the one hand, a multi-sensor enabled smart bike (Holoscene Edge Bike) from Boreal Bikes[5] with built-in ITS-G5 capability is used. On the other hand,

[1] https://www.bike2cav.at/

[2] https://www.c-roads.eu/

[3] https://www.car-2-car.org/

[4] https://www.etsi.org/

[5] https://www.borealbikes.com

a proof-of-concept prototype of a C-ITS-enabled bicycle helmet with high-quality localization as well as C-ITS-communication is evaluated.

This work introduces the implemented prototype of a C-ITS-enabled helmet consisting of a GNSS (Global Navigation Satellite System) device (XSens MTi 680G) to determine the current location and two additional IMUs (MetamotionR by Mbientlab) mounted on the left and right hand to recognize turn intentions indicated by hand signals. A Raspberry Pi 4 device is acting as a local data hub for collecting data from both data sources, wrapping positions and indicated directions into a CAM and sending it via C-ITS IP Based Interface Profile of the C-Roads Specification Version 1.8[6] to a C-ITS broker that distributes the messages to registered roadside ITS stations or other vehicles and bicycles. The broker assembles CAMs to position trajectories, map-matches these trajectories in near real-time onto a local high definition (HD) map and calculates intersection collision risks (ETSI TS 101 539-2 2018). In case of detected collision risks, collision risk warnings (DENMs) are generated and distributed to all connected vehicles or bicycles. The overall goal is to evaluate the proof-of-concept-prototype in real-world situations, especially whether localization accuracies (0.1 m accuracy at 95% confidence) can be achieved.

2. Methodology

This section introduces the bicycle C-ITS prototype and the message broker.

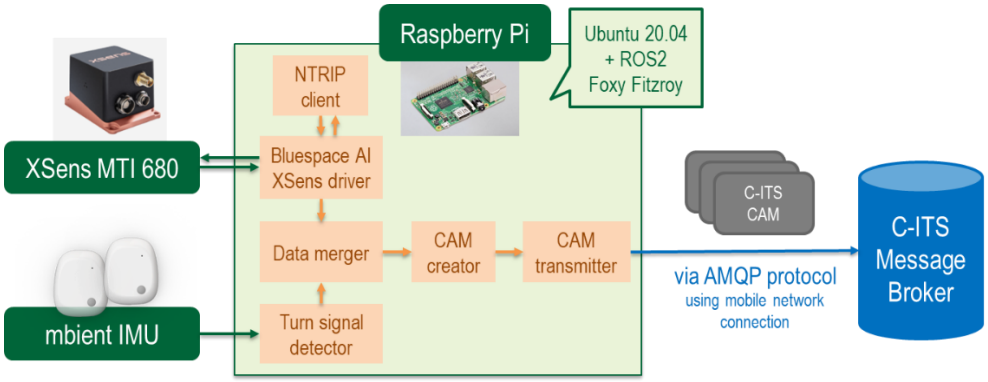

Figure 1. Components of the prototypical acquisition device; green components are devices, orange boxes and lines show ROS nodes and topics, blue represents the C-ITS broker (images © xsens.com, raspberrypi.com, mbientlab.com)

[6] https://www.c-roads.eu/fileadmin/user_upload/media/Dokumente/Harmonised_specs_text.pdf

As mobile data collection node, the prototype uses a Raspberry Pi 4 Model B set up with Ubuntu 20.04 and ROS 2.0 Foxy Fitzroy. All components (Figure 1) of the prototype are introduced in the following list. Technically, these components are ROS[7] nodes that process, subscribe and publish data to each other.

- **XSens MTi driver** reads multi-frequency GNSS locations from the XSens MTi 680G device. The GNSS locations are improved by RTK and an internal filter algorithm using INS data. The latter especially improves localization in areas with limited GNSS coverage. The applied ROS node is forked from the XSens MTI driver for ROS 2.0 developed by Bluespace AI[8], which itself is based on the official XSens driver being only compatible with ROS 1.0. For the prototype, this driver is enhanced to forward NRTK messages to the XSens device. A RTK- and INS-enhanced localization device has been selected in order to meet the proposed positional accuracy targets, which are required for the intended collision detection.
- **Ntrip client** retrieves RTCM (Radio Technical Commission for Maritime Services) messages from a NRTK (Network Real Time Kinematics) service and provides the correction data to the XSens device in order to improve the precision of the GNSS coordinates. The client implemented for the work[9] is based on the implementation offered by XSens (XSens Base 2021). Modifications on the ROS node for this work include the upgrade to ROS 2.0 and the continuous sending of NMEA messages at a 5-second interval.
- **Turn signal detector** reads left and right hand signals to indicate direction or lane changes. The signals are detected from data acquired with IMUs (MetamotionR by Mbientlab) attached to the cycling gloves in real time. The data is transferred via Bluetooth to the turn signal detector ROS node.
- **Data collector/merger** collects the GNSS and turn signal data and merges both to a bicycle data message that is forwarded to the CAM creator. The component also calculates the motion attributes speed and heading from the RTK- and INS-corrected GNSS data.
- **CAM creator** builds CAM (ETSI TS 102 894-2 2014) in XML format from the data stored in the received bicycle message. Due to

[7] https://www.ros.org/

[8] https://github.com/bluespace-ai/bluespace_ai_xsens_ros_mti_driver

[9] https://github.com/SGroe/ntrip_client_ros2

missing dedicated parameters, bicyclist's turn signals are written to the leftTurnSignalOn and rightTurnSignalOn fields within the exteriorLights element of the BasicVehicleContainerLowFrequency.

- **CAM transmitter** sends CAMs via Apache QPID and S-AMQP (Secure Advanced Message Queuing Protocol) to a C-ITS message broker (edge computing node) following the C-Roads C-ITS IP Based Interface Specification 1.8.0.

Challenges during the development of the prototype primarily arose from the two major ROS versions, namely ROS 1.0 and ROS 2.0. Each version is built and recommended for a specific version of Ubuntu and Python. Consequently, all available ROS nodes and required dependencies are implemented for a specific ROS/Ubuntu/Python version. For instance, the official XSens MTI driver is built for ROS 1.0; however, there exists an upgraded version from a third-party company.

Apart from the bicycle prototype, the second major component of the collision detection system is an edge-computing node including a C-ITS broker (Apache ActiveMQ® Artemis[10]) as well as the collision detection module. This broker receives CAMs from the prototype as well as CAMs and CPMs from connected and automated vehicles and a roadside ITS station being enhanced by a camera-based perception system. The further processing of all messages is done on the edge-computing node. Figure 2 shows an exemplary trajectory moving across an intersection represented by a local HD map.

[10] https://activemq.apache.org/components/artemis/

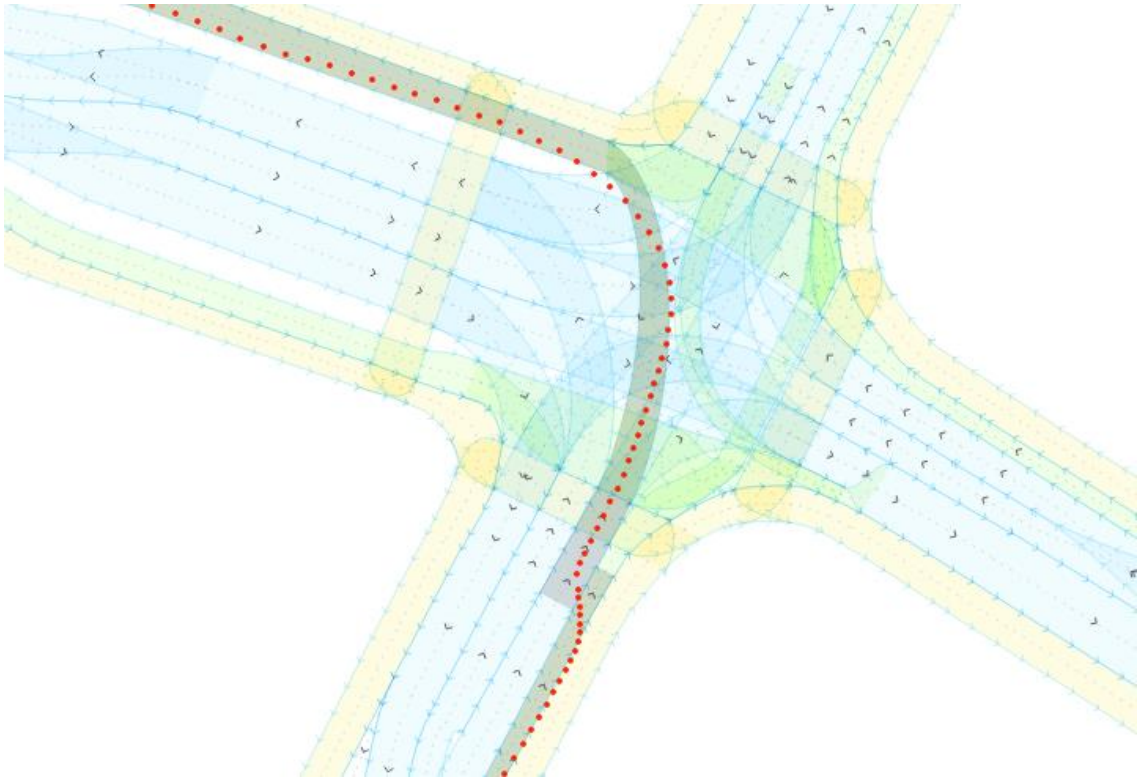

Figure 2: Extract of a trajectory (red points) visualized on a HD map; map-matched HD segments are highlighted grey

2.1. Next Steps and Expected Findings

On the one hand, the localization accuracy of the prototype will be evaluated. This is done by matching the position trajectories of test drives on a lane-accurate HD map including bicycle infrastructure. It should be evaluated whether lane-accurate localization for bicycles can be achieved. On the other hand, algorithms for detecting collision risks for cyclists will be evaluated. The hypothesis is that lane-accurate localization in combination with cyclists' intentions and HD map matching can contribute to improve the detection of collision risks in real-world scenarios (especially at risky intersections). First results are expected for the 2021 LBS symposium.

Acknowledgement

Funded by the Austrian Federal Ministry for Climate Action, Environment, Energy, Mobility, Innovation and Technology.

References

Adminaité-Fodor, Dovilé, and Graziella Jos. 2020. “How Safe Is Walking and Cycling in Europe? Pin Flash Report 38.” 2020. https://etsc.eu/wp-content/uploads/PIN-Flash-38_FINAL.pdf.

Ahmed, Sarfraz, M. Nazmul Huda, Sujan Rajbhandari, Chitta Saha, Mark Elshaw, and Stratis Kanarachos. 2019. “Pedestrian and Cyclist Detection and Intent Estimation for Autonomous Vehicles: A Survey.” *Applied Sciences 2019, Vol. 9, Page 2335* 9 (11): 2335. https://doi.org/10.3390/APP9112335.

Botello, Bryan, Ralph Buehler, Steve Hankey, Andrew Mondschein, and Zhiqiu Jiang. 2019. “Planning for Walking and Cycling in an Autonomous-Vehicle Future.” *Transportation Research Interdisciplinary Perspectives* 1 (June): 100012. https://doi.org/10.1016/J.TRIP.2019.100012.

ETSI EN 302 637-2. 2019. “ETSI EN 302 637-2 V1.4.1 (2019-04), Intelligent Transport Systems (ITS); Vehicular Communications; Basic Set of Applications; Part 2: Specification of Cooperative Awareness Basic Service.”

ETSI EN 302 637-3. 2019. “ETSI EN 302 637-3 V1.3.1 (2019-04) ETSI EN 302 637-3 V1.3.1 (2019-04) Intelligent Transport Systems (ITS); Vehicular Communications; Basic Set of Applications; Part 3: Specifications of Decentralized Environmental Notification Basic Service.” ETSI. https://www.etsi.org/deliver/etsi_en/302600_302699/30263703/01.03.01_60/en_30263703v010301p.pdf.

ETSI TR 103 562. 2019. “ETSI TR 103 562 V2.1.1 (2019-12) Intelligent Transport Systems (ITS); Vehicular Communications; Basic Set of Applications; Analysis of the Collective Perception Service (CPS); Release 2.” ETSI. https://www.etsi.org/deliver/etsi_tr/103500_103599/103562/02.01.01_60/tr_103562v020101p.pdf.

ETSI TS 101 539-2. 2018. “ETSI TS 101 539-2 V1.1.1 (2018-06), Intelligent Transport Systems (ITS); V2X Applications; Part 2: Intersection Collision Risk Warning (ICRW) Application Requirements Specification.”

ETSI TS 102 894-2. 2014. “ETSI TS 102 894-2 v1.2.1 (2014-09) Intelligent Transport Systems (ITS); Users and Applications Requirements; Part 2: Applications and Facilities Layer Common Data Dictionary.”

Festag, Andreas. 2014. “Cooperative Intelligent Transport Systems Standards in Europe.” *IEEE Communications Magazine* 52 (12): 166–72. https://doi.org/10.1109/MCOM.2014.6979970.

Loidl, Martin, and Bernard Zagel. 2014. “Assessing Bicycle Safety in Multiple Networks with Different Data Models.” In *GI_Forum 2014. Geospatial Innovation for Society*, edited by R. Vogler, Adrijana Car, Josef Strobl, and Gerald Griesebner, 144–54. Wichmann Verlag.

Nikolaeva, Anna, Marco te Brömmelstroet, Rob Raven, and James Ranson. 2019. “Smart Cycling Futures: Charting a New Terrain and Moving towards a Research Agenda.” *Journal of Transport Geography* 79 (July): 102486. https://doi.org/10.1016/J.JTRANGEO.2019.102486.

Oliveira, Franklin, Dilan Nery, Daniel G. Costa, Ivanovitch Silva, and Luciana Lima. 2021. “A Survey of Technologies and Recent Developments for Sustainable Smart Cycling.” *Sustainability 2021, Vol. 13, Page 3422* 13 (6): 3422.

https://doi.org/10.3390/SU13063422.

Reid, Tyler G.R., Sarah E. Houts, Robert Cammarata, Graham Mills, Siddharth Agarwal, Ankit Vora, and Gaurav Pandey. 2019. "Localization Requirements for Autonomous Vehicles." *SAE International Journal of Connected and Automated Vehicles* 2 (3): 173–90. https://doi.org/10.4271/12-02-03-0012.

Sandt, Laura, and Justin M Owens. 2017. "Discussion Guide for Automated and Connected Vehicles, Pedestrians, and Bicyclists." Washington, DC.

XSens Base. 2021. "Using an NTRIP Client with the Xsens ROS Driver." 2021. https://base.xsens.com/knowledgebase/s/article/Using-an-NTRIP-client-with-the-Xsens-ROS-driver?language=en_US.

Crime Prevention on the Edge: Designing a Crime-Prevention System by Converging Multimodal Sensing with Location-Based Data

Amna Anwar, Eiman Kanjo

Smart Sensing Lab, Nottingham Trent University
amna.anwar@ntu.ac.uk, eiman.kanjo@ntu.ac.uk

Abstract. Emerging technological innovations have been developed in recent years to prevent crime and enhance public safety. This paper evaluates the recent advances in ubiquitous sensing and pervasive computing to ultimately propose a multimodal crime prevention tool which incorporates several technologies into a single wearable device. The crime prevention tool proposed combines Bluetooth Low Energy (BLE) technology to sense the social context of a person with a violent language sound-based detection system which aims at the real-time spotting of violent behaviours and threats to victims of domestic abuse. The system is currently being developed to safeguard and protect vulnerable individuals.

Keywords. Bluetooth Low Energy (BLE), Crime Prevention, Proximity detection

1. Introduction

Ubiquitous computing for the purpose of crime prevention is a constantly improving subject with a huge impact on society's security and safety. Through the development of edge computing tools and methodologies, cities and the people that live in them can be made even safer through the integration of unobtrusive novel technologies.

The use of technology in crime prevention has been explored in a variety of work, for example applications, such as the tracking of terrorist suspects to gain insights into their spatial and temporal behaviour, have recently been proposed by Griffiths, G et al (2017). Overall, as outlined by Belur, J et al

LBS 2021
16th Conference on Location Based Services
24-25 November 2021 Online

Published in "Proceedings of the 16th International Conference on Location Based Services (LBS 2021)", edited by Anahid Basiri, Georg Gartner and Haosheng Huang, LBS 2021, 24-25 November 2021, Glasgow, UK/online.

https://doi.org/10.34726/1754 | © Authors 2021. CC BY 4.0 License.

(2020), electronic monitoring is an effective tool towards preventing recidivism, especially for sex offenders.

Despite the wider subject being explored by a number of researchers, our work focuses on merging the use of natural language processing and wearable devices.

Our system proposes a novel low-cost wearable device to equip vulnerable individuals with a tool to protect them against violent behaviours, by the use of a multimodal approach based on the evaluation of their social context with BLE technology and the detection of violent language by combining audio processing, machine learning and natural language processing (NLP) techniques. Our existing work has attempted to curate and process a natural language dataset to improve the identification and detection of harmful language. We are now looking to integrate this algorithm on-device alongside location-based sensor data to assist in the real time detection and prevention of violent or harmful language.

This paper is split into four sections, the next section presents the methodologies used throughout the study. *Section 3* is a discussion of the limitations and opportunities of the work. Finally, *Section 4* provides a conclusion and highlights the focus of future studies.

2. Methodology

The proposed system makes use of edge computing to enable onboard complex computations that support the safety of vulnerable individuals. By implementing multimodal data algorithms, including proximity detection using BLE technology and sentiment analysis techniques based on sound and language, the proposed system supports enhanced feedback and monitoring of potential threats and issues. Feedback and notifications are algorithmically triggered to alert authorities or designated contacts of an emergency while presenting the generated information for decisions to be made.

The wearable device includes proximity detection techniques to provide instant information about suspicious behaviour nearby. Along with this, the wearable also integrates violent language detection through Natural Language Processing (NLP) of relevant captured data to safeguard victims. The data generated through both sensing modalities are then combined to support further actions or decisions.

2.1. Proximity Detection

The two most used and known location-based technologies to track and monitor people include radio frequency and the Global Positioning System (GPS) (J. Tully, 2014). However, in recent years there has been an increase attention to BLE probe requests for crowd monitoring (Rekimoto, J et al, 2007) and social context analysis (Anderez D et al, 2020) (Woodward K, 2020).

Our current experiments with different technologies show the continuous broadcasting done by BLE transceivers is more convenient than the interception of intermittent probes sent by WiFi antennas. In line with this, we propose the use of BLE for proximity detection to ensure regular offenders keep their legal distance from the victims and an alert is triggered automatically if the victims are at risk. By monitoring offenders' approximate location to vulnerable individuals (using their phones or enforced tag) enables the detection of suspicious activities such as stalking. *Figure 1* shows how the alerts are sent out depending on the proximity of the devices of interest.

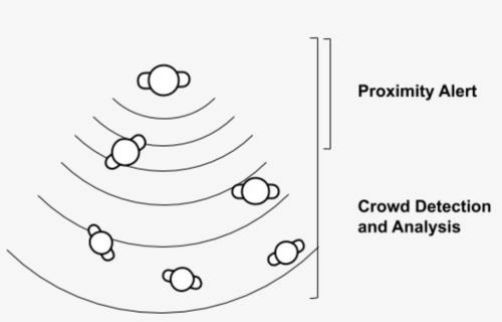

Figure 1. A diagram showing how the proposed proximity alerts will be sent.

3. Challenges and Opportunities

The collected dataset provides useful usability for the outlined purpose of the project; however, we identified a number of challenges that should be taken into consideration:

Privacy - There exist some concerns about data sharing and access to personal information. We propose to process the data locally and only communicate the output of the detection algorithms remotely (alert to police or a family member).

Battery Life - Battery life is another factor that is being tested as the project progresses as the higher the processing power required, the quicker the battery drains. This challenge can be overcome by incorporating adequate hardware for high processing computations.

Processing power - To preserve data we aim to process data locally on the device using edge-computing, however this can be challenging depending on the processing power required. Edge devices are evolving and making strong leaps in advancing its processing power.

4. Conclusion

In this paper we presented our work in progress research relating to the merging of on-device sensor data and a natural language processing algorithm to detect violent or harmful language. Our preliminary results highlight the importance of the multi modal approach as the combination of audio text and BLE for crime prevention has not been explored and the need to further research how this approach can be integrated into an environment like that. We hope to continue the development of our wearable device and further develop the idea behind using location-based technologies alongside Bluetooth and Wi-Fi sensing as part of the project.

The crime prevention system proposed combines different sensing technologies with signal processing and machine learning techniques for ensuring the safety of vulnerable individuals. The rationale of this project is certainly the need for a system of these characteristics, as expressed by several project collaborators (Police and victim support charities).

The research challenges and the limitations of existing technologies suggests that the use of edge computing embedded in unobtrusive wearable devices can help the society to live a better and safer life. Future work will be focused on the implementation and experimental evaluation of the system. The incorporation of additional sensing technologies will be also studied and evaluated.

References

Anderez, D. O., Kanjo, E., Pogrebna, G., Kaiwartya, O., Johnson, S. D., & Hunt, J. A. (2020). A COVID-19-based modified epidemiological model and technological approaches to help vulnerable individuals emerge from the lockdown in the UK. Sensors, 20(17), 4967.

Belur, J., Thornton, A., Tompson, L., Manning, M., Sidebottom, A., & Bowers, K. (2020). A systematic review of the effectiveness of the electronic monitoring of offenders. Journal of Criminal Justice, 68, 101686.

Griffiths, G., Johnson, S. D., & Chetty, K. (2017). UK-based terrorists' antecedent behavior: A spatial and temporal analysis. Applied geography, 86, 274-282.

Rekimoto, J., Miyaki, T., & Ishizawa, T. (2007, September). LifeTag: WiFi-based continuous location logging for life pattern analysis. In LoCA (Vol. 2007, pp. 35-49).

Tully, J., Hearn, D., & Fahy, T. (2014). Can electronic monitoring (GPS 'tracking') enhance risk management in psychiatry?. The British journal of psychiatry, 205(2), 83-85.

Woodward, K., Kanjo, E., Anderez, D. O., Anwar, A., Johnson, T., & Hunt, J. (2020, November). DigitalPPE: low cost wearable that acts as a social distancingreminder and contact tracer. In Proceedings of the 18th Conference on Embedded Networked Sensor Systems (pp. 758-759).

Employee Location Tracking in Retail Stores

Caner Guney*, Emre Tuncel**, Hakan Ulagan**

* Istanbul Technical University, Department of Geomatics Engineering, 34469, Istanbul, TURKEY
** Opthema Teknoloji, 34485, Istanbul, TURKEY

Abstract. Indoor Positioning System generally uses radio signals, visual data or other types of sensor data to determine where assets such as people and objects are located. There are many different indoor solutions and products used in different application areas from smart transportation in smart cities to contact tracking, location-based games to retail. The offered solutions and/or systems by companies for indoor localization, indoor navigation with context-aware provide different accuracy, reliability, installation and maintenance costs according to the techniques and technologies chosen for the purpose. In this study, an innovative hybrid solution is proposed that will bring a different approach to personnel monitoring in a store that will increase productivity in the retail industry. Within the scope of the study, the indoor location determination process will be carried out by using radio frequency and image data together. Map and/or trajectory fusion will be used to integrate different types of results from different sensors. Spatial decision support approach will be used in directing the salesperson to the busy areas in the store.

Keywords. Indoor Positioning, Indoor Tracking, Wireless Radio Technologies, Vision-Based Technologies, Retail Store Efficiency

1. Introduction

The retail industry pays attention to every detail regarding its customers in order to increase its profitability rates. Many technological approaches are used effectively in the retail marketing, such as store cards, customer phone numbers, customer's smartphones, social media, discount campaigns, and data science analysis of which product and how much customers consume. However, it is seen that new technological applications that have become

Published in "Proceedings of the 16th International Conference on Location Based Services (LBS 2021)", edited by Anahid Basiri, Georg Gartner and Haosheng Huang, LBS 2021, 24-25 November 2021, Glasgow, UK/online.

https://doi.org/10.34726/1755 | © Authors 2021. CC BY 4.0 License.

widespread in the retail sector generally focus on the customer and the product. In the scope of this study, innovative solutions for store employee, which is another pillar of the sector, are included. By using the proposed innovative hybrid solution, it is targeted that the store sales team will work more efficiently and effectively, thus improving the loyalty of the customers to the store and their shopping continuity, and ultimately improving the productivity of the store.

To determine whether the customers visiting the store receive the attention they expect regarding the products they are interested in, quickly and appropriately from the store employees a long with to increase the satisfaction of the customers regarding the services they receive from the store employees, a Virtual Merchandisor (vMerch)-Team" has been developing.

The vMerch-Team solution provides real-time tracking of store employees with indoor positioning technologies. Thus, the behaviors and activities of employees, both individually and as a team, can be monitored in the store. The performances of store employees are evaluated with data sets obtained as a result of monitoring over business intelligence approaches.

In summary, vMerch-Team is a solution that automatically performs the tasks of tracking store employees based on location and time. These include finding/capturing store employees, identifying and tracking employees, taking action based on customer density in store, and creating analytics such as location analytics, behavior analytics.

2. Indoor Ecosystem in Retail

Indoor Positioning System generally includes technologies and positioning methods used to determine the location of a receiver in an indoor environment. Today, however, the concept of the indoor ecosystem has expanded substantially and has evolved from indoor location determination to indoor navigation, location-based services, context-aware services and reasoning.

In indoor positioning systems and Location-Based Service applications, roughly, the location of a user is determined using generally wireless radio technology and path planning is executed for the user to reach the place of interest. In the retail sector, however, it is generally desired to follow the customer density or product in the store through indoor localization applications. Proximity Marketing can be given as an example of the prominent indoor application in the retail industry. While employee tracking is carried out with GNSS receivers in the open area, electronic personnel cards are used in enclosed environments. Such an approach through the cards produces only general information in accordance with the Personnel Attendance Control System requirements, such as the hours in which the employee is in the store and the entry-exit hours.

Although there is a wide variety of approaches using different technologies and methods in IPS domain, Radio Frequency (RF) based technology seems to be more common in practice than others. On the other hand, the rapid development of computer vision, video processing, and deep learning makes image-based localization one of the fastest-growing indoor positioning and tracking techniques.

3. The Proposed Solution: "vMerch"

In this study, Indoor Positioning was designed as a hybrid solution. Firstly, the positioning technique with wireless radio waves, in which the user interacts with the wireless sensor network via wearable devices, and secondly, the image-based positioning technique, in which the user does not interact with the system, was developed separately. Although the first technique using radio signal power and the second technique using optical image are different from each other, they are used together to produce location information. The reason why an approach in which data sets obtained from different sources in different structures is used together is preferred within the scope of the study is that both techniques have pros and cons. Thus, the solution, in which two different techniques are used in a way that supports each other, will ensure that the system works continuously with high performance and will produce reliable outputs for other systems and analyzes to be made.

Stores are cluttered and crowded environments. Additionally, crowded customers around the products may prevent the store employee from being viewed by the camera or performing the correct face recognition from the image. In these and similar cases, information about where and how long the store employee has been can be produced by wireless radio technology. On the contrary, the store employee can give his radio signal tag to another employee. In this case, this employee will be followed by being matched with a different identity. Such situations can also be avoided by using image-based systems.

The main problem to be solved in the hybrid approach proposed in the study is how to use two different techniques with different structures in an integrated manner.

Positioning approach with RF techniques is performed by signal strength and is based on RSSI value. By applying classification algorithms to RSSI values, the location information is given generally on the fingerprint map (RF-map).

In image-based technique, stereo image and depth map can be produced from RGB-D source images or using more than one camera. If a single camera is used, location information can be produced by the help of the grids pregenerated on the image.

Apart from these two spatial representations, there is also a basic map (indoor map, metric map) that reflects the geometric representation of the environment.

In this case, the solution of the problem evolves from sensor fusion to map fusion (map matching). The map fusion problem can be solved by transformation. The coordinate system from which the base map was produced should be taken as the base coordinate system and other spatial representations such as fingerprint maps should be integrated in the base coordinate system. Thus, the locations and traces of movements of employees can be visualized on the base map.

Thematic maps like heat maps produced on the subjects, such as what products the customers are particularly interested in in the store, how long the customers stay in which part of the store, or how much time they spend in which product group, were also included in the map fusion.

In summary, the map engine being developed within the scope of vMerch-Team can spatially integrate the base map with topological features and other maps such as fingerprint, grid display and thematic maps. The interface being developed also visualizes the map and map information according to the roles and rights of the user.

References

Benezeth, Y., Emile, B., Laurent, H., "Vision-Based System for Human Detection and Tracking in Indoor Environment", Int J of Soc Robotics (2010) 2: 41. https://doi.org/10.1007/s12369-009-0040-4

Duque Domingo J, Cerrada C, Valero E, Cerrada JA. An Improved Indoor Positioning System Using RGB-D Cameras and Wireless Networks for Use in Complex Environments. Sensors (Basel, Switzerland). 2017;17(10):2391. doi:10.3390/s17102391.

George Galanakis, Xenophon Zabulis, Panagiotis Koutlemanis, Spiros Paparoulis, and Vassilis Kouroumalis. 2014. Tracking persons using a network of RGBD cameras. In Proceedings of the 7th International Conference on PErvasive Technologies Related to Assistive Environments (PETRA '14). ACM, New York, NY, USA, Article 63, 4 pages. DOI: https://doi.org/10.1145/2674396.2674467

Jaime Duque Domingo, Carlos Cerrada, Enrique Valero, and J. A. Cerrada, "Indoor Positioning System Using Depth Maps and Wireless Networks," Journal of Sensors, vol. 2016, Article ID 2107872, 8 pages, 2016. doi:10.1155/2016/2107872

Leykin, A., 2007, "Visual Human Tracking And Group Activity Analysis: A Video Mining System For Retail Marketing", Doctor of Philosophy, in Computer Science and Cognitive Science, Indiana University, December 2007

Luo, Wenhan & Xing, Junliang & Milan, Anton & Zhang, Xiaoqing & Liu, Wei & Zhao, Xiaowei & Kim, Tae-Kyun. (2017). Multiple Object Tracking: A Literature Review.

Massimo Camplani, Adeline Paiement, Majid Mirmehdi, Dima Damen, Sion Hannuna, Tilo Burghardt, Lili Tao, "Multiple human tracking in RGB-depth data: a survey," in IET Computer Vision, vol. 11, no. 4, pp. 265-285, 6 2017. (UK-Bristol)

Paul, M., Haque, S.M.E. & Chakraborty, S., 2013, “Human detection in surveillance videos and its applications - a review,” EURASIP Journal on Advances in Signal Processing. (2013) 2013: 176. https://doi.org/10.1186/1687-6180-2013-176

Yilmaz, A., Javed, O., and Shah, M., 2006, “Object Tracking: A Survey”, Journal of ACM Computing Surveys (CSUR) Surveys Homepage archive, Volume 38 Issue 4, 2006, Article No. 13, ACM New York, NY, USA. (December 2006). DOI=http://dx.doi.org/10.1145/1177352.1177355

Y. Wang, K. Lu and R. Zhai, "Challenge of multi-camera tracking (Technique and Challange for Multi-Camera Tracking)," 2014 7th International Congress on Image and Signal Processing, Dalian, 2014, pp. 32-37.

R. Mautz and S. Tilch, "Survey of optical indoor positioning systems," 2011 International Conference on Indoor Positioning and Indoor Navigation, Guimaraes, 2011, pp. 1-7.

E. Trucco and K. Plakas, "Video Tracking: A Concise Survey," in IEEE Journal of Oceanic Engineering, vol. 31, no. 2, pp. 520-529, April 2006.

Building Rhythms: Reopening the Workspace with Indoor Localisation

Guilherme Spinoza Andreo*, Ioannis Dardavesis*, Michiel de Jong*, Pratyush Kumar*, Maundri Prihanggo*, Georgios Triantafyllou*, Niels van der Vaart *,**, Edward Verbree*

* Faculty of Architecture and the Built Environment, Delft University of Technology

G.SpinozaAndreo@student.tudelft.nl; I.Dardavesis@student.tudelft.nl; M.D.deJong-1@student.tudelft.nl; P.Kumar-12@student.tudelft.nl; MaundriPrihanggo@student.tudelft.nl; G.Triantafyllou-1@student.tudelft.nl; C.G.vanderVaart@tudelft.nl; e.verbree@tudelft.nl;

**Esri Nederland

Nvandervaart@esri.nl

ABSTRACT

Indoor localisation methods are an essential part for the management of COVID-19 restrictions, social distancing, and the flow of people in the indoor environment. Moving towards an open work space in this scenario requires effective real-time localisation services and tools, along with a comprehensive understanding of the 3D indoor space. This project's main objective is to analyse how ArcGIS Indoors can be used with location awareness methods to elaborate and develop space management tools for COVID--19 restrictions in order to reopen the workspace for TU Delft Campus. This was accomplished by using six Arduino micro controllers, which were programmed in C++ to scan all available Wi--Fi fingerprints in the east wing of the Faculty of Architecture and the Built Environment of TU Delft and send over the data to an ArcGIS Indoor Information Model (AIIM). The data stored on the AIIM is then accessed using the app on the user's Android device using REST Application Programming Interface

Published in "Proceedings of the 16th International Conference on Location Based Services (LBS 2021)", edited by Anahid Basiri, Georg Gartner and Haosheng Huang, LBS 2021, 24-25 November 2021, Glasgow, UK/online.

https://doi.org/10.34726/1756 | © Authors 2021. CC BY 4.0 License.

(API) where a kNN based matching algorithm then identifies the location of the user. The results show that the localisation is not consistent for rooms that are directly above each other or share common access points. However, when functioning to locate different tables inside a room, the system proved to uniquely distinguish between the specific tables. As a result, we can conclude that based on the size of the rooms, more Arduino devices should be installed to achieve an ideal accuracy. Finally, recommendations are made for the continuation of this research.

Keywords: Indoor localisation system, Wi-Fi fingerprinting, ArcGIS, Indoor model, Machine Learning

1. Introduction

Recently, the success of outdoor positioning methods has provided the means for high accuracy positioning technologies research to slowly shift towards the indoor environment (Brena et al., 2017; He & Chan, 2016; Liu et al., 2016). This new wave of indoor localisation technologies has been growing at a rapid pace, however, most of them are considered to still be in the early phases of development (Xia et al., 2017). The core aspect of Wi-Fi fingerprint localisation systems is established on the set of measurements of the signal strength from different Wireless Access Points (WAPs). They can be used as a radio-map, or reference points, that can be applied to estimate and match a location of a given device according to its signal strength (Torres et al., 2016).

Indoor models, in broad terms, are a hierarchy of unique classes of different building elements, spaces, topological and semantic information (Liebich, 2009 cited in Tran et al., 2018). Specifically, the topological information model of a building, which can be obtained from either CAD or BIM data, is the first component of creating an indoor localisation and navigation system. These 3D models are vital for the development of navigation assistance applications and emergency responses (Tran et al., 2018) .

Indoor localisation methods are an essential part for the management of COVID-19 restrictions, social distancing, and the flow of people in the indoor environment. To move towards an open workspace in a restricted occupancy scenario requires effective real-time localisation services and tools, along with a comprehensive understanding of the 3D indoor space.

This project consists of three parts which have their own goals and expectations. Accordingly, all of them are combined and each of them subdivided in more specific sections in order to form the final product. The initial one is the main goal of the ”Synthesis Project” course from the MSc Geomatics which aims to combine and apply all the knowledge, skills and insights gained during the core programme (T.U. Delft, 2020b).

The second part relates to the wider TU Delft project ”Building Rhythms” which aims to investigate the impact of COVID--19 on campus life through public data visualisations with high respect to privacy preservation (T.U. Delft, 2020a). Although the general project targets all of the campus, in this project, the focus is only about the indoor environments.

The third and last part is set by the client and stakeholders, mainly by Esri Nederland. Therefore, one of the main goals of the project is to explore the possibilities and capabilities of ArcGIS and ArcGIS Indoors with the combination of a real--time indoor location system with Fingerprinting produced by open source micro-controllers (Arduino MKR-WiFi) and a native mobile application.

To sum up, the combination of these three parts leads to the main research question of the project:

"How can ArcGIS Indoors be combined with indoor Wi-Fi fingerprinting localisation awareness techniques to create a real-time application for understanding COVID-19's impact in the indoor environment of TU Delft with high respect for privacy of the users?"

2. Methodology

The methodology of the project can be summarized into five key stages: Data Acquisition, Indoor modelling, Indoor localisation with Wi-Fi fingerprinting, and, Testing and Visualisation. The indoor model was based on (Computer Aided Design) CAD files with minor adjustments, in order to represent the current floor-plans of the Building of the Faculty of Architecture and Built Environment, TU Delft. The CAD files, combined with an excel file containing information about the layers, were imported into ArcGIS Pro, so that the CAD layers could be transformed into GIS layers.

To accomplish the scope of this project, only the ground and first floor of the Faculty's east wing were investigated. Furthermore, the database, which contains the information about the rooms of the building, was enriched with additional information, such as capacity, occupancy and room types, provided by TU Delft Campus Real Estate and Abdullah Alattas (Alattas et al., 2018). Points of Interest were created for rooms of high importance, such as offices and lecture rooms, based on which the interior network of the model was created. The created model was published in ArcGIS online portal, as a web scene, which works as the main view of the android application and the part of the end product of this project.

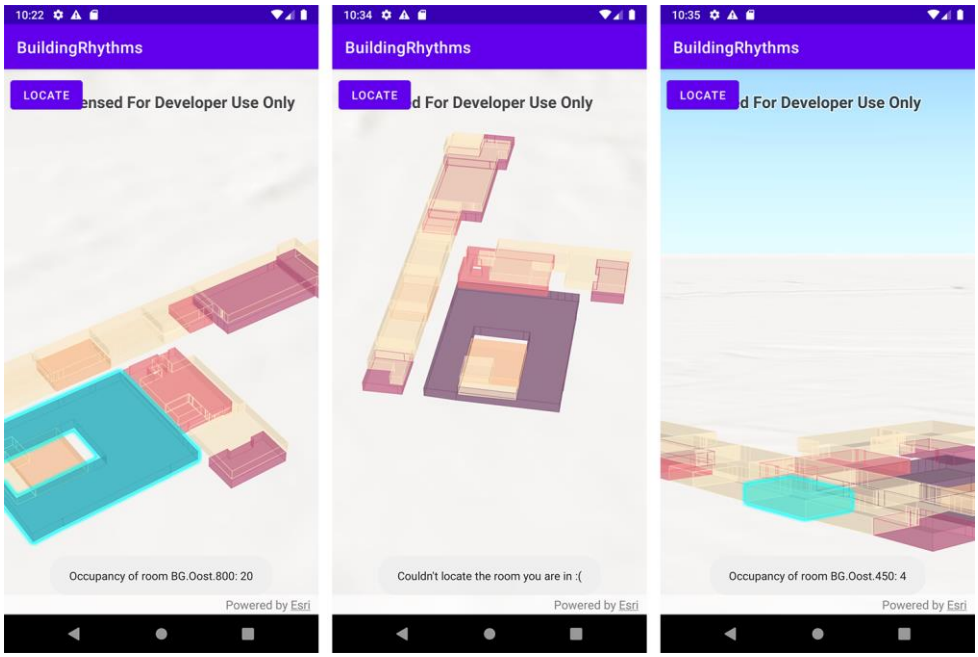

Figure 1: Android Application

To find out if live radio maps combined with Wi-Fi fingerprinting can accurately be used as an indoor localisation system, we use a setup where the rooms we want to test are equipped with a Wi-Fi enabled microcontroller which creates a live radio map of the static Wi-Fi networks at the Campus, and sends this to the server. Studies such as those from (Abdul et al., 2019; Lee et al., 2019), indicate that the microcontroller needs to have an ESP8266 module on board, which acts as both a Wi-Fi access point which scans for Wi-Fi signals in the vicinity as well as a device which connects to a pre-set Wi-Fi access point and pushes data to our server set up on ESRI ArcGIS

Online Server (ESRI, 2021c). The pushed data includes the RSSI, BSSID, SSID and a location tag specific to the location where the particular chipset is located and this is achieved through the use of Arduino MKR 1010 Wi-Fi controller.

The pushed data is then used as input for a simple user app we developed that uses a local user Wi-Fi scan and a kNN machine learning algorithm to match the user to a fingerprint location which is semantically linked to the indoor model. For the purpose of the matching algorithm, different techniques could have been employed, as illustrated by (Lee et al., 2019), a random forest model could be used, or a deep learning-based model (Ayyalasomayajula et al., 2020) could be used, however, the chipset employed returns only about 20 Wi-Fi scan values in one push to the server, hence the amount of data samples involved is not sufficient to train a deep learning or random forest based model. Deriving from studies of (Dai et al., 2019; Ge & Qu, 2016; Hoang et al., n.d.; Oh & Kim, 2018; Yu et al., 2014) , kNN proves to be the most reliable and fast model to predict the room the user is located in. This matching is done locally on the user device, ensuring no user Wi-Fi data is being used anywhere except on the users phone itself. Using this, we can then update the indoor model with live occupancy data on a room level of detail, ensuring that no privacy sensitive data is sent to the server.

Because access to the Wi-Fi chip was paramount for the development of the user app, and with Apple not opening this up for developers in iOS, this led us to start the development of an Android user app. The home screen of the user app is a 3D Scene of the Indoor Model of the study area which is directly added from ArcGIS Online. The main functionality of the app is to provide a visual representation of the real time occupancy of the study area, and to allow the user to locate themselves in this study area (given that they are in a room that is covered by the system).

The ArcGIS Online REST API (ESRI, 2021b) was used to load the table which contains the updated Wi-Fi fingerprints from the Arduino sensors located at different nodes, being hosted on the ArcGIS Online server. The HTTP request returns a JSON string which is then parsed to be loaded into a table, with the columns for MAC address, RSSI values, and Room ID. The Wi-Fi signals received from the Android device are parsed as a JSON string, and loaded directly to a table, which is then cleaned to contain two columns, one for the MAC addresses and one for the signal. Once this is done, the x and y variables for the kNN algorithm are extracted. This is done by the following means: Firstly, in order to take the MAC addresses into account when running a matching algorithm, all the MAC IDs are aggregated and each unique MAC address is given a unique number. The x variables for training data set then

are the Unique MAC numbers and their corresponding RSSI values. The y--variable is the label containing the rooms name from which a particular MAC number and a RSSI was obtained. For the test data-set, only the x-variables need to be created, which should be in the same format as the training data-set, so a unique MAC identifier and RSSI values are needed. To prepare the x-variables for the test data, the MAC addresses are matched to the fingerprint MAC addresses and the unique number assigned to a MAC in fingerprint is given to matching MAC addresses from the test data-set. If a MAC in test data cannot be found in fingerprint data, it is discarded along with its RSSI values, as that particular MAC address would not help us in matching. The y-variable in the case of the test data-set is supposed to be our final label for the room to locate the user's position.

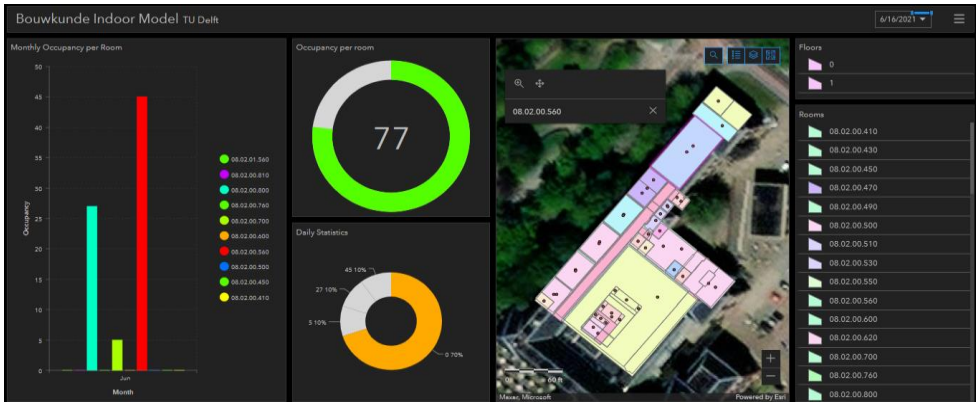

Figure 2: ArcGIS Online Dashboard

On the back-end, to actually implement the updating of the occupancy without storing any more data then needs be, a simple updating function was developed. This function uses the output of the matching algorithm, which will either be a string with the NAME attribute of a feature, or it will output the error string *"Couldn't locate the room you are in :("*. If the output is the error string, nothing happens, as no new occupancy data has not been generated. If the output of the matching algorithm is not the error string, the updating function will be called once or twice, depending on if there is a previous room known to the app or not. If the previous room is known, the app will decrement the occupancy in the previous room, and increment the occupancy in the current room.

One of the main goals of this project was to investigate and analyse the impact of COVID-19 in the indoor environment. The manager of a building, the Faculty of Architecture of TU Delft in this case, should be able to have access to statistics, including movement patterns inside a building, as well as

occupancy data, so that the peak hours of movement and occupancy could be identified. This data aids towards optimizing space planning and avoiding overpopulation of rooms. To accomplish that, a dashboard was created using ESRI ArcGIS Dashboards (ESRI, 2021a), additionally to the main application, in order to provide hourly, daily and monthly statistics, based on occupancy data provided by the Arduino sensors. The dashboard uses the created indoor model of the map and provides several capabilities, such as monthly and daily occupancy per room, as well as information on which rooms are the most populated at the current time. The dashboard is interactive and the included graphs are updated real-time with a small refresh rate.

3. Results

A fully functional hosted indoor model has been implemented using ArcGIS Indoors, with the initial testing of the Android app has proved to successfully obtain the Wi-Fi fingerprints from the selected research area and match them statically to a fingerprint in the database. After expanding to real-time fingerprinting, we found that while for some rooms, the accuracy is very high, for other rooms the accuracy is far lower, due to a number of reasons. The accuracy of the system of both testing setups is presented in table 1 and 2 below.

Room ID	Accuracy in center [%]	Accuracy along sides [%]
BG.Oost.560	100.00	100.00
01.Oost.560	10.00	0.00
BG.Oost.700	30.00	40.00
BG.Oost.800	100.00	100.00

Table 1: The accuracy of our indoor localisation system with n=10

Table ID	Accuracy in center[%]
2.031.O	100.00
2.032.O	100.00
2.033.O	100.00
2.034.O	100.00

Table 2: The accuracy of our indoor localisation system within a room with n=3

After looking at table 1 it would seem that the localisation system we designed is not functioning well, be-cause there is low accuracy on at least two out of four rooms upon first glance. However, when diving into the testing deeper we do see that there are some reasons for this outcome, and then these results are not unexpected.

The first thing to consider is the placement of the rooms, namely the pairs BG.Oost.560 and 01.Oost.560 and BG.Oost.700 and BG.Oost.800. For the two .560 rooms we know that these two rooms are directly above each other, which leads to lots of shared access points, and could lead to a less unique fingerprint for each room, leading the fingerprint matching algorithm to wrongfully assign the BG.Oost.560 room when in the 01.Oost.560 room and vice- versa.

In the case of 700 and 800, the fact that often when the user was in 700, the algorithm would match the user to 800 erroneously is also due to their proximity, with room 700 sharing a wall with windows with room 800. This could also be the reason that the accuracy for room 700 is higher near the walls of the room, the 40% accuracy are the 4 measurements taken nearer to 800 than to the location of the Arduino.

Another thing to consider is the fact that the ratio of different rooms varies quite a bit, with an over-representation of room BG.Oost.560, and an under representation of room 01.Oost.560, leading us to theorise that, this is another reason that 01.Oost.560 is has a very low accuracy. To solve this, in the second testing setup we tried to watch the ratio of the Arduinos feeding

their data, and the high accuracy presented in table 2 shows this does have an effect.

4. Discussion and Conclusions

With this project, we demonstrate the development of an ArcGIS Indoor Model created from CAD data in ArcGIS, which is later applied to an external Android app to display real-time occupancy of the Faculty for COVID-19 scenarios. The process of creating the ArcGIS Indoor Model was easy to follow, given the information provided by Esri, however, there were some issues with the initial structure of the CAD data, therefore, for it to function properly within the ArcGIS Indoors software required some manual adjustments. We have yet to conclude our project, however we believe that there is potential to expand and implement it as a privacy-preserving indoor localisation system, with location information available on a room scale. We think that the system could be expanded to include routing and navigation.

When defining the product, it became quite clear, early on, that we would need to design, develop and test a system that would try to answer the need created in the research question, namely: the combi-nation of ArcGIS Indoors with a privacy proof Wi-Fi fingerprinting localisation technology. To this extent, we have achieved what we wanted, with different levels of success on individual aspects of the system design.

On a more specific level, the system isn't exactly production ready. But we did make a big initial step to show that a reasonably accurate, versatile, cheap and scalable system can be created to provide an answer for the need stated in the research question. In terms of privacy, which was a very important value and key reason the entire system is set up this way, as opposed to using something like Indoors (the native ArcGIS IPS), we have achieved what we wanted. There is no personal data required to display and store occupancy information for an indoor environment like the Faculty of Architecture. Furthermore, we managed to completely separate the client and server side in the sense that the user is not required to share any data with the server concerning Wi-Fi or location as of yet.

Furthermore, we have developed a robust pipeline for converting often readily available CAD data into a semantically rich indoor model suitable for indoor localisation on a room level, using ArcGIS Pro/In-doors. This pipeline can be applied to any indoor environment for which this data is available, which is essential for the scalable nature of the system in its entirety.

In a technical sense, we have shown that using a single scanning point inside a room to create live radio maps can lead to a reasonable accuracy level, and deploying this setup can yield similar levels of accuracy as when constructing a very time consuming radio map at regular intervals as in the traditional Wi-Fi fingerprinting setup. With our system having lower initial time investing, as the scanning devices operate independently and autonomously, this project serves as a proof of concept.

References

Abdul, N., Zghair, K., Croock, M. S., Abdul, A., & Taresh, R. (2019). Indoor Localization System Using Wi-Fi Technology. *Iraqi Journal of Computers, Communications, Control & Systems Engineering*, *19*(2), 69–77. https://doi.org/10.33103/uot.ijccce.19.2.8

Alattas, A. ;, Oosterom, P. v, Zlatanova, S. ;, Diakité, A. A., & Yan, J. (2018). Developing a database for the LADM-IndoorGML model. In *Proceedings of the 6th International FIG 3D Cadastre Workshop*. APA. https://repository.tudelft.nl/islandora/object/uuid%3A31a20fb8-dabc-4f19-82c8-432f410a3ece

Ayyalasomayajula, R., Arun, A., Wu, C., Sharma, S., Sethi, A. R., Vasisht, D., & Bharadia, D. (2020). Deep Learning based Wireless Localization for Indoor Navigation. *Proceedings of the 26th Annual International Conference on Mobile Computing and Networking*, *20*, 1–14. https://doi.org/10.1145/3372224

Brena, R. F., García-Vázquez, J. P., Galván-Tejada, C. E., Muñoz-Rodriguez, D., Vargas-Rosales, C., & Fangmeyer, J. (2017). Evolution of Indoor Positioning Technologies: A Survey. *Journal of Sensors*, *2017*. https://doi.org/10.1155/2017/2630413

Dai, P., Yang, Y., Wang, M., & Yan, R. (2019). Combination of DNN and Improved KNN for indoor location fingerprinting. *Wireless Communications and Mobile Computing*, *2019*. https://doi.org/10.1155/2019/4283857

Esri. (2021a, July). *Create a dashboard—ArcGIS Dashboards | Documentation*. Esri. https://doc.arcgis.com/en/dashboards/get-started/create-a-dashboard.htm

Esri. (2021b, September). *ArcGIS REST APIs | ArcGIS Developers*. Esri. https://developers.arcgis.com/rest/services-reference/enterprise/get-started-with-the-services-directory.htm

Esri. (2021c, September). *ArcGIS Server web services | Documentation*. Esri. https://doc.arcgis.com/en/arcgis-online/reference/arcgis-server-services.htm

Ge, X., & Qu, Z. (2016). Optimization WIFI indoor positioning KNN algorithm location-based fingerprint. *Proceedings of the IEEE International Conference on Software Engineering and Service Sciences, ICSESS*, *0*, 135–137. https://doi.org/10.1109/ICSESS.2016.7883033

He, S., & Chan, S. H. G. (2016). Wi-Fi fingerprint-based indoor positioning: Recent advances and comparisons. *IEEE Communications Surveys and Tutorials*, *18*(1), 466–490. https://doi.org/10.1109/COMST.2015.2464084

Hoang, M. T., Zhu, Y., Yuen, B., Reese, T., Dong, X., Lu, T., Westendorp, R., & Xie, M. (n.d.). *A Soft Range Limited K-Nearest Neighbours Algorithm for Indoor Localization Enhancement*.

Lee, S., Kim, J., & Moon, N. (2019). Random forest and WiFi fingerprint-based indoor location recognition system using smart watch. *Human Centric Computing and Information Sciences*, *9*(6). https://doi.org/10.1186/s13673-019-0168-7

Liebich, T. (2009). *IFC 2x Edition 3 Model Implementation Guide*. https://standards.buildingsmart.org/documents/Implementation/IFC2x_Model_Implementation_Guide_V2-0b.pdf

Liu, Q., Qiu, J., & Chen, Y. (2016). Research and development of indoor positioning. *China Communications*, *13*, 67–79. https://doi.org/10.1109/CC.2016.7833461

Oh, J., & Kim, J. (2018). Adaptive K-nearest neighbour algorithm for WiFi fingerprint positioning. *ICT Express*, *4*(2), 91–94. https://doi.org/10.1016/J.ICTE.2018.04.004

Torres, J., Belmonte, O., Montoliu, R., Trilles, S., & Calia, A. (2016). How feasible is WiFi fingerprint-based indoor positioning for in-home monitoring? *Proceedings - 12th International Conference on Intelligent Environments, IE 2016*, 68–75. https://doi.org/10.1109/IE.2016.19

Tran, H., Khoshelham, K., Kealy, A., & Díaz-Vilariño, L. (2018). Shape Grammar Approach to 3D Modeling of Indoor Environments Using Point Clouds. *Journal of Computing in Civil Engineering*, *33*(1), 04018055. https://doi.org/10.1061/(ASCE)CP.1943-5487.0000800

T.U. Delft. (2020a). *Building Rhythms Project*. T.U. Delft. https://www.tudelft.nl/en/covid/wellbeing#c658811

T.U. Delft. (2020b). *Synthesis Project, GEO1101 Study Guide*. T.U. Delft. https://www.studiegids.tudelft.nl/a101_displayCourse.do?course_id=52691

Xia, S., Liu, Y., Yuan, G., Zhu, M., & Wang, Z. (2017). Indoor Fingerprint Positioning Based on Wi-Fi: An Overview. *ISPRS International Journal of Geo-Information 2017, Vol. 6, Page 135*, *6*(5), 135. https://doi.org/10.3390/IJGI6050135

Yu, F., Jiang, M., Liang, J., Qin, X., Hu, M., Peng, T., & Hu, X. (2014). 5 G WiFi Signal-Based Indoor Localization System Using Cluster k-Nearest Neighbor Algorithm: *Http://Dx.Doi.Org.Tudelft.Idm.Oclc.Org/10.1155/2014/247525*, *2014*. https://doi.org/10.1155/2014/247525

Modeling accident hotspots to locate roadside equipment based on intelligent transportation system

Saman Shafipour*, Mahmoud Reza Delavar **, Abbas Babazadeh ***

* GIS Department, School of Surveying and Geospatial Engineering, College of Engineering, University of Tehran, Tehran, Iran, Email: saman.shafipour1371@gmail.com

** Center of Excellent in Geomatic Eng., School of Surveying and Geospatial Engineering, College of Engineering, University of Tehran, Tehran, Iran, Email: mdelavar@ut.ac.ir,

*** School of Civil Eng., College of Engineering, University of Tehran, Tehran, Iran, Email: ababazadeh@ut.ac.ir

Abstract. Road transport has always attracted immense attention in Iran's planning as one of the main transportation system and economical infrastructures. High number of accidents and road fatalities in Iran reveals the weak safety in Iran's roads, therefore in the era which is called digital era, information technology is a necessary and efficient tool to help the management of transportation and increasing the road safety.
Geospatial information system and intelligent transportation system are among the branches of information technology that are used in transportation management. Intelligent transportation system is composed of various components with different applications can be used in all of the transportation systems. On the other hand installing and setting up the components of this system is very expensive, justifying the accurate and proper location

LBS 2021
16th Conference on Location Based Services
24-25 November 2021 Online

Published in "Proceedings of the 16th International Conference on Location Based Services (LBS 2021)", edited by Anahid Basiri, Georg Gartner and Haosheng Huang, LBS 2021, 24-25 November 2021, Glasgow, UK/online.

https://doi.org/10.34726/1757 | © Authors 2021. CC BY 4.0 License.

determination for these facilities.
To the best of our knowledge, Empirical Bayesian Kriging Regression Prediction (EBKRP) and Forest-based Classification and Regression to model the accident prone areas and predict the hotspots has not been undertaken so far. In addition, preparing, preprocessing and exploring the impact of input variables which varies in number and nature in ArcGIS Pro software has not been done.
Contribution of this research is in predicting high risk areas as an appropriate place for the installation of intelligent speed bumps using machine learning methods and data mining based on artificial intelligence in a locational intelligence field.
The data used in this study consist of the official data of the traffic accidents in the period 2018 to 2019 which are available in the accidents and road transport system and has been obtained using programming in the web environment, intelligent descriptive information obtained from smart cameras of the video surveillance in the context of locational information system, non-intelligent descriptive information obtained from the Ministry of Roads and Urban Development related to the characteristics of suburban roads of Mazandaran Province in the North of Iran and also TanDEM digital elevation model with a spatial resolution of 12.5 meters.
In order to predict high traffic accident risk areas, first the area of Mazandaran Province was divided into a number of hexagons to reduce the error effect of the data fusion process. The accidents data and the surrounding land uses and land covers have been extracted from the images acquired from the smart transportation monitoring cameras.
For predicting the dependent variable and estimating the coefficients of significance considering the available data uncertainty, an automatic method has been proposed in this research. The method is based on heuristic regression, ordinary least squares regression and spatial rhythmic regression by considering distance as an independent variable and regression and forest-based classification with a combination of raster, vector and artificial data were used as independent variables. In addition, a new method of predicting EBK regression with raster format was proposed and implemented in this paper. Heat mapping tools have been used to convert vector variables into raster format. The integration of DEM as a variable containing ground height information with other inputs of the EBKRP method was also employed.
Furthermore, the combination of digital elevation layer was used as a variable containing information about the earth with other inputs of the EBKRP method.
The results showed that the information variable obtained from smart images in the training regression process and forest-based classification methods are among the effective variables in the modeling and predicting high traffic accident risk areas.

In addition, it is shown that the residuals obtained from the spatial statistics employed methods have a random distribution. On the other hand, based on the validation performed for each of the implemented methods, it was found that the adjusted coefficient of determination (Adjusted-R2) for spatial rhythmic regression method has been increased compared to those of the normal least squares regression, regression method and forest-based classification. ٢٠% of the data were selected to validate the results and the mean square error (MSE) was estimated to be 0.012. The Geostatistics toolkit in the two cases has been used in terms of time. The cross-validation method employed showed that in the case of considering the digital layer of height in the modeling process, the accuracy of the model prediction process has been improved.

Keywords. Intelligent Transportation System, Geospatial Information System, EBK Regression Prediction

1. Introduction

The use of geospatial information system (GIS) in the transportation network has been developed in recent years, where GIS transport (GIS-T) is quite common in this field. Therefore, the practical principles of using geospatial information system science and technology in transportation related issues has been widely welcomed by the transportation community (Agyemang 2013).

On the other hand, intelligent transportation systems (ITS) use various technologies such as navigation systems, electronic toll payment systems, traffic control sensors, weather monitoring devices, electronic messaging boards. In order to improve the transportation systems and enhance the infrastructure of the road equipment, collecting, storing, analyzing and integrating the qualified transportation information is necessary. Furthermore, the information in the transportation system, such as road networks are spatially referenced (Khan, Rahman et al. 2017, Zhu, Yu et al. 2018).

2. LITERATURE REVIEW

Previous research on road accidents has focused on spatial factors affecting the distribution and type of accidents in urban and suburban roads(Shafabakhsh, Famili et al. 2017). Accumulation of accidents in any place can not only be affected by human factors and vehicle defects, but also the characteristics of the road, usages of their surrounding facilities, the

frequency and type of accidents and the amount of the associated damages (Shafabakhsh, Famili et al. 2017, Yuan, Zhou et al. 2018).

The analysis of these effects can be used in future road safety planning, including determining the appropriate location for the construction of intelligent accelerators or the proper distribution of conventional accelerators in the absence of proper road intelligent infrastructure, with the aim of reducing accidents by road transport authorities.

3. RESEARCH GAPS AND QUESTIONS

The data may be flawed for a variety of reasons. For example, data may be lost in some cases because a sensor may be temporarily disabled, a sampling point may be inaccessible, or data values may be deliberately hidden for confidential protection. When one or more values are missing, most statistical methods in data preprocessing remove that attribute from the process by default. To bridge this gap, which implies the presence of areas with no data, by filling in the missing values, the nulls are estimated with values based on spatio-temporal data analysis with respect to their neighborhood to minimize the effect of those values with missing data(https://pro.arcgis.com/en/pro-app/latest/tool-reference/space-time-pattern-mining/fillmissingvalues.htm).

Data diversity is another issue in the intelligent transportation system, which is collected in various formats and in different ways including numerical data obtained from sensors on vehicles and roads and textual data obtained from the media. Social and image data contained in the maps are collected in the geospatial information system. This data can be organized from semi-structured data (e.g., text reports, images, videos, and audio files) to structured data (e.g., data received from smart devices such as video surveillance cameras, sensors and traffic accident data in a database) (Khan, Rahman et al. 2017).

Therefore, data infrastructures and systems that can model and predict large volumes of data are needed to convert the equipment information from a technology-based system to a complex data-driven system, such as a geospatial information system (Khan, Rahman et al. 2017).

4. Methodology

Machine learning is a branch of artificial intelligence in which structured data is processed by an algorithm to solve a problem. Deep learning is a subset of machine learning that uses multiple layers of algorithms in the

form of neural networks. Input data is analyzed through different network layers, each layer defining specific features and patterns in the data(L. Bennett).

EBKRP is a geostatistical interpolation method employed in ArcGIS Pro software that combines the Empirical Bayesian Kriging (EBK) method with regression analysis. In the regression models, heuristic variables are often related to each other. The problem of multilinearity is solved by converting the primary independent variables necessary in the raster model to their main components before constructing a regression model (Malcheva, Bocheva et al. 2019).

Official and raw data related to suburban accidents in Mazandaran Province, for the years 2018 and 2019 from the comprehensive information system of accidents and transport accidents in Iran, which has been recorded by the experts of the Roads and Transportation Organization, in the form of a set of Excel files. Accident data for two years were obtained with the JavaScript programming language. After the preprocessing steps, the ground was referenced by the linear reference system method. Because the recorded information from accidents may have been incomplete and subject to change, an indicator is used to identify accident hotspots with fatalities with those accidents that only cause damage which are considered for the road traffic safety analysis.

The distribution and dispersion of land use density, especially educational land uses along the roads in Mazandaran Province, have a significant impact on traffic accidents. Therefore, various information including text reports, roadside user information (e.g. educational and medical land uses) as well as digital model of land height and spatial features (e.g. roads and population centers) are collected and aggregated in a spatial database.

Optimal performance were determined by ordinary least squares (OLS) and geographically weighed regression (GWR) methods with R^2 and AdjR^2 values, Forest-based Classification and Regression methods with R^2 and MSE values, as well as EBK Regression Prediction (EBKRP) and EBKRP + digital elevation model (DEM) methods with Continuous Ranked Probability Score (CRPS) and Root Mean Square Standardized Error (RMSSE) values.

5. Discussion

In order to achieve one of the objectives of the research based on the use of GIS-based emerging machine learning methods, it was determined that from the set of spatial statistics tools, a prediction model based on Forest-

based Classification and Regression due to the diversity in accepting the number and nature of input information, as well as from the Geostatistics toolkit, the EBKRP-based prediction model due to the acceptance of terrestrial raster data such as DEM are suitable models for locating the intelligent accelerators. Figure (1) is a graphical output of areas appropriate to the installation of intelligent accelerators or areas predicted by the EBKRP method.

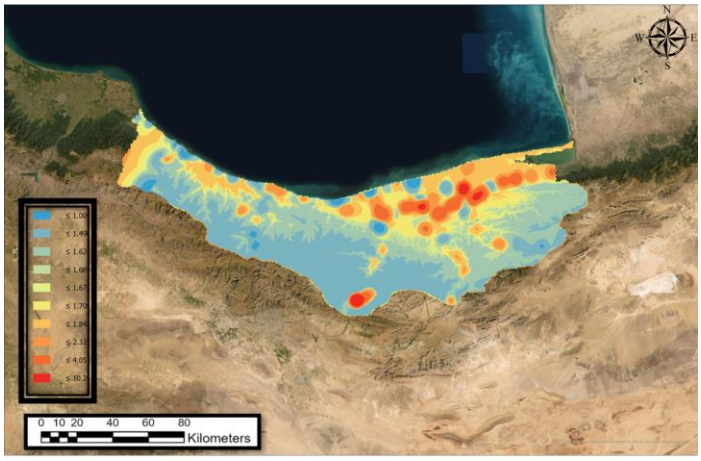

Figure 1. The spatial distribution of some car accidents traffic hot spots

The disadvantages of the exploratory regression and the least squares methods are the limitation in the number of input variables. To best of my knowledge, the limitations of the machine learning methods in GIS can be mentioned as the number as well as the unacceptance of the input variable with raster format (Ali, Sajjad et al. 2021). Therefore, the EBKRP method was selected to determine the importance of variables and the prediction was made based on 25805 hexagonal tessellations employed in dividing the Mazandaran Province. The accuracy of the proposed method based on the coefficient of determination was 0.915 and the error equal to 0.012 was obtained.

6. Conclusion

In comparison with(Effati, Rajabi et al. 2015) who used the classification tree method and fuzzy regression to predict the model, in the present study the forest-based classification and regression method was used. The advantage of this method is in the final predictions that are not based on any single tree but on the whole forest.

References

Agyemang, E. (2013). "A cost-effective Geographic Information Systems for Transportation (GIS-T) application for traffic congestion analyses in the Developing World." Ghana Journal of Geography **5**: 51-72.

Ali, G., M. Sajjad, S. Kanwal, T. Xiao, S. Khalid, F. Shoaib and H. N. Gul (2021). "Spatial–temporal characterization of rainfall in Pakistan during the past half-century (1961–2020)." Scientific reports **11**(1): 1-15.

Effati, M., M. A. Rajabi, F. Hakimpour and S. Shabani (2015). "Prediction of crash severity on two-lane, two-way roads based on fuzzy classification and regression tree using geospatial analysis." Journal of Computing in Civil Engineering **29**(6): 04014099.

https://pro.arcgis.com/en/pro-app/latest/tool-reference/space-time-pattern-mining/fillmissingvalues.htm.

Khan, S. M., M. Rahman, A. Apon and M. Chowdhury (2017). Characteristics of intelligent transportation systems and its relationship with data analytics. Data analytics for intelligent transportation systems, Elsevier**:** 1-29.

L. Bennett, M. l. i. A., "ed: ArcUser, 2018.

Malcheva, K., L. Bocheva and T. Marinova (2019). "Mapping temperature and precipitation climate normals over Bulgaria by using ArcGIS Pro 2.4."

Shafabakhsh, G. A., A. Famili and M. S. Bahadori (2017). "GIS-based spatial analysis of urban traffic accidents: Case study in Mashhad, Iran." Journal of traffic and transportation engineering (English edition) **4**(3): 290-299.

Yuan, Z., X. Zhou and T. Yang (2018). Hetero-convlstm: A deep learning approach to traffic accident prediction on heterogeneous spatio-temporal data. Proceedings of the 24th ACM SIGKDD International Conference on Knowledge Discovery & Data Mining.

Zhu, L., F. R. Yu, Y. Wang, B. Ning and T. Tang (2018). "Big data analytics in intelligent transportation systems: A survey." IEEE Transactions on Intelligent Transportation Systems **20**(1): 383-398.

Machine Learning for Predicting Pedestrian Activity Levels in Cities

Achituv Cohen*, Sagi Dalyot*, Asya Natapov**
* Technion - Israel Institute of Technology, Israel
**Loughborough University, United Kingdom

Abstract. Analysing and modelling pedestrian activity in built environments allows us to understand, assess, predict, and manage its dynamics. Nonetheless, pedestrian activity data might not be available everywhere. An alternative can suggest predicting pedestrian activity by considering environmental characteristics and the geometrical configuration of the environment. This paper presents a Machine Learning pedestrian activity level prediction model, which is trained and tested using data extracted from smart city sensor systems from multiple cities. The proposed model was applied to Greater London, UK, and the prediction results were compared with pedestrian activity data provided by Transport for London. Our results show that the model has high potential to predict pedestrian activity levels in a city, but that further research is needed to obtain more reliable results.

Keywords. Machine Learning, Pedestrian Activity, Spatial Analysis, Crowdsourcing

1. Introduction

Diverse digital technologies and sensors are used today in smart cities to collect different types of data for better city management aimed to improve citizens' quality of life. The Hystreet platform[1], for example, monitors Pedestrian Activity (PA) by continuously counting the number of pedestrians, using laser scanners positioned on building facades. By modelling and analysing PA, city officials can better predict and manage city traffic and understand the resultant movement dynamics (Duives et al. 2015). Dynamic PA data can assist city officials and improve pedestrian routing services by

[1] https://hystreet.com/en/locations#/

LBS 2021
16th Conference on Location Based Services
24-25 November 2021 Online

Published in "Proceedings of the 16th International Conference on Location Based Services (LBS 2021)", edited by Anahid Basiri, Georg Gartner and Haosheng Huang, LBS 2021, 24-25 November 2021, Glasgow, UK/online.

https://doi.org/10.34726/1758 | © Authors 2021. CC BY 4.0 License.

suggesting custom routes for pedestrians wishing to avoid empty streets for safety reasons or overcrowded areas for health reasons. Still, these sensors are sparse, and hence PA data is very limited, forcing cities to rely on site and periodic (household) surveys, which are limited and expensive. Research shows that PA can be predicted by analysing the city structure and its features that represent the urban form (Qin 2016, Omer et al. 2015). These, both static and dynamic, can be retrieved from geospatial catalog, such as OpenStreetMap (OSM) (Cohen & Dalyot, 2020). We propose a Machine Learning (ML) prediction model, which is trained and tested using smart sensor data that counts PA from different cities: the Hystreet platform in Germany and Bluetooth (BT) sensor network in Tel Aviv, Israel. The prediction model reveals the relationships between the urban structure and features and the PA in these areas, and then is applied to new areas.

2. Methods

The proposed supervised ML prediction model uses as features OSM's street segments and different city elements, including their attributes. As model labels, the smart sensors' PA counts corresponding to each street segment. PA counts are classified to five categories (*Table 1*), or levels, based on the work of Helbing and Johansson (2009).

PA Levels	Model Labels	Density range
< 0.7 m/p	5	Highest
< 0.95 m/p	4	
< 1.2 m/p	3	
< 1.5 m/p	2	
> 1.8 m/p	1	Lowest

Table 1. PA levels in units of meters per person, according to Helbing and Johansson (2009).

Figure 1 illustrates the implemented ML workflow. OSM street network was downloaded and transformed into a walkable streets graph by examining the OSM highway tags of the segments to retain pedestrian streets only. *Table 2* depicts the feature engineering used in the model: (1) city features, which are derived from OSM tags; (2) centrality features, which are calculated based on OSM's street network; and (3) time-related features. For the city features we adopted the works of Qin (2016) and Omer et al. (2015) that list city and spatial features that effect PA. Centrality features are generated using graph-

based measures (Cooper 2015) that help identify the most central street segments within a particular area.

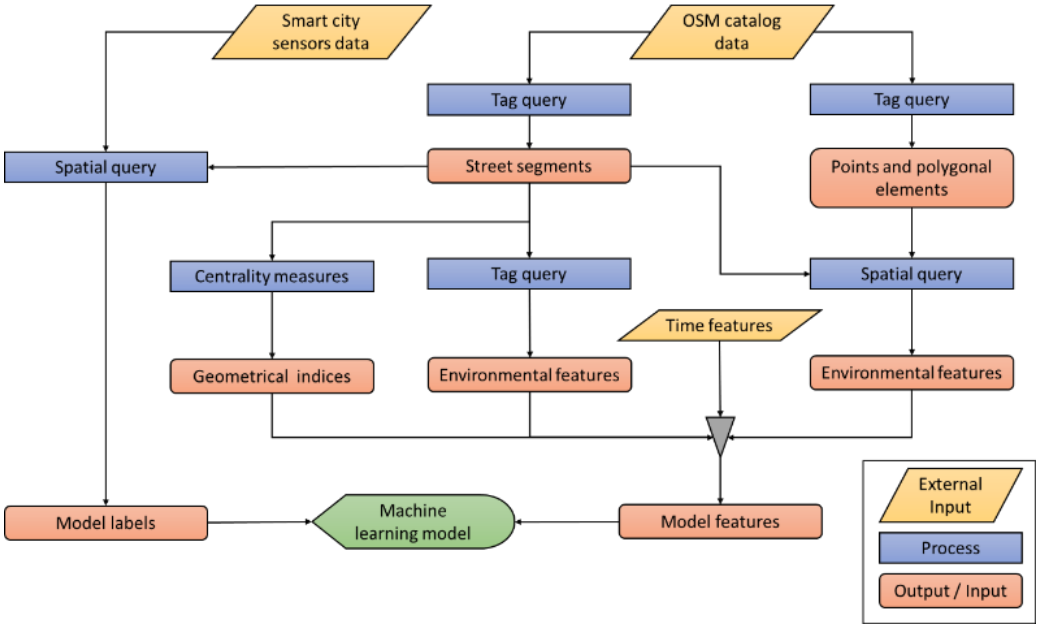

Figure 1. ML prediction model workflow.

Feature Group	Model Features	Calculation method
City Features	Highway	Categorical values based on OSM's highway tag.
	Land use	Categorical values based on OSM's land use tag or nearby element's tag (e.g., residential, retail).
	Amenity	The number of elements with the same tag that are within 20 meters from the street segment.
	Office	
	Tourism	
	Shop	
	Building	
	Natural	
	Leisure	
Centrality Features	Betweenness	Street centrality indices.
	Closeness	
Time Features	Hour	Hour of the day.
	Day	Day of the week order (for example, Sunday=1, Monday=2 …).

Table 2. Feature engineering and calculation method.

PA label data (pedestrian counts translated to levels) were retrieved from two smart monitoring systems: 1) The Hystreet platform, which continuously counts pedestrians on streets in cities throughout Germany; 2) A BT sensor network, located in Tel-Aviv, Israel, consisting of 65 point-to-point BT sensors, and 78 street segment streets (links) between adjacent sensors. PA is measured in meters per person, while the systems provide the number of people per hour. Therefore, PA is calculated (Equation 1) by dividing the street segment length with the number of people per hour multiplied with the time it takes them to cross the street (speed is defined as the commonly used average walking speed, which is 3,000 meters per hour):

$$PA = \frac{street\ segement\ length}{\left\lfloor number\ of\ people\ per\ hour * \left\lceil \frac{street\ segement\ length_{[meter]}}{pedestrain\ speed_{\left[\frac{meter}{hour}\right]}} \right\rceil_{[hour]} \right\rfloor} \left[\frac{meter}{person}\right] \quad [1]$$

Our prediction model is based on the Random Forest (RF) classifier. RF combines tree predictors in such a way that each tree depends on the values of a random vector sampled independently with the same distribution for all trees in the forest. Cross validation was conducted on the data to resolve overfitting, with 70% of the samples used for training, and 30% for testing.

3. Preliminary Findings

The ML prediction model includes 141,384 training samples: 83,544 from 9 German cities (Hystreet data), and 57,840 samples from Tel-Aviv (BT data). All cities represent heterogeneous street arrangements that include variety of urban morphologies, land uses and settings. *Table 3* presents the resulting confusion matrix based on 27,379 test samples and label (PA level) predictions. Despite the high F1-score and accuracy values, it should be noted that labels are not evenly distributed, where most samples (90%) belong to Label 1 (least dense streets), thus the prediction of this label is very accurate. However, although the recall and precision values for the other labels is between 44% and 67%, most of the errors are predictions of adjacent labels, indicating the reliability potential of the resulting prediction model. As an example, of the 927 samples from Label 3, 604 were correctly classified (65%), while 282 samples (30%) were classified as Labels 2 and 4, and only 41 samples (less than 5%) were classified as Labels 1 and 5.

		Predicted Labels						
	Labels	*1*	*2*	*3*	*4*	*5*	*Number of samples*	Recall
True Labels	*1*	**24624**	163	74	22	4	24887	98.9%
	2	197	**333**	191	34	4	759	43.9%
	3	37	147	**604**	135	4	927	65.2%
	4	7	8	127	**390**	47	579	67.4%
	5	12	2	5	79	**129**	227	56.8%
	Number of predicted samples	24877	653	1001	660	188	**F1 score**	**99.0%**
	Precision	99%	51%	60%	59%	69%	**Accuracy**	**95.3%**

Table 3. Prediction model confusion matrix.

As PA levels rely on a set of features, which are considered universal, we further evaluate the prediction model on unseen data – Greater London, UK, and generated PA level values for the entire street network. As reference, we use PA level values provided by the Transport for London (TfL) that documented six years of data consisting of 300,000 walking trips. TfL's PA data is organized as 15,477 hexagons covering the Greater London area, each with a measurement of meters walked per square meter. *Figure 2* depicts the two PA results, showing that the centre of London is the area with the densest PA in the Greater London, and as we move away from the centre there is a clear trend of diminishing PA intensity. Other dense areas, which are located within the suburbs, mostly correspond to local shopping streets, central stations, and schools, which tend to be more crowded. Although the prediction model shows an overall resemblance to TfL's dataset, even in London's outskirts, there exists some differences between the two models (Pearson correlation = 0.487).

In conclusion, the developed PA prediction model relies on more than 140,000 samples, where testing showed a high accuracy of about 95%. Using Greater London for model evaluation, the results show robustness of the model and its potential to predict PA for new, unfamiliar areas. We believe that as we use more PA samples from different cities, the prediction model will be adjusted better to other city arrangements and characteristics, producing more reliable results. Overall, this methodology of using ML to predict PA proves to be accurate and reliable for better city management, having the potential to replace on site and periodic surveys, which are limited and expensive.

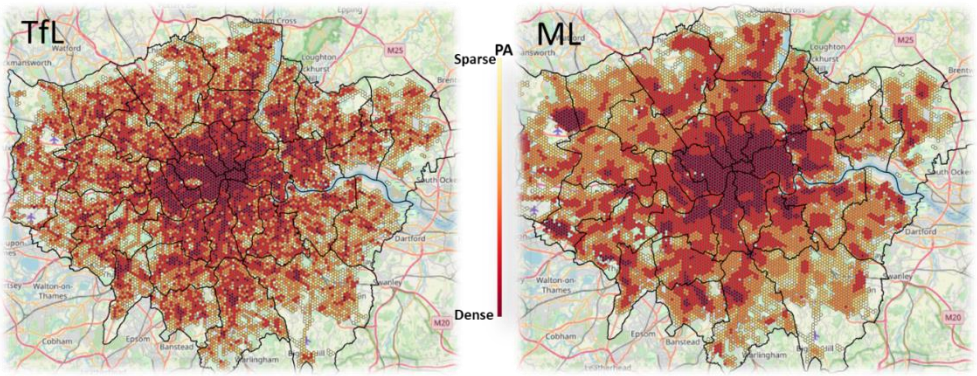

Figure 2. PA in Greater London during the weekdays according to TfL's reference model (left) and the developed ML prediction model (right).

References

Cohen A and Dalyot S (2020) Machine-learning prediction models for pedestrian traffic flow levels: Towards optimizing walking routes for blind pedestrians. *Transactions in GIS* 24(5). Wiley Online Library: 1264–1279.

Cooper CH V (2015) Spatial localization of closeness and betweenness measures: a self-contradictory but useful form of network analysis. International Journal of Geographical Information Science 29(8). Taylor & Francis: 1293–1309.

Duives DC, Daamen W and Hoogendoorn SP (2015) Quantification of the level of crowdedness for pedestrian movements. *Physica A: Statistical Mechanics and its Applications* 427. Elsevier: 162–180.

Helbing D (2009) Pedestrian, Crowd and Evacuation Dynamics. In: *Encyclopedia of Complexity and Systems Science*. New York, NY, pp. 6476–6495.

Omer I, Rofè Y and Lerman Y (2015) The impact of planning on pedestrian movement: contrasting pedestrian movement models in pre-modern and modern neighborhoods in Israel. *International Journal of Geographical Information Science* 29(12): 2121–2142.

Qin Q (2016) *Exploring Pedestrian Movement Patterns with Urban Environmental Factors in Beijing*. The Pennsylvania State University.

The Effect of Post-Processing in Stop-Move Detection of GPS Data: A Preliminary Study

Eun-Kyeong Kim*,**,[1], Elena Ebert*, Robert Weibel*

* Department of Geography, University of Zurich, Switzerland
** University Research Priority Program (URPP) 'Dynamics of Healthy Aging', University of Zurich, Switzerland

Abstract. Stop-move detection has been an essential step to construct semantic trajectories and extract meaningful activity sequences of moving objects. Detecting stop and move segments accurately is critical because errors occurred in stop-move detection can be propagated and amplified in later steps in trajectory data analysis. In particular, post-processing that merges or discards the detected stop-move segments can make an impact on the accuracy and characteristics of detected stops and moves. Although many stop-move detection algorithms exist and new methods are continuously proposed in the field, studies on comparing the performance of the stop-move detection methods are still scarce.

In this study, we evaluated the effect of post-processing in stop-move detection with four selected existing stop-move detection algorithms—CandidateStops, SOC, POSMIT, and MBGP—in two input-data scenarios: (1) original data and (2) sampled data. The detected stops were assessed by two quantitative measures that quantify the accuracy at different levels of aggregation in space and time: (1) accuracy based on individual data points (i.e., F-measure) and (2) the shape of detected stops (i.e., shape compactness). With the case study, we found that the impact of post-processing on the detection results can vary by a selected algorithm and input data sparsity. The results can potentially provide insights into how to adopt and maneuver the stop-move detection methods for GPS data analysis.

Keywords. Stop detection, GPS data analysis, Semantic trajectory, Algorithm comparison.

[1] Corresponding author, eun-kyeong.kim@uzh.ch

Published in "Proceedings of the 16th International Conference on Location Based Services (LBS 2021)", edited by Anahid Basiri, Georg Gartner and Haosheng Huang, LBS 2021, 24-25 November 2021, Glasgow, UK/online.

https://doi.org/10.34726/1759 | © Authors 2021. CC BY 4.0 License.

1. Introduction

Trajectory segmentation, particularly stop-move detection, has been an essential step to construct semantic trajectories and extract meaningful activity sequences of moving objects [1]. Detecting stop and move segments accurately is critical to infer further semantics of segments—activities in stops and transportation modes of moves in the case of human subjects—, because errors occurring in stop-move detection can be propagated and amplified in later steps in trajectory data analysis.

Stop-move detection methods for GPS data often consist of two phases: stop-move detection, in which initial stop-move segments are detected; post-processing, in which the detected segments are merged or discarded upon criteria. Some stop-move detection algorithms inherently integrate such post-processing procedures, e.g., SMUoT – Zhao et al. [2]. Some other approaches conduct additional post-processing after applying an existing algorithm, e.g., Fillekes et al. [3]. As a part of trajectory segmentation, such post-processing can make an impact on the accuracy and characteristics of detected stops and moves. Although many stop-move detection algorithms exist and new methods are continuously proposed in the field, studies on comparing the performance of the stop-move detection methods are still scarce. Hence, this study evaluates the effect of post-processing in stop-move detection for GPS data. First, we select four existing stop-move detection algorithms—CandidateStops, SOC, POSMIT, and MBGP and analyze the post-processing effect in two input-data scenarios, (1) original GPS data and (2) sampled data, by quantifying the accuracy at two levels of spatiotemporal aggregation.

2. Data and Methods

2.1. Data Collection and Labelling

GPS and Accelerometer (ACC) datasets analysed in this study were collected from 161 participants for a 30-day period in the *Mobility, Activity and Social Interaction Study* (MOASIS) [4]. Stop-move detection is based solely on GPS data. The sampling rate of GPS data is 1 Hz and that of ACC is 50 Hz.

To evaluate the accuracy, labelled GPS data were constructed based on ACC and GPS data by manually identifying stops via the interactive visualization tool for data labelling task. Out of 161 participants, 38 participants with relatively more GPS points were sampled and 90 study days with more GPS data points (30 days for each of Tuesday, Thursday, and Sunday) were extracted, in order to construct balanced labelled data across weekdays and participants. The GPS points were labelled as a stop upon the following criteria:

velocity less than 1 m/s [5]; acceleration between −0.3 m/s² and 0.3 m/s² [5]; stop duration at least 10 minutes.

2.2. Stop-Move Detection Algorithms and Post-Processing

To assess the post-progressing effect on stops detected by a variety of stop-move detection algorithms, four stop-move detection algorithms were selected: CandidateStops [5], SOC (Sequence Oriented Clustering) [6], POSMIT (PrObability of Stops and Moves In Trajectories) [7], and MBGP (stop detection method by Montoliu, Blom and Gatica-Perez) [8]. On one hand, the selected algorithms meet the criteria of a good algorithm—maximum parsimony, ease of understanding, and high performance—to different degrees: lower (CandidateStops), moderate (MBGP), and highest (SOC; POSMIT) levels. SOC and POSMIT are expected to outperform CandidateStops and MBGP in stop detection. On the other hand, the selected algorithms implement different key measures and built-in post-processing procedures (Table 1).

Algorithm	**CandidateStops**	**SOC**	**POSMIT**	**MBGP**
Expected Usefulness	Low	High	High	Moderate
Key Measure	Density	Density	Probability	Density
Post-Processing	None	Merging stops	None	Merging stops

Table 1. Algorithmic Characteristics and Built-in Post-Processing of Selected Algorithms.

While CandidateStops and POSMIT do not have inherent post-processing in the algorithm, SOC and MBGP recognize stops too close in time and space as a single stop, using input parameters, i.e., maximum time gap and distance between subsequent GPS points. On top of the built-in post-processing of SOC and MBGP, we applied an additional post-processing procedure to detected stops by each of the four algorithms with the following rules:

- All moves shorter than 3 minutes were removed and classified as noise;
- Two stops are merged if the last GPS point of the preceding stop and the first GPS point of the following stop are within 150-meter distance and 1-hour time interval.

2.3. Evaluation Measures

The detected stops are assessed by two quantitative measures that quantify the accuracy at different levels of aggregation in space and time: (1) accuracy based on individual data points (i.e., F-measure based on confusion matrix [9]) and (2) the shape of detected stops (i.e., shape compactness based on the area and longest axis of a stop [10]).

2.4. Input-Data Scenarios

To observe how the post-processing effect changes over different input datasets, four algorithms are evaluated in two input-data scenarios: (1) original GPS data and (2) sampled data. For the second scenario, the GPS points were sampled with the rate of 1/60 Hz (1 point every minute).

3. Results

3.1. Accuracy at a GPS Data Point Level

The stop classification accuracy is compared at an individual GPS point level for the stops detected with vs. without applying post-processing for each algorithm. Each plot is drawn for each input-data scenario (Figure 1).

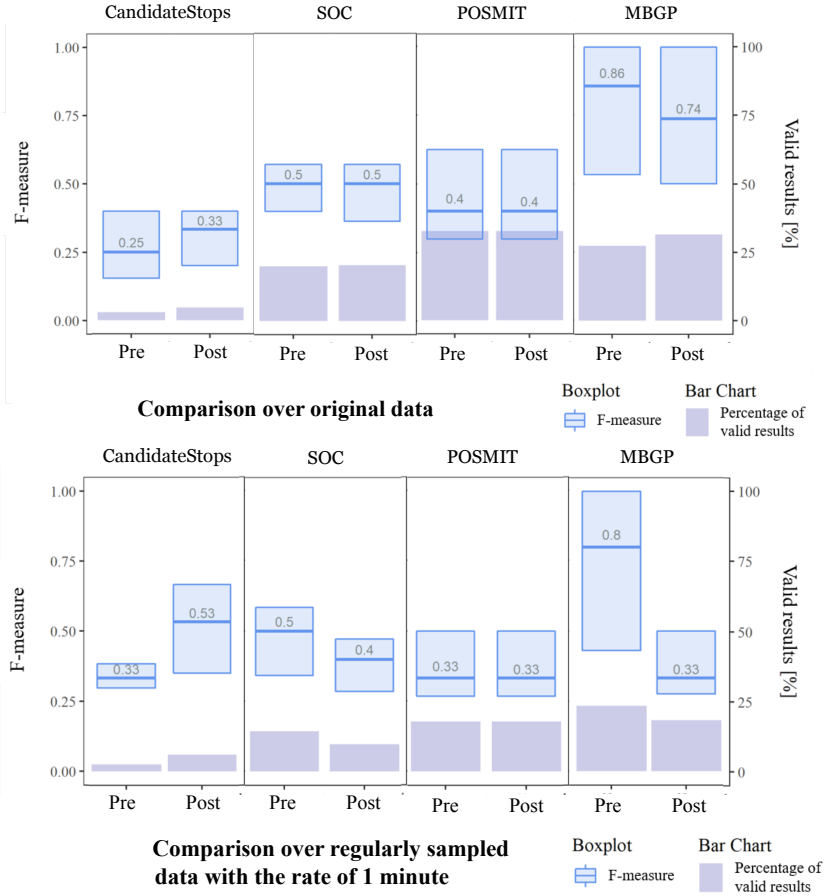

Figure 1. F-measure and percentage of valid results for stop detection accuracy measurement at the GPS point level with vs. without applying post-processing: Comparison over original data (upper) and comparison over regularly sampled data with the rate of 1 minute (lower).

3.2. Shape Compactness at an Individual Stop Level

The shape compactness of the detected stops was evaluated at an aggregated level of an individual stop with vs. without applying post-processing for each algorithm. Each table represents the results based on each input-data scenario (Table 2, Table 3). The larger shape compactness value indicates more circular shape.

Algorithm	Process	Min.	Q1	Median	Q3	Max.	Mean
CandidateStops	Pre	$2.46*10^{-17}$	$6.57*10^{-15}$	$1.91*10^{-15}$	$8.01*10^{-15}$	$5.88*10^{-11}$	$8.04*10^{-14}$
	Post	$3.82*10^{-17}$	$3.87*10^{-11}$	$9.30*10^{-09}$	$1.34*10^{-06}$	$3.38*10^{-03}$	$3.75*10^{-05}$
SOC	Pre	$8.82*10^{-10}$	$7.84*10^{-09}$	$2.55*10^{-08}$	$1.47*10^{-07}$	$2.57*10^{-03}$	$2.03*10^{-05}$
	Post	$8.82*10^{-10}$	$7.33*10^{-09}$	$2.54*10^{-08}$	$2.06*10^{-07}$	$2.57*10^{-03}$	$2.17*10^{-05}$
POSMIT	Pre	$1.39*10^{-08}$	$4.43*10^{-06}$	$4.09*10^{-04}$	$1.72*10^{-02}$	$1.13*10^{01}$	$7.48*10^{-01}$
	Post	$1.39*10^{-08}$	$4.43*10^{-06}$	$4.09*10^{-04}$	$1.72*10^{-02}$	$1.13*10^{01}$	$7.48*10^{-01}$
MBGP	Pre	$2.76*10^{-11}$	$6.55*10^{-08}$	$1.23*10^{-07}$	$2.11*10^{-07}$	$5.35*10^{-06}$	$1.77*10^{-07}$
	Post	$2.76*10^{-11}$	$7.29*10^{-08}$	$1.46*10^{-07}$	$3.18*10^{-07}$	$8.62*10^{00}$	$9.30*10^{-02}$
Labelled data		$1.99*10^{-11}$	$6.72*10^{-10}$	$3.08*10^{-09}$	$7.79*10^{-09}$	$8.71*10^{-07}$	$6.97*10^{-08}$

Table 2. Shape compactness of detected stops based on original data (Scenario 1).

Algorithm	Process	Min.	Q1	Median	Q3	Max.	Mean
CandidateStops	Pre	-	-	-	-	-	-
	Post	$4.44*10^{-13}$	$2.06*10^{-12}$	$1.08*10^{-11}$	$4.63*10^{-05}$	$1.12*10^{-01}$	$9.78*10^{-03}$
SOC	Pre	$5.54*10^{-11}$	$2.38*10^{-09}$	$9.36*10^{-09}$	$3.12*10^{-08}$	$1.39*10^{-04}$	$1.22*10^{-06}$
	Post	$3.07*10^{-10}$	$6.17*10^{-09}$	$5.39*10^{-08}$	$3.55*10^{-04}$	$5.10*10^{00}$	$1.31*10^{-01}$
POSMIT	Pre	$6.26*10^{-09}$	$4.10*10^{-06}$	$3.27*10^{-04}$	$1.47*10^{-02}$	$1.12*10^{01}$	$6.05*10^{-01}$
	Post	$6.26*10^{-09}$	$4.10*10^{-06}$	$3.27*10^{-04}$	$1.47*10^{-02}$	$1.12*10^{01}$	$6.05*10^{-01}$
MBGP	Pre	$9.38*10^{-11}$	$1.11*10^{-08}$	$5.06*10^{-08}$	$1.02*10^{-07}$	$8.26*10^{-07}$	$8.02*10^{-08}$
	Post	$9.01*10^{-10}$	$2.53*10^{-07}$	$2.63*10^{-05}$	$3.56*10^{-03}$	$1.06*10^{01}$	$4.23*10^{-01}$
Labelled data		$1.99*10^{-11}$	$6.72*10^{-10}$	$3.08*10^{-09}$	$7.79*10^{-09}$	$8.71*10^{-07}$	$6.97*10^{-08}$

Table 3. Shape compactness of detected stops based on regularly sampled data with the rate of 1 minute (Scenario 2).

4. Discussion

The evaluation at two aggregation levels implies that the impact of post-processing in stop-move detection varies by base stop-move detection algorithms as well as input data traits. In summary, the major findings are:

- At a data point level, the accuracy of stop-move detection without post-processing is the lowest with CandidateStops and the highest with MBGP, although SOC and POSMIT were expected to perform the best.

- At a data point level, post-processing largely improves the accuracy for CandidateStops, but makes little impact on the outputs of POSMIT, and worsens the accuracy for MBGP and SOC, especially for the sparse input data with low sampling rates.
- At an individual stop level, post-processing tends to change detected stops into more circular-shaped ones, with the highest impact on the outputs of CandidateStops and weaker impacts on the results of SOC and POSMIT. The shape compactness of the detected stops from SOC and MBGP without post-processing is similar to that of the labelled data.

References

[1] Y. Zheng, "Trajectory Data Mining: An Overview," *ACM Trans. Intell. Syst. Technol.*, vol. 6, no. 3, pp. 1–41, 2015, doi: 10.1145/2743025.

[2] Z. Zhao, L. Yin, S.-L. Shaw, Z. Fang, X. Yang, and F. Zhang, "Identifying stops from mobile phone location data by introducing uncertain segments," *Trans. GIS*, vol. 22, no. 4, pp. 958–974, Aug. 2018, doi: 10.1111/tgis.12332.

[3] M. P. Fillekes, E. Giannouli, E.-K. Kim, W. Zijlstra, and R. Weibel, "Towards a comprehensive set of GPS-based indicators reflecting the multidimensional nature of daily mobility for applications in health and aging research," *Int. J. Health Geogr.*, vol. 18, no. 1, p. 17, Dec. 2019, doi: 10.1186/s12942-019-0181-0.

[4] C. Roecke, M. Katana, M. Fillekes, M. Martin, and R. Weibel, "Mobility, physical activity and social interactions in the daily lives of healthy older adults: the MOASIS project," *Innov. Aging*, vol. 2, no. suppl_1, pp. 274–274, Nov. 2018, doi: 10.1093/geroni/igy023.1014.

[5] T. P. Nogueira, R. B. Braga, and H. Martin, "An ontology-based approach to represent trajectory characteristics," *Proc. - 5th Int. Conf. Comput. Geospatial Res. Appl. COM.Geo 2014*, pp. 102–107, 2014, doi: 10.1109/COM.Geo.2014.22.

[6] L. Xiang, M. Gao, and T. Wu, "Extracting stops from noisy trajectories: A sequence oriented clustering approach," *ISPRS Int. J. Geo-Information*, vol. 5, no. 29, pp. 1–18, 2016, doi: 10.3390/ijgi5030029.

[7] L. Bermingham and I. Lee, "A probabilistic stop and move classifier for noisy GPS trajectories," *Data Min. Knowl. Discov.*, vol. 32, no. 6, pp. 1634–1662, 2018, doi: 10.1007/s10618-018-0568-8.

[8] R. Montoliu, J. Blom, and D. Gatica-Perez, "Discovering places of interest in everyday life from smartphone data," *Multimed. Tools Appl.*, vol. 62, no. 1, pp. 179–207, 2013, doi: 10.1007/s11042-011-0982-z.

[9] B. Lamiroy and T. Sun, "Computing precision and recall with missing or uncertain ground truth," *9th Int. Work. GREC 2011, Seoul, Korea, Sept. 15-16, 2011, Revis. Sel. Pap.*, vol. Springer, no. 7423, pp. 149–162, 2013, doi: 10.1007/978-3-642-36824-0_15.

[10] A. M. Maceachren, "Compactness of Geographic Shape: Comparison and Evaluation of Measures," *Geogr. Ann. Ser. B, Hum. Geogr.*, vol. 67, no. 1, pp. 53–67, Apr. 1985, doi: 10.1080/04353684.1985.11879515.

Survey of Leisure Walking Behaviours and Activity Tracking Use: Emerging Themes and Design Considerations

James Williams [1], James Pinchin [1], Adrian Hazzard [2], Gary Priestnall [3]

[1] Nottingham Geospatial Institute, University of Nottingham
[2] Mixed Reality Laboratory, University of Nottingham
[3] School of Geography, University of Nottingham
{firstname.lastname}@nottingham.ac.uk

Abstract. In this paper we present a work in progress analysis of a leisure walking behaviour survey that focuses on walkers' habits and experiences. We are specifically interested in the use of mobile tracking applications in this context to help design and deploy future technologies that can better support engaging leisure walks through synthesising previous behaviours and experiences. This survey collected 329 responses relating to self-reported walking behaviour patterns and mobile activity tracker use. In the emerging analysis we identified design considerations for future walking-focused applications, emphasizing the subjective and personal nature of walking routes.

Keywords. Mobile activity tracking, Walking behaviour, Mobile geospatial computing

1. Introduction

Mobile activity trackers are an increasingly common feature of our everyday activities and routines. They populate our smart phones and adoption of activity tracking wearables is becoming ever more ubiquitous. Such technologies support users exercise (e.g., Diaz et al. 2015), health and well-being routines (e.g., Murphy et al. 2020). This data can be used in social exercising, which allows for the sharing of routines with a broader community (Couture 2020), and gamification where it is used to encourage physical activity (Shameli et al. 2017). Shin et al's (2019) review of activity tracking technology research highlights understanding human-information in-

LBS 2021
16th Conference on Location Based Services
24-25 November 2021 Online

Published in "Proceedings of the 16th International Conference on Location Based Services (LBS 2021)", edited by Anahid Basiri, Georg Gartner and Haosheng Huang, LBS 2021, 24-25 November 2021, Glasgow, UK/online.

https://doi.org/10.34726/1760 | © Authors 2021. CC BY 4.0 License.

teraction as an under explored area. We are interested in how digital technologies can better support leisure walkers, their choice of routes, their engagement with places of interest and how they reflect and share their experiences. We will then look to investigate how this ambient and volunteered geographic information can be applied within a walking route recommendation framework. The survey charted here begins this journey by capturing leisure walkers' current practices through collecting data on three aspects of leisure walking: (1) the frequency and duration of the activity; (2) the use of technology in walking; and (3) an identification of themes in the experiential factors of walking.

This paper is structured in five sections; the following section explains the survey design and recruitment, while *section 3* presents the preliminary results. *Section 4* is a discussion of design considerations and *section 5* is the conclusion.

2. Survey Design and Recruitment

We designed an online self-reported survey of five sections and 19 questions, split into: walking behaviours, reasons to walk, two on mobile technologies and demographic data relating to the participant. The question format used was a combination of behavioural questions to collect data on activity patterns and qualitative open questions to help identify subjective opinions and themes. We recruited 329 participants through social media and snowballing; participants were thus allowed to self-select for involvement. Our participant group included a range of age and genders, interestingly 52% reported their age as being between 45-64 and 81% of respondents were reported as female.

3. Preliminary Results

Analysis of the survey are work in progress. A sample of emerging results are presented in the following sections.

3.1. Activity Tracking Usage

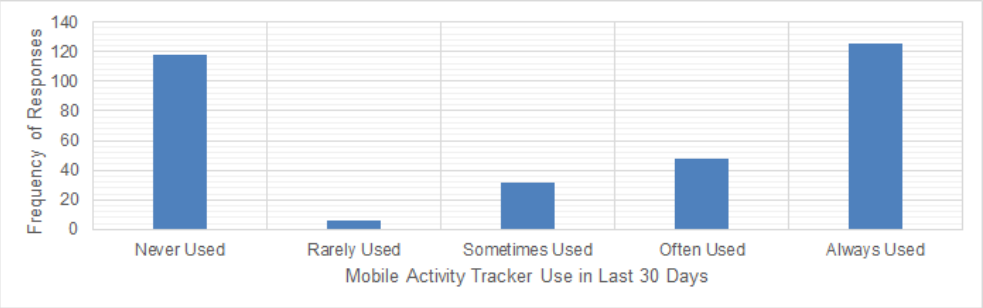

Figure 1. Frequency of mobile activity tracker use.

We gathered responses about the duration and frequency of leisure walking and the use of mobile activity trackers. Our preliminary analysis finds that 65% of participants used a mobile activity tracker; most of which used the application either 'often' or 'always' as in *Figure 1*. The current findings suggest that both walking frequency and duration influence a partial role in activity tracking use. For instance, filtering out participants who walked for less than one hour or once a week found that 70% of the remaining responses used an activity tracking application.

3.2. Applications Used

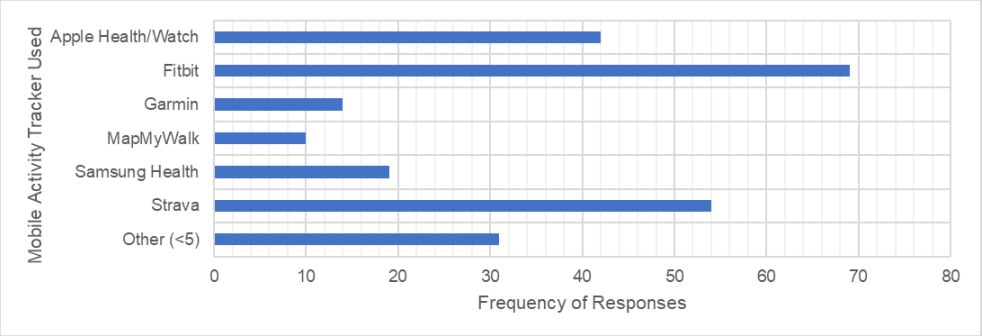

Figure 2. Highest frequency walking activity trackers used by respondents.

We asked participants what activity tracking applications they used and found the most popular were Fitbit, Strava and Apple Health as in *Figure 2*. Our emerging analysis also investigated those who did not use an activity tracking application. For this purpose, we identified several themes from an open-ended question, we found 70% of these responses were just not interested, 15% found the technology too difficult to use, and 10% wanted to be completely offline while walking.

3.3. Route Planning

Participants were asked whether they planned routes using technology or local knowledge. We found a significant association between these variables, with 51% of respondents saying that they never used technology to plan walks, contrasting with the 77% which said they sometimes or always use local knowledge in this process. In addition, we identified the effect that meeting other people had on the willingness to travel to start a walk. Respondents who usually met 1-3 other people were more likely to travel (54%) when compared to those who walked individually (30%).

3.4. Walking Rationale

The participants were presented with two open ended questions asking what they enjoyed about leisure walks and their rationale for taking them. These question responses have been coded to reveal some emerging themes, for example, 72% of respondents enjoy walking due to being able to get outside, 30% enjoyed walking for wellbeing, and 17% enjoyed exploration. Similar themes were identified in the rationale for walking, with 70% of participants walking for health and exercise purposes, 9% for social activities and 20% for dog walking. We found participants who walked for health or exercise to be the most likely to use an activity tracking application.

4. Discussion

This work in progress survey is to lay the groundwork for further study and development of a framework that can shape the design of future technologies that can support and curate engaging leisure walking experiences. Our emerging findings point towards the following design considerations:

Capturing and harnessing users' local knowledge to help support route planning appears to be an important consideration, of which sharing could also factor as an important facilitator. The ability to effectively capture and process high quality crowdsourced geographic information (See et al. 2016) could thereby contribute to the potential relevance of a design.

Escaping or avoiding technology while walking offers an interesting challenge, and one that could be addressed through careful design, but also whether the role of the technology is to support the route planning process, rather than the walk itself. The adoption of mobile activity tracking should also be considered in this context as previous research has found older demographics less likely to engage with such technology when difficult to use (Mercer et al. 2016).

People can walk for leisure for a variety of reasons, so the target rationale should be explicit in the design. The nature of each activity should be carefully considered, and relevant constraints should be identified, for example, a walk for exercise may need to be circular and of a certain distance or time. A challenge in this respect is linking these demands to other contextual factors to increase the enjoyment of a walk.

5. Conclusion

In this work we presented the emerging results of a self-reported leisure walking behaviour survey. The analysis captured statistics and identified themes for the rationale and enjoyment of walking, notably the importance of getting outside and exercise to our respondents. We discussed the potential design implications of the work which support the notion of capturing local knowledge, escaping technology and activity constraints. To further develop this knowledge, we will continue to study the contextual variables of walking to help in the design of a leisure route recommendation framework.

Acknowledgements

The James Williams author is supported by the Horizon Centre for Doctoral Training at the University of Nottingham (UKRI Grant No. EP/S023305/1) and by the Ordnance Survey external partner.

References

Couture, J. (2020). Reflections from the 'Strava-sphere': Kudos, community, and (self-)surveillance on a social network for athletes. Qualitative Research in Sport, Exercise and Health, 13(1), 1–17. doi:10.1080/2159676x.2020.1836514.

Diaz, K. M., Krupka, D. J., Chang, M. J., Peacock, J., Ma, Y., Goldsmith, J., Schwartz, J. E., & Davidson, K. W. (2015). Fitbit®: An accurate and reliable device for wireless physical activity tracking. International Journal of Cardiology, 185, 138–140. doi:10.1016/j.ijcard.2015.03.038.

Mercer, K., Giangregorio, L., Schneider, E., Chilana, P., Li, M., & Grindrod, K. (2016). Acceptance of Commercially Available Wearable Activity Trackers Among Adults Aged Over 50 and With Chronic Illness: A Mixed-Methods Evaluation. JMIR MHealth and UHealth, 4(1), e7. doi:10.2196/mhealth.4225.

Murphy, J., Uttamlal, T., Schmidtke, K. A., Vlaev, I., Taylor, D., Ahmad, M., Alsters, S., Purkayastha, P., Scholtz, S., Ramezani, R., Ahmed, A. R., Chahal, H., Darzi, A., & Blakemore, A. I. F. (2020). Tracking physical activity using smart phone apps: assessing the ability of a current app and systematically collecting patient recommendations for future develop-

ment. BMC Medical Informatics and Decision Making, 20(1), 17. doi:10.1186/s12911-020-1025-3.

See, L., Mooney, P., Foody, G., Bastin, L., Comber, A., Estima, J., Fritz, S., Kerle, N., Jiang, B., Laakso, M., Liu, H.-Y., Milčinski, G., Nikšič, M., Painho, M., Pődör, A., Olteanu-Raimond, A.-M., & Rutzinger, M. (2016). Crowdsourcing, Citizen Science or Volunteered Geographic Information? The Current State of Crowdsourced Geographic Information. ISPRS International Journal of Geo-Information, 5(5), 55. doi:10.3390/ijgi5050055.

Shameli, A., Althoff, T., Saberi, A., & Leskovec, J. (2017). How Gamification Affects Physical Activity. Proceedings of the 26th International Conference on World Wide Web Companion - WWW '17 Companion, 2017, 455–463. doi:10.1145/3041021.3054172.

Shin, G., Jarrahi, M. H., Fei, Y., Karami, A., Gafinowitz, N., Byun, A., & Lu, X. (2019). Wearable Activity Trackers, Accuracy, Adoption, Acceptance and Health Impact: A Systematic Literature Review. Journal of Biomedical Informatics, 93, 103153. doi:10.1016/j.jbi.2019.103153.

Personalized POI recommendation using deep reinforcement learning

Jing Huang, Tong Zhang

jing_h@whu.edu.cn, zhangt@whu.edu.cn

Wuhan University

Abstract. As an important location based service, next Point-Of-Interest (POI) recommendation has been widely utilized in helping people discover attractive and interesting locations. However, the sparsity of check-in data, the cold start issue and complicated contextual and semantic relationships between users and POIs bring severe challenges. To cope with these challenges, we develop a novel deep reinforcement learning based personalized POI recommendation framework. Within the proposed framework, a joint graph embedding model is proposed to compute users' dynamic preferences, accounting for inter-user relationships, historical check-in sequence, and category information of visited POIs. We are working on the experiments of applying the proposed POI recommendation framework on two typical real-world location-based social network datasets.

Keywords. POI recommendation, deep reinforcement learning, graph embedding

1. Introduction

With the rapid prevalence of smart mobile devices, users can post their locations and location-related contents on various social platforms, which underpin the building of online virtual society and generate massive user behavior data. Massive information of POIs has imposed serious information overload on mobile users. The selection dilemma faced by regular users has motivated the development of next POI recommendation algorithms in both computer science and location-based service communities.

Published in "Proceedings of the 16th International Conference on Location Based Services (LBS 2021)", edited by Anahid Basiri, Georg Gartner and Haosheng Huang, LBS 2021, 24-25 November 2021, Glasgow, UK/online.

https://doi.org/10.34726/1761 | © Authors 2021. CC BY 4.0 License.

Unlike traditional recommender systems, next POI recommendation faces several challenges. (1) **Data sparsity**. Due to high cost and privacy protection, users' check-in data generated in location based social networks (LBSNs) is much sparser than their rating data generated for music and movies. The performance of most existing collaborative filtering (CF) methods is significantly degraded by the sparse user-item matrix. (2) **Cold Start** is a common but critical problem in the field of recommender system. In POI recommendation tasks, there are broadly two main cold start issues: locations that have never been visited are called cold-start POIs, and users who have never visited any location are called cold-start users. Traditional research predicts a user's next POI based on the individual's sufficient historical data, which are difficult to be applied in cold start scenarios (Mazumdar et al. 2020). (3) **Dynamic User Preferences**. As time goes by or environments change, users' preferences for POIs and items may vary (Hu et al. 2021). We aim to deal with all above challenges and propose an effective data-driven POI recommendation method.

The primary contributions of this paper are summarized as follows:

- We develop a joint graph-based embedding model to learn the representations of POIs, timestamps, function zones, user comment and trajectory data in a shared low-dimension space. To track the changes of user preferences, we model the dynamic user preferences based on the learnt embedding of POIs.
- We propose a POI recommendation framework based on deep reinforcement learning techniques, which are used to produce a list of POIs by incorporating real-time feedbacks from users and unified representations of various factors such as temporal effect, geographical influence, semantic information and sequential features.

2. Methodology

2.1. Problem Statement

Definition 1. (**User check-in profile**) For each user u, we create a user profile vector D_u, which is a set of check-in activities associated with u and sorted by timestamp. A check-in activity is expressed as a tuple (u, v, l_v, t, M_v), denoting user u visits POI v at time t, l_v is v's geographical location including latitude and longitude coordinates and M_v is the set of words describing v, such as POI categories, reviews, and ratings. The dataset D used in our model includes the profiles of all users, $D = \{D_u : u \in U\}$.

Definition 2. (**POI-POI Graph**) A POI-POI graph, denoted as $G_{vv} = (V \cup V, \varepsilon_{vv})$, V is a collection of POIs and ε_{vv} is a collection of edges between POIs. In the given comment set C_{review}, the corresponding text set w_v is extracted for each POI v. w_v is then be used to calculate the topic feature $\overrightarrow{w_v}$ using the Latent Dirichlet Allocation (LDA) model (Chen et al. 2020). The cosine distance is used to calculate the similarity between the topic feature vectors of each POI. If the cosine similarity s_{ij} between the topic feature vectors of v_i and v_j is greater than the threshold α, then v_i and v_j are connected to an edge e_{ij} and the weight w_{ij} is set to s_{ij}.

Definition 3. (**POI-Zone Graph**) POI-Zone graph, denoted as $G_{vz} = (V \cup Z, \varepsilon_{vz})$, is a bipartite graph, where ε_{vz} is a set of edges between POIs and function zones. Considering the semantic connectivity among spatial entities, regions segmented based on their typical core functions are termed as function zones (Wang et al. 2020). If POI v_i is located in function zone z_j, there will be an edge e_{ij} connecting v_i and z_j, otherwise none. The weight w_{ij} is set to 1 if edge e_{ij} exists.

Definition 4. (**POI-Time Graph**) POI-Time graph, denoted as $G_{vt} = (V \cup T, \varepsilon_{vt})$, is a bipartite graph, where ε_{vt} is a set of edges between POIs and pre-defined time slots. If POI v_i is visited by users at time slot t_j, there will be an edge e_{ij} connecting v_i and t_j, otherwise none. The weight w_{ij} is set to frequency of POI v_i checked in at time slot t_j.

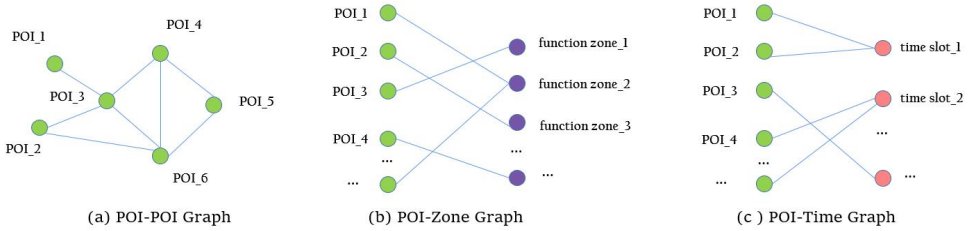

Figure 1. Bipartite graphs.

Problem Definition. (**Location-based Recommendation**) Given a user check-in sequence dataset D and a query user u with her current location l and time t (denoted as a query $q(u, l, t)$), our goal is to recommend top-k POIs that user u would be interested in and enhance her experience with these POIs.

2.2. Model description

We first propose a joint graph-based embedding approach using bipartite graph and produce the integrated representation of a user, spatial entities

(e.g., POIs, activity types, function zones), sequence and semantic information in a latent space. Then, we present a POI recommendation framework based on graph embeddings using an actor-critic reinforcement learning framework (Zhao et al. 2018).

Joint Graph Embedding Learning. We adopt a bipartite graph embedding model with a joint training algorithm (Xie et al. 2016) to embed the POI-POI graph, POI-Zone graph and POI-Time graph into a low dimension latent space, in which visited POI, visit time slot and associated function zone of each user, are represented as a low dimensional vector, $\vec{v}$, $\vec{t}$ and $\vec{z}$, respectively. An intuitive way is to minimize the sum of all objective functions as following:

$$O = O_{vt} + O_{vv} + O_{vz} \quad (1)$$

To optimize the objective function Eqn. (1), we first merge all the edges in the three sets e_{vv}, e_{vt}, e_{vz} together, and then update the corresponding embedding model by alternatively sampling an edge from it at each step.

Deep Reinforcement Learning Based POI Recommendation. We model the POI recommendation task as a Markov Decision Process (MDP) and use Deep Reinforcement Learning (DRL) to learn and update the optimal recommendation strategies during the interactions between users and POIs. A recommender agent (RA) interacts with environment $\mathcal{E}$ over a sequence of time steps. We formally define the tuple of five elements $(\mathcal{S}, \mathcal{A}, \mathcal{P}, \mathcal{R}, \gamma)$ of **MDP Environment** $\mathcal{E}$, which informs the actor (i.e., user) about its states in the POI graph and possible actions to take. The environment also rewards the actor if the current policy fits the observed user interactions. (1) **State** $\mathcal{S}$. The state s is to describe the environment composed by users and spatial entities (e.g., POIs, activity types, function zones); (2) **Action** $\mathcal{A}$. An action $a = \{a^1, \cdots, a^M\} \in \mathcal{A}$ is to recommend a list of M POIs to a user based on the current state s; (3) **Transition** $\mathcal{P}$. Transition $p(s'|s, a)$ defines the state transition from s to s' when recommender agent (RA) takes action a; (4) **Reward** $\mathcal{R}$. After the RA takes an action a at the state s, i.e., recommending a list of POIs to a user, the user browses these POIs and provides her feedbacks. She can skip (not visit) or visit the recommended POIs. We consider the length of stay duration at POIs as an implicit feedback, and the agent receives immediate reward $r(s, a)$ according to the user's feedbacks; (5) **Discount factor** γ. $\gamma \in [0,1]$ defines the discount factor when we measure the present value of future reward.

At each time step, the *RA* takes an action $a \in \mathcal{A}$ according to $\mathcal{E}$'s state $s \in \mathcal{S}$, and receives a reward $r(s, a)$. According to action a, the environment $\mathcal{E}$ updates its state to s' with transition probability $p(s'|s, a)$. The recommendation task can then be solved via reinforcement learning (Afsar

et al. 2021), which aims to find a recommendation policy $\pi : \mathcal{S} \rightarrow \mathcal{A}$, which maximizes the cumulative reward for the POI recommender system. In this work, our recommending policy builds upon the Actor-Critic framework which is appropriate to handle enormous and dynamic action space and reduce redundant computation.

The Actor-Critic framework consists of two components: Actor and Critic. The Actor component inputs the current state s and outputs a deterministic action (or recommending a deterministic list of M points), i.e., $s \rightarrow a = \{a^1, \cdots, a^M\}$.

The Critic component is designed to leverage an approximator to learn an action-value function $Q(s, a)$, which determines whether the action a (or a recommendation list of POIs) generated by Actor matches the current state s. The approximation function can be defined as follows:

$$Q(s, a) = \mathbb{E}_{s'}[r + \gamma Q(s', a') | s, a]. \quad (2)$$

Then, according $Q(s, a)$, the Actor updates its' parameters in a direction of improving performance to generate proper actions (or recommendations) in the following iterations. In practice, the action-value function is highly nonlinear. Thus we choose deep Q-value function (DQN) (Volodymyr et al. 2015) as the approximator.

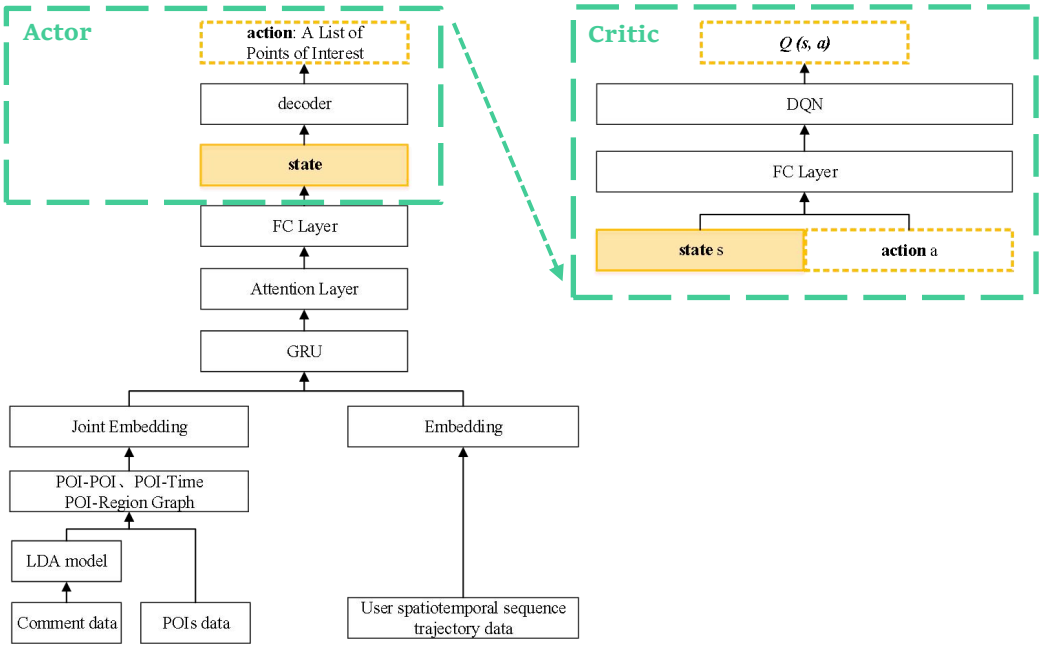

Figure 2. The proposed POI recommendation architecture.

We use Gated Recurrent Units (GRU) (Chung et al. 2014) to capture users' sequential behavior as user's initial preference. The input of GRU is a low-dimensional dense vector representing the information from the users' profile and spatial entities graphs, while the output vector is the representation of users' initial preference. To capture user's dynamic preference, we employ an attention mechanism (Sachdeva et al. 2018), which allows the *RA* to adaptively combine different parts of the input sequence in a linear manner. Given user's current preference (state) s, we aim to recommend a list of POIs to maximize the reward. It is the inverse process of what the joint embedding and GRU layer do. We use the decoder model (Cho et al. 2014) to restore one list from the low-dimensional representation s. The entire embedding and Actor-Critic based recommendation workflow is illustrated in Figure 2.

3. Current State and Future Work

Our experiments will be performed on two real large-scale LBSNs datasets: Foursquare (Chen et al. 2020) and Gowalla (Luo et al. 2019) to evaluate the effectiveness of the proposed framework. We will mainly focus on two questions: (1) how the proposed framework performs compared to the state-of-the-art baselines; and (2) how different components of the proposed model contribute to the performance.

We divide the dataset by sorting users' check-in records according to the check-in time, taking the earlier 80% as the training/validation set and the later 20% as the test set. To evaluate the recommendation performance and explainability, we adopt two widely-used metrics including *Precision@M* and *Recall@M*. The evaluation metrics are defined as follows:

$$Precision@M = \frac{|D_{test} \cap \text{Top\_}M|}{|\text{Top\_}M|} \tag{3}$$

$$Recall@M = \frac{|D_{test} \cap \text{Top\_}M|}{|D_{test}|} \tag{4}$$

where $|D_{test}|$ denotes the test set and $|\text{Top\_}M|$ denotes the list of recommendations of size M generated for the user. In the experiments, we evaluate the performance of the recommendation framework using the mean accuracy and mean recall of all users. Each time the *RA* recommends a list of $M = 5$ POIs to users. The rewards r of one skipped/visited POI is empirically set as 0 and 1 and the discounted factor $\gamma = 0.95$.

We will design experiments to perform parameter sensitivity analysis and explore the impacts of the number of topics, thresholds and the dimensions

of the embedding vectors on the recommendation performance of the proposed framework.

References

Mazumdar P, Patra B. K, Babu K S (2020) Cold-start Point-of-interest Recommendation through Crowdsourcing. ACM Transactions on the Web, 14(4), 19:1-19:36.

Hu X, Xu J, Wang W, Li Z, Liu A (2021) A graph embedding based model for fine-grained poi recommendation. Neurocomputing, 428:376-384.

Chen J, Meng X, Ji W, Zhang Y (2020) POI Recommendation Based on Multidimensional Context-Aware Graph Embedding Model. Journal of Software, 31(12):3700-3715 (in Chinese).

Wang P, Liu K, Jiang L, Li X, Fu Y (2020) Incremental Mobile User Profiling: Reinforcement Learning with Spatial Knowledge Graph for Modeling Event Streams. Proceedings of the 26th ACM SIGKDD International Conference on Knowledge Discovery & Data Mining, pp.853-861.

Xie M, Yin H, Wang H, Xu F, Chen W, Wang S (2016) Learning Graph-based POI Embedding for Location-based Recommendation. CIKM '16: Proceedings of the 25th ACM International on Conference on Information and Knowledge Management, pp.15-24.

Afsar M.M, Crump T, Far B (2021) Reinforcement learning based recommender systems: a survey.

Zhao X, Xia L, Zhang L, Ding Z, Yin D, Tang J (2018) Deep reinforcement learning for page-wise recommendations. Proceedings of the 12th ACM Conference on Recommender Systems (RecSys '18), pp.95-103.

Zhao X, Gu C, Zhang H, Yang X, Liu X, Tang J, Liu H (2019) DEAR: Deep Reinforcement Learning for Online Advertising Impression in Recommender Systems.

Volodymyr M, Koray K, David S, Andrei A. R, Joel V, et al. (2015) Human-level control through deep reinforcement learning. Nature, 518(7540):529-533

Chung J, Gulcehre C, Cho K. H, Bengio Y (2014) Empirical evaluation of gated recurrent neural networks on sequence modeling. Proceedings of the 2014 Conference on Empirical Methods in Natural Language Processing, pp.1724-1734.

Sachdeva N, Cupta K, Pudi V (2018) Attention neural architecture incorporating song feature for music recommendation. Proceedings of the 12th ACM Conference on Recommender Systems (RecSys '18), pp.417-421.

Cho K, Merrienboer B. V, Gulcehre C, Ba Hdanau D, Bougares F, Schwenk H, et al (2014) Learning phrase representations using RNN encoder-decoder for statistical machine translation. Computer Science.

Luo A, Zhao P, Liu Y, Xu J, Li Z, Zhao L, et al. (2019). Adaptive attention-aware gated recurrent unit for sequential recommendation. Database Systems for Advanced Applications – 24th International Conference, pp.317-322.

Understanding Mobility of Aalborg Commuters: A case study with a Floating Car Dataset

Irma Kveladze*, Pelle Rosenbeck Gøeg**, Niels Agerholm**

* Department of Planning, Division of Lang Management and Geoinformatics, Aalborg University, Copenhagen, Denmark. ikv@plan.aau.dk

** Department of the built Environment, Division of Transportation Engineering, Aalborg University, Aalborg, Denmark. {prg, niag}@build.aau.dk

Abstract. This research focuses on investigating human commuting patterns within the GeoVisual Analytics (GVA) environment using Floating Car Datasets (FCD) collected in Aalborg municipality between years 2012 – 2014. According to studies in the transportation domain, physical commuting remains an actual routine in the everyday lifestyle of modern society. And yet, insufficient number of studies have been conducted in this direction nor presented from the GVA analytics perspective that would provide a more in-depth understanding. To contribute to the existing studies, we investigate the spatio-temporal distribution of the travel behaviour of Aalborg commuters from location-to-location during peak and off-peak hours throughout working days and weekends with morning and afternoon rush hours. Accordingly, we propose an interactive GVA environment as an essential tool for the extensive analysis of human mobility data to ensure effective exploratory interpretation of the commuters' travel behaviour while following the analysis workflow provided by the traffic experts. The GVA reveals ongoing dynamic processes in traffic flow over space and time to help local authorities for a better decision-making process in traffic management.

Keywords. GeoVisual Analytics, Floating Car Dataset, Commuting

1. Introduction

According to the studies conducted by the Confederation of Danish Industry (DI), on average in Denmark, people commute 40 – 45 km between work and home places. However, these numbers can differ in some parts of the country

LBS 2021
16th Conference on Location Based Services
24-25 November 2021 Online

Published in "Proceedings of the 16th International Conference on Location Based Services (LBS 2021)", edited by Anahid Basiri, Georg Gartner and Haosheng Huang, LBS 2021, 24-25 November 2021, Glasgow, UK/online.

https://doi.org/10.34726/1781 | © Authors 2021. CC BY 4.0 License.

due to significant distances between municipalities. For instance, in the northern part of Denmark, some workplaces require employees to commute on average 53 – 56 km between home to work depending on whether they are full-time or half-time employed (Dansk Industri 2018). Besides the morning and afternoon rush hours, traffic congestion causes adverse ecological and health outcomes, plus a significant time burden and fuel consumption (Bopp et al. 2018, Novaco 2015). From an environmental and health perspective, long time commuting results in a more extensive exposure to air pollution, traffic noise and possible mental health associated with stress and fatigue (Bopp et al. 2018b). The study provided by Dansk Industri (2018) gives an overall understanding of the commuting behaviour of Danes across the country. However, more in detail investigations are needed for individual regions. Therefore, to comprehend Aalborg commuters' spatial behaviour and mobility patterns during rush and off rush hours over the weekdays, we investigate their spatial distribution and temporal variation over space and time using FCD. The FCD contains valuable information on commuters' whereabouts. One of the effective ways to get better insight into the human mobility characteristics from a visual exploration perspective is a flow map (Kraak 2014, Verbeek et al. 2011). According to the literature in transportation research, traditional micro and macro simulation and modelling approaches focus on providing tools to support planning challenges by determining travel needs for origin and destination (Saeedi 2018). Therefore, differing from those traditional methods, we propose a GVA environment for the interactive visual investigation of commuting patterns, where the focal representation of a flow map is supported by various graphs for a profound analysis of the origin-destination data. The GVA will help the users to answer the following questions: What variations exist in commuting patterns, and how did they change over space and time? How far and how often do people commute between work and living places? How does commuting affect traffic congestion, the environment and commuters' health?

Thus, this study will be interesting for the local municipality representatives due to the increased traffic problems during morning and afternoon rush hours that causes some health and ecological issues.

2. Related Work

Over the years, various Origin-Destination (OD) flow map visualizations have been introduced in the scientific literature. For instance, Dewulf et al. (2015) introduced OD matrices to study commuting time differences between cars and public transport during rush hours based on FCD. To overcome overlapping problems, Wood et al. (2013) proposed to map OD as cells rather than flows. Differing from them, Zhou et al. (2019) presented an interactive visualization interface focusing on the OD flow wheel supported by

graphs to reveal human mobility characteristics through a mobile phone location dataset. These authors used different techniques to avoid visual overclutter. However, studies on usability issues indicate the importance of the cartographic design of OD flow maps (Koylu & Guo 2017). For instance, Purchase et al. (2012) and Xu et al. (2012) found that the users performed better with straight edges than curved edges due to considerable visual clutter. Ware et al. (2002) and Huang et al. (2005) revealed that reducing the number of crossings between edges improves the effectiveness and efficiency of flow maps. The above studies tackle visual clutter issues and focus on understanding commuting patterns through interactive interfaces. Differing from them, we suggest an interactive GVA environment as a visual solution space to allow the users data filtering and selection on demand options. This will facilitate visual clutter and increase the effectiveness and efficiency of the visual communication for knowledge extraction. To do so, the proposed GVA incorporates a flow map with various graphs to enhance in-depth data analysis. This will lead to understand the dynamic processes in the mobility of Aalborg commuters on micro and macro geographical scales.

3. Data and Methodology

3.1. Study area

Aalborg Municipality is situated in the Northern Jutland region of Denmark and covers approximately 1,144 km2 with a population of 215,312. The center of municipality, Aalborg city is the 4th largest city in Denmark and plays an essential role in the social and economic development of the Northern region.

Figure 1. Location of the Aalborg municipality in Denmark.

3.2. Data collection and processing

The Floating Car Datasets (FCD) was collected from 425 vehicles registered in Aalborg Municipality over three years. The data were gathered for a Danish big data project focusing on the Intelligent Transportation System (ITS) platform. The information about vehicle whereabouts and technical conditions was transmitted and stored in the database based on the installed onboard tracking devices. After data collection, FCD was map-matched to the real-world traffic network and anonymized. And after the anonymization, only data recordings gathered from 389 vehicles with 0,74 billion positions covering 9.7 million km have been published as an open source for data sharing (Figure 2a) (Gøeg et al. 2019).

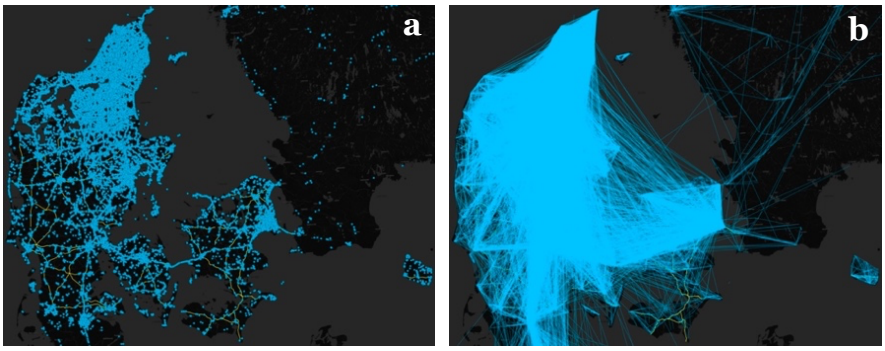

Figure 2. a) Row FCD and b) trips extracted with Origin-Destination (OD).

The anonymized FCD dataset was further processed for this research to extract relevant data characteristics and geographic knowledge with Origin-Destination (OD) trips for the GVA application. The extracted origin-destination points were again processed to separate weekdays from weekends and then connected to the municipality centres.

3.3. Designing the GeoVisual analytics environment

To gain an in-depth understanding of the mobility of Aalborg commuters, a user-friendly interface that allows enhanced characteristic analysis of human mobility from a spatio-temporal perspective was designed. The developed GVA environment aims to provide comprehensive information on the connectivity and volume of the Aalborg commuters across the country. Thus, flow maps can aggregate large streams of movements into flows to avoid visual over-clutter and reveal movement intensity between pairs of Origin and Destination locations (OD). OD flow maps require a careful cartographic design approach to overcome occlusions on the representation, for instance, between vectors and their arrowheads (Jenny et al. 2016). A graph drawing

criterion of a flow map could be grouped in edge geometry, arrangement of edges, and direction indication categories. The origin-destination node positions on the flow map are fixed to the centre of the municipality. At the same time, their thickness indicates the volume of the traffic flow within particular time windows. To follow some temporal uniformity, those time windows were generated based on the typical 24-hour traffic rhythm of the Danish Road network. The other important aspect was to define commuting distance in terms of space and time between home and work locations. However, according to traffic experts, it cannot be represented accurately as it depends on the different modes of transport. Therefore, trips with more than 5km were considered consistent. A large portion of the analytical environment consists of the geographical map view that specifically was designed in Mapbox and linked via API to the GVA. While the implementation of the flow map partially relies on the solutions described in Graser et al. (2019) and Koylu & Guo (2017). To operate displayed context on the map view, selection and filtering options are integrated into the system. This should allow a better visual perception of the flow map and information extraction. For better analysis and interpretation of commuter movements, graph views of time graph and parallel coordinate plot were also embedded in the GVA. The graphs and flow map are being constructed based on the user requirements and design recommendations gathered from the literature.

4. Results

Origin Destination (OD) flow maps are one of the interesting forms to visualize human mobility. Accordingly, the spatial view of the flow map allows interactive exploratory analysis on Aalborg commuters' distribution over space and time. The primary results show different trends in travelling distance and time behaviour over the weekdays. According to Danish Industry (DI) (Dansk Industri 2018), the length of the trips between work and home places for mobile Danes can vary across Denmark, and the average commuting is 42,5 km per day. Besides, there is a trend that the majority of the commuters prefer an early trip to the workplace to avoid morning rush hours. Alternatively, they will commute to the workplace late and accordingly return home late. Of course, family obligations have a crucial role to play in the commuting behavioural pattern. Therefore, the proposed GVA environment, reveals and answers a diversity of the complex questions for a profound understanding of commuters' mobility patterns In Aalborg municipality.

References

Bopp M, Sims D, Piatkowski D (2018). Benefits and Risks of Bicycling. In Bicycling for Transportatio, Elsevier, 21–44.. doi:org/10.1016/B978-0-12-812642-4.00002-7

Dansk Industri (2018). Stor forskel i pendlingsafstand på tværs af køn, alder og kommuner. In DI Transport. http://publikationer.di.dk/dikataloger/857/. Accessed 7 July 2021

Dewulf B, Neutens T, Vanlommel M, Logghe S, de Maeyer P, Witlox F, de Weerdt Y, & van de Weghe N (2015). Examining commuting patterns using Floating Car Data and circular statistics: Exploring the use of new methods and visualizations to study travel times. Journal of Transport Geography, 48: 41–51.. doi:org/10.1016/j.jtrangeo.2015.08.006

Gøeg P, Kveladze I, Lahrmann H S, Agerholm N, & Koskinen S (2019). Anonymised Floating Car Data – the long path to data sharing. In ITS congress (Ed.), 13th ITS Europe Conference 2019 (p. 9). Online Publication. https://vbn.aau.dk

Graser A, Schmidt J, Roth F, Brändle N (2019). Untangling origin-destination flows in geographic information systems. Information Visualization, 18(1):153–172.. doi:org/10.1177/1473871617738122

Huang W, Hong SH, Eades P (2005). Layout Effects on Sociogram Perception. Lecture Notes in Computer Science, 3843 LNCS, 262–273.. doi:org/10.1007/11618058_24

Jenny B, Stephen DM, Muehlenhaus I, Marston BE, Sharma R, Zhang E, Jenny H (2016). Design principles for origin-destination flow maps. 45(1):62–75.. doi:org/10.1080/15230406.2016.1262280

Koylu C, Guo D (2017). Design and evaluation of line symbolizations for origin–destination flow maps. Information Visualization, 16(4):309–331.. doi:org/10.1177/1473871616681375

Purchase HC, Hamer J, Nöllenburg M, Kobourov SG (2012). On the Usability of Lombardi Graph Drawings. Lecture Notes in Computer Science (Including Subseries Lecture Notes in Artificial Intelligence and Lecture Notes in Bioinformatics), 7704 LNCS, 451–462.. doi:org/10.1007/978-3-642-36763-2_40

Saeedi S (2018). Integrating macro and micro scale approaches in the agent-based modeling of residential dynamics. International Journal of Applied Earth Observation and Geoinformation, 68: 214–229.. doi:org/10.1016/j.jag.2018.02.012

Ware C, Purchase H, Colpoys L, McGill M (2002). Cognitive Measurements of Graph Aesthetics: 1(2):103–110.. doi:org/10.1057/PALGRAVE.IVS.9500013

Wood J, Dykes J, Slingsby A (2013). Visualization of Origins, Destinations and Flows with OD Maps. 47(2): 117–129.. doi:org/10.1179/000870410X12658023467367

Xu K, Rooney C, Passmore P, Ham DH, Nguyen PH (2012). A User Study on Curved Edges in Graph Visualization. IEEE Transactions on Visualization and Computer Graphics, 18(12): 2449–2456.. doi:org/10.1109/TVCG.2012.189

Zhou Z, Meng L, Tang C, Zhao Y, Guo Z, Hu M, Chen W (2019). Visual Abstraction of Large Scale Geospatial Origin-Destination Movement Data. IEEE Transactions on Visualization and Computer Graphics, 25(1): 43–53.. doi:org/10.1109/TVCG.2018.2864503

Climate change and populists in geolocated Twitter

Francisco Porras-Bernardez, Georg Gartner

Research Group Cartography, TU Wien, Vienna, Austria.
francisco.porras.bernardez@tuwien.ac.at, georg.gartner@tuwien.ac.at

Abstract. Surveys have been one of the traditional tools to collect public opinions. However, social media are an important alternative to surveys, being a source of information easily available, in high volume and at low cost. There is plenty of literature dealing with the study of different social, political or environmental topics through social media such as Twitter. Climate change is one of these topics and has major relevance in our current society. In addition, politics is a common element of analysis in the platform. Nevertheless, there is not enough insight about the overall quantitative relevance of climate change compared with other topics such as politicians. Moreover, some of the literature focus specifically on geolocated tweets, which are a small fraction of the total posts generated. This work in progress deals with the identification and semantic analysis of geolocated posts in social media. We analyse and compare the presence of climate change with populist politicians in the platform. These political figures often have a controversial stance on climate change while enacting policies affecting millions of citizens. We aim to study how suitable is the platform for spatiotemporal analysis of public opinion on climate change, and how relevant is the topic on it compared to the presence of some populists. We also aim to provide guidance for further research based on geolocated tweets by estimating how much geolocated data is produced by which countries. More than 170 M geolocated tweets were extracted and analysed. Those tweets containing terms related to climate change in the official languages of the 14 most popular countries in the dataset, as well as the names of several politicians were filtered. Then, an analysis was performed to characterise the spatial and temporal global distribution of these posts during most of the past decade. This was compared with the dates of major events related with climate change and politics. Additionally, sentiment analysis was used to characterise the polarity of the posts. This paper presents an estimation of the relative presence of climate change in Twitter based on probably one of the largest geolocated tweets datasets existing.

LBS 2021
16th Conference on Location Based Services
24-25 November 2021 Online

Published in "Proceedings of the 16th International Conference on Location Based Services (LBS 2021)", edited by Anahid Basiri, Georg Gartner and Haosheng Huang, LBS 2021, 24-25 November 2021, Glasgow, UK/online.

https://doi.org/10.34726/1782 | © Authors 2021. CC BY 4.0 License.

This work will also offer a semantic analysis of the posts including a graph of the main terms used by country, as well as the polarity of the sentiments associated with climate change. This study has the potential to benefit policy makers, non-governmental organizations, activists, journalists and social media researchers worldwide.

Keywords. Twitter, Climate change, Populism, NLP, Sentiment Analysis

1. Introduction

Twitter is one of the most popular SM platforms offering geolocated content generated by its users. This and other SM have been used for the public discussion of topics of diverse relevance. This medium is a platform used by the general public, activists, governments, NGOs or public figures such as celebrities or politicians. Twitter has been widely used in research for the analysis of different phenomena including social, political or environmental issues (Doğu, 2019; Milleville et al., 2019; Yaqub et al., 2017). Climate change is an extremely relevant topic nowadays that is in the intersection of society, politics and environment.

Climate change presence in Twitter has been explored in previous studies attending to different topics such as its impacts, its causes, or even the acceptance of the phenomenon itself (Chen et al., 2019; Pathak et al., 2017). Additionally, many works have concentrated on analysing the sentiments associated to the tweets mentioning the term (Cody et al., 2015; Veltri & Atanasova, 2017). Moreover, other studies have focused on geolocated tweets to analyse regional differences or language and culture-based disparities (Bennett et al., 2021; Singleton et al., 2018). Nevertheless, most works have been limited to a few number of regions and languages and have built their conclusions on top of relatively limited datasets, spatially and temporally.

The role of politics in the platform has been analysed in terms of international events, political actions or direct communication related with climate change (Ebrey et al., 2020; Sanford et al., 2021). However, there has not been a specific focus on populist politicians and how prominent is their presence in the platform, compared directly to climate change. This is relevant due to their often-controversial stance towards the topic.

To the best of our knowledge, a comparative analysis of the overall presence of both topics in Twitter based on a large global geolocated dataset has not been carried out until now. There are differences in the rate of tweets geolocated among countries and the proportion of tweets geolocated is estimated in a 1% (Tasse et al., 2017). However, this kind of analysis could shed some light on the relative relevance of climate change in the overall public interest within Twitter. A differentiated analysis by countries and languages based on

geolocated tweets could contribute to build a better picture across regions and cultures.

For this study, we have processed more than 170 million geolocated tweets generated worldwide (2011-2020). The evolution of tweets produced in the countries with more users is being analysed and compared with the number of tweets dealing with climate change or four relevant populist politicians. We aim to estimate the overall presence of climate change in the platform compared to these political figures. This analysis has a wide coverage temporally, spatially and linguistically by taking into account terms in 14 languages. We are performing a basic analysis of the sentiments and the main terms of interest on these tweets in order to depict the topics commonly related to climate change and these politicians in this medium.

This study has the potential to benefit policy makers, non-governmental organizations, activists or journalists by providing an insight into the public debate about climate change in Social Media. Additionally, academics could benefit by an enlarged knowledge about the quantitative impact of some populist politicians along different countries within a specific platform. Moreover, by focusing on and quantifying geolocated tweets we provide additional hints for further research aiming to target specific regions.

2. Method

2.1. Data preparation

Given the Twitter API limitations, we decided to use an existing large collection of tweets built by The Internet Archive. The Twitter Stream Grab[1], contains more than 10 billion tweets mined from the Twitter Stream API. This API delivers a 1% random sample of their public daily global tweets[2]. It is available as thousands of TAR and JSON files that contain the tweets accounting for approximately 4TB of data. We developed multiple Python scripts to mine all the tweets available in the collection at that moment. Then we extracted and further processed only those posts geolocated. For one part of the geolocated tweets only a bounding box was available, thus a centroid was computed in such cases to obtain a point location.

2.2. Tweet filtering by terms

For filtering tweets related to “climate change” or “global warming” in our dataset, the terms were used translated to 14 languages. These include the top 13 languages in number of tweets in our dataset. In a second analysis

[1] https://archive.org/details/twitterstream
[2] https://developer.twitter.com/

phase, four world leaders considered populists by multiple sources[3] were selected. These politicians were presidents of their countries during the development of this work: Donald Trump, Vladimir Putin, Jair Bolsonaro and Recep Tayyip Erdoğan. These four figures were chosen because of their controversial public profiles, and the potential for global and regional analysis in the platform.

2.3. Sentiment Analysis

In this phase, we perform sentiment analysis on the filtered tweets in order to estimate the polarity of the posts generated by the users, analyse its temporal evolution and explore possible relations with real world events. The sentiment analysis determines sentiment orientation and classifies the tweets into classes of polarity: positive, neutral or negative. For the analysis, we use the VADER model (Hutto & Gilbert, 2014).

2.4. Topics extraction and visualization

We will follow a simple approach using NLP in order to analyse and visualize the most frequent words in the tweets. We can consider these words topics of interest (TOIs). For our objectives, we use a script in R based on the packages tm and igraph. The script cleans and counts the frequency of appearance of the words. First, the text is cleaned. Then, a corpus is built with all the cleaned words and a term-document matrix is generated considering each tweet a document. Those words with a frequency of appearance above a threshold are selected. Finally, graphs are created with nodes and edges representing the terms and their relations. Graphic elements are proportional to the total frequency of appearance and co-appearance.

3. Preliminary results

We present here a sample of some current results. *Figure 1* shows the amount of tweets in our dataset by country of posting for the top countries. In *table 1* is shown the amount of tweets generated in the top 24 countries and which share it represents from the total dataset.

[3] https://ips-dc.org/the-rising-tide-of-the-populist-right/
https://www.diepresse.com/5695513/trump-bolsonaro-erdogan-die-stunde-der-populisten
https://www.theguardian.com/commentisfree/2020/apr/26/trump-to-erdogan-men-who-behave-badly-make-worst-leaders-pandemic-covid-19

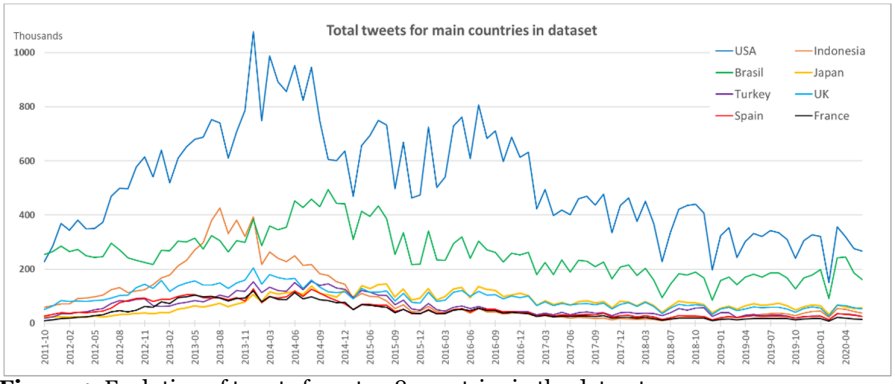

Figure 1. Evolution of tweets from top 8 countries in the dataset.

Number of tweets per country of generation (Top 24 countries)							
	Country	**Tweets**	**% of total**		**Country**	**Tweets**	**% of total**
1	USA	51.819.811	30,34	**13**	Russia	2.545.795	1,49
2	Brazil	25.592.957	14,98	**14**	Canada	2.172.296	1,27
3	Indonesia	9.666.053	5,66	**15**	Italy	1.720.884	1,01
4	UK	9.444.855	5,53	**16**	Saudi Arabia	1.668.118	0,98
5	Japan	7.622.546	4,46	**17**	Thailand	1.554.671	0,91
6	Turkey	6.275.875	3,67	**18**	Chile	1.494.398	0,87
7	Argentina	6.244.591	3,66	**19**	Colombia	1.471.555	0,86
8	Spain	5.204.510	3,05	**20**	India	1.456.484	0,85
9	France	4.415.451	2,58	**21**	The Netherlands	1.242.471	0,73
10	Malaysia	4.276.622	2,50	**22**	South Africa	1.113.650	0,65
11	Mexico	3.791.270	2,22	**23**	Portugal	1.070.508	0,63
12	Philippines	3.702.589	2,17	**24**	Germany	865.517	0,51
					TOTAL dataset	**170.813.099**	**100**

Table 1. Number of tweets in the dataset per country of generation.

Figure 2 compares the evolution of all tweets produced worldwide (blue line) in our dataset with the proportion of those mentioning *Trump* (red line).

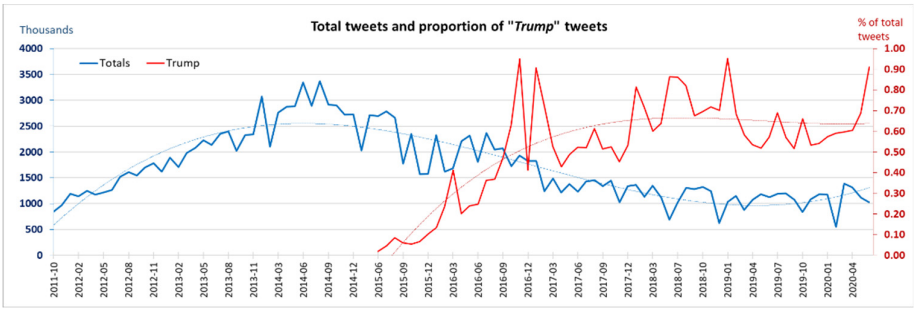

Figure 2. Share of global tweets mentioning Trump vs. total.

Figure 3 compares the evolution of geolocated tweets produced worldwide with the proportion of those mentioning *climate change*.

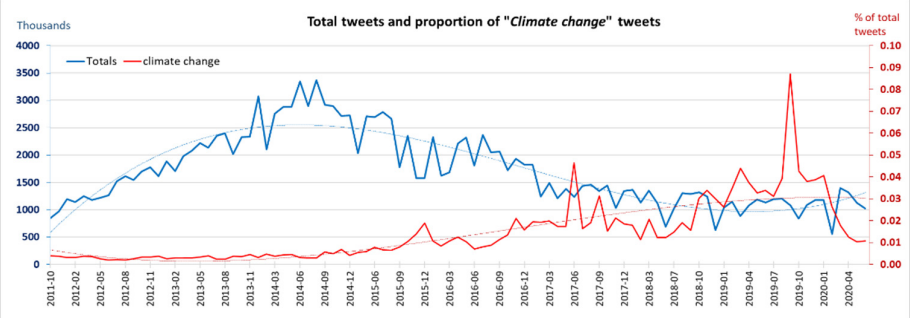

Figure 3. Share of global tweets mentioning Climate Change vs. total.

In *figure 4* we can see the evolution of the polarity of the *Trump* tweets in English after performing sentiment analysis. There is an overall positive polarity until May 2016 when he became his party's nominee. After this event, most of the months present a slightly negative mean polarity.

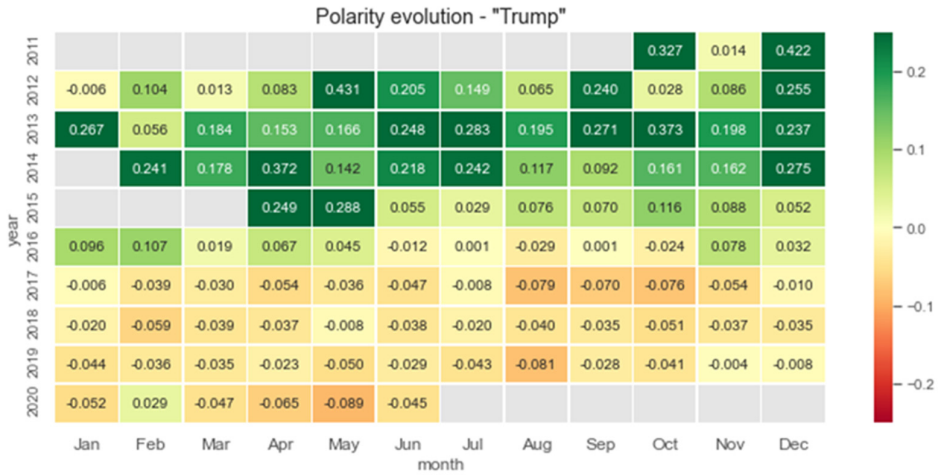

Figure 4. Polarity of tweets mentioning "trump".

Figure 5 compares the share of tweets for *Trump* and *climate change* in several countries. Distance between *climate change* and *Trump's* curves is lower in the European countries considered, compared to the USA and its neighbour Canada.

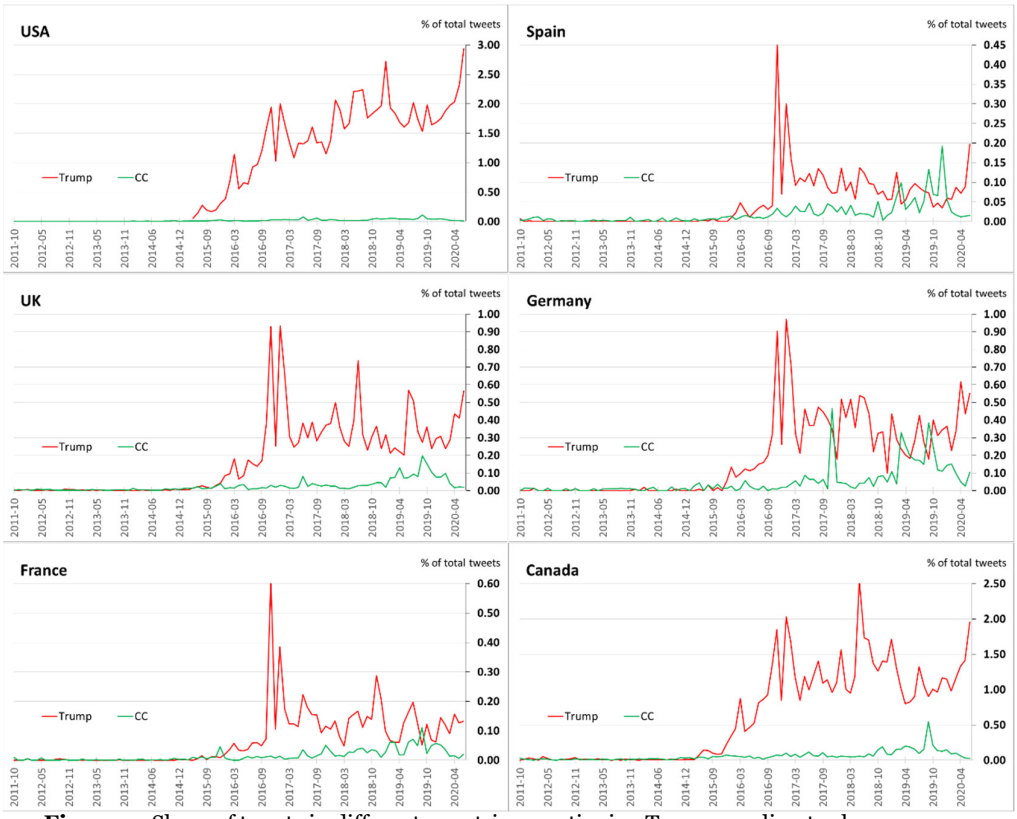

Figure 5. Share of tweets in different countries mentioning Trump vs. climate change.

Figure 6 shows in logarithmic scale the evolution of each group of tweets. Trump's global presence is outstanding. *Erdogan* and *Putin* show a similar impact during time, whereas *Bolsonaro* evolves from a modest global presence to overpass both. At a global level, all of the politicians have had a much bigger direct presence in Twitter than climate change.

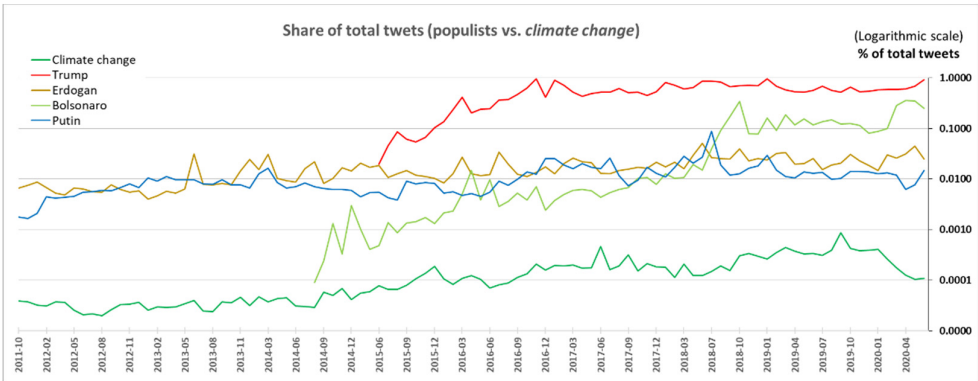

Figure 6. Global tweets dealing with climate change and selected politicians

4. Conclusion

The selected politicians are far more present in the platform than *climate change*. *Climate change* is comparatively more mentioned in the European countries considered, even overpassing *Trump* in short periods. We are mining a big and unique geolocated dataset that allows for a large data analysis spatially and temporally. Once completed, this work might allow us to provide a better insight into the geolocated conversation in the platform.

References

Bennett, J., Rachunok, B., Flage, R., & Nateghi, R. (2021). Mapping climate discourse to climate opinion: An approach for augmenting surveys with social media to enhance understandings of climate opinion in the United States. *PLOS ONE*, *16*(1), e0245319. https://doi.org/10/gmpv2q

Chen, X., Zou, L., & Zhao, B. (2019). Detecting Climate Change Deniers on Twitter Using a Deep Neural Network. *Proceedings of the 2019 11th International Conference on Machine Learning and Computing*, 204–210. https://doi.org/10/gmpv68

Cody, E. M., Reagan, A. J., Mitchell, L., Dodds, P. S., & Danforth, C. M. (2015). Climate change sentiment on Twitter: An unsolicited public opinion poll. *PloS One*, *10*(8), e0136092. https://doi.org/10/gj2w3k

Doğu, B. (2019). Environment as Politics: Framing the Cerattepe Protest in Twitter. *Environmental Communication*, *13*(5), 617–632. https://doi.org/10/gmn6rg

Ebrey, R., Hall, S., & Willis, R. (2020). Is Twitter Indicating a Change in MP's Views on Climate Change? *Sustainability*, *12*(24), 10334. https://doi.org/10/gmpv69

Hutto, C. J., & Gilbert, E. (2014). *VADER: A Parsimonious Rule-based Model for Sentiment Analysis of Social Media Text*. 10.

Milleville, K., Ali, D., Porras-Bernardez, F., Verstockt, S., Van de Weghe, N., & Gartner, G. (2019). *WordCrowd: A location-based application to explore the city based on geo-social media and semantics*. 231–236.

Pathak, N., Henry, M. J., & Volkova, S. (2017). *Understanding Social Media's Take on Climate Change through Large-Scale Analysis of Targeted Opinions and Emotions*. 2017 AAAI Spring Symposium Series.

Sanford, M., Painter, J., Yasseri, T., & Lorimer, J. (2021). Controversy around climate change reports: A case study of Twitter responses to the 2019 IPCC report on land. *Climatic Change*, *167*(3), 1–25.

Singleton, S., Kumar, S. A. P., & Li, Z. (2018). Twitter Analytics-Based Assessment: Are the United States Coastal Regions Prepared for Climate Change*f*. *2018 IEEE International Symposium on Technology and Society (ISTAS)*, 150–155. https://doi.org/10/gmpv2k

Tasse, D., Liu, Z., Sciuto, A., & Hong, J. (2017). State of the Geotags: Motivations and Recent Changes. *Proceedings of the International AAAI Conference on Web and Social Media*, *11*(1), 250–259.

Veltri, G. A., & Atanasova, D. (2017). Climate change on Twitter: Content, media ecology and information sharing behaviour. *Public Understanding of Science*, *26*(6), 721–737. https://doi.org/10/gf6dqd

Yaqub, U., Chun, S. A., Atluri, V., & Vaidya, J. (2017). Analysis of political discourse on twitter in the context of the 2016 US presidential elections. *Government Information Quarterly*, *34*(4), 613–626. https://doi.org/10/gcqjp8

A Real-Time Spatio-Temporal Bigdata System for Instant Analysis of Twitter Data to Monitor of Advertising Campaigns; Case Study New York City

Seyed Ali Hoseinpour*

* PHD student, GIS Dept, School of Surveying and Geospatial Engineering, College of Engineering, University of Tehran, Tehran, Iran
s.alihosein.p@ut.ac.ir

Abstract. Advertising monitoring is useful for detecting and determining user reaction, campaign performance and their challenges. Popular social networks especially Twitter are one of the best resources that could been analyzed for this purpose. Twitter's data analyzing needs different methods and tools because Twitter is one of the bigdata sources. In this paper, a system is developed dealing with Twitter data streams and can monitor advertising keyword spatio-temporal trends, real time. Also, it can predict the location of later tweets using MLP model. The prediction accuracy is 0.78.

Keywords. Location Based Services, Geotagged Big Data, Twitter, Advertising Campaigns, Spatio-Temporal

1. Introduction

Advertisement plays an important role in marketing, branding and business developing (Frolova 2014; Dib 2016), but it's not useful alone and to increase the performance and choose the best strategy, users' reactions and feedbacks must be controlled (Dib 2016). For example, after an advertise teaser, which group of customers, when and where were attracted (Frolova 2014; Dib 2016)?

Today, most of people share information on social media in different subjects such as products purchases (Varol et al. 2017). Twitter is one of the most important of them and is considered to be very important in the bigdata era (Shirdastian et al. 2019). There are 500 million tweets sent each day (Alotaibi et al. 2020). Twitter has an impact on marketing, so that, 40% of Twitter users purchased something after seeing it on Twitter (Alotaibi et al. 2020). Twitter contains spatial-temporal information so it can be used to spatio-temporal analytics (Martín et al. 2019).

The main purpose of this article is designing a real-time system for monitoring the spatial and temporal distribution of a particular keyword on

LBS 2021
16th Conference on Location Based Services
24-25 November 2021 Online

Published in "Proceedings of the 16th International Conference on Location Based Services (LBS 2021)", edited by Anahid Basiri, Georg Gartner and Haosheng Huang, LBS 2021, 24-25 November 2021, Glasgow, UK/online.

https://doi.org/10.34726/1783 | © Authors 2021. CC BY 4.0 License.

Twitter. Second purpose is adding a predicting model to it. So, this scenario is considered: A company has done an advertising with one keyword, and now, it needs this information to identify spatial and temporal hotspots to find the best location for a new store or billboard. What users have used this keyword in their tweets? How is the spatial and time sequence of these tweets on the map? What other keywords have been used with this keyword? Which hashtags are frequent in these tweets? What is the time distribution of tweets per hour? At next hour, how many tweets and where will be tweeted?

There are some challenges in this research that this paper tries to solve them:

- Twitter is one of the big data sources and has data stream. So, there are difficulties related to managing the 4V[1] characteristics(Alotaibi et al. 2020). Therefore, some special technologies and architectures (eg particular indexing) must be used.
- The base data in Twitter is text, so we need NoSQL databases, preprocesses and NLP[2].
- Many of Twitter's data don't have exact position. Also, although Twitter has an API to geocode request, but there is limitation for making requests number. So, we need location interpolation or estimation.

Martín et al (2019), with Python, MongoDB and Apache Pyspark, developed an architecture and work flow (*Figure 1.a)* to evaluate and locate the activity in the city of Valencia by Heatmap visiualization (Martín et al. 2019). Alotaibi et al (2020), developed a big data analytics tool (named Sehaa) for healthcare symptoms and diseases detection (*Figure 1.b)* using Twitter, Python and Apache Spark (Alotaibi et al. 2020). Sehaa uses machin learning method to detect various diseases in the Saudi Arabia.

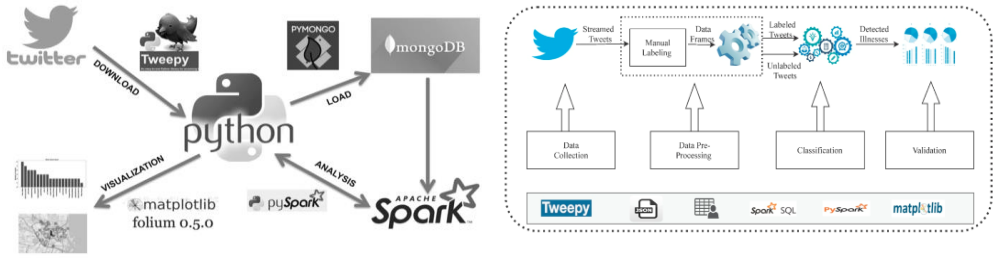

Figure 1. System architecture. **Left.** (Martín et al. 2019). **Rigth:** (Alotaibi et al. 2020)

2. Methodology

Figure 2 shows System's architecture; this system has 3 sections.

[1] i.e., volume, velocity, variety, and veracity

[2] Natural language processing

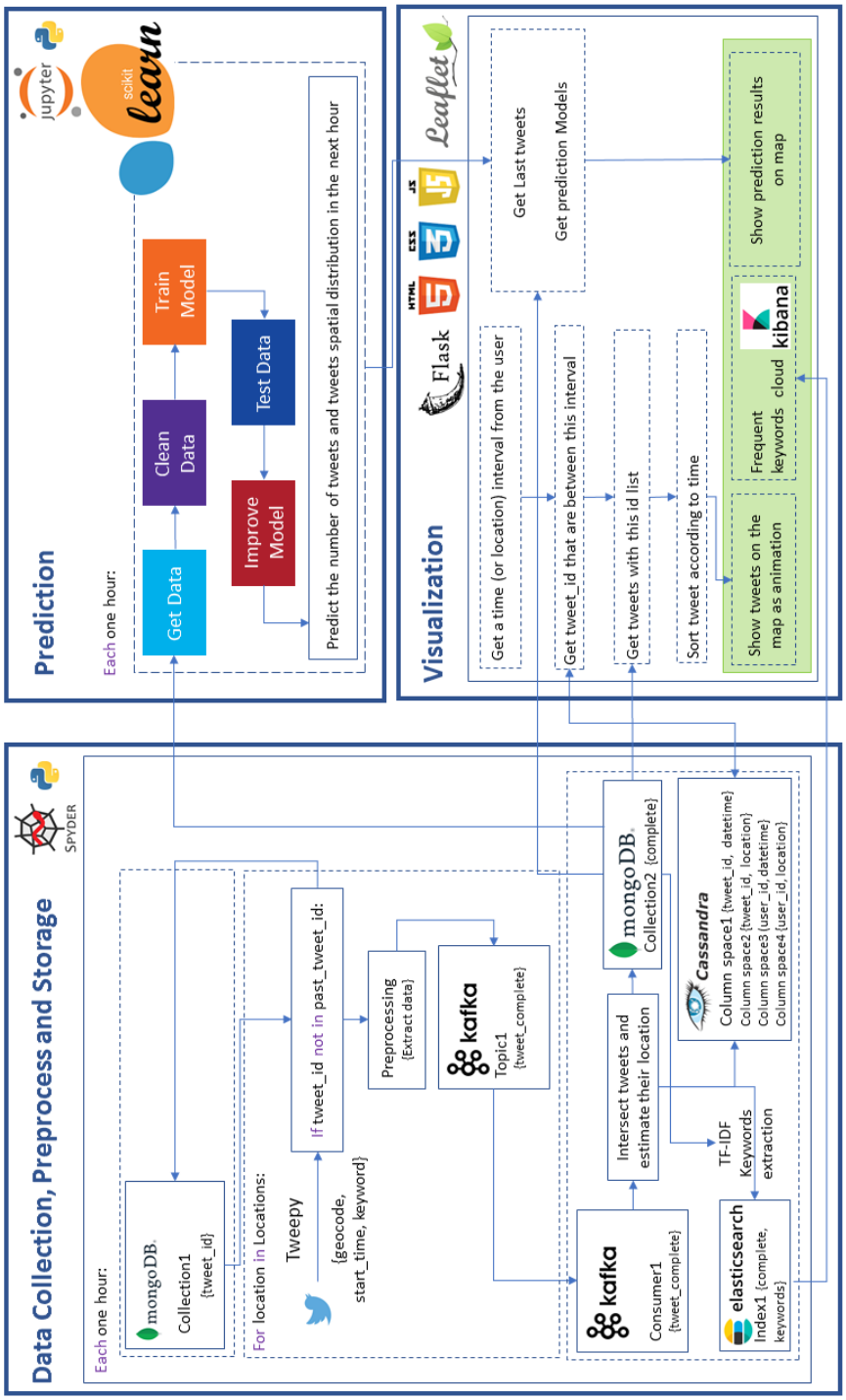

Figure 2. Architecture of proposed system

2.1. Data Collection, Preprocess and Storage

First a list of locations is defined as *Figure 3* according to them, geocode request with Twitter API by Python tweepy library is sent. Then a Python script code, sends a request with 4 parameters per hour for all locations: location geographic coordinates – keyword - start date - radius of search

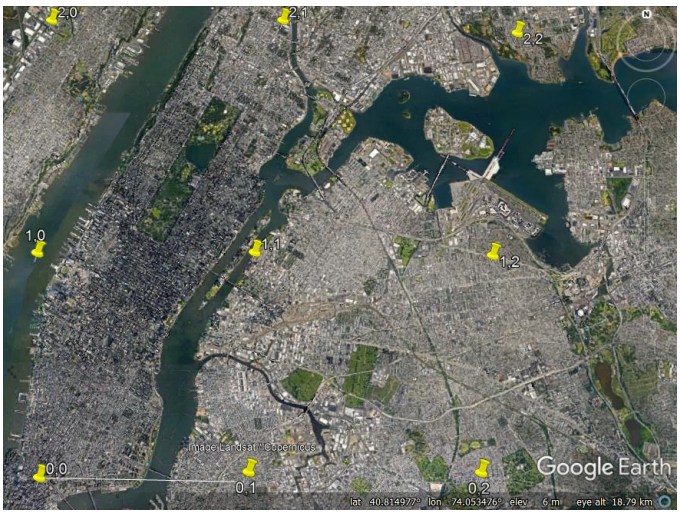

Figure 3. Locations list, New York. Distance between two neighbor points is 5km.

This paper used 'fire', '2021-09-01' and '5km'. Then all tweets with these features were returned. Then, for each tweet, if 'tweet-id' is not duplicated:

1. 'tweet-id' is saved in MongoDB first collection (MongoDB is optional).
2. **Preprocess**. All of tweet's essential data (eg hashtags) are extracted as a json.
3. The json is sent to Kafka topic using producer (Apache Kafka is an open-source distributed event streaming platform for high-performance data pipelines and streaming). Therefore, there is no need to worry about system disconnecting and reconnecting, and Kafka handles it. Kafka lets several consumers to use data separately.

When all tweets's json was sent to Kafka topic, a Kafka gets them. Then for each one:

1. **Spatial intersection.** It is possible that one tweet is returned by several requests. It means that this tweet is in the intersection of neighbors, as shown in *Figure 4*. The average of their coordinate is considered as tweet location and is added to json and the json is sent to MongoDB's other collection.
2. Tweet’s id and datetime is sent to Cassandra column space. Cassandra has been used for indexing and fast retrieval.
3. According to tweet’s text and other tweets's text, keywords are extracted by TF-IDF (Term Frequency — Inverse Document Frequency) technique and are added to json and the json is sent to Elasticsearch index. Elasticsearch has been used for text query and visualization dashboards.

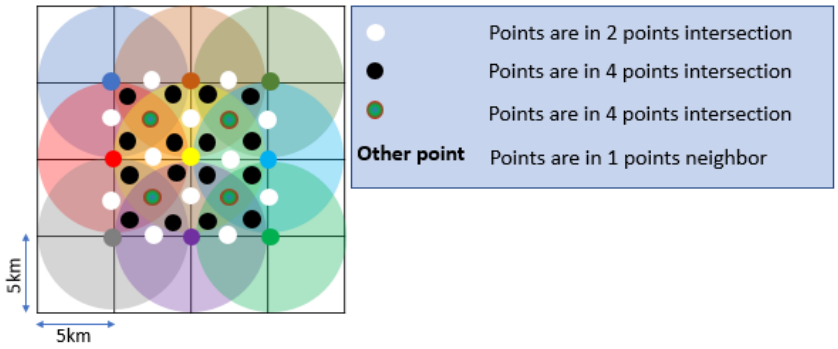

Figure 4. Spatial Intersection

2.2. Prediction

In another Python script code, each hour, all saved tweets are taken and after feature extraction and normalization, with sckit-learn library, a Multi-layer Perceptrons (MLP) model and a Random Forest model is trained for computing next hour tweets's count (function approximation) and distribution of 3 later tweets (classification). Then, the model's parameter is saved.

2.3. Visualization

A web application is been developed with FLASK framework. The user can select datetime interval, then tweets's spatio-temporal trend is shown on the map as animation. Also, users can see visualization dashboards (keywords' cloud, tweets count per hour, most frequent hashtags). Users can predict next hour tweets's count and 3 later tweets location on the map.

3. Results

This research has achieved its goals and has responded to scenario 'questions. Results are shown as several snapshot in *Figure 5-7*. *Figure 5* shows two snapshots of web app at different times while spatial distribution of tweets showing on the map. For each tweet, one red circle is added to the map in location that estimated for tweet. Also, some of tweet data such as id, text, user name, and tweet time are shown at same time. So, user can see tweets release direction and also can detect spatial and temporal hotspots that have more eager audience. *Figure 6* shows results of prediction on the map. *Figure 7* shows three dashboards on the map for most frequent Hashtags, keywords 'cloud and Tweets per hour. The full result can be seen at https://youtu.be/KOFikjf-vJ4. The MSE[3] of tweets' count prediction model is 0.00069. The average accuracy of 3 later tweets' location prediction model using MLP is 0.78 and using Random Forest is 0.7. So, MLP model is more suitable for this purpose. Research is ongoing to improve the accuracy of forecasting models using other ensemble and fusion methods,

[3] Mean Square Error

implement them using the Apache Spark and simultaneous use of Telegram data.

Figure 5. Tweets' spatio-temporal distribution for specified interval: **Top**.snapshot-1 **Bottom**.snapshot-2

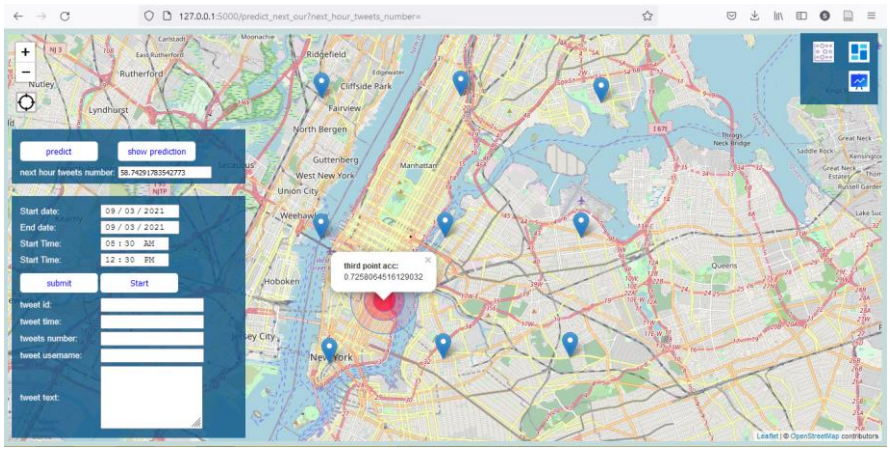

Figure 6. Prediction results. Predicted location for next three tweets.

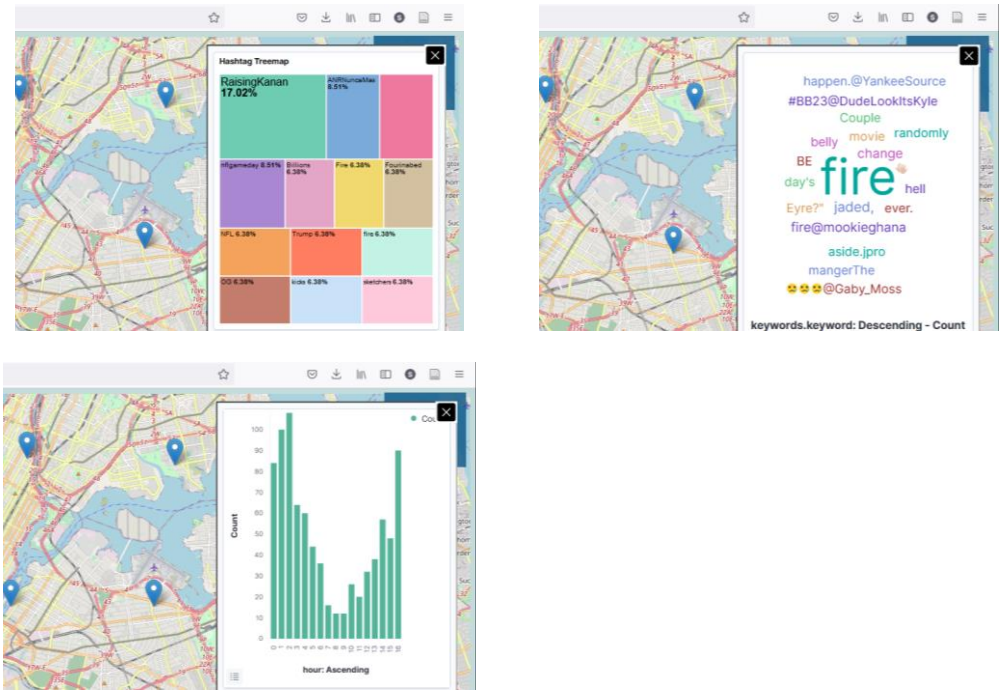

Figure 7. Elasticsearch dashboards that added to the web app: **Top-left**. Most frequent Hashtags **Top-right**. keywords 'cloud **Bottom**. Tweets-per-hour

References

Alotaibi S, Mehmood R, Katib I, et al (2020) Sehaa: A Big Data Analytics Tool for Healthcare Symptoms and Diseases Detection Using Twitter, Apache Spark, and Machine Learning. Applied Sciences 10:1398. https://doi.org/10.3390/app10041398

Dib A (2016) The 1-Page Marketing Plan: Get New Customers, Make More Money, And Stand Out From The Crowd. Successwise

Frolova S (2014) The role of advertising in promoting a product

Martín A, Julián ABA, Cos-Gayón F (2019) Analysis of Twitter messages using big data tools to evaluate and locate the activity in the city of Valencia (Spain). Cities 86:37–50. https://doi.org/10.1016/j.cities.2018.12.014

Shirdastian H, Laroche M, Richard M-O (2019) Using big data analytics to study brand authenticity sentiments: The case of Starbucks on Twitter. International Journal of Information Management 48:291–307. https://doi.org/10.1016/j.ijinfomgt.2017.09.007

Varol O, Ferrara E, Menczer F, Flammini A (2017) Early detection of promoted campaigns on social media. EPJ Data Science 6:1–19

Would Citizens Contribute their Personal Location Data to an Open Database? Preliminary Results from a Survey

Vilma Jokinen*, Ville Mäkinen*, Anna Brauer*† and Juha Oksanen*

* Finnish Geospatial Research Institute FGI, National Land Survey of Finland
† Department of Computer Science, University of Helsinki

Abstract. The amount of movement data that people record using their mobile phones via different tracking apps is vast. In a typical case the data can be viewed within the app but using the data by the third-party for other purposes is cumbersome, or practically impossible. One way to improve the situation is to establish an open trajectory data repository, where the users could save their movement tracks as open data. However, this data is considered personal data and the users may not be willing to share full trajectories as they might reveal for example their home locations. Thus, the trajectory data must be processed to minimize the amount of information that can be used to identify person while keeping the utility of the data as high as possible. We launched a survey of peoples' opinions about sharing their movement data and what kind of privacy guarantees they would expect. Based on the preliminary results, a large part of the potential users appears to be interested in sharing their tracking data, when adequate privacy-preserving pre-processing is performed.

Keywords. Human trajectory data, mobile tracking data

1. Introduction

The diffusion of smartphones and other GNSS-enabled mobile devices among the population has been exceptionally fast and extensive (Bento 2016), and a notable amount of people are recording their movement by fitness and other tracking applications provided by private companies. Typically, the companies keep the data mostly to themselves and allow access to users' data often only through their web sites. Exceptions, such as Strava

Published in "Proceedings of the 16th International Conference on Location Based Services (LBS 2021)", edited by Anahid Basiri, Georg Gartner and Haosheng Huang, LBS 2021, 24-25 November 2021, Glasgow, UK/online.

https://doi.org/10.34726/1784

Metro (Strava 2021), do exist, but they provide only aggregated data and limit access to the data only for actors directly involved in active transportation infrastructure planning. This leaves out large number of potential data users, like scientists, from the end users (Personal communication 2021). Thus, the data is fragmented and heavily processed, and access to the data is arbitrarily restricted, which inhibits its full utilization potential. On the other hand, there are various reasons hindering sharing of the tracking data openly. Most importantly, human mobility data is personal data whose use in the EU is regulated by the General Data Protection Regulation (GDPR).

In the GeoPrivacy project, we study methods on how human mobility data could be collected, used, and shared in a privacy-protected open database. One objective of the project is to find out citizens' attitudes about sharing their mobile tracking data, and possible motivations for it. We conducted an online survey and in this abstract, we present our preliminary findings related to 1) citizens' willingness to contribute to an open location data repository, 2) the adequate level of privacy protection, 3) motivation and 4) obstacles for sharing personal location data.

2. Materials and Methods

The survey was conducted using an online questionnaire form. The form was distributed through a number of email lists and social media channels, mainly for Finnish audiences. The survey consisted of 17 questions about the participants' mobile tracking habits, their opinions and worries about sharing their tracking data publicly, and background information. A Finnish and an English version of the questionnaire were distributed.

The preliminary findings presented in this abstract are based on the 325 responses collected between the 28th of June and the 31st of August 2021. The main method used for analysing the survey data was cross tabulation.

The four questions under investigation in this abstract were presented in the survey as follows:

1. Would you consider sharing your tracking data to an open data repository? (A five-step Likert scale from one ("definitely no") to five ("definitely yes"))
2. Which level of privacy protection should the repository guarantee, so that you would be willing to contribute? (Table 1)
3. What would motivate you to share your tracking data? (Table 2)
4. What would prevent you from sharing your tracking data? (Table 3)

Table 1. The answer options and their abbreviations for Question 2 "Which level of privacy protection should the repository guarantee, so that you would be willing to contribute?" (Single-choice)

Answer option	Abbreviation
Level 0: Your tracks are published as they are.	Level 0
Level 1: Your tracks are published as they are, but your identifying information is replaced by a pseudo-identifier (for example, a random number).	Level 1
Level 2: Places that you visit (and spend a considerable amount of time) are removed, including your start location and destination. The remaining parts of the tracks are published as they are.	Level 2
Level 3: Your tracks are processed before publication, so that it is very unlikely that any part of the track can be traced back to you.	Level 3
Level 4: Your data is combined with the data of all other users, and only this summarized data is published. Information about any individual cannot be extracted.	Level 4
You are not willing to contribute, no matter what the privacy guarantee of the repository would be.	Never
Other (free text field)	

Table 2. The answer options and their abbreviations for Question 3 "What would motivate you to share your tracking data?" (Multiple-choice)

Answer option	Abbreviation
getting summary statistics about yourself (e.g., comparisons to your past activity)	ownSummary
comparison of your summary statistics to other contributors	compSummary
possible improvements in cycling and/or pedestrian lane infrastructure	imprLanes
possible improvements to the safety of lanes used by cyclists and pedestrians/runners	imprSafety
possible improvements to the cost-effectiveness of investments in infrastructure	imprCost
enthusiasm for supporting open data	openData
contribution in scientific research	research
a possibility to influence policy-making in the long term	policymaking
other (free text field)	

Table 3. The answer options and their abbreviations for Question 4 "What would prevent you from sharing your tracking data? (Multiple-choice)

Answer option	Abbreviation
concerns that the data might reveal some personal information	persInfo
concerns about the causes my data will be used for	dataUse
not having enough time	lackTime
not being interested enough	noInterest
technical difficulties in sharing my data	techDiffic
other (free text field)	

3. Preliminary results

General attitude: According to the preliminary results, the respondents' attitudes towards sharing their tracking data were mostly positive (Figure 1). The positive general attitude (GA) groups 4 and 5 covered 54 % of the replies, and 77 % had no clear objections to sharing their data.

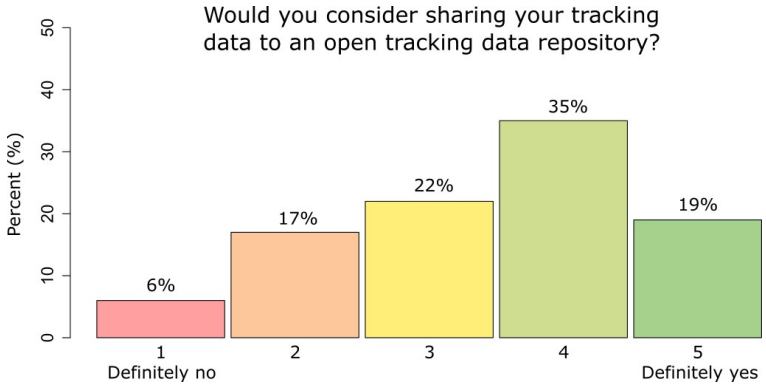

Figure 1. Respondents' general attitude about sharing mobile tracking data.

Privacy level requirements: Concerning the respondents' opinions about the privacy protection levels of the tracking data repository, level 3 was the most popular option with 33 % of the replies (Figure 2). The levels 0 and 1 were clearly less popular than the other levels. In the following cross tabulation analysis, they are therefore merged to level 2. Only 3 % of respondents said they would not be willing to contribute, regardless of the privacy guarantee of the repository.

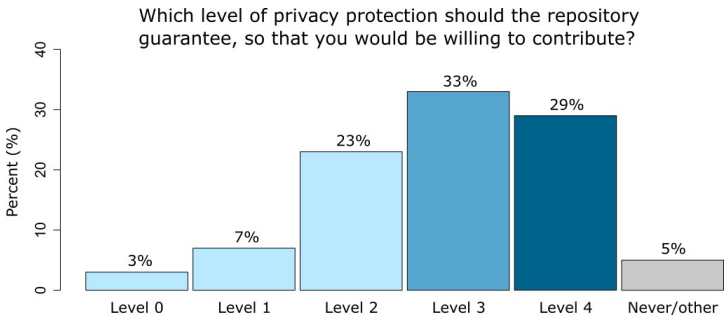

Figure 2. Respondents' privacy requirements for sharing their data.

The more positive a respondent's attitude towards data sharing was, the lower the level of privacy protection they would be satisfied with appeared to be (Figure 3, n = 309, p <= 0,001). Among those respondents who had either neutral or positive attitudes towards sharing their data (GA groups 3, 4, and 5), 75 % would be willing to contribute if the privacy protection level was 3 or higher. Focusing only on the people who have positive attitudes towards sharing the data (GA groups 4 and 5), 79 % would be pleased with level 3 or higher. In contrast, among the respondents who have negative attitudes towards sharing their data, 53 % require the strictest privacy protection level 4 before considering sharing their data.

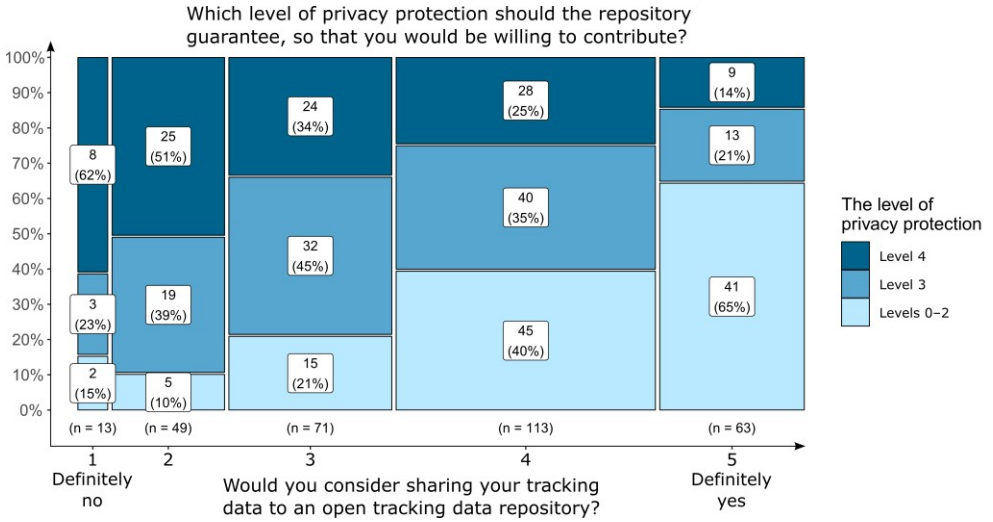

Figure 3. Respondents' requirement of privacy level vs. their willingness to share their tracking data. The privacy levels 0 and 1 are merged to level 2.

Motivators and preventors: The three most popular motivators for sharing data were development of cycling and/or pedestrian lane infrastructure, improvements of lane safety, and the contribution in scientific research (Figure 4a). Of the reasons that could prevent the respondents from sharing

their data, two clearly stand out: concerns about the causes the data will be used for (90 %) and concerns that the data might reveal personal information (79 %) (Figure 4b).

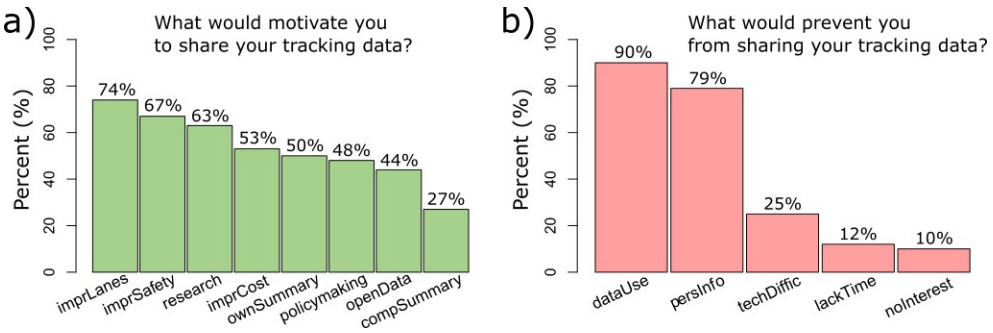

Figure 4. a) Respondents' motivators and b) reasons that would prevent them from sharing their data.

4. Conclusion

Generally, based on our survey, the attitude towards donating personal tracking data to a privacy-protected open data repository appears to be positive. Most respondents are privacy conscious and require advanced levels of data protection. The most popular motivators for donating the data are related to seeing improvements in biking and pedestrian infrastructure, but such changes are long-term and raise the question of how immediate feedback could be provided for the contributors. The small sample size and bias in the responses must be considered carefully. All findings provide important insights on issues related to designing a privacy-protected open repository for personal location data.

5. Acknowledgements

GeoPrivacy project funding from the Finnish Cultural Foundation is gratefully acknowledged.

References

Bento, N. (2016). Calling for change? Innovation, diffusion, and the energy impacts of global mobile telephony. Energy Research & Social Science, 84–100.

Personal Communication (2021). Strava Metro Application Update. Personal email June 29th 2021.

Strava (2021). Better cities for cyclists and pedestrians. On-line: https://metro.strava.com/

Small differences: Limits of Legibility of Cartographic Symbols on High- and Ultra-High-Resolution Mobile Displays

Florian Ledermann florian.ledermann@tuwien.ac.at

TU Wien, Research Division Cartography

Abstract. This paper reports on a lab study that attempts to experimentally establish the limits of legibility of fundamental cartographic symbology on modern smartphone screens. Participants were presented six classes of stimuli on four different displays of varying pixel densities, and were asked to identify the cartographic symbol shown among a set of choices. The results of the experiment should help to develop updated guidelines for minimal dimensions of cartographic symbology for use on mobile phones and other high resolution digital displays.

Keywords. Map perception, map symbols, user study, cognition, controlled experiment

1. Introduction and Problem Statement

Cartographic design guidelines usually demand that maps presented on screens use larger and coarser symbology than paper-based maps, due to the reduced fidelity of the display medium (Neudeck, 2001; Lobben & Patton, 2003; Jenny et al., 2008). However, such recommendations were generally derived from the state of development of display hardware around the turn of the millennium, when desktop monitors were limited at pixel densities around 100 pixels per inch (ppi) (Malić, 1998). In recent years, screens of mobile devices have become available with ever higher pixel densities. Today, there are virtually no technical limitations in manufacturing displays of ultra-high pixel densities (Katsui et al., 2019), and the highest pixel density for commercially available mobile phones currently lies at 801ppi (Sony Xperia Z5 Premium). However, guidelines for the dimensions of cartographic symbology have not been updated to reflect those developments. Does the increased fidelity of digital displays mean that cartographers can now revert

LBS 2021
16th Conference on Location Based Services
24-25 November 2021 Online

Published in "Proceedings of the 16th International Conference on Location Based Services (LBS 2021)", edited by Anahid Basiri, Georg Gartner and Haosheng Huang, LBS 2021, 24-25 November 2021, Glasgow, UK/online.

https://doi.org/10.34726/1785|

to the minimum dimensions that have been traditionally used for printed maps? Can even smaller symbol sizes be used for smartphones due to the increased contrast ratio and the reduced viewing distance? Or does the recommendation to use larger symbology for presentation on screens still hold, even for displays of the highest resolutions?

2. Study Design, Apparatus and Stimuli

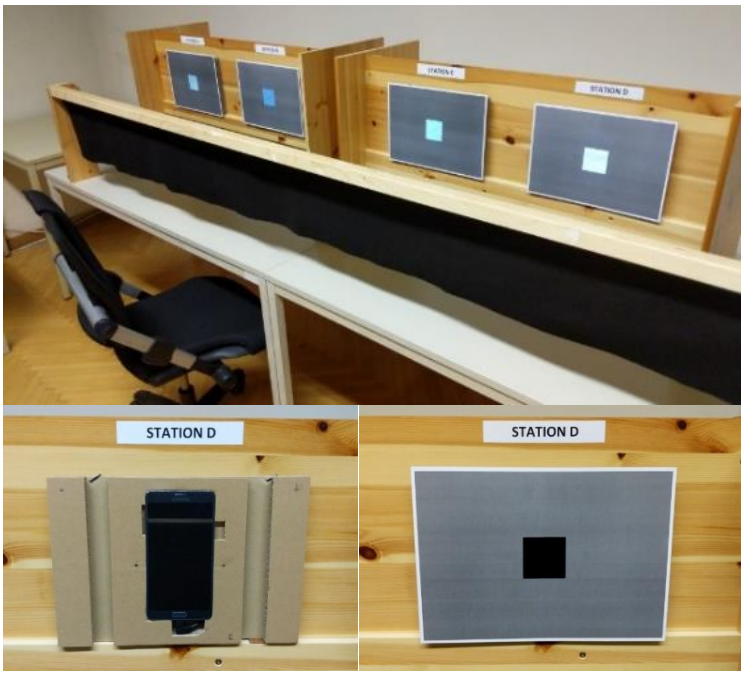

Figure 1. Lab setup for the study. Top: viewing stations with mobile phones of varying pixel densities mounted behind bezels, rail to ensure constant viewing distance, curtain to minimize reflections. Bottom left: mobile phone mounting fixture. Bottom right: Bezel covering mounting fixture to reveal an area of identical size for each station.

This paper reports findings of a lab study that attempts to experimentally establish the limits of legibility for fundamental cartographic symbology on modern smartphone screens of varying pixel densities. For the experiment, four mobile phones with screens of varying pixel densities (228 / 342 / 522 / 801 ppi) were mounted behind bezels, revealing only a square portion of 48 x 48mm of each phone display (as mandated by the smallest screen size used in the study). In front of these viewing stations, a rail was mounted to ensure equal viewing distance of approximately 30cm (see Fig. 1). Participants were presented a sequence of stimuli on each display, and were asked to select the

symbol best matching each stimulus by pressing the corresponding on-screen button on a separate response device. Stimulus size was specified in millimeters and adjusted using a staircase procedure, which upon three consecutive correct responses decreased the stimulus size, and upon one incorrect response increased the stimulus size. Using this procedure, the limit at which stimuli could still be reliably discriminated was established for each participant, display and stimulus class.

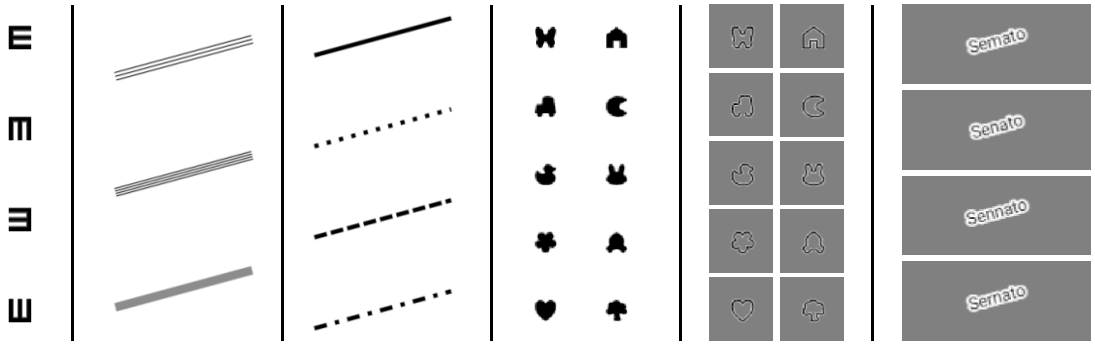

Figure 1. Types of stimuli which participants were asked to distinguish in the experiment. (1) Tumbling E's (2) parallel lines (3) dashed/dotted lines (4) "Auckland Optotypes" symbols (5) "vanishing" symbols (6) word variants. (The orientation of stimuli for tasks 2,3 and 6 was randomized for each trial in the experiment)

Each participant would perform all tasks of the experiment on all four display stations, in randomized order. At each station, the identical sequence of tasks was run, each representing a specific class of stimuli related to cartographic symbology (see Fig. 2) – (1) "tumbling E's", which are established as a standard test for visual acuity; (2) three / four parallel lines or a grey line, random orientation; (3) dotted, dashed, dot-dash and solid lines, random orientation; (4) point symbols taken from the "Auckland Optotypes" symbol set (Hamm et al., 2018); (5) Point symbols, drawn with a white-black-white outline against a grey background ("vanishing" into grey when beyond legibility) ; (6) Short words, made up to look plausible as a toponym without being a dictionary word or a well-known toponym, with a white outline against grey background, rotated randomly ±90°.

The experiment was implemented using our in-house framework for running distributed experiments, stimsrv (Ledermann & Gartner, 2021), and run with 28 participants recruited among student volunteers.

3. Results and Conclusions

In line with our hypotheses, the display with lowest pixel density (228ppi) was outperformed significantly by the one of next higher pixel density (342ppi) in five out of six tasks. The display of yet higher density (522ppi) outperformed this display significantly in three tasks (2,4,5), while, surprisingly, performing significantly *worse* in the tumbling E task (1). The display with highest pixel density (801ppi) outperformed the 522ppi display significantly only in the tumbling E tasks (with no significant improvement over the 342ppi display in that task). Although a plateau for further improving the legibility of most cartographic symbols seems to have been reached with the 522ppi display, the display of highest pixel density was the only display on which participants did not perform significantly worse in any task than on any other display. Surprisingly, no significant difference in performance has been found for any pair of devices for the text legibility task (6).

Further analysis of these results lets us conclude that for high-resolution devices (> 500ppi), which are now commonly available, and near viewing distance (≈30cm), cartographic symbology can be differentiated at significantly smaller sizes than conventionally recommended for screen-based maps. Point symbols were reliably identified at a size of 0.6mm on the two highest-resolution displays, and dash patterns of lines could be reliably discriminated at a line width of 0.12mm – both of these values are approaching the minimum dimensions conventionally recommended for printed maps (0.6mm and 0.1mm, respectively) (Imhof, 1972; Schweizerische Gesellschaft für Kartografie, 1980). The viewing conditions of the presented experiment approximated ideal contrast, so these findings would need to be adapted for less-than-ideal viewing conditions and more complex cartographic symbology.

It is important to note that this is clearly not a recommendation to use such minimal dimensions to depict important information on a map. However, these minimum dimensions may establish the foundation of the visual hierarchy of cartographic symbols of a map (Dent et al., 2008), from which the dimensions of the symbols at higher importance or the parameters for cartographic generalization may be derived. Lines and point symbols of the smallest size may be used for purely optional or contextual information, such as graticules or contour lines.

Two results of our study stand out as going against our intuitive expectations: the poor performance of the 522ppi device in the “Tumbling E’s” task, and the virtually identical performance of all devices in the text legibility task. Closer inspection of the stimuli presented of the tumbling E’s tasks reveals

that this stimulus was subject to strong aliasing effects due to its intensity gradients being aligned with the pixel grid. This caused the stimulus to appear enlarged on the 228ppi display, leading to better performance than the physical pixel resolution should allow on this device, while degrading the stimulus in an unfortunate way for the 522ppi display, leading to worse-than-expected performance. Only the device with the highest resolution (801ppi) was not affected by such sampling artefacts for this task. While this result serves as a reminder that sampling artefacts must be taken into account for some classes of stimuli on digital displays, in real-world cartographic applications such high-frequency stimuli in perfect alignment with the pixel grid would rarely be encountered.

A detailed report on the findings of the presented study and a table of guidelines for cartographic symbology derived from the results can be found in a forthcoming publication (Ledermann, forthcoming).

In the future, we are planning to investigate whether novel techniques could be deployed to make use of the highest resolutions available and further increase user's map reading performance on those devices. Furthermore, we want to verify the findings of our lab study in real-world cartographic applications, potentially in collaboration with institutions for which detailed maps are important and which could deploy high-resolution devices to their staff, such as emergency services in alpine areas.

References

Dent, B., Torguson, J., & Hodler, T. (2008). Cartography: Thematic Map Design (6th edition). McGraw-Hill Education.

Hamm, L. M., Yeoman, J. P., Anstice, N., & Dakin, S. C. (2018). The Auckland Optotypes: An open-access pictogram set for measuring recognition acuity. Journal of Vision, 18(3), 13–13. https://doi.org/10.1167/18.3.13

Imhof, E. (1972). Thematische Kartographie (Vol. 10). Walter de Gruyter.

Jenny, B., Jenny, H., & Räber, S. (2008). Map design for the Internet. In International perspectives on maps and the internet (pp. 31–48). Springer Berlin Heidelberg. http://link.springer.com/chapter/10.1007/978-3-540-72029-4_3

Katsui, S., Kobayashi, H., Nakagawa, T., Tamatsukuri, Y., Shishido, H., Uesaka, S., Yamaoka, R., Nagata, T., Aoyama, T., Nei, K., Okazaki, Y., Ikeda, T., & Yamazaki, S. (2019). A 5291-ppi organic light-emitting diode display using field-effect transistors including a c-axis aligned crystalline

oxide semiconductor. Journal of the Society for Information Display, 27(8), 497–506. https://doi.org/10.1002/jsid.822

Ledermann, F., & Gartner, G. (2021). Towards Conducting Reproducible Distributed Experiments in the Geosciences. AGILE: GIScience Series, 2, 1–7. https://doi.org/10.5194/agile-giss-2-33-2021

Ledermann, F. (forthcoming). The Effect of Display Pixel Density on Minimum Legible Size of Fundamental Cartographic Symbols. The Cartographic Journal, forthcoming.

Lobben, A. K., & Patton, D. K. (2003). Design Guidelines for Digital Atlases. Cartographic Perspectives, 44, 51–62. https://doi.org/10.14714/CP44.515

Malić, B. (1998). Physiologische und technische Aspekte kartographischer Bildschirmvisualisierung [PhD Thesis]. Rheinische Friedrich-Wilhelms-Universität.

Neudeck, S. (2001). Zur Gestaltung topografischer Karten für die Bildschirmvisualisierung [PhD Thesis]. Universität der Bundeswehr.

Schweizerische Gesellschaft für Kartografie (Ed.). (1980). Kartographische Generalisierung: Topographische Karten (2nd ed.). Bern.

Game Engine-based Point Cloud Visualization and Perception for Situation Awareness of Crisis Indoor Environments

Zhenyu Liu*, Runnan Fu*, Linjun Wang*, Yuzhen Jin*, Theodoros Papakostas*, Xenia Una Mainelli*, Robert Voûte*,**, Edward Verbree*

* Faculty of Architecture and the Built Environment, Delft University of Technology
z.liu-46@student.tudelft.nl, r.fu-1@student.tudelft.nl, l.wang-21@student.tudelft.nl, y.jin-10@student.tudelft.nl, t.papakostas@student.tudelft.nl, x.u.mainelli@student.tudelft.nl, E.Verbree@tudelft.nl, R.L.Voute-1@tudelft.nl
** CGI Nederland B.V.
robert.voute@cgi.com

Abstract. Because unknown interior layouts can have serious consequences in time-sensitive situations, crisis response teams request many potential solutions for visualizing indoor environments in crisis scenarios. This research uses a game engine to directly visualize point cloud data input of indoor environments for generating clear interaction between the environment and viewers, to aid decision-making in high-stress moments. The prospective final product is an integration of game-oriented visualization and cartography, hosted within Unreal Engine 4 (UE4), allowing users to navigate throughout an indoor environment, and customizing certain interaction features. The UE4 project consists of 4 modules: data preprocessing, render style, functional module, and user interface. Finally, this research uses a single-floor indoor point cloud dataset collected from a building in Rotterdam, the Netherlands for the implementation.

Keywords. Game Engine, Unreal Engine 4, 3D Visualization, Situation Awareness, Point Cloud, Indoor Environment, Crisis Scenario

Published in "Proceedings of the 16th International Conference on Location Based Services (LBS 2021)", edited by Anahid Basiri, Georg Gartner and Haosheng Huang, LBS 2021, 24-25 November 2021, Glasgow, UK/online.

https://doi.org/10.34726/1786 | © Authors 2021. CC BY 4.0 License.

1. Introduction

Crisis response teams often encounter situations in which unfamiliar buildings need to be reached, where floor plans can be out of date, or real-time situations are different from what is briefed. Unknown interior layouts can have serious consequences in time-sensitive situations when command centers direct first responders on the basis of out-of-date information. Compared with the other 3D data, point clouds are very suitable for visualizing crisis indoor environments as they can retain accurate details, and can be easily captured and updated. However, first responders usually lack geo-spatial experts who are proficient in terminology and the structure of spatial data (Zlatanova, 2010). Therefore, exploring the intuitive spatial-information transfer and easy-to-use environment interaction potential of point cloud-based visualization solutions for crisis indoor environments can aid first responders in the correct decision-making and situation awareness.

This research focuses on the visualization and perception of crisis indoor environments, emphasizing the direct use of point clouds with the great interaction potential offered by game engines (Virtanen et al., 2020). The research aims to answer the following question: *Can we harness the potential that point clouds have, to effectively convey the visual contents of an indoor environment to first responders?* The prospective final product is an integration of game-oriented visualization and cartography, hosted within *Unreal Engine 4* (*UE4*)[1], allowing users to navigate throughout an indoor space, and customizing certain interactive features.

2. Methodology

The product software is designed in a game-oriented scope using *UE4* aiding users in decision-making and situation awareness. 3D adventure games often have high similarities to real crisis environments, so game-oriented features can offer many design inspirations. *UE4* provides official support for point cloud data and some easy-to-use interactive interfaces, which make the development of the software more convenient.

The software consists of four modules, including the **data preprocessing**, **render styles**, **functional system**, and **user interface**. *Figure 1* describes the workflow of module design and development. Finally, the single-floor indoor point cloud data collected from a building in Rotterdam is used to test the software.

[1] www.unrealengine.com

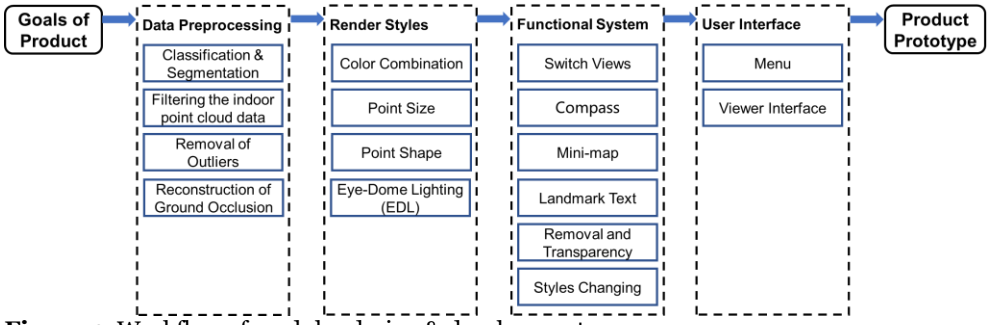

Figure 1. Workflow of modules design & development

3. Module Design & Development

3.1. Data Preprocessing Module

Before importing a point cloud into *UE4*, the data should be preprocessed. The classification and segmentation operations can yield many benefits, such as significantly reducing the computation complexity, providing semantic information, offer the possibility to be demonstrated in different rendering styles, and switch between displayed and hidden states independently. A method was designed (*Figure 2*) to classify the point cloud into 4 categories: (1) **roof**, (2) **architecture components** (walls, columns, etc.), (3) **non-architecture components** (furniture, etc.), and (4) **ground** (*Figure 3*).

Figure 2. Workflow of point cloud classification & segmentation

Figure 3. Four segmented categories

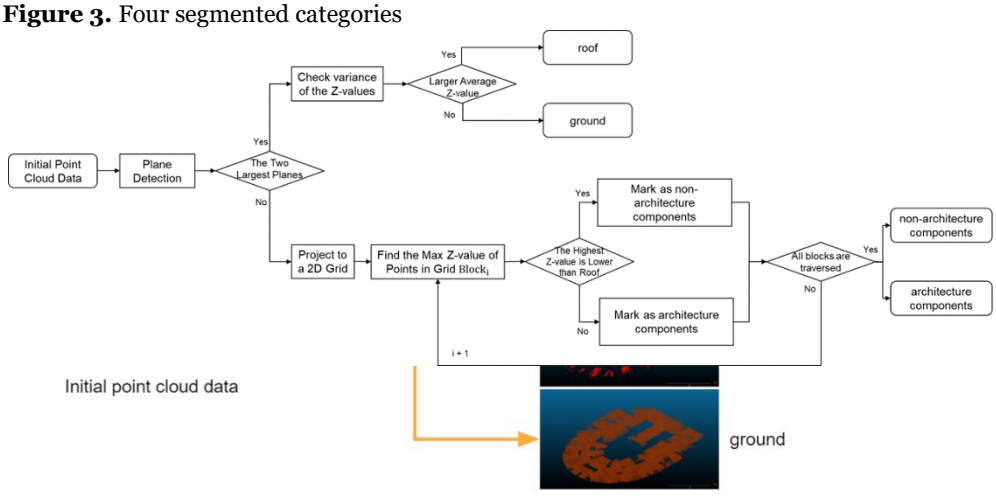

To remove the external environment objects (*Figure 4*), segmented points are projected onto a 2D-grid. Each grid cell will be preserved as an indoor area only if it contains enough roof and ground points, and its density exceeds the preset threshold. The outliers (noise points) can cause non-trustworthy rendering results. Therefore a denoising method, which should keep the balance between denoising, feature-preservation, and avoiding degradation of the input (Rakotosaona et al., 2019), is also needed in this phase.

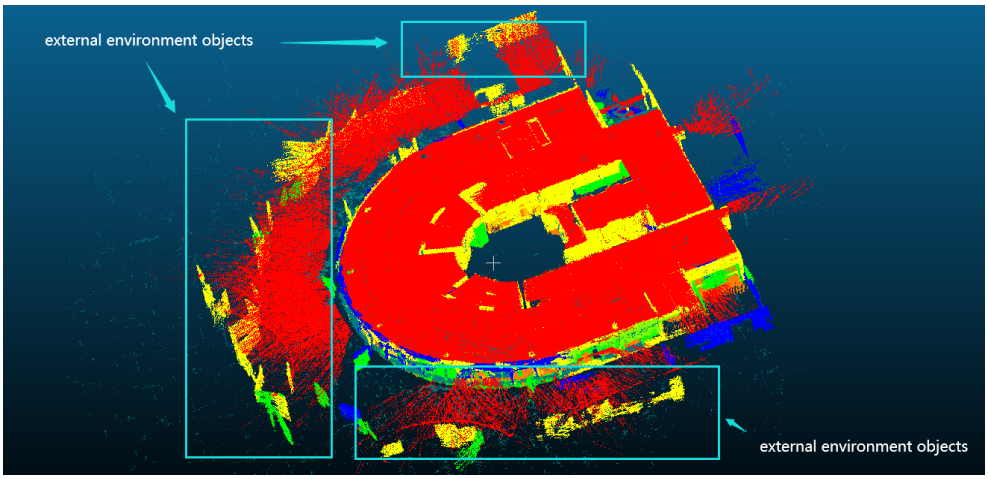

Figure 4. External environment objects

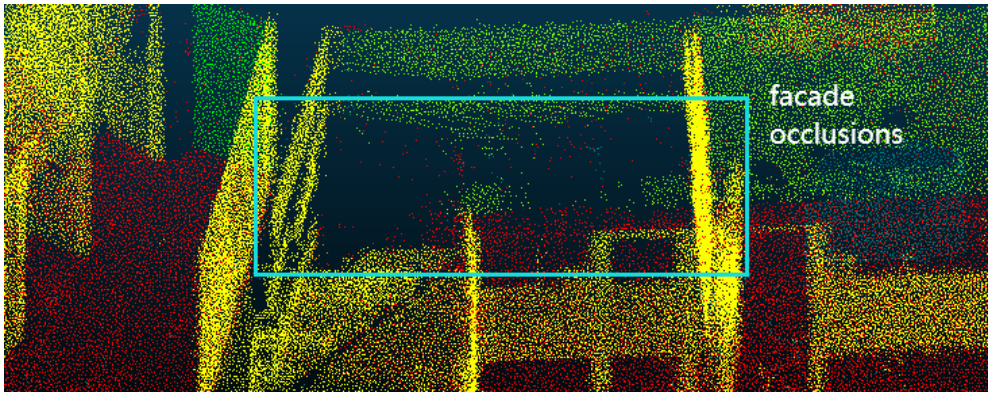

Figure 5. Facade occlusions

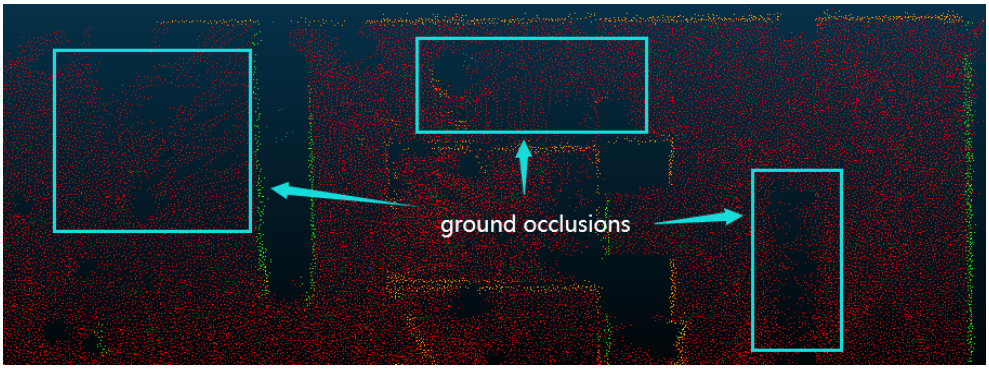

Figure 6. Ground occlusions

Many indoor point clouds contain both facade occlusion (*Figure 5*) and ground occlusion (*Figure 6*) problems (Friedman & Stamos, 2012). But only the latter may obviously hinder exploration, such as the user may fall through holes (occluded areas) in the ground. So we insert a transparent plane object with a collision property to fill the ground occlusions in *UE4*.

3.2. Render Styles Module

In order to enhance the visual effect of the built environment with topographic cartography, we follow the visualization principles summarized by (Andrienko et al., 2020) and use some 3D static visual variables (Neuville et al., 2018) to design the render module.

Color Combinations: We set three different color styles. The default (brighter) one is closer to the real materials of the objects, enabling the user to quickly understand the indoor environment. The two darker styles can highlight the architecture and non-architecture features respectively according to the users' needs.

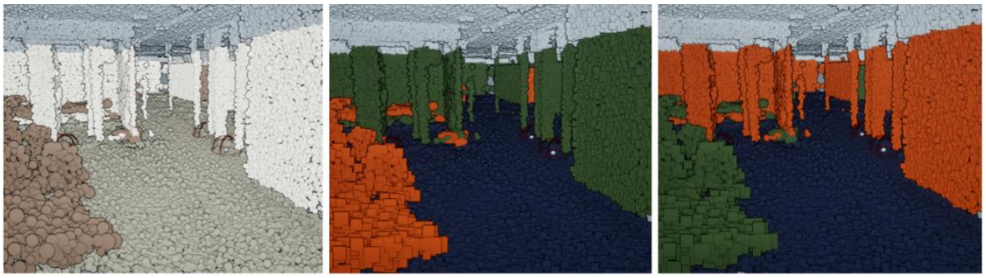

Figure 7. Default style (left), darker style 1 (middle) and darker style 2 (right)

Point Size & Point Shape: Users can adjust the shape and size of the points to change the visual and physical properties. For instance, adjusting point size to circumvent the effects of the point cloud density such as forming voids between points when the density is too low (Kharroubi et al., 2019).

Figure 8. Enlarge point size to reduce the hole area

Figure 9. Sphere points (left) and cube points (right)

Eye-Dome Lighting (EDL): Point cloud data often do not have realistic depth information, so *EDL* as a non-photorealistic lighting model can group points close to each other and shade their outlines, which accentuates the shapes of objects within a point cloud (Ribes & Boucheny, 2011). *EDL* can improve the visual quality and can quickly and self-adaptively apply to other point cloud data.

Figure 10. Visualization results without (left) and with (right) EDL

3.3. Functional Module

The functional module is based on some interaction and enhancement techniques (Andrienko et al., 2020) and 3D adventure game features, which are well designed for the exploration functions needed by users in a crisis environment.

Switch Views: Users can switch between the first-person view, the third-person view, and the bird's eye view (*Figure 11* & *Figure 12*). This function is essential to improve the immersion of the virtual environment and allows users to discover the indoor environment more comprehensively.

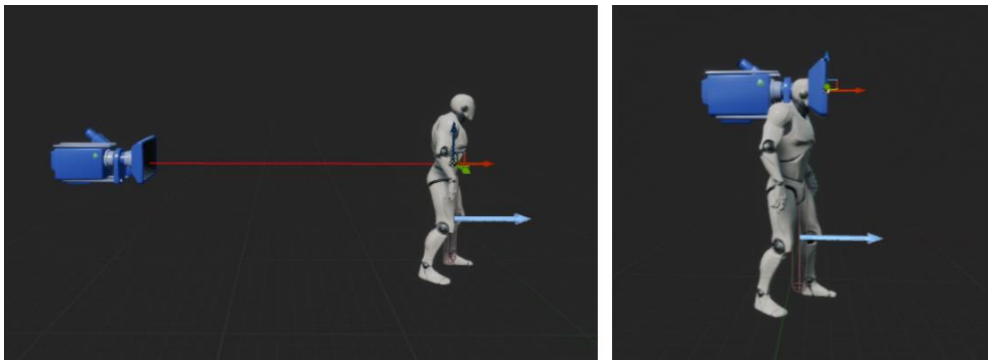

Figure 11. Camera location in third-person view (left), and first-person view (right)

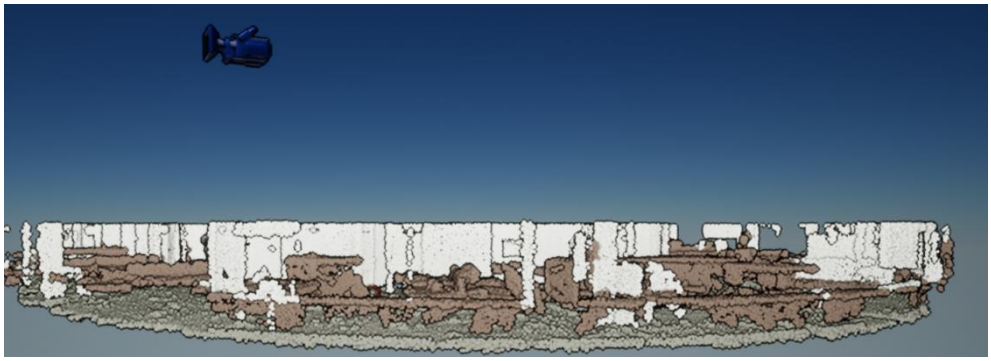

Figure 12. Camera location in bird's eye view

Compass: Compass is an important feature to improve the experience of interaction with the virtual environment. We apply a compass like a dynamic ruler and add some color marks for crucial landmarks of the building in the compass.

Figure 13. The compass with color marks

Mini-Map: A mini-map is a typical integrated feature of game visualization and 2D-cartography which aids users in orienting themselves within the virtual world. The blue triangle on the character icon in *Figure 14* shows the viewing direction.

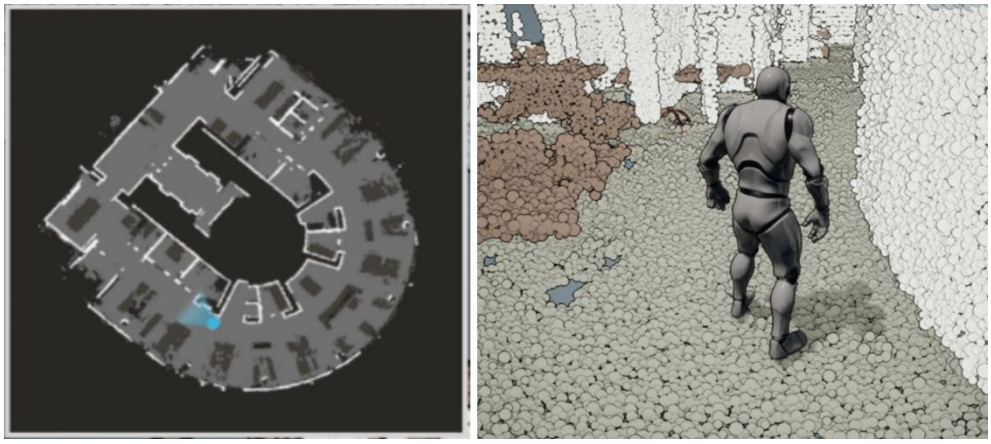

Figure 14. The mini-map

Landmark Text: Landmarks are static objects with predefined distinctive features in the model environment (Gim et al., 2021) and are often used as cues for action in situations of route navigation (Foo et al., 2005). The verbal indicator is a visual text animation, which fades in and progressively fades off to notify the users that they crossed an important landmark.

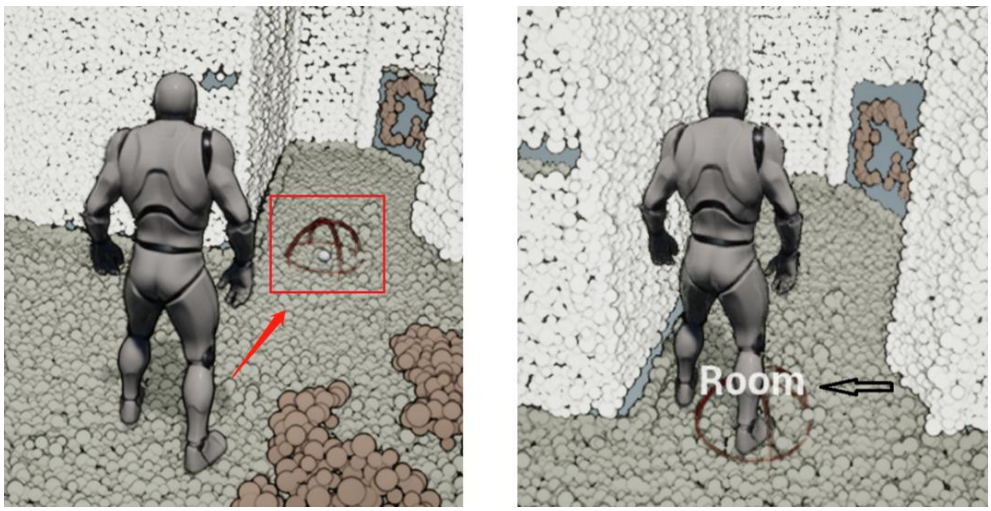

Figure 15. The collision sphere-landmark (left) and the Pop-Up text animation (right)

Roof Removal & Wall Transparency: Besides the bird's eye view, the roof can be removed, and glass materials can be applied on the wall to see the objects behind for facilitating gaining an overview of all the data. This has a better visualization effect compared with applying transparent rendering directly due to the overlapping effect (*Figure 16*).

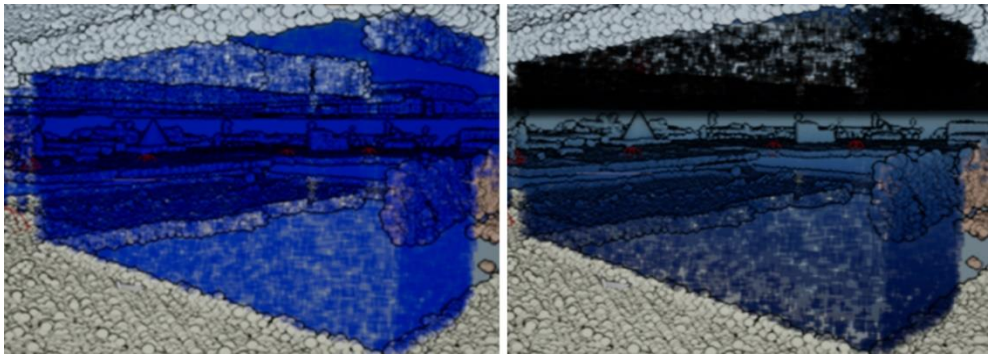

Figure 16. The wall displayed in transparency effect (left) and realistic glass materials (right)

Styles Changing: Users can switch between three different color styles to distinguish different objects and change the shape and size of points for different kinds of objects respectively.

4. Preliminary Results

We use a single-floor indoor point cloud data captured from a building in Rotterdam to test our designed modules by interacting with the point cloud data in the software (*Figure 17* & *Figure 18*).

Figure 17. The model with (left) and without (right) roof

5. Conclusion & Future Research

Visualization results show the game engine-based point cloud visualization has advantages in preprocessing and rendering efficiency, detail level, and volume perception, which are well suited for exploring crisis indoor environments. In the next stage, this research will focus on the more self-adaptive preprocessing module (such as dynamically adjusted denoising algorithms based on point density), automatic point cloud model import mechanisms (automatic alignment between the point cloud model and the transparent ground plane object), higher levels of customization (such as user-defined landmarks), and finally forming a 3D cartography and visualization framework suitable for indoor point cloud models. At last, our method will be compared with the mainstream mesh-based and voxel-based methods to evaluate its performance. In the future, the application potential of this research can be further explored by expanding to the multi-floor model, integrating with the outdoor model, and supporting VR/AR devices.

Figure 18. Visualization results: (A) circle points (first-person view), (B) square points (first-person view), (C) third-person view, (D) bird's eye view, (E) the smallest size points, (F) the biggest size points, (G) darker style 1, and (H) darker style 2

References

Andrienko, N., Andrienko, G., Fuchs, G., Slingsby, A., Turkay, C., & Wrobel, S. (2020). Principles of Interactive Visualisation. In N. Andrienko, G. Andrienko, G. Fuchs, A. Slingsby, C. Turkay, & S. Wrobel (Eds.), Visual Analytics for Data Scientists (pp. 51–88). Springer International Publishing. https://doi.org/10.1007/978-3-030-56146-8_3

Foo, P., Warren, W. H., Duchon, A., & Tarr, M. J. (2005). Do Humans Integrate Routes Into a Cognitive Map? Map- Versus Landmark-Based Navigation of Novel Shortcuts. Journal of Experimental Psychology: Learning, Memory, and Cognition, 31(2), 195–215. https://doi.org/10.1037/0278-7393.31.2.195

Friedman, S., & Stamos, I. (2012). Online facade reconstruction from dominant frequencies in structured point clouds. 2012 IEEE Computer Society Conference on Computer Vision and Pattern Recognition Workshops, 1–8. https://doi.org/10.1109/CVPRW.2012.6238908

Gim, J., Ahn, C., & Peng, H. (2021). Landmark Attribute Analysis for a High-Precision Landmark-Based Local Positioning System. IEEE Access, 9, 18061–18071. https://doi.org/10.1109/ACCESS.2021.3053214

Kharroubi, A., Hajji, R., Billen, R., & Poux, F. (2019). CLASSIFICATION AND INTEGRATION OF MASSIVE 3D POINTS CLOUDS IN A VIRTUAL REALITY (VR) ENVIRONMENT. ISPRS - International Archives of the Photogrammetry, Remote Sensing and Spatial Information Sciences, XLII-2/W17, 165–171. https://doi.org/10.5194/isprs-archives-XLII-2-W17-165-2019

Neuville, R., Pouliot, J., Poux, F., De Rudder, L., & Billen, R. (2018). A Formalized 3D Geovisualization Illustrated to Selectivity Purpose of Virtual 3D City Model. ISPRS International Journal of Geo-Information, 7(5), 194. https://doi.org/10.3390/ijgi7050194

Rakotosaona M.-J., La Barbera V., Guerrero P., Mitra N. J., & Ovsjanikov M. (2019). PointCleanNet: Learning to Denoise and Remove Outliers from Dense Point Clouds. https://arxiv.org/abs/1901.01060v3

Ribes, A., & Boucheny, C. (2011). Eye-Dome Lighting: A non-photorealistic shading technique.

Virtanen, J.-P., Daniel, S., Turppa, T., Zhu, L., Julin, A., Hyyppä, H., & Hyyppä, J. (2020). Interactive dense point clouds in a game engine. ISPRS Journal of Photogrammetry and Remote Sensing, 163, 375–389. https://doi.org/10.1016/j.isprsjprs.2020.03.007

Zlatanova S. (2010). Formal modelling of processes and tasks to support use and search of geo-information in emergency response. Proceedings of the 13th annual international conference and exhibition on geospatial information technology and applications - map India 2010 - defining geospatial vision for India, 19-21 January 2010. https://repository.tudelft.nl/islandora/object/uuid%3Abd37a6e6-5f3f-4cca-a929-8ff0e40e8c84

On the Detection of Moving Objects in Laser Scan Data: the Highest Point of Interest (HPOI) Method

Lars De Sloover*, Bart De Wit*, Samuel Van Ackere*, Laure De Cock*, Nico Van de Weghe*
*Ghent University, Faculty of Sciences, Department of Geography, CartoGIS Research Group

Abstract. There are many sensors and measuring methods for detecting moving objects, each with its advantages and disadvantages. In active tracking methods (based on e.g. GNSS technology), the user is informed and actively participates, for instance by installing a smartphone app. These methods typically have the problem that only a limited part of the moving objects is tracked. In passive tracking methods (e.g. video recognition), the moving person is not informed of being subject to the data acquisition. These methods are typically privacy-invasive. Many techniques also require complex calculations to transform the raw data into accurate and meaningful trajectories of moving objects. However, such trajectories usually require only one point of the moving object at any given time. If the moving object is a person walking or cycling, then such a point of interest is the highest point of the person's head (i.e. “highest point of interest” or HPOI). Detecting this point typically demands computationally intensive mining of the trajectory data, for example using deep learning approaches in video recognition. We present the use of static LiDAR technology, a well-established, precise and anonymous 3D data acquisition method, for this use case. By continuously (i.e. at a high temporal rate) laser scanning an environment in which pedestrians or cyclists move, multiple epochs of point clouds are obtained. A robust vertical threshold filtering allows reducing aforementioned high-dimensional, bulky point cloud data to easily visualisable and interpretable trajectories of HPOIs.

Keywords. LiDAR, object tracking, trajectory data mining, point cloud processing, spatiotemporal data, visual analytics

Published in “Proceedings of the 16th International Conference on Location Based Services (LBS 2021)”, edited by Anahid Basiri, Georg Gartner and Haosheng Huang, LBS 2021, 24-25 November 2021, Glasgow, UK/online.

https://doi.org/10.34726/1787 | © Authors 2021. CC BY 4.0 License.

1. Introduction

3D laser scanning is often used for data acquisition in complex situations, ranging from acquiring surface or terrain characteristics in environmental sciences to detection of obstacles surrounding autonomous cars in the field of robotics to (Chen, Fragonara, and Tsourdos 2021; Fan et al. 2021). This work presents the use of LiDAR technology for a simple, but overlooked situation: scanning moving objects from a single stationary point of view. Although not new, the concept of people tracking with 3D LiDAR data has typically relied on computationally intensive deep learning techniques (Yoon, Bae, and Kuc 2020; Brščić et al. 2020; Ma et al. 2019). We propose a passive but non-privacy-intrusive approach entitled the "highest point of interest" (HPOI) method. HPOI has great potential for real-time anonymous trajectory acquisition of moving objects. It exploits a very important intrinsic strength of 3D scanning: fast and precise acquisition of dense point clouds with known (x, y, z, t)-coordinates. Using simple methods from trajectory data mining (Wang, Miwa, and Morikawa 2020) and some principles from time geography, the highest points of objects moving throughout the scene can be quickly and easily filtered, forming the basis for the trajectories. This robust technique has great potential to provide data input for numerous applications within trajectory data analysis, both in outdoor and indoor environments.

This work-in-progress paper is organised as follows: first, in the methodology section, an experimental data acquisition set-up is discussed. Second, the pre-processing of the point cloud data is outlined. The third part of the methods section encompasses the idea behind HPOI. Next, in the results section, the potential of HPOI is demonstrated using meaningful visualisations. Finally, potential applications are highlighted.

2. Methodology

2.1. Experimental Set-Up

An Ouster™ OS1-64 mid-range high-resolution LiDAR sensor (Ouster, 2021) was installed on the first floor of a building near an open window, overlooking a roadway

and sidewalk on De Sterre Campus of Ghent University (https://goo.gl/maps/HEUZW8bnrhZ7TmAv6). This particular route on the campus was chosen because of the frequent passage of cars, cyclists and pedestrians. During a period of 15 minutes, the roadway, sidewalk and surroundings were scanned with a vertical resolution of 64 channels and a horizontal resolution of 1024 channels at a rotation rate of 10 Hz. To avoid an overload of data acquisition, the vertical field-of-view was set at 45° and the horizontal field-of-view at 90°.

Figure 1. HPOI method laser scan set-up of case study at Ghent university campus (Belgium)

2.2. Pre-Processing

This subsection gives an overview of the pre-processing, step-by-step. The source code used to process the point cloud data can be found on a GitHub repository (https://github.com/samuvack/Highest-Point-of-Interest-HPOI-Method). Due to the static way of setting up the laser scanner, all raw backscattered points were observed in coordinates relative to the origin of the laser sensor. Because we were mainly interested in the absolute Z-coordinates,

perpendicular to the topographic surface of the terrain, a local plane was determined by averaging out the Z-value of a subset of points on the road. Then, a coordinate transformation was applied to the point cloud to rotate and translate all points to a local coordinate system with the Z-axis along the normal of the surface of the road.

2.3. Highest Point of Interest (HPOI)

In most cases, 3D laser scanning is used to model objects in great detail. In the case of the HPOI method, the shape of the object during tracking is of minor importance. Moreover, an oriented bounding box, or even a single point (e.g. the highest point of the scanned point cloud in relation to the surrounding terrain) is sufficient to track an object along its path. As a result, this method requires a low computational load, making it possible to easily track moving objects in near real-time. Additionally, the position of an object along its trajectory is measured relatively accurately compared to image recognition of camera images.

3. Results

3.1. Visual Exploration

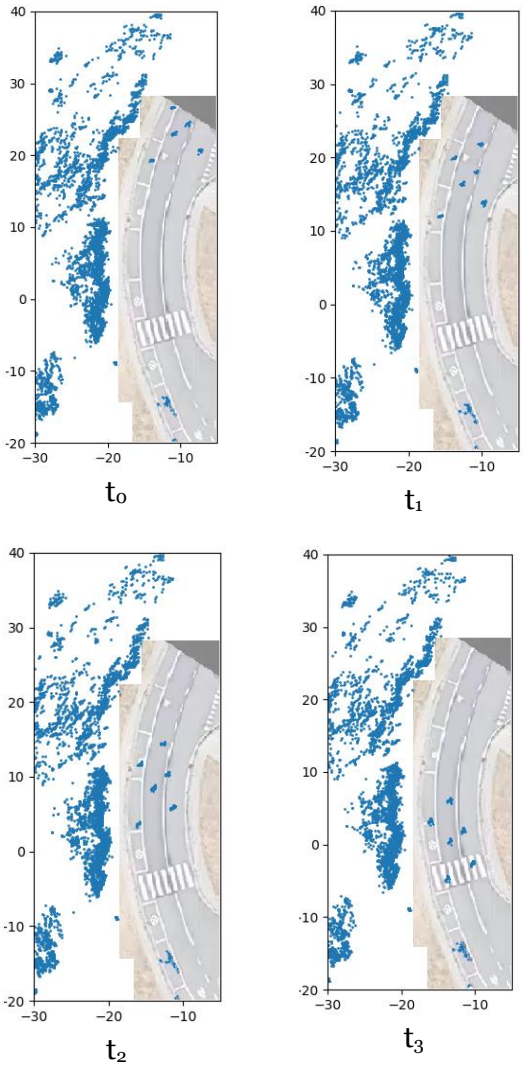

Figure 2. Processed point cloud, in which six cyclists are detected via the HPOI method

First of all, the figure above shows that the HPOI method clearly distinguishes six moving objects on the road segment. Since the position of the HPOI points varies with respect to each other and the six representative trajectories also differ from each other, it can be concluded that these six HPOIs represent six independent moving objects. From the height, speed and context (moving objects along a road segment), one can conclude that six cyclists were tracked in this case study.

Second, when looking at the road segment in the above figure, we can spot a parked car in the parking lane (bottom right of the time frames). Although the shape of the car obviously does not change in reality, the shape of the point cluster (extracted with HPOI) does change. Therefore, in addition to the benefits of HPOI, this case study also shows that further research is needed to avoid dubious interpretations of the result.

It must be noted that at no point in time the privacy of the six tracked cyclists was at risk. It can also be stated with certainty that a parked car was detected in this short recording via the HPOI method, without registering the type of vehicle or its number plate.

4. Discussion

4.1. Accuracy

The position of the highest measured point (relative to the surrounding terrain) of an object will change in the oriented bounding box along its trajectory. This can be caused by several things. First of all, depending on the distance, speed and direction of the object, more or fewer points of the object will be measured. Secondly, depending on the type of object (e.g. reflective, wet, rough) the number of measured points of the moving object can vary. Next, the object can also change shape during the trajectory (e.g. oscillating movement of a cyclist on his bicycle).

4.2. Potential Applications

The highest point of interest method (HPOI) can be used in all kinds of applications where the presence and movement of an object must be detected easily and quickly, and where the nature of the object is of secondary importance or can be inferred easily. The type of movement, the spatiotemporal and environmental context, the oriented bounding box (taking into account shadow effects, reflection and noise) can be used to determine which object was detected. For example, a moving object whose trajectory is mainly along a bicycle path, with a fairly constant speed, can be assumed to be a cyclist. Different types of animals (e.g. sheep and cows) can be determined to a certain extent by means of variation in height in a meadow full of cattle, or by linking the type of livestock at the starting point (e.g. by having the animals enter from different gates) or any other point in time along their trajectory.

The nature of the moving object needs to be determined only once along its trajectory, and, moreover, the level of detailed definition of the nature of the object can be fully determined. Of course, this is only the case if the path of the moving object is not interrupted at any time. In this case, shadow effects from obstacles in the environment must be taken into account when setting up the laser scanner. If it is still not possible to detect all trajectories of the objects uninterruptedly, a combination of several laser scanners may be a solution.

In the near future, an extensive feasibility study will be conducted to test under which conditions (weather, range and incidence angle of the scanner, density and speed of the moving objects, size of the scanning area, …) this method works optimally and for which applications in mobile data research and activity analysis it can be best used.

5. Conclusion

This work presents the use of LiDAR technology for a simple but overlooked situation: scanning moving objects from a single stationary point of view.

Although not new, the concept of tracking people from 3D LiDAR data has typically relied on computationally intensive deep learning techniques. In contrast, the HPOI method offers great advantages in tracking objects in a simple, fast and non-privacy-invasive manner. As the privacy of every moving object is guaranteed with the HPOI method, contextual information is needed to determine the nature of a tracked object. Further research is needed to test under which conditions (weather, range and incidence angle of the scanner, density and speed of the moving objects, size of the scanning area, …) this method works optimally and for which applications in mobile data research and activity analysis it can be best used.

References

Brščić, Dražen, Rhys Wyn Evans, Matthias Rehm, and Takayuki Kanda. 2020. "Using a Rotating 3D LiDAR on a Mobile Robot for Estimation of Person's Body Angle and Gender." *Sensors20*20(14), 3964. https://doi.org/10.3390/S20143964.

Chen, Can, Luca Zanotti Fragonara, and Antonios Tsourdos. 2021. "RoIFusion: 3D Object Detection from LiDAR and Vision." *IEEE Access* 9: 51710-21. https://doi.org/10.1109/ACCESS.2021.3070379.

Dewan, A., Caselitz, T., Tipaldi, G. D., & Burgard, W. (2016, May). Motion-based detection and tracking in 3d lidar scans. In 2016 IEEE international conference on robotics and automation (ICRA) (pp. 4508-4513). IEEE.

Fan, Yu Cheng, Chitra Meghala Yelamandala, Ting Wei Chen, and Chun Ju Huang. 2021. "Real-Time Object Detection for LiDAR Based on LS-R-YOLOv4 Neural Network." *Journal of Sensors* 2021. https://doi.org/10.1155/2021/5576262.

Hasan, M., Hanawa, J., Goto, R., Fukuda, H., Kuno, Y., & Kobayashi, Y. (2021). Person Tracking Using Ankle-Level LiDAR Based on Enhanced DBSCAN and OPTICS. IEEJ transactions on electrical and

electronic engineering, 16(5), 778-786.

Ma, Yuchi, John Anderson, Stephen Crouch, and Jie Shan. 2019. "Moving Object Detection and Tracking with Doppler LiDAR." *Remote Sensing 2019, Vol. 11, Page 1154* 11 (10): 1154. https://doi.org/10.3390/RS11101154.

Ogawa, T., Sakai, H., Suzuki, Y., Takagi, K., & Morikawa, K. (2011, June). Pedestrian detection and tracking using in-vehicle lidar for automotive application. In 2011 IEEE Intelligent Vehicles Symposium (IV) (pp. 734-739). IEEE.

Ouster. (2021, February 11). *Ouster OS1 Datasheet*.

https://data.ouster.io/downloads/datasheets/datasheet-revd-v2p0-

os1.pdf

Wang, Di, Tomio Miwa, and Takayuki Morikawa. 2020. "Big Trajectory Data Mining: A Survey of Methods, Applications, and Services." *Sensors 2020, Vol. 20, Page 4571* 20 (16): 4571. https://doi.org/10.3390/S20164571.

Yoon, Jae Seong, Sang Hyeon Bae, and Tae Yong Kuc. 2020. "Human Recognition and Tracking in Narrow Indoor Environment Using 3D Lidar Sensor." *International Conference on Control, Automation and Systems* 2020-October (October): 978-81. https://doi.org/10.23919/ICCAS50221.2020.9268208.

Zhao, J., Xu, H., Liu, H., Wu, J., Zheng, Y., & Wu, D. (2019). Detection and tracking of pedestrians and vehicles using roadside LiDAR sensors. Transportation research part C: emerging technologies, 100, 68-87.

Towards Perceived Space Representation using Brain Activity, Eye-Tracking and Terrestrial Laser Scanning

Gabriel Kerekes, Volker Schwieger

Institute of Engineering Geodesy, University of Stuttgart,
Geschwister-Scholl-Str. 24D,
70174 Stuttgart, Germany

Abstract. Deciphering how humans perceive physical spaces can lead to new reality capture methods and eventually replace measurement instruments like terrestrial laser scanners (TLSs). The current approach pursues this goal using non-invasive wearable sensors like Brain Computer Interfaces (BCIs) and mobile eye-trackers. Work in progress from static experiments shows that positions of targets on a wall at 4 m can be determined with differences up to several dm and better w.r.t. ground truth using homography.

Keywords. Space perception, TLS, human perception

1. Introduction

There are multiple methods of capturing reality and representing physical space. One method implies TLS scans and physical space is represented by point clouds. Similar to how a scanner measures only what it "sees", humans create a representation of their surroundings mostly based on vision and knowledge. Therefore, the question arises if human perception can be deciphered with non-invasive sensors and used to represent physical space similar to how a TLS measures it. The expected precision of this method is currently lower than the TLS one. Nevertheless, it may be fit-for-purpose for tasks like semantic segmentation of 3D scenes.

Perception of space happens in the neocortex of the human brain (Buzsáki & Llinás, 2017). A non-invasive approach for analyzing brain activity during an action is electroencephalography (EEG) (Bellmund et al., 2018). Additionally, space perception is mostly based on vision; therefore, eye activity

LBS 2021
16th Conference on Location Based Services
24-25 November 2021 Online

Published in "Proceedings of the 16th International Conference on Location Based Services (LBS 2021)", edited by Anahid Basiri, Georg Gartner and Haosheng Huang, LBS 2021, 24-25 November 2021, Glasgow, UK/online.

https://doi.org/10.34726/1788 | © Authors 2021. CC BY 4.0 License.

is also used as input for this approach (Authié et al., 2017). Previous approaches as Plöchl et. al. (2012) also combined eye-tracking and EEG with the aim of eliminating EEG artefacts caused by eye movements, but the current one strives to use them. Similar ongoing research as Kastrati et al. (2021) aims at classifying the saccade (voluntary rapid eye movements) direction based on EEG signal analysis. Other related work (cf. Mlot et al., 2016, Hirzle et al., 2018) use gaze data to estimate position within ranges less than 1 m.

Complementary to these studies we take steps towards using the human perception as input for a close-range representation method that can eventually replace a TLS if the accuracy is satisfactory.

2. Experiments and preliminary results

The planned experiments combine data obtained from a Pupil Core mobile Eye-Tracker from Pupil Labs and an 8-chanel EEG BCI from Neuroelectrics for the brain activity. Ground truth geometry of a scene is defined by TLS, which is a 3D polar measurement system used to generate point clouds describing surroundings up to a certain range. Experiments are limited to indoor spaces, therefore a Leica BLK360 TLS is chosen. The accuracy of a single 3D point is 6 mm at 10m.

2.1. The Experiment

The experiment (fig. 1) can be described as follows: a subject equipped with the BCI and Eye-tracker stands in front of a wall at about 4 m distance with black & white targets fixed on it. The whole scene is captured by TLS.

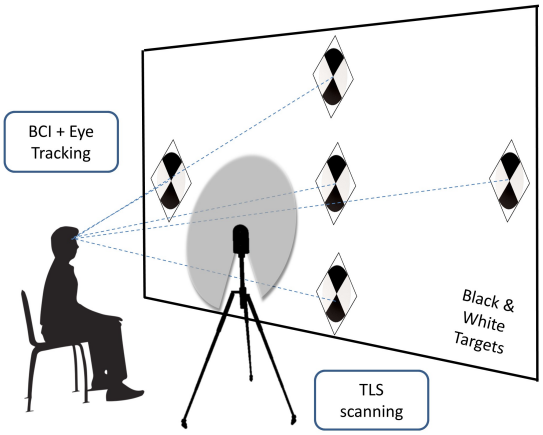

Figure 1. Example of experiment set-up.

While BCI and Eye-tracker data is recorded, the subject successively focuses on each target. The goal is to reconstruct the targets position based solely on EEG and eye-tracking data, practically making the TLS scan redundant if successful.

2.2. Up to now

First experiments were conducted with a subject facing the wall with 10 targets on it. After scanning, target positions were defined in a wall-based coordinate system.

Firstly, EEG patterns were analyzed in the BCI signals. The EEG protocol is defined with electrodes placed symmetrical on both brain hemispheres (Fig. 2).

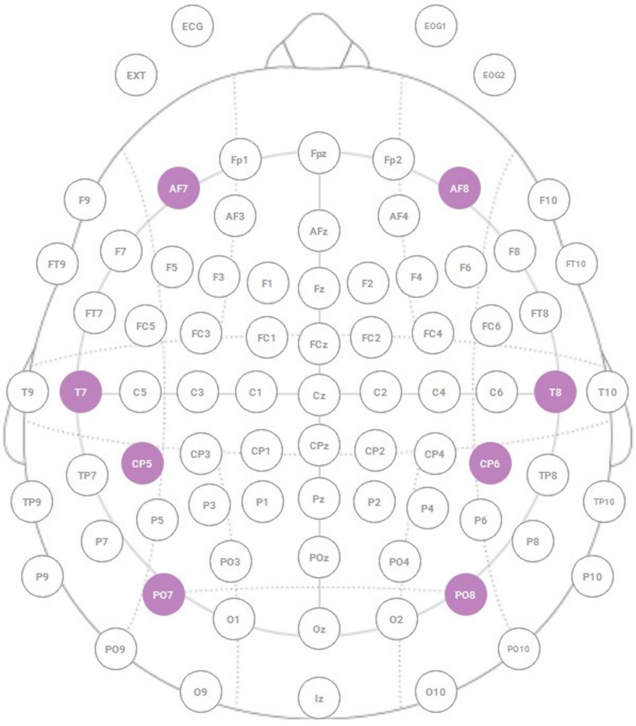

Figure 2. The 8-Chanel EEG Setup protocol

The intention is to differentiate between hemispheric brain activity and analyze patterns depending on a specific action of the observer. The subject was instructed to observe only three targets on the wall placed on a horizontal line. Additionally, between observations, the subject was asked to blink, since this is a clearly indefinable EEG artefact. Based on the EEG signal, it

is possible to distinguish saccades performed by the observer (see fig. 3) especially due to the signals read from the electrodes placed near the forehead (AF7 and AF8).

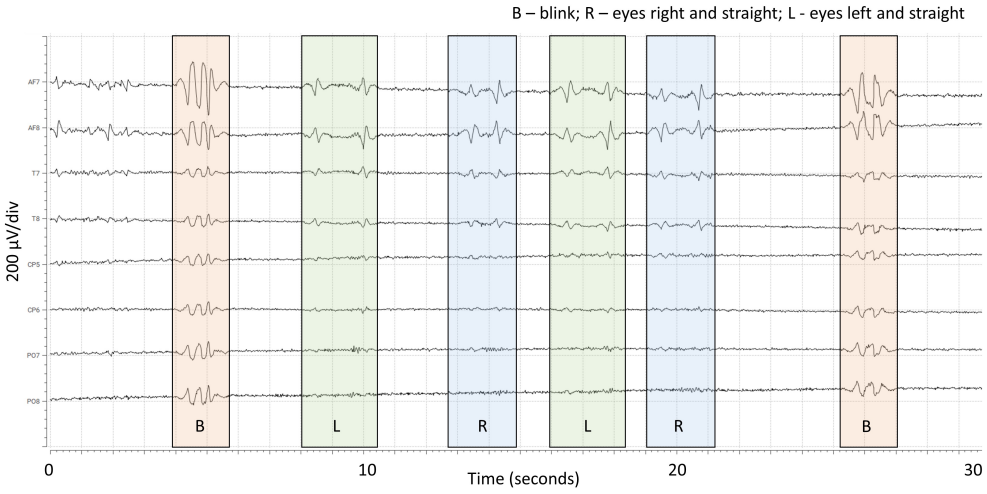

Figure 3. EEG signal

When the eyes performed a saccade from the center target to the left one, the AF7 signal shows a decrease of about 200 µV whilst the AF8 presents a mirrored profile. If the center target is fixed again, an increase of the same magnitude occurs in AF7 and AF8 gives the mirrored profile.

For the pursued goal, results are obviously unsatisfactory, since the only spatial information depicts if an observed target is on the left side or on the right side w.r.t. the previously fixed one.

Further on, gaze data from the eye-tracker is analyzed and the fixations (cf. Hering & Martin, 2017) identified in the world camera images were then projected with the help of homography (Luhmann et al., 2020) onto the wall-defined coordinate system. Afterwards, differences to the reference position (TLS scan) were computed. Three trials lead to the results presented in fig. 4.

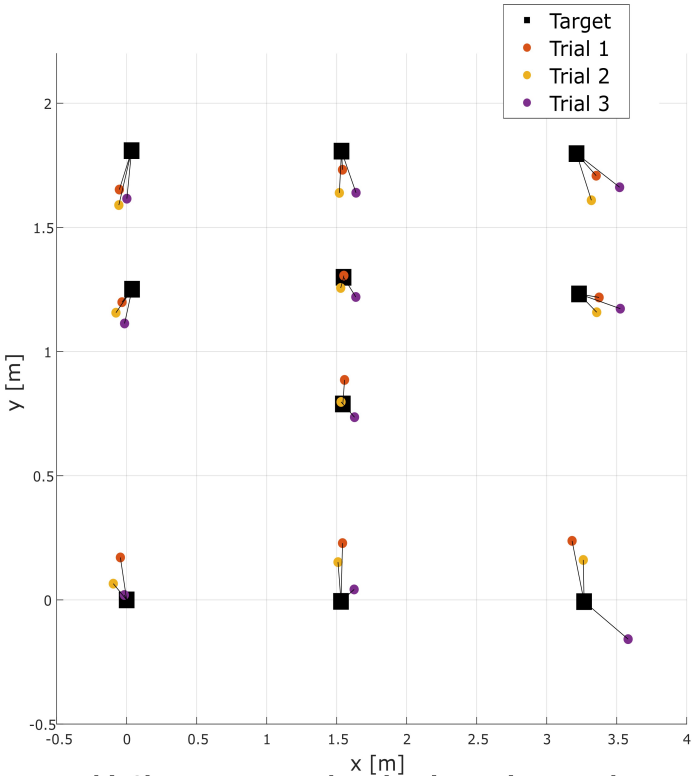

Figure 4. Fixations projected on wall (colored dots) and reference positions of the targets (black squares)

At this range, differences in both directions vary from 14 to 18 cm. This cannot be compared to currently available TLS precision, but can be better if fixation detection of the eye-tracker is improved. Additional depth-sensitive set-ups are foreseen to extend the current experiment.

3. Beyond findings

Currently, EEG can be limitedly used to discriminate between a left-hand side and right-hand side target, but not to precisely position it. Using gaze data captured with a mobile eye-tracker positioning accuracy on a plane reached the level of some dm. This approach presented intermediate steps towards using human perception for reality capture with the intention of establishing a connection between instrument-measured space and human-perceived space.

Acknowledgment

This research was conducted within a RISC (Research Seed Capital) project financed by the University of Stuttgart and Ministerium für Wissenschaft, Forschung und Kunst Baden-Württemberg from 2020 to 2022.

References

Authié, C. N., Berthoz, A., Sahel, J-A., Safran, A. B. (2017): Adaptive Gaze Strategies for Locomotion with Constricted Visual Field, Frontiers in Human Neuroscience 11:387, doi:10.3389/fnhum.2017.00387.

Bellmund, J. L. S., Gärdenfors, P., Moser, E. I., Doeller, C. F. (2018): Navigating cognition: Spatial codes for human thinking, Science 362, eaat6766.

Buzsáki, G., Llinás, R. (2017): Space and time in the brain, Science 358, Challenges in Neuroscience, p. 482-485.

Hering, E., Martin, R. (ed.) (2017): Geometrische Optik, Optik für Ingenieure und Naturwissenschaftler, Grundlagen und Anwendungen, Carl Hanser Verlag München.

Hirzle, T., Gugenheimer, J., Geiselhart, F., Bulling A., Rukzio, E. (2018) Towards a Symbiotic Human-Machine Depth Sensor: Exploring 3D Gaze for Object Reconstruction. In Adj. Proc. of UIST '18. doi:10.1145/3266037.3266119.

Kastrati, A., Płomecka, M., Langer, N. (2021). Using Deep Learning to Classify Saccade Direction from Brain Activity. ETRA '21 Virtual Event 25-27 May, 2021 doi:10.1145/3448018.3458014.

Luhmann, T., Robson, S., Kyle, S., Boehm, J. (2020). Close Range Photogrammetry and 3D Imaging. 3rd Ed. Walter de Gruyter GmbH, Berlin/Boston 2020.

Mlot, E.G., Bahmani, H., Wahl, S., Kasneci, E. (2016) 3D Gaze Estimation using Eye Vergence. In HEALTHINF. 125–131.

Plöchl M., Ossandón J., König P. (2012) Combining EEG and eye tracking: identification, characterization, and correction of eye movement artifacts in electroencephalographic data, Frontiers in Human Neuroscience, Vol. 6/2012, p. 278, doi:10.3389/fnhum.2012.00278.

What Can I Do There? Extracting Place Functionality Based on Analysis of User-Generated Textual Contents

Mina Karimi*, Mohammad Saedi Mesgari*, Omid Reza Abbasi*

* GIS Department, Faculty of Geodesy and Geomatics Engineering, K. N. Toosi University of Technology, Tehran, Iran

Abstract.

Recently, due to the rapid increase of social networks, user-generated textual contents have grown significantly. Sense of place emerges when a place is functionally different from its surroundings and is therefore recognizable. This paper aims to extract place functionality by analyzing user-generated textual contents. Therefore, using different natural language processing and machine learning methods, we show how much place functionality can be represented through the whole text with lemmatized words and only action verbs in descrining place. The evaluation results demonstrate that using the whole text achieves better performance and among different classifiers, SVM leads to better accuracy and f1-score.

Keywords. Place-Based GIS, Place Functionality, User-Generated Textual contents (UGTC), Natural Language Processing (NLP).

1. Introduction

In GIScience, spatial information is mostly presented in the form of space and coordinates while human reasoning, behavior and perception is based on place, not space (Goodchild 2015). Place is related to the human experience of the world (Couclelis 1992) and is usually ambiguous and context-dependent. In recent decades, the speed of urbanization has increased, enabling cities to engage in a wide range of human functions and activities. Sense of place emerges when a place is functionally different from its surroundings and is therefore recognizable (Purves et al. 2019). In this case, GIS should link functionality and space using data and knowledge about human activity to answer questions such as "What can I do there?" or

LBS 2021
16th Conference on Location Based Services
24-25 November 2021 Online

Published in "Proceedings of the 16th International Conference on Location Based Services (LBS 2021)", edited by Anahid Basiri, Georg Gartner and Haosheng Huang, LBS 2021, 24-25 November 2021, Glasgow, UK/online.

https://doi.org/10.34726/1789 | © Authors 2021. CC BY 4.0 License.

"How can I find places that provide a particular functionality?" In particular, GIS should be able to extract place functionality (Papadakis et al. 2019) that do not necessarily exist explicitly in the stored data.

Today, due to the rapid increase in using social networks, textual contents have grown significantly. Among the different types of user-generated contents, textual contents are often the most unstructured form and highly dependent on context and application. In the case of unstructured or semi-structured texts, first, they have to be structured and then different methods of natural language processing (NLP) can be applied to extract information and knowledge. Various studies have used user-generated textual contents such as place descriptions and user reviews to extract place information (Alazzawi 2012, Ballatore 2015, Chen et al 2018, Gao2021, Richter et al 2013).

This paper aims to extract place functionality based on analysis of user-generated textual contents such as users' reviews on travel blogs. Khoury et al. (2006) believe that the activity described by a sentence shows most of semantic information. Also, we are going to find how much place functionality can be represented through verbs that people use to describe or comment on a place. Therefore, the performance of action verbs on extracting place functionality is compared with the case when the whole sentence with lemmatized words is used.

2. Methodology

The general framework of the proposed method is summarized in *Figure 1*.

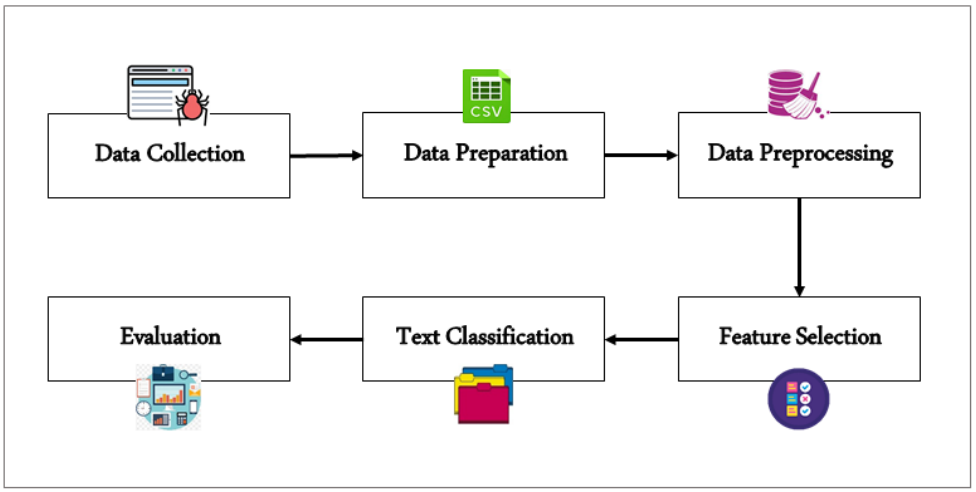

Figure 1. The general workflow of the proposed method

First of all, places and users' reviews on TripAdvisor were collected through web crawling by python. New York City (NYC) which is the most populous and also the most densely populated major city in the United States is chosen as our study area. These data were collected in October, 2020, and only English reviews are considered. For each place, place ID, name, type, sub-type, and geographical location of all realted places are extracted. Then, for each place, place ID, review ID, review title, review text and review rating of a maximum of 1000 top reviews are extracted. Finally two files are created, one for places and one for users' reviews. These two files can be joined using place ID.

It is clear that these data were unstructured and unprepared. In order to prepare data, places without geographic coordinates, those that were not located at the study area, NYC, duplicates, and places whose types are unknown were removed. There are five place types in TripAdvisor blog. *Table 1* shows the number of places and user's reviews in each category after preparing data.

Place Type	Attraction	Food Place	Hotel	Shopping	Vacation Rental
No of Places	1203	13282	842	1049	1080
No of Reviews	95661	325774	157625	31404	3334

Table 1. Number of places and user's reviews in each category

Data preprocessing is the most time consuming and important part in any text mining and machine learning task (Han & Kamber 2001). Therefore, first of all, the users' reviews should be preprocessed. NLTK library is used for this purpose. First, each review is converted to lower case and tokenized, then punctuations and stop words were removed. Afterward, all tokens are stemmed and lemmatized. In the first approach, these review texts with lemmatized words are considered. In the second approach, for each review verbs are extracted using NLTK and WordNet part-of-speech (POS) tagging. Then state verbs and auxiliary verbs are then removed and only action verbs in the review are selected for prediction process.

In the next step, the features should be generated and selected. As candidate words for feature selection, we only consider sufficiently frequent words. Bag of Words (BoW), Word2Vec, and Doc2Vec are different methods for feature selection that are used in our method.

Finally, place functionality of each user's review can be predicted using text classification methods in NLP. Crucially, our method is fully supervised, requiring a bag of words/word2vec/doc2vec representation of the objects

and place types as input. Logistic regression (LogReg), support vector machine (SVM), stochastic gradient decant (SGD), multinomial naïve bayes (MNB), k nearest neighbors (KNN), random forest (RF), gradient boosting (GB), decision tree (DT), and multi-layer perception (MLP) classifiers are different machine learning classifiers that are tested on both review text with lemmatized words and just action verbs of the review using three different methods of feature selection (BoW, Word2Vec, Doc2Vec). The performance of the text classifiers are evaluated using common machine learning evaluation measures such as accuracy, precision, recall, and f1-score by computing confusion matrix.

3. Results

Evaluation results demonstrate that in all the three feature selection methods and in all the different classification algorithms, using whole sentence with lemmatized words achieves better performance rahter than considering just action verbs. This shows that words with differnt part-of-speach and the sementic relations between words are important for extracting place functionality. Among different classifiers, although SVM leads to better accuracy and f1-score, the execution time of the algorithm is about 317 times and 758 times that of LogReg for lemmatized words and verbs with just 1% less accuracy. Also, MNB is the fastest algorithm. The best prediction results are achieved for Food Places, Hotels, Attractions, Shops, and Vacation Rentals, respectively. Figure 2 shows the confusion matrix of SVM for lemmatized words and verbs using BoW feature selection method.

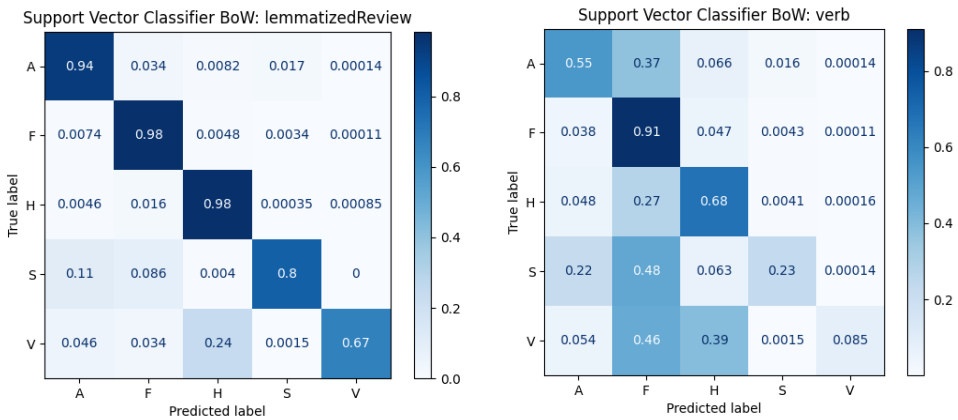

Figure 2. The confusion matrix of SVM for lemmatized words and verbs using BoW feature selection method.

4. Conclusion

Applying human cognition in defining and extracting place information is necessary. Today, this would be possible due to the growth of technologies related to artificial intelligence such as natural language processing and machine learning algorithms. Place functionality is considered important information in defining a place by humans. The propose of this paper was extracting place functionality through analyzing user-generated textual contents. Therefore, the activity of people in the place was extracted using action verbs, and then by using machine learning methods, the place functionality was predicted from the whole text and only action verbs. The results show that using whole sentence with lemmatized words achieve better performance rahter than considering just action verbs. Also, among different classifiers, SVM leads to better accuracy and f1-score.

References

Alazzawi, A. N., Abdelmoty, A. I., & Jones, C. B. (2012). What can I do there? Towards the automatic discovery of place-related services and activities. *International Journal of Geographical Information Science, 26*(2), 345-364

Ballatore, A., & Adams, B. (2015). *Extracting place emotions from travel blogs*. Paper presented at the Proceedings of AGILE.

Chen, H., Vasardani, M., Winter, S., & Tomko, M. (2018). A graph database model for knowledge extracted from place descriptions. *ISPRS International Journal of Geo-Information, 7*(6), 221.

Couclelis, H. (1992). Location, place, region, and space. *Geography's inner worlds, 2*, 15-233.

Gao, S., Liu, Y., Kang, Y., & Zhang, F. (2021). User-Generated Content: A Promising Data Source for Urban Informatics.

Goodchild, M. F. (2015). Space, place and health. *Annals of GIS, 21*(2), 97-100

Khoury, R., Karray, F., & Kamel, M. (2006). *Extracting and representing actions in text using possibility theory*. Paper presented at the Proceedings of the 3rd annual e-learning conference on Intelligent Interactive Learning Object Repositories (i2LOR 2006).

Papadakis, E., Baryannis, G., Petutschnig, A., & Blaschke, T. (2019). Function-based search of place using theoretical, empirical and probabilistic patterns. *ISPRS International Journal of Geo-Information, 8*(2), 92

Purves, R. S., Winter, S., & Kuhn, W. (2019). Places in information science. *Journal of the Association for Information Science and Technology, 70*(11), 1173-1182.

Richter, D., Winter, S., Richter, K.-F., & Stirling, L. (2013). Granularity of locations referred to by place descriptions. *Computers, environment and urban systems, 41*, 88-99.

Han, J., & Kamber, M. (2001). Data mining: Concepts and techniques. San Francisco, CA: Morgan Kaufman.